Endocannabinoid modulation of astroglial cells in multiple sclerosis

DOCTORAL THESIS

Álvaro Moreno García
Thesis supervisors: Susana Mato and Giovanni Marsicano
University of the Basque Country UPV/EHU – University of Bordeaux
Leioa, 2022

Summary

Multiple sclerosis (MS) is an immune-mediated, chronic inflammatory disease of the central nervous system and a leading cause of disability in young adults. It is well-established that **astrocyte activation** drives chronic inflammation and neurodegeneration in the **experimental autoimmune encephalomyelitis (EAE)** model of MS and *in vivo* modulation of astrocyte signaling exhibits beneficial effects during disease progression. It is thus envisaged that the identification of factors driving pathogenic astrocyte activity in MS will contribute to the development of novel and more successful treatment strategies. In this context, a neurotoxic population of **neurotoxic reactive astrocytes** induced by activated microglia that contributes to the death of neurons and oligodendrocytes has been recently identified in MS.

Astrocytes present complex and tightly controlled **Ca^{2+} dynamics** which are fundamental to intracellular signaling and intercellular communication. Activity-dependent Ca^{2+} signals in astrocyte regulate directly the biological functions of these cells and affect the integration and processing of synaptic information, modulating synaptic transmission, plasticity and behavior. Indeed, astrocytes respond with cytosolic Ca^{2+} elevations to a wide variety of neurotransmitters released by neurons and subsequently release a plethora of neuroactive molecules, called **gliotransmitters**, which comprise glutamate, ATP, D-serine and GABA. Reactive astrocytes displaying deregulated Ca^{2+} signaling have been found in several neurological disorders. However, astrocyte Ca^{2+} dynamics have not been investigated in the context of MS.

Astrocytes and **microglia** are modulated by **endocannabinoids** and participate in the biosynthesis and metabolism of these compounds. However, the role of neuroglial cells as targets and mediators of endocannabinoid signaling in MS remains poorly understood. **(Endo)cannabinoids** acting through **cannabinoid type 1 receptors (CB_1Rs)** exert symptom control in MS. These beneficial effects are mainly mediated by the activation of neuronal CB_1Rs that engage protection from glutamate excitotoxicity. On the other hand, **CB_1Rs expressed in astrocytes induce intracellular Ca^{2+} elevations that promote glutamate release**. This mechanism underlies working memory impairment by acute cannabinoids in rodents and may contribute to excitotoxic events in neurodegenerative conditions such as MS.

In this work, we have addressed several objectives aimed at deciphering **the role of the endocannabinoid system in modulating astrocytes during MS**. In the EAE model of chronic MS we have 1) investigated the temporal dynamics of endocannabinoid signaling deregulation in reactive astrocytes, 2) characterized changes in astrocyte Ca^{2+} signaling and 3) examined the role of astroglial CB_1Rs during autoimmune demyelination using conditional mutant mice. Our results show that astrocyte activation during EAE involves early **transcriptional alterations affecting endocannabinoid signaling associated molecules**. Secondly, we have identifies **CB_1Rs as crucial regulators of astrocytic Ca^{2+} dynamics** in the mouse cortex *in vivo* and uncover **aberrant Ca^{2+} signaling in MS**. Lastly, we unveil that **astrocyte CB_1Rs exacerbate neurological disability and neuroinflammation during EAE** pointing out to a previously unexpected role of the ECS in the pathophysiology of myelin. These data broaden current knowledge on the mechanisms involved in benefits/side effects of currently available MS treatments targeting CB_1Rs and pave the way for the development of novel, more efficacious endocannabinoid system-modulating drugs to treat MS.

Résumé

La **sclérose en plaques (SEP)** est une maladie inflammatoire chronique à médiation immunitaire du système nerveux central et est une cause majeure de handicap chez les jeunes adultes. Il est bien établi que **l'activation des astrocytes** est à l'origine de l'inflammation chronique et de la neurodégénérescence dans le modèle **d'encéphalomyélite auto-immune expérimentale (EAE)** de la SEP et que la modulation *in vivo* de la signalisation astrocytaire a des effets bénéfiques sur la progression de la maladie. L'identification des facteurs conduisant à l'activité pathogène des astrocytes dans la SEP contribuera donc au développement de nouvelles stratégies de traitement plus efficaces. Dans ce contexte, a récemment été identifiée dans la SEP une **population neurotoxique d'astrocytes réactifs**, induits par la microglie activée, qui contribue à la mort des neurones et des oligodendrocytes.

Les **astrocytes** présentent une **dynamique Ca^{2+}** complexe qui est fondamentale pour la signalisation intracellulaire ainsi que la communication intercellulaire. Les signaux Ca^{2+} dépendants de l'activité dans les astrocytes régulent directement les fonctions biologiques de ces cellules et affectent l'intégration et le traitement des informations synaptiques. En effet, les astrocytes répondent par une élévation du Ca^{2+} cytosolique à une grande variété de neurotransmetteurs libérés par les neurones. Ils libèrent ensuite une pléthore de molécules neuroactives, appelées **gliotransmetteurs**. Des astrocytes réactifs présentant une signalisation déréglée du Ca^{2+} ont été trouvés dans plusieurs troubles neurologiques. Cependant, la dynamique du Ca^{2+} des astrocytes n'a pas encore été étudiée dans le contexte de la SEP.

Les **astrocytes** et la **microglie** sont modulés par les **endocannabinoïdes** et participent à la biosynthèse et au métabolisme de ces composés. Cependant, le rôle des cellules neurogliales en tant que cibles et médiateurs de la signalisation endocannabinoïde dans la SEP reste très peu compris. Les **(endo)cannabinoïdes** agissant par l'intermédiaire des **récepteurs cannabinoïdes de type 1 (CB_1Rs)** permettent de contrôler les symptômes de la SEP. Ces effets bénéfiques sont principalement modulés par l'activation des CB_1Rs neuronaux qui engagent une protection contre l'excitotoxicité du glutamate. D'autre part, **les CB_1Rs exprimés dans les astrocytes induisent des élévations intracellulaires de Ca^{2+} qui favorisent la libération de glutamate.** Ce mécanisme sous-tend l'altération de la mémoire de travail par les cannabinoïdes aigus chez les rongeurs et pourrait contribuer aux événements excitotoxiques dans les conditions neurodégénératives telles que la SEP.

Dans ce travail, nous avons abordé plusieurs objectifs visant à déchiffrer **le rôle du système endocannabinoïde dans la modulation des astrocytes pendant la SEP.** Dans le modèle EAE de SEP, nous avons 1) étudié la dynamique temporelle de la dérégulation de la signalisation endocannabinoïde dans les astrocytes réactifs, 2) caractérisé les changements dans la signalisation Ca^{2+} astrocytaire et 3) examiné le rôle des CB_1Rs astrogliaux pendant la démyélinisation auto-immune. Nos résultats montrent que l'activation des astrocytes au cours de l'EAE implique des **altérations transcriptionnelles précoces affectant les molécules associées à la signalisation endocannabinoïde.** Ensuite, nous avons identifié les **CB_1Rs comme régulateurs cruciaux de la dynamique du Ca^{2+} astrocytaire** dans le cortex de la souris *in vivo* et découvert une **signalisation aberrante du Ca^{2+} dans la SEP**. Enfin, nous dévoilons que les **CB_1Rs astrocytaires exacerbent l'incapacité neurologique et la neuroinflammation au cours de l'EAE**, ce qui met en évidence un rôle précédemment inattendu du système endocannabinoïde dans la physiopathologie de la myéline. Ces données élargissent les connaissances actuelles sur les mécanismes impliqués dans les bénéfices ainsi que les effets secondaires des traitements actuels de la SEP, ciblant les CB_1Rs.

Introduction

1. Multiple sclerosis (MS)

Multiple sclerosis (MS) is an immune-mediated, chronic inflammatory disease of the central nervous system (CNS) characterized by the destruction of the myelin sheath giving rise to widespread areas of focal demyelination (Lassmann, 2014). Myelin harm disrupts neuronal signaling processing leading to neurological deficits.

MS was first clinically described by Jean-Martin Charcot in 1865 and today is the commonest non-traumatic neurological disease among young adults affecting 2.8 million people worldwide according to the Atlas of MS database (2020). MS is a global problem and its prevalence is increasing, being almost 3 times more frequent in women than in men. The global distribution of the disease increases moving away from the equator. The highest prevalence is found in North America, Western Europe, and Australasia (>100 cases per 100.000 population) (Wallin et al., 2019).

MS is a heterogeneous, multifactorial disease in which complex gene-environment interactions are involved. The major hallmark of MS is the accumulation of **demyelinating lesions** in the white matter and the grey matter of the brain and spinal cord that lead to **inflammation, axonal degeneration** and **astrogliosis** (Compston and Coles, 2008). Although the etiology of MS remains unclear, it is generally accepted that these lesions are caused by autoreactive lymphocytes that migrated across the blood-brain barrier (BBB) followed by glial activation and chronic neurodegeneration (Weiner, 2004).

1.1. Phenotypic classification

Diagnostic criteria for MS have evolved over time, thanks to new scientific discoveries and the development of clinical techniques, specially imaging by magnetic resonance (MRI), that enable an earlier, more sensitive and more reliable diagnosis, potentially facilitating treatment at initial disease stages (Brownlee et al., 2017). The disease course and clinical manifestations of MS are highly heterogeneous. Based on clinical relapse rate, MRI and disease progression, MS has been classified into different subtypes (Thompson et al., 2018) (**Figure 1**).

Relapsing-remitting MS (RRMS). It is the most common form of MS, affecting approximately 85% of patients and characterized by defined acute exacerbations with complete or incomplete recovery. During periods between relapses, patients show relative clinical stability with no disease progression. Numerous patients diagnosed with RRMS eventually develop a secondary progressive disease phase.

Secondary progressive MS (SPMS). Characterized by gradual progression after a relapsing course. Around 40% of patients develop this form of MS within 20 years of the initial event. In most of the cases, SPMS involves a gradual decline in neurologic functioning and affects areas previously involved in the relapsing course of the disease.

Primary progressive MS (PPMS). Patients with this form of the disease experience a progressive decline in neurological functions from disease onset and an absence of relapses. This form represents about 10% of MS cases. PPMS patients tend to have a later age onset and the prognosis is worse compared to RRMS patients.

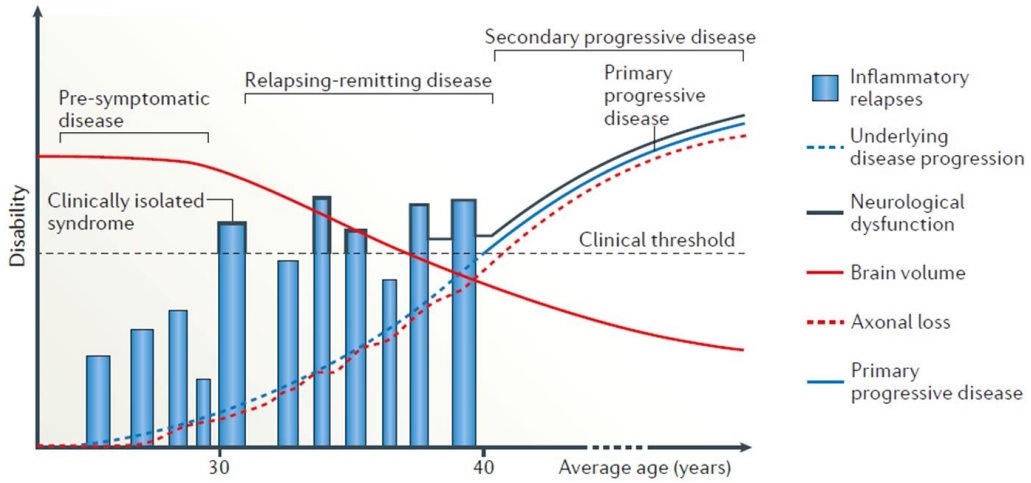

Figure 1. Representation of MS subtypes depicting the characteristic neurological dysfunction, brain atrophy and axonal loss associated to each subtype. From Dendrou *et al*., 2015.

The importance of an early and accurate diagnosis of MS is essential for an optimal treatment. This evidence is supported by the observation that certain disease-modifying therapies (DMTs) for MS are contraindicated in some of the different types of the disease (Thompson et al., 2018). As the characterization of different forms of MS improves, a key challenge is to determine whether different disease forms can truly be classified as a single disease or not. This knowledge will help to better understand pathophysiological mechanisms that are either unique of MS or shared with other neurodegenerative diseases, improving the accuracy of diagnostics and therapeutic targeting (Dendrou et al., 2015).

1.2. Etiology and pathophysiology

The cause of MS is still unknown, although it is now known that environmental, genetic and epigenetic factors are involved in disease pathogenesis (Olsson et al., 2017). **Environmental risk factors** such as vitamin D deficiency, obesity in early life, cigarette smoking and infection by Epstein-Barr virus have been associated with enhanced risk for developing MS (Filippi et al., 2018; Kjetil et al., 2022). Some of these risk factors interact with different **genetic and epigenetic modifications**, including the human leukocyte antigen (HLA) or major histocompatibility complex (MHC) gene family, among other genes, conferring a higher risk of MS (Cotsapas and Mitrovic, 2018; Hafler et al., 2007). Most risk alleles are associated with immune-pathway genes, consistent with the notion that autoimmune mechanisms play a major role in disease pathogenesis. Further efforts are required to elucidate how environmental risk factors interact with MS susceptibility genes to contribute to disease progression (Reich et al., 2018).

Detailed histopathological analysis has revealed a high heterogeneity between MS lesions, which suggest that disease initiation and progression are driven by complex pathogenic mechanisms that include autoimmune and primary demyelination, astroglial and microglial activation, glutamate excitotoxicity and neuroaxonal degeneration, among others (Reich et al., 2018) (**Figure 2**).

Immune dysregulation leading to altered 'crosstalk' between the innate and adaptive immune systems is considered a key event mediating CNS damage in MS (Grigoriadis et al., 2015). This process appears to involve dendritic cells, which migrate across de blood brain

barrier and secrete a variety of cytokines inducing T cell differentiation. In this regard, the secretion of IL-12 mediates $CD4^+$ T cell differentiation into IFNγ-secreting Th1 helper cells. On the other hand, in the predominant presence of IL-23, $CD4^+$ T cells differentiate into IL-17 or IL-22 secreting Th17 cells. Pathogenicity triggered by these activated T cells consists in many events. On one hand, they induce an increase in BBB permeability by producing matrix metalloproteinases (MMPs) and radical oxygen species. Secondly, they promote the recruitment of monocytes from the bone marrow and produce cytokines that induce **macrophage**, **microglial and astrocyte activation**, which in turn release pro-inflammatory mediators, oxygen and nitric oxide radicals (ROS, NOS) that participate in myelin breakdown, oligodendrocytes damage and axonal degeneration. Besides that, $CD8^+$ T cells also release pro-inflammatory mediators such as IL-17 and lymphotoxin, and their presence in CNS has been associated to axonal injury. Moreover, other cell types such as natural killer cells -by stimulating APC maturation and cytokine production- and B cells -by antibody and autoantibody production- have also been implicated in the immunopathogenesis of MS.

Although the predominant view has been that acute demyelinating lesions start with deregulation of the immune system, newly forming lesions of MS patients exhibit profuse oligodendrocyte apoptosis with early microglial activation, in the virtual absence of infiltrating lymphocytes or myelin phagocytes. By contrast, older lesions in the same patients exhibited positive expression of these immune cells (Barnett and Prineas, 2004; Lucchinetti et al., 2000). These observations suggest that, at least in a subset of MS patients, autoimmunity might be a secondary response to massive **primary oligodendrocyte apoptosis**. This process suggest that **primary demyelination** is a relevant as mechanism of MS pathogeny lesions (Lassmann, 2018).

In the last years, **neurodegeneration** has been highlighted as a primary cause of long-term neurological disability in MS. Indeed, synaptic alterations, axonal injury and neuronal loss have been consistently described in the context of MS (Centonze et al., 2009; Seehusen and Baumgärtner, 2010; Vercellino et al., 2009). Furthermore, neurodegeneration might occur early in the disease course and not only because of myelin loss. In this regard, converging lines of evidence support the hypothesis that **glutamate-mediated excitotoxicity** is a key etiopathogenic mechanism of neurodegeneration and demyelination in MS. Overactivation of ionotropic glutamate receptors results in a massive entry of extracellular calcium (Ca^{2+}), which triggers a depolarization of the mitochondrial membrane and ROS production leading to the initiation of death cascades. The relevance of glutamate excitotoxicity to MS is supported by consistent observations that AMPA and NMDA receptors mediate Ca^{2+} dependent injury to oligodendrocytes and myelin (Micu et al., 2006; Sánchez-Gómez et al., 2003) and that glutamate levels are significantly higher in the brain of MS patients (Sarchielli et al., 2003; Srinivasan et al., 2005), a feature that correlates with altered glutamate homeostasis in lesions and with oligodendroglial and axonal damage (Werner et al., 2001). Moreover, impaired glutamate clearance and beneficial effects resulting from AMPA/kainate and NMDA receptor antagonists have been reported in mouse MS models (Bolton and Paul, 1997; Pitt et al., 2000). These results also support the hypothesis that disturbances in Ca^{2+} homeostasis in MS patients potentially contribute to MS pathogenesis (see below).

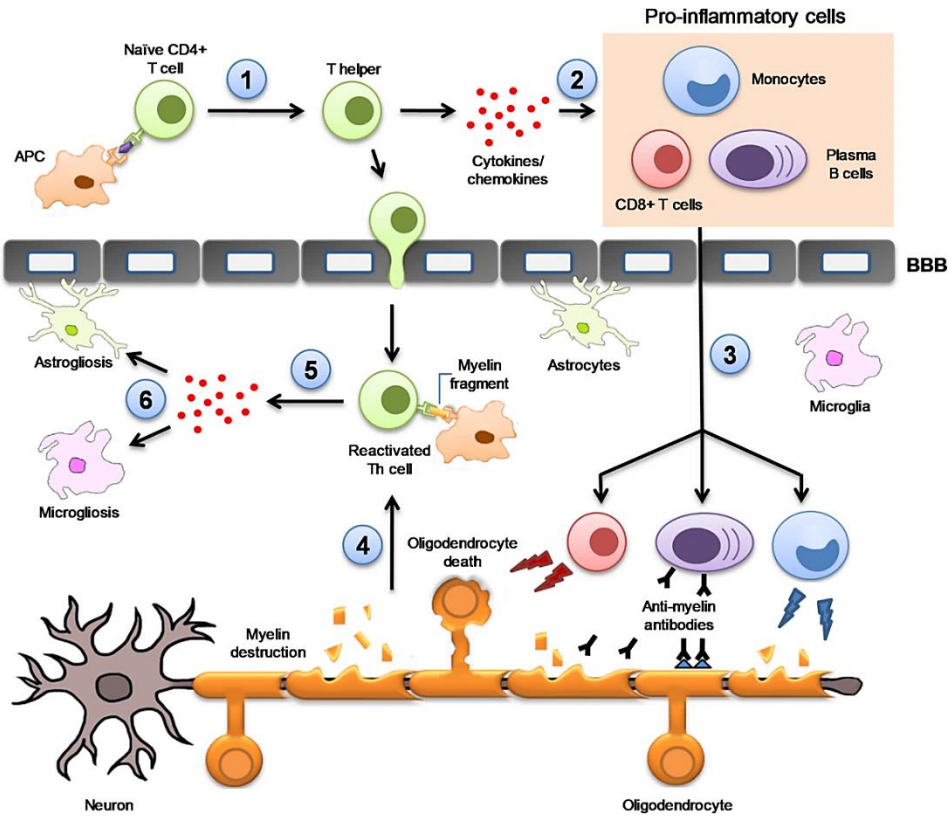

Figure 2. The underlying pathophysiological mechanism of MS. In the first instance, autoreactive $CD4^+$ T cells are activated in the periphery by antigen presenting cells (APC) that present, in conjunction with class II MHC molecules, similar antigens to those synthesized by the CNS. (**1**) This interaction activates the differentiation of $CD4^+$ T naïve cells into $CD4^+$ T helper cells (Th). (**2**) Upon activation, Th produces interferon-gamma (IFN-γ), a cytokine responsible for recruiting $CD8^+$ T cells, B cells and monocytes in the periphery. (**3**) These pro-inflammatory cells migrate to the blood-brain barrier (BBB) and pass into the CNS. Inside the brain, plasma B cells produce autoantibodies against CNS self-antigens contributing to myelin sheath damage. This process is aggravated when infiltrated cytotoxic $CD8^+$ T cells attack oligodendrocytes causing their destruction and neuronal death. Monocytes, on the other hand, increase local inflammatory response by releasing pro-inflammatory cytokines and contributing to demyelination through myelin phagocytosis. (**4**) In parallel, infiltrated $CD4^+$ T cells are reactivated upon interaction with myelin fragments presented by resident APCs which favors (**5**) pro-inflammatory cytokines and chemokines release, (**6**) astrogliosis and microgliosis. From Celarain and Tomas-Roig, 2020.

Regardless the primary mechanisms driving the formation of MS lesions it is well established that neuroglial cells are important contributors to MS pathology (Dendrou et al., 2015). **Microglia** are abundant in demyelinating lesions and play dual roles in disease progression, sometimes promoting destructive inflammation but in other circumstances promoting repair by clearance of myelin debris thus facilitating repair mechanisms (Aguzzi et al., 2013). Astrocytes are crucially involved in MS initiation and progression through a variety of mechanisms that range from the recruitment and activation of microglia and monocytes to the production of factors that facilitate regeneration of the myelin sheath (Thompson et al., 2018).

Despite the fact that most of MS lesions remain permanently demyelinated, myelin repair occurs spontaneously in some of them, named “shadow plaques” (Chang et al., 2012). **Remyelination**, which is considered a physiological response, is defined as a regenerative

process whereby myelin sheaths are restored. This process occurs through the activity of oligodendrocyte precursor cells (OPCs), which are recruited into MS lesions and differentiate into myelinating oligodendrocytes (Franklin and Ffrench-Constant, 2017; Kremer et al., 2018) giving rise to shorter and thinner myelin sheaths than the original ones. The mechanisms responsible for OPC activation and recruitment are still poorly defined, but it is speculated that may be related to tissue injury-associated innate immune responses mediated by **microglia-astrocyte interactions** (Franklin and Ffrench-Constant, 2017). Although remyelination is a consistent finding in MS, the efficiency of myelin repair varies considerably between patients and lesions. It is also well established that a number of factors such as aging, chronic inflammation, and the production of extracellular matrix proteins limit endogenous myelin repair.

Over the years, a variety of complementary MS models mimicking specific aspects of MS pathology have been developed (Burrows et al., 2019). These models include immune-mediated, toxic-induced and virus-induced models that cannot replicate the whole complexity and heterogeneity of human MS, although they have proved useful for the development of several drugs approved for treatment of MS patients. **Experimental autoimmune encephalomyelitis** (EAE) induced by myelin oligodendrocyte glycoprotein (MOG) in C57BL/6 mice resembles the chronic progressive phase of human MS and is, by far, the most studied animal model for MS pathology. The onset of EAE is characterized by perivascular infiltration of peripheral immune cells in the white matter of the CNS accompanied by activation of astrocytes and microglia, demyelination and axonal loss, mainly seen at the peak of the disease. The most pronounced changes are observed in the spinal cord, but alterations are also present in the brain in a lower extent (Schmitt et al., 2012).

1.3. General features of Ca^{2+} dynamics: a focus in MS

Ca^{2+} is one of the most important intracellular second messengers in eukaryotic cells, playing key roles in signal transduction for neurotransmitter release, synaptic plasticity, cell growth, differentiation, metabolism, gene transcription, learning and memory, immunity and apoptosis, among other cellular functions (Berridge et al., 2003). These cellular processes take place over a wide dynamic range and require a Ca^{2+} signaling system that operates in many different ways to achieve multifunctional roles (**Figure 3**). At the synaptic junction, for example, Ca^{2+} triggers neurotransmitter exocytosis within microseconds, whereas minutes or even hours are required to drive events such as gene transcription and cell proliferation (Berridge et al., 2003).

The concentration of Ca^{2+} is tightly regulated and kept low both extracellularly and intracellularly under physiological conditions. Extracellular Ca^{2+} levels are kept at a range of 1.5-2 mM. The resting cytosolic Ca^{2+} concentration in neurons is 100-150 nM but most Ca^{2+} signaling is mediated within subcellular microdomains that maintain very distinct Ca^{2+} concentrations, and have specific roles in physiological and pathological Ca^{2+} signaling (Lim et al., 2021). Ca^{2+} homeostasis consists thus in a coordinated transport of Ca^{2+} ions through several sets of membranes that define distinct intracellular compartments.

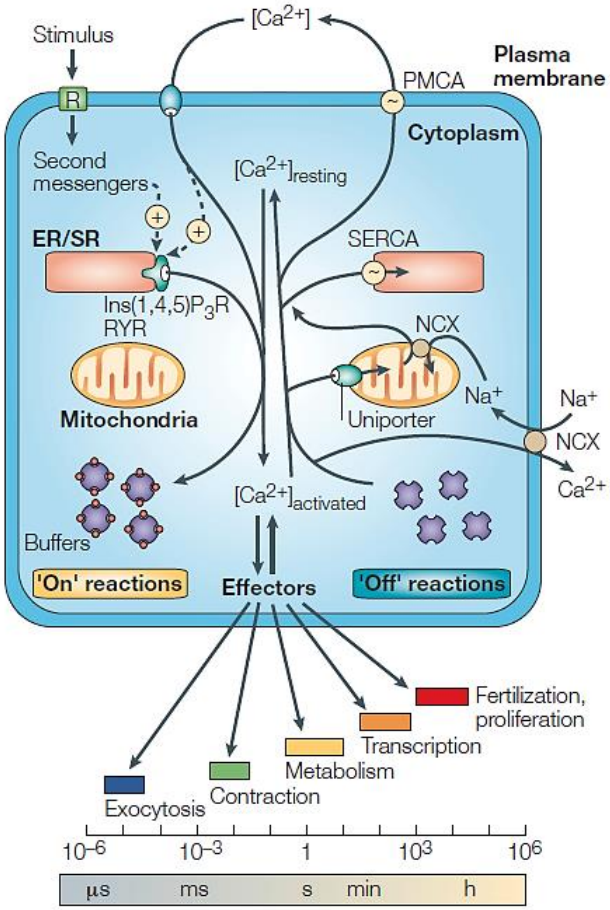

Figure 3. Ca^{2+} signaling dynamics and homeostasis. During the 'on' reactions, stimuli induce both the entry of external Ca^{2+} and the formation of second messengers that release internal Ca^{2+} that is stored within the endoplasmic/sarcoplasmic reticulum (ER/SR). Most of this Ca^{2+} (shown as red circles) is bound to buffers, whereas a small proportion binds to the effectors that activate various cellular processes that operate over a wide temporal spectrum. During the 'off' reactions, Ca^{2+} leaves the effectors and buffers and is removed from the cell by various exchangers and pumps. The Na^+/Ca^{2+} exchanger (NCX) and the plasma-membrane Ca^{2+}-ATPase (PMCA) extrude Ca^{2+} to the outside, whereas the endoplasmic/sarcoplasmic reticulum (ER/SR) Ca^{2+}-ATPase (SERCA) pumps Ca^{2+} back into the ER/SR. Mitochondria also have an active function during the recovery process in that they sequester Ca^{2+} rapidly through a uniporter, and this is then released more slowly back into the cytosol to be dealt with by the SERCA and the PMCA. [Ca^{2+}], Ca^{2+} concentration; Ins(1,4,5)P_3R, inositol-1,4,5-trisphosphate receptor; RYR, ryanodine receptor. From Berridge *et al,* 2003.

Ca^{2+} ions flow into the cytosol in response to stimuli via two main pathways (i) along their electrochemical gradient from the extracellular space through plasma membrane Ca^{2+} channels, and (ii) from intracellular Ca^{2+} stores such as the endoplasmic reticulum (ER) or the mitochondria, which instantly accumulate Ca^{2+} ions and release them during certain cellular events (**Figure 3**) (Clapham, 2007). Cytosolic Ca^{2+} concentrations are maintained low by active ion pumping into the extracellular space through plasma membrane Ca^{2+}-ATPases (PMCAs) and the Na^+/Ca^{2+} exchanger (NCX). Certain proteins of the cytoplasm and cell organelles additionally act as buffers by binding free Ca^{2+} so that the cytosolic Ca^{2+} level is only briefly increased when required (Clapham, 2007). Cellular Ca^{2+} homeostasis is thus maintained by several mechanisms

including influx, extrusion, buffering and sequestration. The malfunction of any of these processes can lead to Ca^{2+} dyshomeostasis, initiating injury mechanisms that lead to neuronal dysfunction and death. Indeed, dysregulation of Ca^{2+} homeostasis has been associated with several neurodegenerative disorders such as Parkinson's disease (PD) (Surmeier et al., 2017), Alzheimer's disease (AD) (Briggs et al., 2017), Huntington's disease (HD) (Raymond, 2017), as well as MS (Enders et al., 2020).

Mitochondria are fundamentally involved in intracellular Ca^{2+} signaling through a variety of mechanisms. This organelle provide the ATP required to fuel the numerous Ca^{2+} pumps that maintain low cytosolic Ca^{2+} levels at the same time that import Ca^{2+} actively against its concentration gradient. Mitochondria thus act as a broad Ca^{2+} store, buffering large Ca^{2+} loads and preventing cell from cytotoxic Ca^{2+} overload leading to apoptosis and cell death (Luongo et al., 2017). The movement of Ca^{2+} ions in and out of mitochondria is mediated through two membranes. The first is the outer membrane, which is relatively permeable to ions and where Ca^{2+} transport is facilitated by the non-selective voltage-dependent anion channel (VDAC or mitochondrial porin) (Rapizzi et al., 2002). Conversely, Ca^{2+} transport through the second, inner mitochondrial membrane is tightly regulated and depends on the activity of specialized transporters. Inward Ca^{2+} flux across this membrane is mediated primarily via a highly selective pathway termed the mitochondrial Ca^{2+} uniporter (MCU) (Kirichok et al., 2004). The ability to take up substantial amounts of Ca^{2+} underlines two principal roles of mitochondria: it enables mitochondria to shape the spatiotemporal profile of cytosolic Ca^{2+} signals and to simultaneously transmit these events into the mitochondrial matrix. In the matrix, Ca^{2+} up-regulates the activity of Ca^{2+}-sensitive dehydrogenases of the Krebs cycle and the ATP synthase thus controlling ATP production (Das, 2003). Conversely, accumulated Ca^{2+} efflux from the mitochondria is primarily mediated by the mitochondrial Na^{+}/Ca^{2+} exchanger (NCXL) (Werth and Thayer, 1994) and via transient opening of the mitochondrial permeability transition pore (mPTP) (Bernardi and Petronilli, 1996).

Our understanding of Ca^{2+}-dependent processes in the context of autoimmune demyelination is continuously improving. Free Ca^{2+} in the cytosol regulates various mechanisms directly involved in immune cell activation and selection upon antigen recognition among other immune-related disease mechanisms. In particular, it is well known that Ca^{2+}-dependent processes play an important role in the elimination of autoreactive lymphocytes during the maturation process in the thymus (Valdor and Macian, 2010). Alterations in the expression and/or activity of Ca^{2+} pumps and exchangers, such as PMCA2 and NCX, may affect Ca^{2+} homoeostasis and thereby induce intracellular injury mechanisms in MS (Kurnellas et al., 2007). The inhibition of activated T-cells by regulatory T-cells is also Ca^{2+}-dependent. In particular, it has been shown that regulatory T-cells from MS patients block Ca^{2+} signals in autoreactive, activated T-cells less efficiently than regulatory T-cells from healthy subjects (Schwarz 2013). Importantly, dysregulated Ca^{2+} signals in T-cells can also lead to undesired autoreactive immune responses to self-antigens and trigger autoimmune inflammation (Hundehege et al., 2017).

BBB dysfunction and the following transendothelial migration of activated, autoreactive lymphocytes are among the first pathological changes in MS (Minagar and Alexander, 2003). Although the complex signaling pathways underlying the pathological changes in BBB permeability remain unclear, deregulation of extra- and intracellular Ca^{2+} concentrations is known to be centrally involved. Extracellular Ca^{2+} drops lead to disruption in cell-cell and cell-

extracellular matrix interactions whereas intracellular increases in Ca^{2+} concentration trigger Ca^{2+}-dependent signaling pathways that ultimately induce restructuring of the cytoskeleton together with a reorganization of tight junctions proteins, which results in the weakening of the BBB (De Bock et al., 2013).

Intracellular Ca^{2+} concentration disturbances are considered to be one of the initial steps involved in neurodegeneration (Herz et al., 2010). Concerning MS, axons and neurons in autoimmune-inflammatory lesions display increased free Ca^{2+} levels as compared to those in non-inflamed areas in the EAE rodent model of the disease. Mechanistically, imbalanced Ca^{2+}concentrations were associated with immune-neuronal interactions and postulated as important mediators of sustained damage during neuroinflammation (Siffrin et al., 2015). Recently RNA sequencing (RNA-seq) datasets show that genes encoding Ca^{2+}, K^+ Na^+ and Cl^- channels, ryanodine receptors and others are significantly and uniquely dysregulated in active, chronic active, inactive, remyelinating lesions and normal-appearing white matter of SPMS patients, and it is postulated that ionic dyshomeostasis has profound implications for tissue damage and repair in MS (Boscia et al., 2021). Finally, a number of studies have demonstrated that Ca^{2+} accumulation in the mitochondria following excitotoxic insults is a crucial event initiating death signaling cascades in neurons and oligodendrocytes (Marchi et al., 2018).

To summarize, Ca^{2+} signaling pathways are involved in many relevant steps of MS pathogenesis, such as the alteration of BBB permeability, the autoimmune reactivity and migration of lymphocytes into the CNS, and the neuro-axonal degeneration (Hundehege et al., 2017). It is thus hypothesized that the modulation of Ca^{2+} influx into the cells and the targeting of Ca^{2+}-mediated signaling pathways may represent promising therapeutic avenues for MS among other neuro-immunological disorders (Enders et al., 2020).

1.4. Current therapeutic strategies

MS symptomatology during relapses has been classically treated with anti-inflammatory steroid medications. Combined with improved understanding of the immunological and neurobiological disease processes underlying MS, advances in diagnosis have led to the development of several DMTs that intervene in different pathogenic mechanisms, including antigen presentation, peripheral immune response or target tissue within the CNS itself (Weissert, 2013). These agents aim at reducing relapse rate and thus ameliorate the course of RRMS and the quality of life and delay, at least in part, the progression of MS. However, current DMTs fail to benefit the progressive phase of MS mainly due to the lack of understanding of pathogenic mechanisms driving this form of the disease. Thus, new strategies focused on the protection of CNS from inflammatory injury or aimed at promoting neuroprotection and remyelination need to be developed for efficacious treatment of progressive MS stages. A myriad of drugs that might target immune system dysfunction, glial cells or neurons, metabolic abnormalities associated with mitochondrial injury or different ion channels are nowadays under investigation for MS therapy (Correale et al., 2017).

2. Astrocytes in health and disease

The study of astrocytes is a thrilling field in Neuroscience. Since their first description by Camilo Golgi in 1872 and their morphological representation in Cajal's drawings in 1897, substantial progress has been made in the knowledge of their functions, heterogeneity and morphology.

2.1. Physiology of astroglia

Astrocytes are the main glial population within the CNS representing around 20-40% of the total number of cells in the mammalian brain (Herculano-Houzel, 2014). Astrocytes perform a broad array of functions in the developing and adult brain, including ion and water homeostasis (Simard and Nedergaard, 2004), neurotransmitter recycling (Weber and Barros, 2015), BBB formation and maintenance (Alvarez et al., 2011), immune signaling (Mayo et al., 2012), myelination (Molina-Gonzalez and Miron, 2019) and, synaptic transmission (Araque et al., 2014). Astroglial cells also participate in the maintenance, pruning and remodeling of synapses during development, aging and injury (Chung et al., 2016; Liddelow et al., 2017). To fulfill these complex roles, astrocytes maintain a bi-directional crosstalk with other glial cell populations, such as oligodendrocytes and microglia with complex consequences in neurodegenerative and demyelinating disorders (Lian et al., 2016).

The term "astrocytes", literally "star-shaped" cells, was coined in 1893 by Michael von Lenhossék referring to their ramifications from the soma (Lenhossék, 1893). Like neurons and oligodendrocytes, astrocytes arise from a radial glial cell population surrounding the ventricular zone in the early developing brain (Rowitch and Kriegstein, 2010). During adulthood, they are not subject to secondary lateral migration, but instead they form stable domains throughout the CNS and get specialized to support the local neuronal network (Morel et al., 2017). This fact may explain, at least in part, the high degree of astroglial heterogeneity within the same as well as different regions of the CNS and the broad physiological roles in which astrocytes are involved in the brain. Although astrocyte morphological diversity was documented over a century ago, the landscape of their functional and physiological heterogeneity has only recently emerged thanks to the use of novel combinatorial approaches such as single-cell RNA-seq, immunohistochemistry, Ca^{2+} and glutamate imaging, among others (Chai et al., 2017).

2.1.1. Classification of astroglial cells

Classically, astrocytes have been classified into two main subtypes based on differences in their cellular morphologies and anatomical locations: protoplasmic or fibrous (Miller and Raff, 1984). **Protoplasmic** astrocytes represent the biggest population of astrocytes in the grey matter and are predominantly found in the hippocampus and cerebral cortex. Their cell bodies exhibit several stem branches that give rise to many finely branching processes, which probably allows them to be close to numerous synapses, thus performing neuromodulatory roles (Bushong et al., 2002; Oberheim et al., 2012). The **fibrous** astrocytes are located along white matter tracts and are morphologically less complex than protoplasmic astrocytes. They are characterized by unbranched, long and thin processes that envelop nodes of Ranvier, thus contributing to keep the homeostasis in the area (Lundgaard et al., 2014; Sofroniew and Vinters, 2010). Besides these two main subtypes of astrocytes, other astrocyte-like cells types have been added to this classification, including interlaminar astrocytes, velate astrocytes, varicose projection astroglial, Bergmann glia and Müller glia (Ben Haim and Rowitch, 2016) (**Figure 4**).

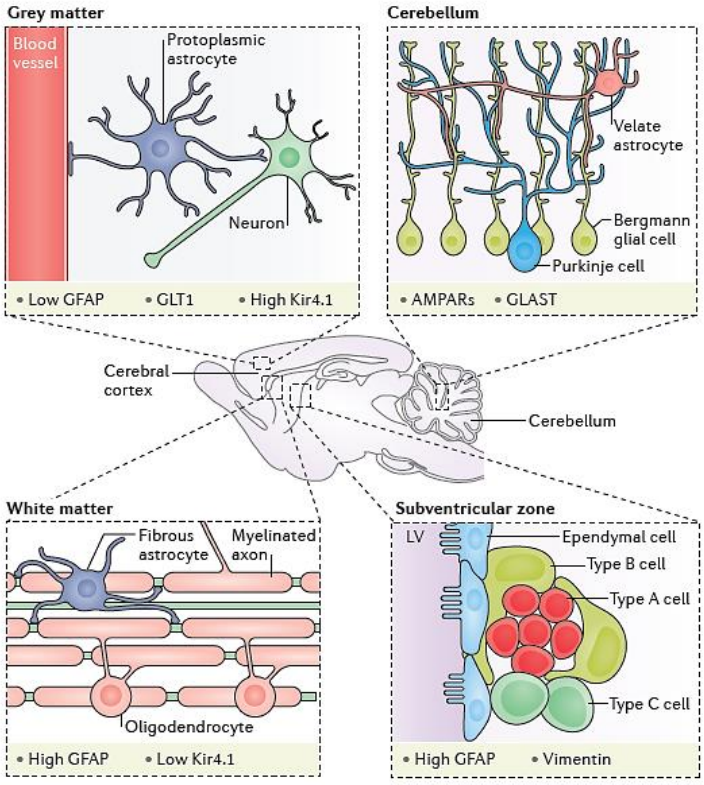

Figure 4. Astrocytes have a range of morphologies and molecular profiles. The schematics illustrate the location and characteristics of several different types of astrocytes in the rodent brain. Protoplasmic astrocytes in the grey matter have a radial morphology and contact neuronal synapses and blood vessels (upper left panel). By contrast, fibrous astrocytes in the white matter have an elongated morphology and are in close contact with oligodendrocytes and myelinated axon tracts (bottom left panel). In the cerebellum, Bergmann glia extend long processes into the molecular layer and enwrap Purkinje cell dendrites (upper right panel). Velate astrocytes are protoplasmic astrocytes found in the cerebellar molecular layer. In the rodent subventricular zone, astrocyte-like type B cells line the lateral ventricles (LVs). These different types of astrocytes differentially express generic astrocyte markers and display inter- and intra-regional molecular differences. From Ben Haim *et al.,* 2016.

New studies based on the morphology of astrocytes as well as on the expression of astrocyte-enriched proteins, however, clearly outdated the early classification of astrocytes. As an example, Emsley and colleagues described nine putative “astrocyte types” in the murine CNS (Emsley and Macklis, 2006), including the types mentioned above, based on their morphology, astroglial density and proliferation rates. A recent study using fluorescence-assisted cell sorting (FACS) and immunological approaches defined five different populations of astrocytes within the adult mouse CNS (John Lin et al., 2017). These astrocyte subsets were characterized by their differential expression of selected surface antigens (CD51, CD63, CD71) and show extensive molecular and functional specific properties as identified by RNA-seq. It is generally accepted that further subpopulations of astrocytes that play diverse roles in health and disease are yet to be defined (Miller, 2018).

2.1.2. Astrocytic markers

Over the past few years, several astrocyte markers have been identified and found to be differentially expressed in subsets of astrocytes. These molecular observations, coupled with morphological and anatomical criteria, can further delineate the cellular and functional diversity

of prospective subpopulations. However, none of the current astrocytic markers is able to label all subpopulations successfully which limits their utility for analysis purposes (Zhang et al., 2019).

Glial fibrillary acidic protein (**GFAP**) is the major intermediate filament composing astrocytic cytoskeleton and the most commonly used astrocytic marker, but it presents some limitations. For instance, GFAP immunostaining covers only about 15% of the total astrocyte volume, and it is not broadly expressed by all astrocytes across brain areas in the healthy CNS (Verkhratsky and Nedergaard, 2018). In particular, GFAP is expressed by astrocytes in the spinal cord, hippocampus, superficial and deep layers of the cortex, but not in the middle layers of the cortex and the thalamus (Khakh and Sofroniew, 2015). Additionally, GFAP has at least eight different isoforms generated by different splicing patterns, and they may be variably expressed in specific subsets of astrocytes (Middeldorp and Hol, 2011). GFAP plays a key role in modulating astrocyte motility and shape by providing structural stability to astrocytic processes. For this reason, it is speculated that GFAP expression is highly regulated during injury and disease (Eng et al., 2000), during aging in specific areas of the rodent and human brain (Morgan et al., 1999; Nichols et al., 1993). In fact, GFAP was first isolated from demyelinated plaques of MS patients, where it was found in high levels (Eng et al., 1970). This led to the immunohistochemical association of GFAP with reactive astrocytes. To complicate things further, GFAP has also been detected in cells that are not astrocytes, such as enteric glia (Kato et al., 1990), Schwann cells (Bianchini et al., 1992), and other non-neuronal cells, such as myoepithelial cells and fibroblasts (Hainfellner et al., 2001). An additional limitation is that GFAP-expressing progenitor cells derived from radial glia in the CNS appear during late development and generate neurons and glia in various CNS areas throughout life (Garcia et al., 2004). An alternative commonly used as astrocytic marker is S100β, a Ca^{2+} binding peptide abundant in the cytoplasm and nucleus of astrocytes, which is involved in cell cycle regulation and cytoskeleton modification (Brozzi et al., 2009). However, S100β is also expressed in a subpopulation of mature oligodendrocytes, ependymal cells and some neurons (Hachem et al., 2005; Steiner et al., 2007).

Other astrocytic markers comprise astrocyte-specific glutamate transporters such as GLT-1 (EAAT2) and GLAST (EAAT1) (Rothstein et al., 1996) that were found to be very useful to stain several astrocytes subtypes like radial glia, Bergmann glia and Müller cells (Schmitt et al., 1997; Shibata et al., 1997). Glutamine synthetase (GS) stains an extensive range of astrocytes subtypes in many regions where GFAP is not an effective marker, mainly astrocytes in the entorhinal cortex (Anlauf and Derouiche, 2013). However, these markers are less specific to astrocytes than GFAP: expression of GLT-1, GLAST and GS has been reported in neurons and oligodendrocytes (Arranz et al., 2008; Matute et al., 1999; Schmitt et al., 2002). Astrocyte processes are rich in the aquaporin 4 (AQP4) water channel, potassium channels such as Kir4.1 and the gap junction/hemichannel proteins Cx30 and Cx43. Nevertheless, these markers are mostly located at astrocytes endfeet rather than throughout the cell soma and their distribution is also limited to some population of brain astrocytes (Higashi et al., 2001; Nagelhus and Ottersen, 2013). Aldehyde dehydrogenase 1 family member L1 (Aldh1l1), a metabolic enzyme responsible for the folate metabolism, was identified as a highly specific antigenic marker for astrocytes that strongly labels a wider population of astrocytes than GFAP (Cahoy et al., 2008).

2.1.3. Astrocyte purification strategies

For many years, progress in understanding astrocyte biology has been hindered by the lack of techniques to study the functions of these cells *in vitro* and *ex vivo*. Since the development of an astrocyte culture preparation from rodent neonatal brains (McCarthy and de Vellis, 1980) nearly all studies of astrocyte function have exploited this system. However, gene profiling analyses have demonstrated that astrocytes cultured in the presence of serum express hundreds of genes not normally expressed *in vivo* making them a sort of combination of developing and reactive astrocytes (Cahoy et al., 2008; Foo et al., 2011). Thus, classical *in vitro* systems are not suitable for addressing the pathogenic functions of astrocytes in disease conditions. The limitations of flow cytometry for accurate isolation and purification of astrocytes has further hampered the advance in the study of astrocyte function. Indeed, the majority of the mentioned astrocytic markers are intracellular proteins that cannot be readily used for direct isolation and subsequent characterization of living cells using this technique. To overcome these limitations, several transgenic mouse lines expressing a reporter gene under an astrocytic-specific promoter, such as GFAP, Aldh1l1, S100b, GLT-1 or GLAST have been generated (Nolte et al., 2001; Regan et al., 2007; Vives et al., 2003; Zhuo et al., 1997). These lines have been helpful for the isolation and identification of astrocytes subpopulations using cell-sorting techniques followed by gene expression analysis. However, the reporters did not always mimic the intrinsic expression pattern driven by the endogenous promoter and show off-target effects in non-astrocytic populations (Jungblut et al., 2012; Srinivasan et al., 2016).

The above mentioned drawbacks have prompted the search for an astrocytic-specific extracellular epitope targetable for direct antibody-mediated cell isolation. An ACSA-1 antibody that specifically detects an extracellular epitope of the astrocyte-specific glutamate transporter GLAST was developed and characterized for flow-cytometry purposes a decade ago (Jungblut et al., 2012). However, the GLAST epitope recognized by ACSA-1 shows sensitivity to papain, which is regarded as less damaging and more effective method for CNS tissue digestion, this feature limiting its utility for the isolation of living cells. Recently, an anti-ACSA-2 antibody was developed as the second available antibody that reacts with the extracellular domain of an astrocyte-specific cell surface antigen (Kantzer et al., 2017). This antibody recognizes the glycoprotein ATP1B2 (ATPase Na^+/K^+ transporting subunit beta 2) which was found to be stably expressed in a pattern similar to GLAST in the healthy brain and in multiple models of CNS disease and injury (Batiuk et al., 2017). ACSA-2 epitope is insensitive to papain digestion and this antibody was therefore proposed as an ideal tool for successful purification and following characterization of adult astrocytes. A potential limitation of ACSA-2 for FACS purposes however, is the concomitant isolation of oligodendrocyte-lineage cells (Kantzer et al., 2017; Schroeter et al., 2021).

2.1.4. Functions of astroglia in the central nervous system

Astrocytes are involved in a wide array of brain homeostatic functions including control of the BBB, clearance of K^+ and neurotransmitters, regulation of metabolism and modulation of synaptic transmission, among others (**Figure 5**) (Lundgaard et al., 2014). This multifunctional capacity of astrocytes is related to the fact that a single astrocyte can enwrap from 100 thousand to 2 million synapses in rodents and humans, respectively (Oberheim et al., 2009).

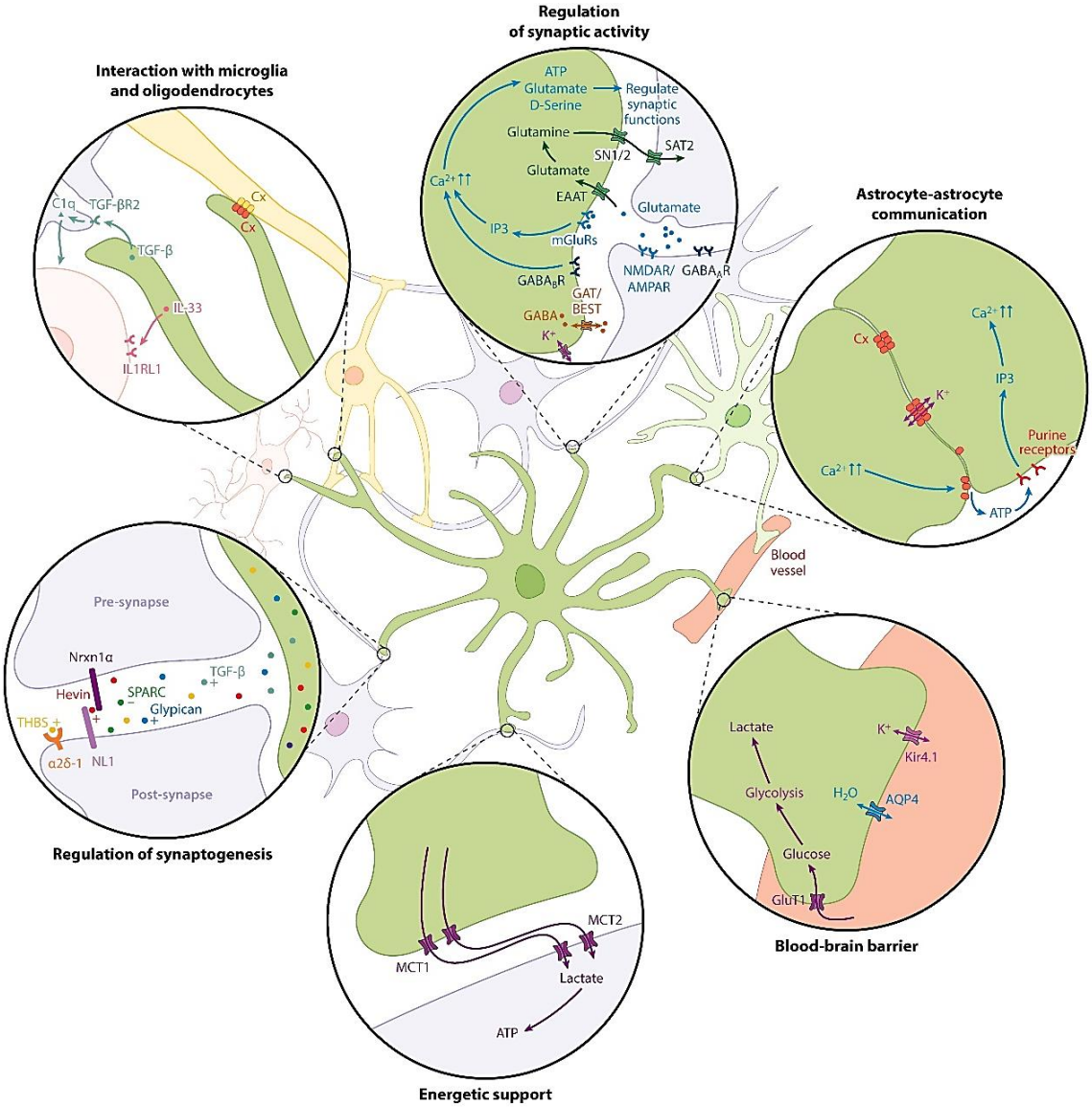

Figure 5. A schematic summary of the diverse roles performed by astrocytes in the brain. Abbreviations: AMPAR, α-amino-3-hydroxy-5-methyl-4-isoxazolepropionic acid receptor; BEST, bestrophin; Ca^{2+}, calcium ion; Cx, connexin; EAAT, excitatory amino acid transporter; GABA, γ-aminobutyric acid; GAT, GABA transporter; GluT1, glucose transporter 1; IL, interleukin; IP_3, inositol triphosphate; K^+, potassium ion; MCT1/2, monocarboxylate transporter 1/2; mGluRs, metabotropic glutamate receptors; NMDAR, *N*-methyl-d-aspartate receptor; Nrxn1α, Neurexin 1α; THBS, thrombospondin. From Khakh and Deneen, 2019.

The **BBB** is highly selective and protects the brain from toxic substances, ions and immune cells (Abbott et al., 2006). Astrocytic endfeet cover more than 90% of the cerebral vasculature and play a crucial role in BBB formation and maintenance (Jukkola et al., 2013). Astrocytes express tight junction proteins, such as occludins and claudins, whose reduction is associated to an increase in BBB permeability allowing influx of neurotoxic factors and immune cells that initiate multiple pathways of neurodegeneration (Castro Dias et al., 2019). Genetic deletion of gap junction/hemichannel proteins Cx30 and Cx43, enriched in the astrocytic endfeet, also weakens the BBB (Ezan et al., 2012). The relevance of astrocytes in the control of the BBB is further evidenced by studies associating astrocytic dysfunction to the infiltration of peripheral

immune cells in neurodegenerative conditions such as MS, AD, HD or ALS, among others (Sweeney et al., 2018).

Neuronal activity causes the local accumulation of K^+ in the extracellular space which produces hyperexcitability and can alter the generation and propagation of action potentials (Bellot-Saez et al., 2017). Maintaining ion homeostasis is thus crucial for proper nervous system function. Astrocytes are endowed with **K^+ channels** and coupled via gap junctions forming a syncytium, which enables these cells to tightly regulate extracellular K^+ concentrations (Ma et al., 2016). Impaired gap junction coupling results in insufficient extracellular K^+ clearance and has been associated to the generation of epileptic seizures (Steinhäuser et al., 2012). Defective extracellular K^+ clearance has also been postulated in a variety of neurodegenerative diseases such as ALS, AD and HD (Bellot-Saez et al., 2017).

Astrocytes are essential for **uptaking and catabolizing neurotransmitters**, including glutamate, GABA, adenosine and monoamines. Through the clearance of these compounds, astrocytes fine-tune the spatial and temporal dynamics of neurotransmitter signaling (Perea et al., 2009). Particular attention has been focused on the role of astrocytes in glutamate uptake given its crucial role as the main excitatory neurotransmitter in the CNS and its implications in the pathogenesis of several neurodegenerative diseases (Murphy-Royal et al., 2017). Around 80% of glutamate in the CNS is taken up through the activation of **EAAT1/GLAST** and **EAAT2/GLT-1**, predominantly expressed by astrocytes (Danbolt, 2001). The genetic removal of either transporter causes an increase in glutamate levels, leading to neuronal hyperexcitability and degeneration (Rothstein et al., 1996), or to spontaneous seizures and eventual cell death (Tanaka et al., 1997), thus highlighting the importance of astrocyte-mediated glutamate homeostasis in brain function. More recently, astrocytes have also been involved in the modulation of inhibitory transmission. Neuronal GABA transporter 1 (GAT1) is classically regarded as the most important transporter in the homeostasis of GABA levels (Zhou and Danbolt, 2013). However, recent evidence suggests that astrocytic GAT3 may be a key component in the regulation of GABA signaling (Boddum et al., 2016), and that astrocytes may play important modulatory roles at inhibitory synapses (Ishibashi et al., 2019). The regulated expression and activity of astrocyte neurotransmitter transporters is therefore, an important mechanism by which astrocytes shape synapse function.

The brain has high energy requirements accounting for at least 20% of the human body's energy consumption despite representing only 2% of the total body mass (Magistretti and Allaman, 2015). Most of the ATP consumed in the brain is dedicated to maintain and restore ion gradients faded upon the generation of action potentials, as well as to the uptake and recycling of neurotransmitters (Alle et al., 2009; Rangaraju et al., 2014). The long-established fuel for physiological brain metabolism is **glucose**, which is taken up by astrocytes from blood vessels by selective transporters, mainly GLUT1 (Mergenthaler et al., 2013). Consistent with their high energy requirements, neurons utilize glucose mainly by mitochondrial oxidative metabolism with high ATP production (Boumezbeur et al., 2010) whereas astrocytes present a highly glycolytic metabolic profile yielding relatively low amounts of ATP and producing important amount of lactate (Barros and Deitmer, 2010; Bittner et al., 2011). Lactate generated as a result of astrocyte metabolism is released to the extracellular medium through monocarboxlylate transporters (MCTs) and taken up by neurons for ATP production (Magistretti and Allaman, 2015). This is a crucial process of the **astrocyte-neuron lactate shuttle** model, which affirms that

neuronal activity relies on lactate released from astrocytes (Pellerin and Magistretti, 1994). These two different and complementary metabolic profiles suggest an important cooperation between both cell types, and a large body of evidence indicates that disturbances in these interactions contribute to neurodegenerative disorders (Bélanger et al., 2011). In addition, brain glycogen is located exclusively in astrocytes and used as substrate for lactate production that sustains neuronal activity in the absence of other energy substrates (Bak et al., 2018). Abnormal astrocyte glycogen metabolism has been associated to neurodegenerative diseases such as epilepsy and AD (Bak et al., 2018).

Neuronal energy metabolism relies mostly on oxidative phosphorylation and generates a high amount of ROS and NOS that need to be scavenged to avoid cellular toxicity. However, neurons have low levels of endogenous antioxidants and rely on astrocytes to neutralize toxic levels of oxygen species. An additional homeostatic function of astrocytes is thus the production and release into the microenvironment of antioxidant glutathione (GSH) and superoxide dismutase (SOD) in the maintenance of the CNS antioxidant system (Bélanger et al., 2011). Astrocytes also release neurotrophic factors such as glial cell line-derived neurotrophic factor (GDNF) and nerve growth factor (NGF), which support neuronal survival (Rocha et al., 2012). The active secretion of **antioxidants** and **neuroprotective factors** by astrocytes aids attenuating excitotoxicity and failure of these mechanisms has been involved in the pathogenesis of neurodegenerative diseases such as PD (Rizor et al., 2019).

2.1.5. Astrocytic Ca^{2+} signaling

Astrocytes are classically regarded as non-excitable cells, and indeed, they do not fire action potentials. However, the “non-excitable” definition is not accurate, since these cells present activity-dependent Ca^{2+} signals. Astrocytes respond to multiple extracellular stimuli, including neurotransmitters such as glutamate, γ-aminobutyric acid (GABA), ATP/adenosine, dopamine and acetylcholine, by rising cytosolic Ca^{2+} levels, this process representing the basis of ‘glial excitability’ (Khakh and McCarthy, 2015) (**Figure 6**). Fluctuations in astrocytic Ca^{2+} levels are present *in vivo* in response to different stimuli such as locomotion and startle (Shigetomi et al., 2016) and have been implicated in the regulation of complex mouse behaviors (Halassa and Haydon, 2010). Neurotransmitter mediated signaling also evokes Ca^{2+} increases in white matter astrocytes which allows coupling the homeostatic functions of these cells to axonal activity, thus ensuring rapid electrical conduction (Butt et al., 2014).

The hypothesis that **astrocytes contribute to neural circuit function** was first proposed almost 30 years ago based on the observation that these cells were able to respond to neuronal activity via increases in intracellular Ca^{2+} both *in vitro*, *ex vivo* and *in vivo* (Cornell-Bell et al., 1990; Newman and Zahs, 1997; Wang et al., 2006). An early finding was also that Ca^{2+} transients could propagate across networks of astrocytes by means of gap-junctions generating intercellular Ca^{2+} waves that allow astrocytes to process information in a coordinated way (Dani et al., 1992). These discoveries raised the possibility that astrocytic Ca^{2+} activity represents a novel-signaling pathway that allows bidirectional communication between neurons and glia for information processing (Attwell, 1994; Nedergaard, 1994). Since then, Ca^{2+} signals in astrocytes have been extensively investigated and found to be fundamental to intracellular signaling and intercellular communication (Araque et al., 2014). Recently, many laboratories have focused their studies on the characteristics and mechanisms of astrocytic Ca^{2+} activity as a way to

evaluate, identify, and define the roles of these cells within neural circuits (Bazargani and Attwell, 2016; Khakh and McCarthy, 2015).

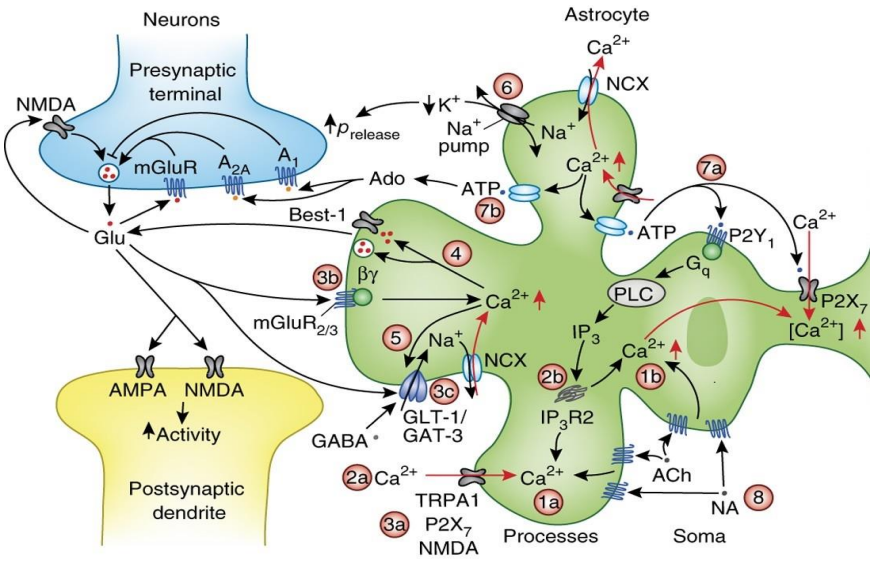

Figure 6. Ca^{2+} signaling in astrocytes. **1**. Cytosolic Ca^{2+} transients astrocyte processes (**1a**) differ from those in the soma (**1b**) in terms of frequency, kinetics and spatial spread. 2. Astrocytic Ca^{2+} transients in the processes depend roughly equally on extracellular Ca^{2+} entry (**2a**) through ion channels (40%) and on Ca^{2+} release from intracellular stores (60%), while those in the soma (**2b**) depend largely (90%) on intracellular Ca^{2+} release. **3**. Cytosolic Ca^{2+} transients can be generated by entry through spontaneously opening TRPA1 channels or neurotransmitter-gated channels (**3a**), by mGluR2 or mGluR3 (**3b**) and by neurotransmitter uptake raising intracellular Na^+ and reversing Na^+/Ca^{2+} exchange (**3c**). **4**. Astrocytic Ca^{2+} rises may release gliotransmitters via ion channels such as Best-1 as well as via exocytosis. **5**. Cytosolic Ca^{2+} rises alter the surface expression of neurotransmitter transporters in astrocytes. **6**. Activation of Na^+/Ca^{2+} exchange can raise intracellular Na^+ and activate the sodium pump thus lowering extracellular K^+ and hyperpolarizing nearby neurons. This increases the release probability ($p_{release}$) for action potential-driven vesicle release and thus decreases synaptic failure rate. **7**. ATP released by astrocytic Ca^{2+} rises may act on P_2X or P_2Y receptors to raise Ca^{2+} levels and propagate a Ca^{2+} wave along the cell (**7a**), or be converted to adenosine, which acts on presynaptic receptors to increase (A_2A) or decrease (A_1) transmitter release (**7b**). **8**. Noradrenaline (NA) and acetylcholine (ACh) released from locus coeruleus and nucleus basalis and neurons, respectively, produce large Ca^{2+} rises in astrocytes. Adapted from Bazargani and Attwell, 2016.

Astrocytic Ca^{2+} homeostasis is a tightly controlled process. Resting Ca^{2+} concentrations in the cytosol of astrocytes is in the range of 50-100 nM of free Ca^{2+} (Shigetomi et al., 2010; Zheng et al., 2015). Like neurons, astroglial cells display complex molecular machinery and mechanisms in order to (i) maintain low cytosolic Ca^{2+} levels, (ii) allow controlled elevations of intracellular Ca^{2+} and (iii) propagate Ca^{2+} signals intracellular and intercellularly (Lim et al., 2021). Thanks to this cellular Ca^{2+} toolkit, astrocytes display Ca^{2+} signals of different magnitude, temporal and spatial characteristics in an organized way leading to different cellular responses (Berridge, 2005). Ca^{2+} signals in astrocytes can occur spontaneously, in the absence of external signals, or induced by endogenous or exogenous stimuli (Bradley and Challiss, 2012; Guerra-Gomes et al., 2018). Cytosolic Ca^{2+} fluctuations are produced by promptly increases in the concentration of free Ca^{2+} ions by the opening of channels permeable to Ca^{2+} either in the surface cell membrane or in the membranes of intracellular organelles containing high Ca^{2+} concentrations, mainly the

ER and mitochondria (Blaustein, 1993; Volterra et al., 2014). The ER of most cell types presents two types of intracellular Ca^{2+} release channels: the ryanodine receptors (RyRs) and the inositol 1,4,5-trisphosphate receptors (IP_3Rs) (Go et al., 1995). The main mechanism of astrocytic Ca^{2+} signaling depends on the **phospholipase C** (**PLC**)**/IP_3 pathway**. Briefly, upon the activation of **$G_{q/11}$-protein-coupled receptors** (**GPCR**), PLC hydrolyzes the membrane lipid phosphatidylinositol 4,5-bisphosphate (PIP_2) to generate diacylglycerol (DAG) and IP_3, which leads to the release of Ca^{2+} from the ER upon activation of IP_3Rs. Cytosolic Ca^{2+} rises in astrocytes occur mainly through the activation of **type 2 IP_3Rs** (**IP_3R_2**) predominantly expressed by these cells (Bazargani and Attwell, 2016). Indeed, genetic deletion of IP_3R_2 prevents astrocytic Ca^{2+} responses in many experimental settings (Petravicz et al., 2008), although recent research supports the existence of Ca^{2+} responses in astrocyte processes that occur independently of IP_3R_2 (Okubo et al., 2019). On the other hand, RyRs control Ca^{2+} release from the ER in response to cyclic ADP ribose or Ca^{2+} itself. This mechanism seems to have a minor role in astrocytic Ca^{2+} signaling during physiological synaptic transmission but has been pointed out as relevant to astrocyte motility (Matyash et al., 2002).

Concerning extracellular signals mediating astroglial Ca^{2+} responses, these cells are endowed with a variety of **neurotransmitter receptors** and channels coupled to the modulation of cytosolic Ca^{2+} levels. In particular, astroglial cells are enriched with type I metabotropic glutamate receptors (mGluRs), which contains both $mGluR_1$ and $mGluR_5$ subtypes (Shelton and McCarthy, 1999), whose interaction with $G_{\alpha q/11}$ proteins stimulates phospholipase C activity and IP_3 formation causing Ca^{2+} release from the ER in astrocytes (D'Ascenzo et al., 2007; Fellin et al., 2004). Astrocytes also express type II and III mGluRs as well as metabotropic receptors coupled to intracellular Ca^{2+} signals in response to ATP, adenosine and endocannabinoids (Lim et al., 2021; Verkhratsky and Nedergaard, 2018). Astroglial cells are also equipped with Ca^{2+} channels such as α-amino-3-hydroxy-5-methyl-4-isoxazolepropionic acid (AMPA) and N-methyl-D-aspartate (NMDA) glutamate receptors as well as P_2X purinoreceptors allowing Ca^{2+} entry from the extracellular space (Lalo et al., 2011). Some members of the tyrosine kinase receptor family have also been related with the integration and processing of neuronal inputs by astrocytes. For instance, ErbB receptors may regulate the release of gliotransmitters and GDNF, as well as the glutamate-glutamine metabolism (Sharif and Prevot, 2010).

In astrocytes, changes in cytosolic Ca^{2+} related to **mitochondrial buffering** have been linked to glutamate release (Reyes and Parpura, 2008). Recently, mitochondrial Ca^{2+} release via the mPTP during brief openings has been suggested to contribute to spontaneous and evoked Ca^{2+} signals in astrocytic processes *in vivo* even in the absence of IP_3-dependent release from ER (Agarwal et al., 2017). Notably, mitochondrial function in astrocytes has aroused special attention during the last years as proposed to be specifically involved in deregulation of synaptic transmission (Jackson and Robinson, 2018). Finally, it is also well established that mitochondria-endoplasmic reticulum contacts (MERCs) are key players of Ca^{2+} signaling in both neurons and astrocytes (Göbel et al., 2020; Rosario et al., 1993). MERCs are postulated to behave as signaling hubs and to act as critical players in different neurodegenerative diseases (Wilson and Metzakopian, 2021).

2.1.6. Astrocyte modulation of synaptic transmission: the tripartite synapse

Work published over the last two decades has highlighted the roles of astrocytes in the modulation of synaptic transmission and neuronal function giving rise to the concept of **tripartite synapse**, where astrocyte-neuron interactions are combined to shape information processing in the CNS (Araque et al., 1999). Astrocytes have emerged as key players in the regulation of synaptic physiology due to findings that demonstrate that these cells are able to integrate and process synaptic information, subsequently modulating synaptic transmission, plasticity and behavior (Perea et al., 2009).

Astrocytes respond with cytosolic Ca^{2+} elevations to a wide variety of neurotransmitters released by neurons and subsequently release a plethora of neuroactive molecules, called **gliotransmitters**, that comprise glutamate, ATP, D-serine and GABA (Araque et al., 2014; Savtchouk and Volterra, 2018) (**Figure 6**). These gliotransmitters feedback to neuronal receptors located on pre- and post-synaptic terminals and cause new responses in adjacent neurons, fine-tuning synaptic transmission (Hamilton et al., 2010; Navarrete et al., 2013). In addition to gliotransmitters, astrocytes release several neuroactive molecules such as tumor necrosis factor α (TNFα), prostaglandins, proteins and peptides, that further shape synaptic physiology and neuronal activity (Volterra et al., 2002).

Concerning the mechanisms for astrocyte gliotransmitters release, Ca^{2+} dependent vesicle fusion (Bezzi et al., 2004; Montana et al., 2006) and lysosome exocytosis (Li et al., 2008; Zhang et al., 2007) have been proposed. These mechanisms are further supported by the detection of vesicles in astrocytic processes close to the synapse cleft by electron microscopy (Jourdain et al., 2007). More recently, ultrastructural studies using immunogold electron microscopy revealed that these small synaptic-like vesicles contain glutamate and, separately, D-serine (Bergersen et al., 2012). Other alternative mechanisms include the release of glutamate or ATP through permeable channels such as pannexin and connexin hemichannels (Kang et al., 2008; Ye et al., 2003), the reversal of glutamate uptake (Szatkowski et al., 1990) and the activation of pore-forming P_2X_7 receptors (Duan et al., 2003).

2.2. Reactive astrocytes in neurodegenerative diseases

The concept that elevations of astrocytic Ca^{2+} provokes the release of gliotransmitters able to regulate neuronal function has been a matter of intense debate (Hamilton and Attwell, 2010). Discoveries supporting gliotransmission have been questioned for decades due to the high variability observed in the results obtained by several laboratories, associated to the lack of methods allowing specific manipulation of astrocytes (Bazargani and Attwell, 2016). Initial studies were performed on astrocytes cultured from rodent neonatal brains, raising the question of whether physiological gliotransmitter release actually occurs *in vivo* (Cahoy et al., 2008). Unfortunately, astrocytes cultured in alternative culture conditions in order to preserve a physiological non-reactive phenotype failed to release glutamate upon stimulation (Foo et al., 2011), further fueling discussion in the field. In addition, the use of bulk loading membrane-permeable organic dyes such as Fura-2 or Fluo-4 allowed the detection of Ca^{2+} elevations within astrocyte somata but failed to efficiently track them in the fine processes and complicated the comprehensive interpretation of astrocytic Ca^{2+} dynamics (Nizar et al., 2013; Takata and Hirase, 2008; Wang et al., 2006). Some of these controversies have been recently resolved thanks to technical advances in the field, including the development of genetically encoded Ca^{2+} indicators (GECIs) that allow the cellular expression of a fluorescent protein that binds to Ca^{2+} (Shigetomi

et al., 2010). GECIs expression is able to detect events from the very thinner branches of the astrocyte enabling the recognition of different types of Ca^{2+} signals through the complex morphology of an astrocyte: somatic events, proximal processes events and distal processes or territories events (Volterra et al., 2014). During the last years, numerous novel techniques have been developed allowing a more detailed and specialized study of astrocyte Ca^{2+} dynamics such as three-dimensional Ca^{2+} imaging, transgenic mice expressing ultrasensitive Ca^{2+} indicators (Kanemaru et al., 2014; Srinivasan et al., 2016), and *in vivo* fiber photometry (Kim et al., 2016). This last technique represents an excellent method to study the functions of astrocytes both in physiological and pathological conditions as it allows deep-tissue measurements in freely behaving animals, thus avoiding interferences in Ca^{2+} dynamics due to anesthesia and restrain-associated stress (Qin et al., 2020).

2.2.1. Definition, classification and mechanisms of reactive astrogliosis

Astrocytes undergo a pronounced transformation during CNS pathology, called **reactive astrogliosis**, whereby they upregulate many genes involved in tissue damage and repair in a context-specific manner (Liddelow et al., 2017; Zamanian et al., 2012) and undergo morphological and functional changes (**Figure 7**). This process is regarded as a pathological hallmark of CNS structural lesions (Pekny et al., 2016; Sofroniew and Vinters, 2010). The nomenclature of astrocytes in disease conditions was recently revisited and reactive astrogliosis described as the process whereby, in response to pathology, *astrocytes display molecularly defined programs involving changes in transcriptional regulation, as well as biochemical, morphological, metabolic, and physiological remodeling, which ultimately result in gain of new function(s), loss or upregulation of homeostatic roles* (Escartin et al., 2021).

Among the insults that lead to reactive astrogliosis we find (i) the release of pro-inflammatory cytokines in response to CNS injury, (ii) damage-associated molecular patterns (DAMPs), (iii) pathogen-associated molecular patterns (PAMPs) produced by microbial infection and, (iv) oxidative or chemical stress. Depending on the severity of the injury, reactive astrogliosis can result in the formation of the **glial scar** around the core of the damaged tissue. The glial scar isolates the inflamed area, restricts the widespread of the damage, and provides structural support to the CNS parenchyma (Brosnan and Raine, 2013; Sofroniew and Vinters, 2010), but also has some undesirable effects because it hinders axonal regeneration, neurite outgrowth and remyelination (Bannerman et al., 2007; Rolls et al., 2009). GFAP upregulation - both at the mRNA and protein levels- is the most widely used marker of reactive astrocytes, but the functional contribution of GFAP in the activation process is still not well defined. In addition to GFAP, expression of other astrocytic markers is also upregulated in reactive astrocytes, including Aldh1l1, GS and S100β (Khakh and Sofroniew, 2015; Yang et al., 2011).

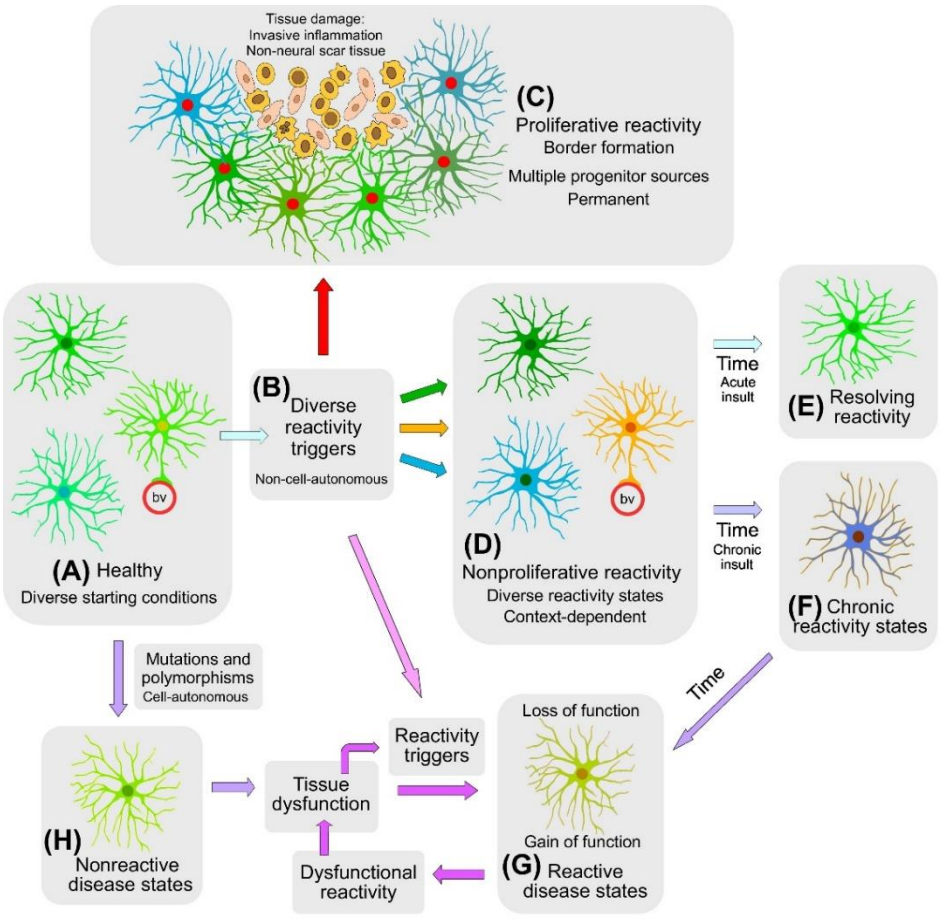

Figure 7. Diverse astrocyte responses to CNS disorders. (**A**) In healthy tissue, astrocytes exhibit regional and local heterogeneity in gene expression and function. (**B**) Different forms of astrocyte reactivity are triggered by diverse non-cell-autonomous signals emanating from diverse CNS insults. (**C**) Proliferative astrocyte reactivity occurs in response to tissue damage caused, for example, by traumatic or ischemic cell degeneration, BBB leakage, infection, or autoimmune leukocytic inflammation. Newly proliferated astrocytes (red nuclei) form borders that permanently separate areas of damage, inflammation, and non-neural scar tissue from adjacent viable neural tissue. (**D**) Nonproliferative astrocyte reactivity can exhibit diverse states with different gene expression patterns and functions that are context-dependent, as determined by astrocyte starting conditions and incoming reactivity triggers. Nonproliferative reactive astrocytes maintain but modify their interactions with surrounding cells in preserved tissue architecture. Astrocyte reactivity can resolve over time if acute triggers recede (**E**) or become chronic if triggers persist (**F**). (**G**) Chronic astrocyte reactivity can lead to loss or gain of function resulting in disease states with dysfunctional reactivity that can exacerbate tissue pathologies and worsen disorder outcome. (**H**) Genetic mutations and polymorphisms can lead to cell-autonomous dysfunctions in astrocytes that promote nonreactive disease states. Such disease states can, in the absence of astrocyte reactivity, cause or contribute to tissue dysfunctions that in turn lead to the production of astrocyte reactivity triggers. The ensuing dysfunctional astrocyte reactivity exhibits gain or loss of function that can contribute to further tissue pathology in a vicious cycle. From Sofroniew, 2020.

The functions of reactive astrocytes in the diseased brain remain a subject of debate, but there is consensus that these cells play fundamental roles in the pathogenesis of neurodegenerative, inflammatory disorders, including MS (Aharoni et al., 2021; Burda and Sofroniew, 2014). Numerous studies have found reactive astrocytes play a dual role in neurological disorders being involved both in detrimental and beneficial processes regardless

the presence of a glial scar (Heppner et al., 2015; Liddelow and Sofroniew, 2019). For example, reactive astrocytes can promote BBB leakage and stimulate the development and maintenance of autoimmune inflammation (Sofroniew, 2015; Sweeney et al., 2018) and chronic pain by releasing pro-inflammatory signaling molecules (Gao and Ji, 2010; Ji et al., 2019). Conversely, reactive astroglia can also facilitate the reparation of the damaged BBB, limiting the infiltration of peripheral leukocytes (Bush et al., 1999; Hara et al., 2017).

Microglia are crucial for regulating astrocyte phenotype in CNS injury. Classically activated microglial cells produce plenty of pro-inflammatory molecules that promote leukocyte recruitment and cytotoxicity to oligodendrocytes and neurons. Recently, resident microglia and infiltrating immune cells have been implicated in shifting physiological astrocytes to pathological astrocytes (Liddelow et al., 2017; Zamanian et al., 2012). In particular, it is generally accepted that microglial cells respond first to many injury signals, in particular to DAMPs and PAMPs, promoting subsequent astrocyte activation through cytokine release (Burda and Sofroniew, 2014). Supporting this mechanism, astrocytes from $Csf1r^{-/-}$ mice, that lack microglia, failed to produce reactive astrocytes *in vivo* in response to lipopolysaccharide (LPS) injection, showing that microglial cells are required to induce astrocytic reactivity (Liddelow et al., 2017). In turn, astrocytes can both respond to and elaborate a wide variety of cytokines, chemokines, growth factors, and other molecules, interacting directly with microglia an additional cells types, such as perivascular cells and blood-borne leukocytes, thus establishing a quite complex intercellular communication (**Figure 8**) (Burda and Sofroniew, 2014; Sofroniew, 2015). Consistently, local innate immune responses driven by microglia-astrocyte crosstalk are thus crucially involved in many neurodegenerative diseases, including MS onset and progression (Mayo et al., 2012, 2014; Rothhammer et al., 2018).

Concerning the modulation of reactive astrogliosis by microglial cells, recent landmark studies propose a mechanism by which microglial release the inflammatory molecules interleukin-1_α (IL-1α), TNFα and complement component 1q (C1q) to induce a neurotoxic population of reactive astrocytes termed A1 (Liddelow et al., 2017). This subset of reactive astrocytes is characterized by the upregulation of complement component 3 (C3) and has been identified in numerous neurodegenerative diseases, including MS (Yun et al., 2018). **Neurotoxic A1 astrocytes** display genomic changes, lose physiological astrocytic functions and release factors that harm neurons and oligodendrocytes (**Table 1**). Astrocyte-mediated toxicity in response to IL-1α, TNFα and C1q seems to be driven through the delivery of saturated lipids contained in APOE and APOJ lipoparticles (Guttenplan et al., 2021). Additional pathogenic features of A1 astrocytes include the formation of fewer and weaker synapses associated to a deregulated expression of certain glypicans and thrombospondin, as well as deficiencies in phagocytosis of myelin debris with potential remyelination-impairing effects (Liddelow and Barres, 2017). Remarkably, these A1 astrocyte-specific responses induce long-term synaptic inhibition and cognitive deficiencies *in vivo* (Li et al., 2020). Finally, the observation that neurotoxic astrocytes are present in most neurodegenerative diseases raises the possibility that may this subset of reactive astroglia plays a relevant role in the pathogenesis of neurological disorders (Liddelow and Barres, 2017; Tassoni et al., 2019; Yun et al., 2018).

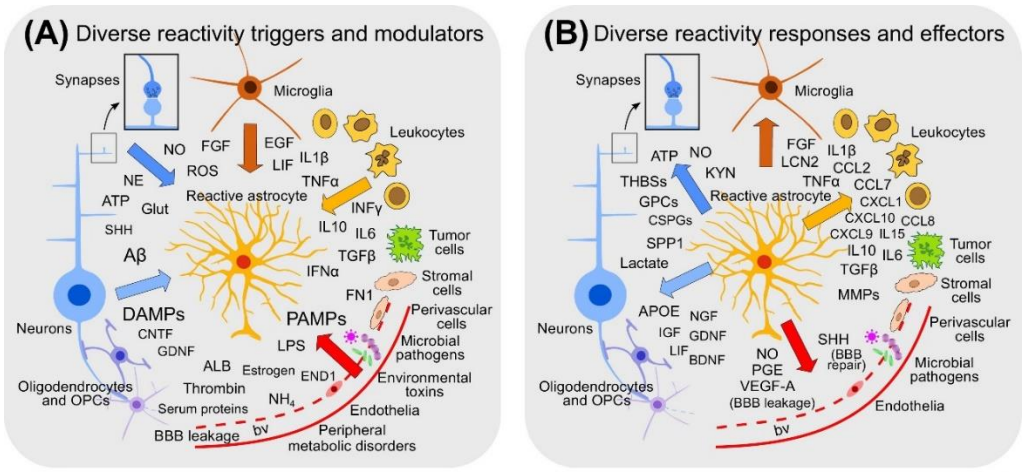

Figure 8. Mammalian astrocytes respond to diverse reactivity-inducing triggers and produce diverse molecular effectors. (**A**) Astrocyte reactivity can be triggered by a wide variety of molecules from diverse sources, including any cell type in CNS tissue, as well as from microbial pathogens, circulating inflammatory cells, serum proteins, peripheral metabolic disorders, or environmental toxins. (**B**) Reactive astrocytes can exhibit diverse functional responses to these triggers and can elaborate a wide variety of effector molecules that can influence many different cell types in a context-specific manner. Abbreviations: Aβ, amyloid β; ALB, albumin; APOE, apolipoprotein E; BBB, blood–brain barrier; bv, blood vessel; BDNF, brain-derived neurotrophic factor; CNS, central nervous system; CNTF, ciliary neurotrophic factor; CSPGs, chondroitin sulfate proteoglycans; CCL/CXCL, chemokines; DAMP, damage- or danger-associated molecular pattern; EGF, epidermal growth factor; FGF, fibroblast growth factor; GDNF, glial cell-derived neurotrophic factor; Glut, glutamate; GPCs, glypicans; KYN, kynurenine; IFN, interferon; IGF, insulin-like growth factor; IL, interleukin; Lcn2, lipocalin 2; LIF, leukemia inhibitory factor; LPS, lipopolysaccharide; MMP, matrix metallopeptidase; NE, norepinephrine; NGF, nerve growth factor; NO, nitric oxide; OPC, oligodendrocyte progenitor cell; PAMP, pathogen-associated molecular pattern; PGE, prostaglandin E; ROS reactive oxygen species; SHH, sonic hedgehog; SPP1, secreted phosphoprotein 1; TGF, transforming growth factor; THBSs, thrombospondins; TNFα, tumor necrosis factor α; VEGF, vascular endothelial growth factor. From Sofroniew, 2020.

The characterization of neurotoxic astrocytes was paralleled by the definition of a neuroprotective population of reactive astrocytes, termed A2, which is induced after ischemic stroke. A2 astrocytes secrete neuroprotective molecules that promote CNS recovery and repair, such as brain-derived neurotrophic factor (BDNF) and nerve growth factor (NGF) (Cheng et al., 2020; Fulmer et al., 2014). The gene profiles of **A2 astrocytes** also showed upregulated expression of genes encoding anti-inflammatory cytokines such as interleukin-6 (IL-6), interleukin-10 (IL-10) and leukemia inhibitory factor (LIF), as well as glypicans and thrombospondins, which may help promote neuronal survival and synapses remodeling (Christopherson et al., 2005; Eroglu, 2009) (**Table 1**). Interestingly, A2 astrocytes transfer functional mitochondria to injured neurons and this mechanism might contribute CNS recovery after stroke (Hayakawa et al., 2016). A2 astrocytes also show increased GLAST expression and glutamate uptake *in vitro*, which suggests that this subtype of astrocytes may potentially protect neurons from excitotoxicity (Neal et al., 2018). However, despite significant progress has been made in recent years regarding the pathogenic effects of neurotoxic A1 astrocytes, the implications of A2 astrocytes on CNS function remain largely unexplored (Fan and Huo, 2021).

Table 1. Molecular changes in reactive A1 and A2 astrocytes. Adapted from Li et al., 2019.

Molecular expression	Molecular changes	References
A1 astrocytes		
Up-regulation	Inflammatory signaling through NFκβ	(Brambilla et al., 2005; Lian et al., 2015)
	Glutamate and ATP release	(Orellana et al., 2011b, 2011a)
	Prostaglandin D2, IFN-γ and TGF-β	(Aebischer et al., 2011; Phatnani et al., 2013)
	Lcn2	(Bi et al., 2013)
	C3, IL-1α, C1q, TNFα	(Liddelow et al., 2017)
	THBS1 and THBS2	(Liddelow et al., 2017)
Down-regulation	*Gpc4, Gpc6, Sparcl1* expression	(Allen et al., 2012; Kucukdereli et al., 2011)
	EAAT2/GLT-1	(Behrens et al., 2002; Howland et al., 2002)
	Trophic factor release	(Chou et al., 2008; Liddelow and Barres, 2017)
	Lactate transport	(Ferraiuolo et al., 2011)
	GABA release through GAT-3	(Wójtowicz et al., 2013)
A2 astrocytes		
Up-regulation	Inflammatory signaling through STAT3	(Herrmann et al., 2008; Okada et al., 2006)
	THBS1, THBS2, IL-6, IL-10	(Eroglu, 2009; Zamanian et al., 2012)
	AQP-4	(Zador et al., 2009)
	HMGB1 and β-2 integrin	(Hayakawa et al., 2014)
	BDNF, NGF, VEGF	(Arregui et al., 2011; Liddelow and Barres, 2017)
	EAAT1/GLAST	(Neal et al., 2018)
Down-regulation	*H2-D1, Gbp2, Fkbp5, Srgn*	(Liddelow et al., 2017)

Abbreviations: AQP-4, aquaporin-4; ATP, adenosine triphosphate; BDNF, brain-derived neurotrophic factor; C1q, complement 1q; C3, complement 3; EAAT1, excitatory amino acid transporter 1; EAAT2, excitatory amino acid transporter 2; Fkbp5, FKBP prolyl isomerase 5; GABA, gamma-aminobutyric acid; GAT-3, GABA transporter-3; Gbp2, guanylate binding protein 2; GLAST, glutamate aspartate transporter 1; GLT-1, glutamate transporter-1; Gpc4, glypican 4; Gpc6, glypican 6; H2-D1, histocompatibility 2-D region locus 1; HMGB1, high-mobility group box 1; IFN-γ, interferon-γ; IL-1α, interleukin-1α; IL-6, interleukin-6; IL-10, interleukin-10; Lcn2, lipocalin 2; NFκβ, nuclear factor-κβ; NGF, nerve growth factor; Sparcl1, SPARC-like protein 1; Srgn, serglycin; STAT3, signal transducer and activator of transcription 3; TGF-β, transforming growth factor-β; THBS1, thrombospondin 1; THBS2, thrombospondin 2; TNFα, tumor necrosis factor α; VEGF, vascular endothelial growth factor.

2.2.2. Deregulated Ca^{2+} signaling in reactive astrocytes

Reactive astrocytes displaying deregulated Ca^{2+} signaling have been found in a number of neurological disorders such as AD, ALS, Alexander's disease and Down syndrome, among others. Although this is still an emerging field, astrocyte Ca^{2+} dynamics seem to vary differently depending on the specific neuropathological situation, phase (acute or chronic) and anatomical brain region. In most cases, Ca^{2+} signals increase in terms of amplitude, duration and frequency in reactive astrocytes, but reduced astrocytic Ca^{2+} transients have also been reported in brain pathophysiology (Shigetomi et al., 2019). The emerging landscape is that there are many mechanisms underlying aberrant Ca^{2+} signals in reactive astrocytes. One main mechanism is the astrocytic Ca^{2+} release via IP_3R_2, whose disruption is a cause of neuropathological disorders in the brain (Okubo et al., 2019). Given the fundamental roles of Ca^{2+} signals in astrocyte biology, deregulation of intracellular Ca^{2+} levels and dynamics in reactive astrocytes might become a good indicator of disease state and disease severity.

2.2.3. Role of reactive astrocytes in MS

Astrocytes are involved in all stages of the formation and development of demyelinating lesions. Reactive astrocytes produce MMPs that alter BBB permeability and facilitate immune cell infiltration to the CNS parenchyma, thus promoting disease progression (Ponath et al., 2018). BBB dysfunction in MS it is also related to the release of factors such as IL-1β, TNFα, glutamate and nitric oxide (NO) by reactive astrocytes that downregulate tight junction proteins, promoting the apoptosis of endothelial cells (Aharoni et al., 2021). Activated astrocytes further drive chronic inflammation in MS through the release of chemokines that attract both peripheral immune cells and resident microglia to lesion sites (Mayo et al., 2012). Also in terms of secreted factors, astrocytes have been described both inhibiting and enhancing roles in relation to myelin repair by modulating OPC recruitment, proliferation and maturation (Lundgaard et al., 2014). In particular, reactive astrocytes close to the border of demyelinating lesions secrete compounds such as chondroitin sulfate proteoglycans and fibronectin that inhibit OPC recruitment and differentiation thus hindering remyelination process (Stoffels et al., 2013). In addition, reactive astrocytes produce fewer cholesterols, which are required for myelin production, thereby inhibiting remyelination (Itoh et al., 2018). Furthermore, alterations in mitochondrial energy metabolism in reactive astrocytes would imply loss of coupling between astrocytic lactate and neuronal energetic needs, promoting neurodegeneration (Rahman and Suk, 2020). Supporting the crucial roles of astrocytes in MS, *in vivo* modulation of astrocyte signaling limits inflammation and attenuates neurological disability during autoimmune demyelination (Mayo et al., 2014; Rothhammer et al., 2016, 2018).

Although reactive astrocytes drive inflammatory and neurotoxic responses in MS lesions, they may also reduce inflammation, promote lesion repair, neuroprotection and remyelination by releasing neurotrophic factors and growth factors with tissue-protective and regenerative properties (Linnerbauer and Rothhammer, 2020). Increased astrocytic production of various such factors, such as BDNF and vascular endothelial growth factor (VEGF), has been demonstrated both in MS and EAE (Brambilla, 2019). Altogether, these observations point out to astrocytes as emergent therapeutic targets for MS.

3. The endocannabinoid system

The endocannabinoid system is an important neuromodulatory system implicated in a wide variety of physiological processes, including movement, memory and cognition, mood, pain, temperature regulation and appetite, among others. The endocannabinoid system is comprised of cannabinoid receptors, their endogenous ligands, termed **endocannabinoids**, and the enzymes for the biosynthesis and degradation of these compounds (**Figure 9**). Cannabinoid receptors are the main molecular targets of **Δ^9-Tetrahydrocannabinol** (**Δ^9-THC**), a phytocannabinoid compound known to mediate the psychoactive effects of the marijuana plant (*Cannabis sativa* L), which has been used for over 5000 years as a recreational and medicinal drug (Mechoulam, 1986).

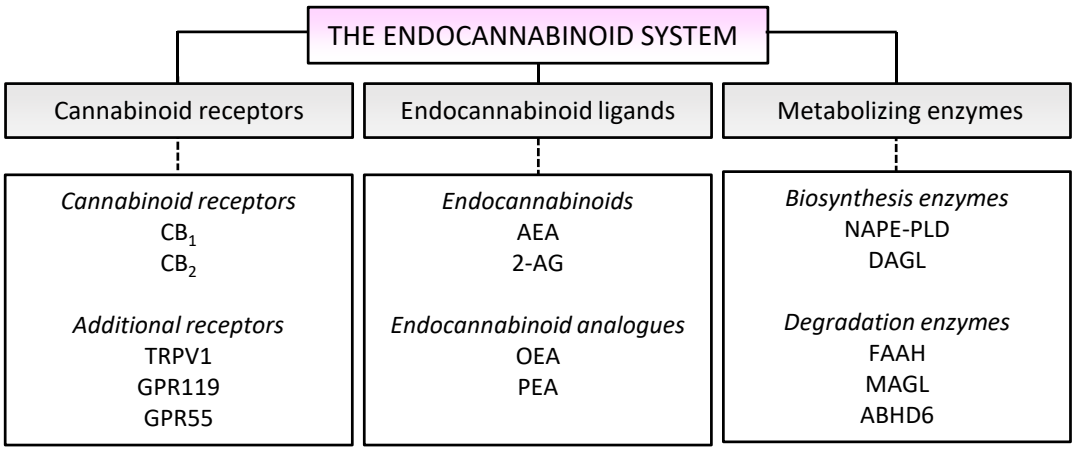

Figure 9. Over-view of molecular composition of endocannabinoid system. Adapted from André and Gonthier, 2010.

3.1. Brain cannabinoid receptors

The isolation of Δ^9-THC in 1964 (Gaoni and Mechoulam, 1964) from confiscated hashish led to the generation of a large amount of synthetic compounds with a similar structure to phytocannabinoids, which finally resulted in the identification of two types of cannabinoid receptors, termed **cannabinoid receptor 1** (**CB_1R**) and **cannabinoid receptor 2** (**CB_2R**) (Matsuda et al., 1990; Munro et al., 1993). The CB_1R is predominantly expressed in the brain whereas CB_2R is mainly localized in peripheral cells derived from immune system. Although each receptor is associated to specific signaling pathways, both share the ability to couple G_i proteins and thereby inhibit adenylate cyclase (Howlett, 2002). CB_1R is one of the most abundant G-protein coupled receptors (GPCRs) in the mammalian brain and mediates the psychoactive effects of cannabis (Herkenham et al., 1990). CB_1Rs are present across the brain at different structural, cellular and subcellular locations, with variable expression levels and functions (Busquets-Garcia et al., 2015). Brain areas with high CB_1R levels include the hippocampus, cerebral cortex, basal ganglia and cerebellum, where they play relevant neuromodulatory roles in brain physiology (Chevaleyre et al., 2006; Zou and Kumar, 2018).

Concerning the cellular distribution of CB_1Rs, these proteins are mainly localized in **mature neurons** within the CNS. In particular, CB_1Rs are expressed at highest levels in GABAergic neurons and in to a lower extent in glutamatergic cells of the forebrain (Gutiérrez-Rodríguez et

al., 2017; Kawamura et al., 2006; Marsicano and Lutz, 1999). The majority of neuronal CB_1Rs are accumulated **presynaptically on axons terminals** and are centrally involved in the maintenance of synapse homeostasis by negatively regulating neurotransmitter release through the inhibition of Ca^{2+} influx driving neurotransmitter exocytosis (**Figure 10**) (Katona and Freund, 2012). A number of anatomical and functional studies have reported the existence of CB_1Rs at postsynaptic sites where could participate in cell autonomous regulation processes (Marinelli et al., 2008; Maroso et al., 2016; Rodriguez et al., 2001). On the other hand, the presence of CB_1R levels in **glial cells** has also been convincingly demonstrated during the last decade. In particular, **astrocytes** express significant amounts of CB_1Rs as demonstrated by electron microscopy (Gutiérrez-Rodríguez et al., 2018; Han et al., 2012). Despite being expressed at low levels, astroglial CB_1Rs engage elevations of cytosolic Ca^{2+} and play a crucial role in neuron-astrocyte communication, memory and behavior (see below). A number of *in vitro* studies also support the localization of CB_1Rs in additional glial cells types, namely oligodendrocytes (Bernal-Chico et al., 2015; Gomez et al., 2010) and microglia (Stella, 2010). However, both the *in vivo* distribution and the physiological role of CB_1R populations in these subsets of glial cells remain poorly investigated *in vivo*.

Like many other GPCRs, CB_1Rs are primarily localized at the **plasma membrane**. Nevertheless, recent outstanding studies have demonstrated that this receptor is also present in different intracellular compartments such as **endosomes** (Leterrier et al., 2004) and **mitochondria** (Bénard et al., 2012). Mitochondria-associated CB_1Rs ($mtCB_1$Rs) have been found in neurons and astrocytes where they seem to be crucially implicated in the regulation of energy metabolism (Hebert-Chatelain et al., 2016; Jimenez-Blasco et al., 2020). On the other hand, astrocytic $mtCB_1$Rs have been recently found to modulate MERCs-dependent Ca^{2+} signaling in astrocytes (Serrat et al., 2021). In particular, activation of $mtCB_1$Rs favors Ca^{2+} transfer from ER to mitochondria thus shaping the dynamics of cytosolic Ca^{2+} events. This mechanism is proposed to facilitate lateral synaptic potentiation thus regulating complex information processing in the brain (Serrat et al., 2021).

Cannabinoid **CB_2Rs** are localized at highest levels in **peripheral immune cells** and tissues and regarded as the main substrate for cannabinoid immunomodulatory activity (Berdyshev, 2000; Howlett, 2002). Healthy CNS tissue contains only very low CB_2R expression levels and the presence of this protein in neurons remains controversial (Atwood and Mackie, 2010). Pharmacological studies in cultured cells also support a marginal expression of CB_2Rs in astrocytes and oligodendroglia (Gomez et al., 2011; Stella, 2010). Conversely, it is well established that CB_2Rs are localized in brain **microglia** during neuroinflammation and that their expression levels vary depending on the activation state of the cell (Mecha et al., 2016). Notably, microglial CB_2Rs regulate the migration and infiltration of these cells into brain areas during active neurodegeneration (Fernández-Ruiz et al., 2008; Navarro et al., 2016). Thus, CB_2R activation affects a myriad of innate and adaptive immune responses from inflammation to neuroprotection.

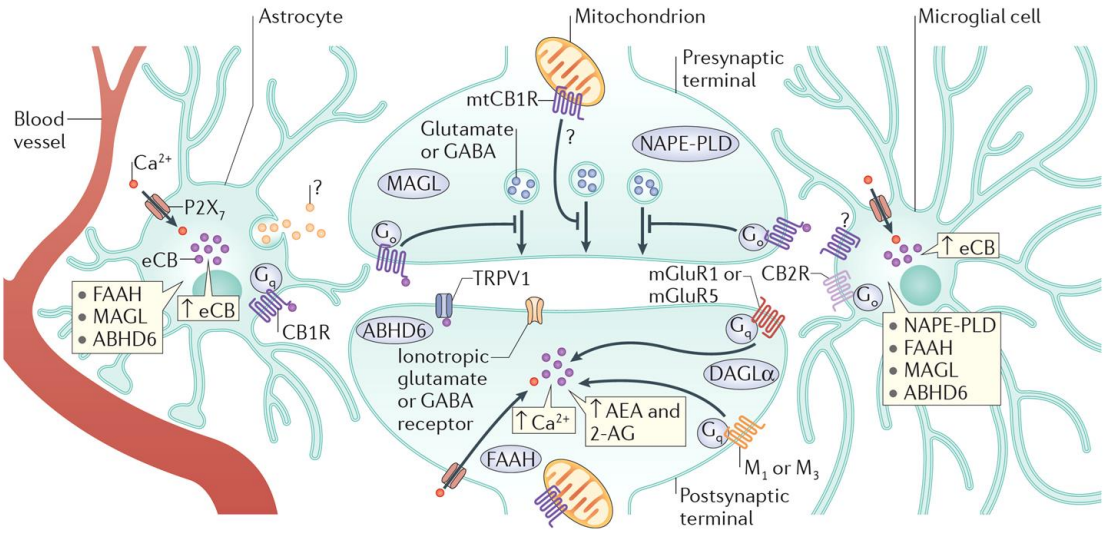

Figure 10. Architecture of neuronal and glial endocannabinoid system. Cannabinoid CB_1 receptors (CB_1Rs) are typically present at presynaptic terminal and coupled to $G_{i/o}$ proteins. Activation of neuronal CB_1R by 2-arachidonoylglycerol (2-AG) or *N*-arachidonoylethanolamine (AEA) triggers the suppression of neurotransmitter release. CB_1R are also expressed by mitochondria ($mtCB_1R$) at pre- and post-synaptic sites. Stimulation of $mtCB_1R$ leads to the inhibition of oxidative phosphorylation and ATP production in the mitochondria. AEA can also activate postsynaptic type-1 transient receptor potential vanilloid receptor channels (TRPV1), increasing the postsynaptic current while 2-AG can stimulate postsynaptic $GABA_A$ receptors. Postsynaptic depolarization following activation of several receptors, including group I metabotropic glutamate receptors ($mGluR_{1/5}$) and muscarinic M_1 and M_3 receptors, leads to on demand synthesis of 2-AG by the action of diacylglycerol lipase-α (DAGLα). Consecutively, 2-AG activates presynaptic CB_1R in a retrograde manner acting as a negative-feedback mechanism to suppress synaptic transmission. The major 2-AG degrading enzyme monoacylglycerol lipase (MAGL) is located at presynaptic terminals and in astrocytes. In contrast, α-β-hydrolase domain 6 (ABHD6) regulates 2-AG levels at the site of production. The major enzyme involved in AEA synthesis, N-acyl phosphatidyl ethanolamine-phospholipase D (NAPE-PLD), is predominantly located in the presynaptic terminal, although it may also be expressed postsynaptically. The enzyme responsible for AEA hydrolysis (FAAH) is present at the postsynaptic terminal. Microglial cells express CB_2 receptors, and possibly CB_1R, involved in the control of inflammatory reactions. Moreover, astrocytes show G_q-coupled CB_1R, that once stimulated lead to an increase in intracellular Ca^{2+} concentration with the subsequent release of 'gliotransmitters'. Endocannabinoid biosynthesis in microglia and astrocytes can be stimulated by ATP through the activation of $P2X_7$ purinoreceptors. From Lutz *et al*., 2015.

In addition to their activity at CB_1Rs and CB_2Rs, endocannabinoids can non-specifically activate many other receptors (Gorzkiewicz and Szemraj, 2018). In particular, type-1 transient receptor potential vanilloid (TRPV1) ion channels, non-selective cation channels such as TRPA1 or TRPM8 (Covelo et al., 2021; Gómez-Gonzalo et al., 2015).

3.2. Endocannabinoid production and metabolism

Endocannabinoids can be defined as a group of lipid messengers synthesized from cellular membrane components. Although several molecules have been identified, the lipids ***N*-arachidonoylethanolamine** (**anandamide, AEA**) (Devane et al., 1992) and **2-arachidonoylglycerol** (**2-AG**) (Sugiura et al., 1995) are the best-characterized endocannabinoids, both of which are **synthesized on demand** usually in response to elevations of intracellular Ca^{2+} (Pertwee et al., 2010). Although both AEA and 2-AG are able to bind and activate CB_1Rs and

CB_2Rs, these compounds play differential roles in the regulation of biological responses (Busquets-Garcia et al., 2011). In this regard, it is worth mentioning that 2-AG is a full agonist of cannabinoid receptors, whereas AEA usually behaves as partial agonist (Howlett, 2002). Notably, 2-AG levels in the CNS are around 200-800 times higher than those for AEA (Sugiura et al., 2002) and it is increasingly accepted that the former is the main ligand for presynaptic CB_1R mediated control of synaptic function (Katona and Freund, 2008).

The main pathways for the biosynthesis of the two major endocannabinoids 2-AG and AEA involve reactions catalyzed by **diacylglycerol lipase α/β isoforms** (**DAGLα/β**) and **N-acyl phosphatidyl ethanolamine-phospholipase D** (**NAPE-PLD**), respectively (Iannotti et al., 2016) (**Figure 11**). 2-AG is preferentially metabolized by the **serine hydrolases monoacylglycerol lipase** (**MAGL**), **α/β-hydrolase domain containing 6** (**ABHD6**) and **12** (**ABHD12**) (Blankman et al., 2007; Savinainen et al., 2012). Regarding AEA metabolism, **fatty acid amide hydrolase** (**FAAH**) is the principal AEA hydrolase in nervous tissue, although the physiological actions of this and other *N*-acylethanolamides can also be terminated by alternative lipid amidases, such as **N-acylethanolamine acid amidase** (**NAAA**) (Ahn et al., 2008). More recently, a number of **fatty acid binding proteins** (**FABPs**) have been identified as intracellular carriers that deliver endocannabinoids, mostly AEA, to their catabolic enzymes (Kaczocha et al., 2009). In addition to their canonical role in intracellular endocannabinoid transport, recent studies have reported that certain FABPs facilitate the extracellular delivery of 2-AG to the synaptic cleft thus modulating retrograde endocannabinoid signaling in certain brain areas (Haj-Dahmane et al., 2018). The synthesis and degradation of endocannabinoids are tightly regulated processes that determine the extent of cannabinoid receptor-mediated signaling. Indeed, pharmacological and/or genetic inactivation of the main 2-AG and AEA hydrolytic enzymes (MAGL and FAAH) and carrier proteins (FABPs) augments CNS endocannabinoid levels and engages cannabinoid receptor-dependent (and independent) effects *in vivo* (Ahn et al., 2008; Cravatt et al., 2001; Griebel et al., 2018; Kaczocha et al., 2015; Long et al., 2009).

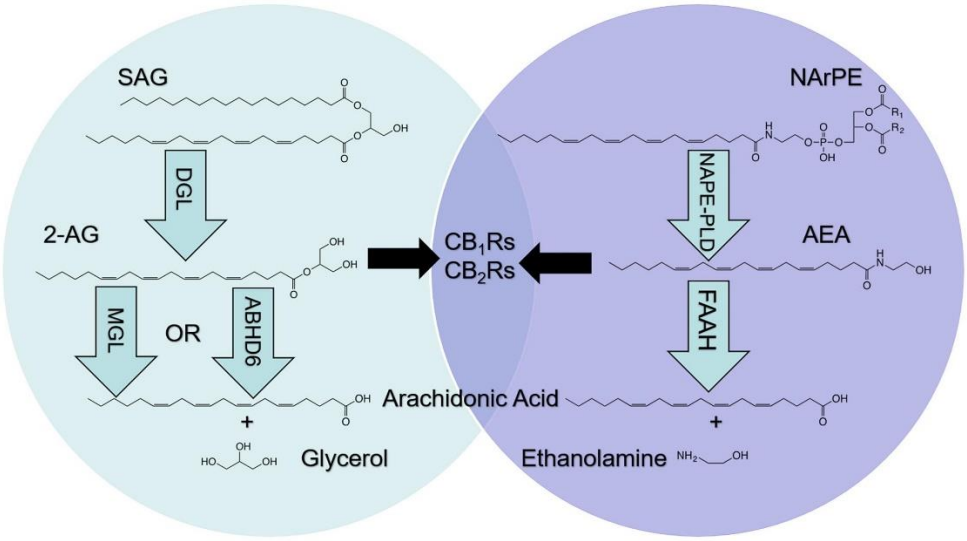

Figure 11. Metabolism of endocannabinoids. The endocannabinoids, 2-arachidonoylglycerol (2-AG) and arachidonoylethanolamide (AEA) activate cannabinoid receptor subtypes 1 (CB_1Rs) and 2 (CB_2Rs) located in cells throughout the body. However, metabolic pathways are not shared. 2-AG is produced following hydrolysis of the precursor, 1, stearoyl,2-arachidonoyl-sn-glycerol (SAG) by diacylglycerol lipase (DGL). 2-AG is degraded by monoacylglycerol lipase (MGL) and alpha/beta hydrolase domain-6 (ABHD6) into arachidonic acid (AA) and glycerol (*left*). AEA is produced following hydrolysis of the AEA precursor, *N*-arachidonoylphosphatidylethanolamide (NAPE) by N-acylphosphatidylethanolamide phospholipase D (NAPE-PLD) and degraded by fatty acid amide hydrolase (FAAH) into AA and ethanolamine (*right*). From Wiley et al., 2021.

3.3. CB_1 receptor signaling

Activation of CB_1Rs is associated to a variety of cellular responses that depend on the cellular type, ligand and ligand-receptor interaction (**Figure 12**). Agonist binding to the receptor can trigger signaling cascades via G protein-dependent and -independent pathways. Canonical CB_1R activation involves the activation of $G_{i/o}$ proteins and the subsequent exchange of GDP with GTP, which triggers the release of the α-subunit from the βγ dimer. Activation of the α_i subunit induces the inhibition adenylyl cyclase with a consequent reduction in cyclic adenosine monophosphate (cAMP) and decrease in protein kinase A (PKA) dependent signaling cascades, effects that are shared by CB_2R (Howlett, 2002). At the same time, released βγ dimers activate other signaling pathways including extracellular regulated kinases such as mitogen-activated protein kinases (MAPK) including ERK, c-Jun and p38 (Bouaboula et al., 1995; Galve-Roperh et al., 2002; Rueda et al., 2000). Additionally, CB_1Rs can also activate a number of different signal transduction pathways involved in cell survival and differentiation, such as the phosphatidylinositol 3-kinase cascade (PI3K/Akt) (Gómez del Pulgar et al., 2000) and the mammalian target of rapamycin (mTOR) pathway (Puighermanal et al., 2009). Non-canonical signaling of CB_1Rs involves the activation of alternative G proteins depending on the ligand or the cell type. Finally, several studies have demonstrated that CB_1Rs are able to form CB_1/CB_1 oligomers and CB_1 heterodimers with other GPCRs (Morales and Reggio, 2017) whose activation triggers complex pharmacological effects that cannot be solely attributed to CB_1R signaling.

Neuronal CB_1Rs are classically coupled to **$G_{\alpha i/o}$ proteins** and their activation leads to the inhibition of adenylyl cyclase and of voltage-gated Ca^{2+} channels (VGCCs) at the presynaptic site and the activation of inwardly rectifying K^+ channels (GIRK), leading to the inhibition of neurotransmitter release (Castillo et al., 2012; Howlett, 2002). CB_1R mediated modulation of transmitter release has been demonstrated for both glutamate and GABA and mediates short- and long-term forms of synaptic plasticity through the brain, which confers this protein an outstanding ability to fine-tune neurotransmission. Remarkably, the ability of CB_1Rs to limit excitatory transmission has been proposed as underlying mechanism of neuroprotection against excitotoxicity (Chiarlone et al., 2014; Monory et al., 2006).

Astrocyte CB_1Rs differ from their neuronal counterparts in that they are coupled to the activation of **$G_{\alpha q/11}$ proteins** and promote Ca^{2+} release through IP_3R_2 in the ER. Indeed, a number of studies addressing the impact of astrocyte-neuron communication on synaptic physiology show that astrocytic CB_1Rs respond to endocannabinoids produced during neuronal activity by inducing Ca^{2+} elevations (Araque et al., 2017). Astrocyte Ca^{2+} mobilization upon activation of CB_1Rs has been demonstrated by two photon imaging *ex vivo* in the rodent hippocampus (Gómez-Gonzalo et al., 2015; Navarrete and Araque, 2008, 2010), neocortex (Min and Nevian, 2012), dorsal striatum (Martín et al., 2015), in spinal cord (Hegyi et al., 2018), among other CNS regions, as well as in cortical and hippocampal human brain tissue (Navarrete et al., 2013). Although studies showing cytosolic Ca^{2+} responses associated to the activation of astrocytic CB_1Rs in living mice are still lacking, these observations suggest that the elevation of intracellular Ca^{2+} levels is a general and relevant mechanism of CB_1R signaling in the regulation of astrocyte function.

Beyond intracellular signaling mechanisms, the *in vivo* functional consequences of astroglial CB_1R activation are only beginning to be deciphered. The generation of conditional mutant mice bearing a specific deletion of the *Cnr1* gene in astrocytes has allowed to delineate specific roles of this receptor population in the control of behavioral performance and, in particular, of memory processes (Han et al., 2012). Using conductual and *in vivo* electrophysiological approaches, Han and collaborators (2012) demonstrated that astroglial CB_1R mediate the disrupting effects of acute exogenous cannabinoids on working memory. This crucial observation not only reveals the importance of CB_1Rs in astrocytic regulation of neuronal activity, but also points to the specific involvement of astroglial CB_1R in the effects of cannabis based medicines in humans. A recent study performed in the suprachiasmatic nucleus showed that astrocytic CB_1Rs regulate the molecular circadian clock suggesting that endocannabinoid signaling through astrocytes fine-tune circadian rhythms (Hablitz et al., 2020).

Neuronal and astroglial $mtCB_1Rs$ activate $G_{\alpha i}$ proteins leading to the inhibition of mitochondrial soluble adenylyl cyclase and PKA-dependent phosphorylation of specific mitochondrial electron transport system subunits. In neurons, $mtCB_1Rs$ are coupled to the inhibition of complex I subunit NDUFS2 which leads to reduced respiration and has been implicated in the amnesic effects of cannabinoids (Hebert-Chatelain et al., 2016). Conversely, activation of $mtCB_1R$ in astrocytes inhibits complex I NDUFS4 and inhibits glycolytic lactate production resulting in altered social behavior (Jimenez-Blasco et al., 2020).

Despite the complexity of the underlying mechanisms, the current scenario is that modulation of synaptic transmission through the activation of CB_1Rs underlie most of the

biological actions of endogenous and exogenous cannabinoids in the CNS. In addition to regulating **memory and learning** (Han et al., 2012; Marsicano and Lafenêtre, 2009), CB_1Rs participate in **nociception** (Woodhams et al., 2017), **motor behavior** (Fernández-Ruiz, 2009), **anxiety** and **stress responses** (Lutz et al., 2015), **appetite** and **feeding behavior** (Lau et al., 2017), among other physiological processes. As such, deregulation of CB_1R signaling has been implicated in a variety of a CNS disease conditions (Fernández-Ruiz et al., 2010; Kendall and Yudowski, 2017). The capability of endocannabinoids to normalize glutamate homeostasis, reduce **excitotoxicity** and decrease **oxidative injury** and **inflammation** has prompted active research on the utility of the endocannabinoid system as a source of novel therapeutic targets in neurodegenerative diseases.

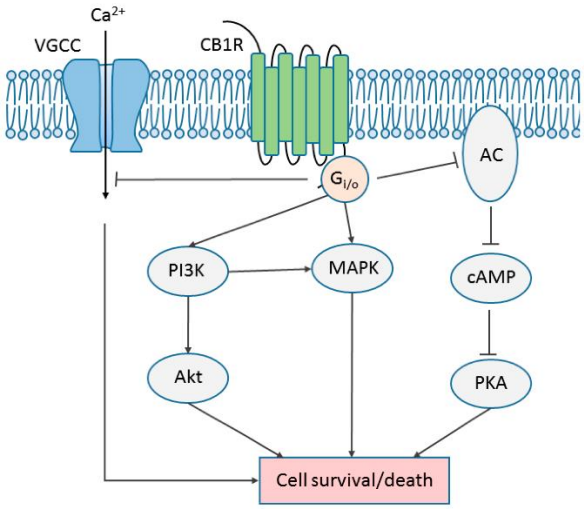

Figure 12. Major signaling pathways modulated by CB_1Rs. The CB_1R is canonically coupled to $G_{i/o}$ proteins and inhibits the activity of adenylyl cyclase (AC) and protein kinase A (PKA) leading to the suppression of Ca^{2+} influx via voltage gated Ca^{2+} channel (VGCC). Under certain circumstances or in specific cell types (mainly astrocytes) CB_1Rs can switch its coupling of G protein from $G_{i/o}$ to G_s or G_q. Several mitogen-activated protein kinases (MAPKs), including ERK1/2, p38, and JNK, are also activated by the CB_1R. The phosphoinositide 3-kinase (PI3K)/protein kinase B (Akt) pathway is activated by CB_1Rs as well. Depending on the ligand and subcellular environment, the outcome of CB_1R-mediated signaling could be the promotion of cell survival or cell death. Arrows indicate stimulation; blunted arrows indicate inhibition. From Zou and Kumar, 2018.

3.4. The endocannabinoid system in MS

The involvement of the endocannabinoid system in MS control is supported by two main lines of evidence. On the one hand, a number of studies have reported dysregulated levels of endocannabinoids and endocannabinoid signaling elements in MS patients and animal models of the disease. Second, and most important, cannabinoid agonists and endocannabinoid hydrolysis or transport inhibitors exert beneficial effects in experimental models of MS that include neuroprotection and attenuated inflammatory responses mediated by adaptive and/or innate immune cells.

In terms of cannabinoid receptors, both decreased and unaltered CB_1R levels have been reported in the EAE model (Berrendero et al., 2001; Cabranes et al., 2006), while increased CB_2R

gene and protein expression is a consistent finding in rodent models of MS (Loría et al., 2008; Maresz et al., 2007; Palazuelos et al., 2008). Results concerning endocannabinoid levels are often controversial. MS is associated to increased concentrations of AEA as determined in brain tissue, cerebrospinal fluid and plasma from MS patients (Centonze et al., 2007; Eljaschewitsch et al., 2006; Jean-Gilles et al., 2009). From a mechanistic perspective, elevated concentrations of AEA have been related to upregulated NAPE-PLD and reduced FAAH expression or activities in EAE mice and MS patients (Baker et al., 2001; Centonze et al., 2007). Nevertheless, lower levels of AEA have also been reported in patients with MS (Di Filippo et al., 2008). Findings in animal models are equally conflicting, since reduced (Cabranes et al., 2005; Manterola et al., 2018a), increased (Baker et al., 2001; Centonze et al., 2007) and unaltered (Witting et al., 2006) concentrations of AEA have been reported. Concerning 2-AG, the majority of the studies report unaltered (Manterola et al., 2018a; Maresz et al., 2007) or increased 2-AG levels (Baker et al., 2001). In all, most of these studies support the hypothesis that deregulated endocannabinoid signaling may be disease-stage dependent and modulate MS initiation and progression, but do not establish the cell-type specificity of endocannabinoid activity dysregulation in MS. Astrocytes and microglia are endowed with cannabinoid receptors and endocannabinoid synthetic/metabolic machinery. However, the specific role of these cellular populations as targets and mediators of endocannabinoid signaling in MS remains to be fully characterized.

The **therapeutic potential** of cannabinoids in MS has been studied for many years based on early reports on the beneficial effects of cannabinoids in the control of relapse frequency, spasticity or tremor by self-medicating MS patients (Consroe, 1998). Consistently, exogenously administered cannabinoid agonists exert a variety of therapeutic benefits in MS animal models, which include **attenuated neurodegeneration**, **demyelination** and **inflammatory responses** as well as **remyelination promoting effects** (Arévalo-Martín et al., 2003; Cabranes et al., 2005; Maresz et al., 2007; Palazuelos et al., 2008). On mechanistic grounds, early studies in constitutive and conditional CB_1R mutant mice showed that the clinical benefits of cannabinoids in experimental mouse models of the disease rely mainly on the activation of CB_1Rs expressed in neurons (Maresz et al., 2007; Pryce et al., 2003). Specifically, the protective efficacy of neuronal CB_1Rs in MS has been attributed to the limitation of glutamate excitation, based on the observations that mice lacking CB_1R exhibit poor tolerance to excitotoxicity and develop more severe neuronal damage and clinical deficits following excitotoxic insults and EAE induction (Marsicano et al., 2003; Pryce et al., 2003). On the other hand, most of anti-inflammatory effects of cannabinoids in MS models are ascribed to CB_2Rs regulating microglial and peripheral immune cell function (Eljaschewitsch et al., 2006; Maresz et al., 2007; Palazuelos et al., 2008). A number of *in vitro* and *in vivo* studies also suggest that (endo)cannabinoids prevent oligodendrocyte death and promote differentiation of OPCs and remyelination in MS by acting though CB_1Rs and CB_2Rs expressed by these cells (Aguado et al., 2021; Bernal-Chico et al., 2015; Gomez et al., 2011)

Research on the therapeutic potential of cannabinoids in MS has successfully culminated in the commercialization of nabiximols (Sativex®), an oromucosal spray containing a 1:1 combination of the phytocannabinoids Δ^9-THC and cannabidiol, for the treatment of spasticity (Kmietowicz, 2010). However, clinical experience with cannabis-based medicines in MS has demonstrated that the use of these compounds is usually accompanied by the appearance of unwanted effects including psychoactivity or memory impairments, associated to the stimulation of bulk CB_1R populations in the CNS. Indeed, the therapeutic efficacy of the

phytocannabinoid Δ^9-THC in animal models and MS patients is restricted to their administration at high doses, which activate the complex array of biological actions mediated by CB_1R at different cellular locations (Baker et al., 2012). Current research on the therapeutic potential of the endocannabinoid system in MS aims thus at developing strategies allowing CB_1R/CB_2R-mediated beneficial effects, whilst limiting adverse responses. In this context, enhancing the concentration of the endocannabinoids AEA and/or 2-AG by decreasing their enzymatic metabolism has been postulated as a potential alternative to the use of exogenous cannabinoids for MS control. In this regard, several studies have suggested that **FAAH inhibitors** ameliorate spasticity in animal models of the disease (Baker et al., 2001; Ligresti et al., 2006; Pryce et al., 2013). However, the effects of FAAH on the MS progression of EAE have been poorly investigated using chronic models of the disease. Concerning 2-AG metabolism, a number of recent studies have consistently demonstrated that administration of **MAGL inhibitors** decreases neurological deficits and inflammation and promotes remyelination in MS animal models (Bernal-Chico et al., 2015; Feliú et al., 2017; Hernández-Torres et al., 2014). On the other hand, evidence suggesting that **ABHD6 blockade** engages protective effects in MS is controversial (Manterola et al., 2018a, 2018b). Finally, inhibition of FABPs also attenuates immune responses and neurological disability in the EAE mouse model but the mechanistic implications of such effects are still obscure (Cheng et al., 2021; Rao et al., 2015).

3.5. Role of astrocytic CB_1 receptor in MS

Preclinical evidence has provided solid support to the neuroprotective potential of cannabinoids and endocannabinoids in MS but the underlying mechanisms and the cell-specificity of the observed effects are not completely understood. Astroglial cells are nowadays regarded important targets of endocannabinoid signaling in the brain and certain functions of the endocannabinoid system depend almost exclusively on its ability to regulate astroglial activity. Anatomical analyses have consistently pointed-out perivascular expressions of astrocytic CB_1Rs through the brain (Bosier et al., 2013; Han et al., 2012; Moldrich and Wenger, 2000), suggesting that endocannabinoids may modulate neurovascular coupling as well as BBB permeability during CNS autoimmunity, by targeting astrocyte endfeet.

It is also well established that astrocytes present the machinery to produce, mobilize and degrade endocannabinoids, pointing to the presence of an astroglial autocrine and/or paracrine signaling regulating the function of these cells through CB_1Rs (Metna-Laurent and Marsicano, 2015; Viader et al., 2015; Schüle et al., 2021). In particular, astrocytic MAGL plays a crucial role in 2-AG metabolism in nervous tissue (Viader et al., 2015), and it seems plausible that *in vivo* blockade of the enzyme will promote the activation of CB_1Rs expressed by these cells both in physiological and pathological conditions. Thus, astrocytic CB_1Rs most probably participate in the disease modulating activity of (endo)cannabinoids in MS. However, the implications of endocannabinoid signaling mediated by astrocytes in MS pathology and therapy remain unexplored.

Objectives

Astroglial cells are the most abundant cell population in the central nervous system and are crucially involved in the pathogenesis of MS. According to preclinical studies, astrocyte activation drives chronic inflammation and neurodegeneration in EAE model, and *in vivo* modulation of astrocyte signaling exhibits beneficial effects in this MS mouse model. In human MS, demyelinating lesions exhibit neurotoxic astrocytes amenable to contribute to axonal and oligodendroglial damage during disease progression. Based on the above-mentioned evidence, it is envisaged that the identification of factors driving pathogenic astrocyte activity in MS will contribute to the development of novel and more successful treatment strategies.

Cannabinoids and **endocannabinoids** acting through **CB_1Rs** exert symptom control in MS. However, the therapeutic efficacy of cannabinoid preparations in MS patients is restricted to their administration at high doses that activate the complex array of biological actions mediated by CB_1Rs in different cellular locations. The benefits of cannabinoids in the EAE mouse model rely mainly on the activation of neuronal CB_1Rs, whose stimulation negatively regulates neurotransmitter release and engages protection from glutamate excitation. This hypothesis relies on the observation that mice lacking CB_1Rs exhibit poor tolerance to excitotoxicity and develop more severe neuronal damage and clinical deficits following EAE induction. Conversely, **CB_1Rs expressed in astrocytes induce intracellular Ca^{2+} elevations resulting in the release of glutamate**. This mechanism underlies working memory impairment by acute cannabinoids in rodents, and may contribute to excitotoxic events in neuroinflammatory degenerative conditions such as MS.

In the above mentioned context, the **global aim** of this Doctoral Thesis is to broaden current knowledge on the role of the endocannabinoid system in modulating astrocytes in MS, with a particular emphasis in astrocytic CB_1Rs. Our **specific aims** were as follows:

Objective 1. To investigate the temporal dynamics of endocannabinoid signaling deregulation in astrocyte and microglia populations in the context of their phenotypic alteration during EAE.

Objective 2. To evaluate the functional coupling of CB_1Rs to the modulation of intracellular Ca^{2+} dynamics in astrocytes activated during autoimmune demyelination using complementary *in vivo* and *in vitro* approaches.

Objective 3. To evaluate the phenotype of conditional mutant mice lacking astrocytic CB_1Rs in the EAE model of MS using histological, molecular and Ca^{2+} imaging techniques.

Materials and Methods

1. Animals

All experimental procedures were approved by the Committee on Animal Health and Care of INSERM and the French Ministry of Agriculture and Forestry (authorization number 3306369) and by the Bioethics Committee of the UPV/EHU (authorization numbers M202017140, M202017144) in accordance with the Spanish legislation (RD53/2013). Female C57BL/6N wild type mice purchased from Janvier or bred at the UPV/EHU, female CB_1-KO mice (Marsicano et al., 2002) bred at the Neurocentre Magendie and female inducible GFAP-CB_1R-KO mutant mice (Han et al., 2012) and their wild-type littermates bred at the Neurocentre Magendie were used in this study. Astrocytic conditional mutants were generated by crossing mice carrying the "floxed" *Cnr1* gene with GFAP-CreERT2 mice using a three-step backcrossing procedure to obtain $CB_1R^{f/f;GFAP\text{-}CreERT2}$ (GFAP-CB_1R-KO) and $CB_1R^{f/f}$ littermates (GFAP-CB_1R-WT), used as controls. Deletion of the CB_1R gene was obtained in adult mice (8-10 weeks-old) by daily i.p. injections of tamoxifen (1 mg dissolved at 10 mg/ml in 90% sesame oil, 10% ethanol, Sigma-Aldrich, St Quentin, France) for 7 days. Mutant mice were used 3 weeks after tamoxifen treatment. Animals were maintained under standard laboratory conditions with food and water *ad libitum*. The experiments were performed during the first part of the light phase (9:00 h to 14:00 h). Experimenters were always blinded to genotypes.

2. Experimental autoimmune encephalomyelitis (EAE)

$MOG_{30\text{-}35}$ (MEVGWYRSPFSRVVHLYRNGK) corresponding to the fragment of mouse MOG from amino acids 35 to 55 was synthesized at the Peptide Synthesis Core Facilities of the Pompeu Fabra University (UPF) and the Príncipe Felipe Research Center Foundation (CIPF). Mice were immunized s.c. in the flank with 200 µg MOG30-35 peptide in incomplete Freund's adjuvant supplemented with 8 mg/ml Mycobacterium tuberculosis H37Ra (Difco Laboratories). Pertussis toxin (500 ng; Calbiochem, Merck Millipore) was injected i.p. on the day of immunization and again 2 days later. In FACS experiments aimed at purifying astrocytes and microglia during the time-course of EAE a total number of 20 mice were immunized in 4 independent experimental sessions separated 2-5 days each (n = 5 mice per EAE experiment). Body weight and motor symptoms were recorded daily and scored from 0 to 8 as follows: 0, no detectable changes in muscle tone and motor behavior; 1, flaccid tail; 2, paralyzed tail; 3, impairment or loss of muscle tone in hindlimbs; 4, hindlimb hemiparalysis; 5, complete hindlimb paralysis; 6, complete hindlimb paralysis and loss of muscle tone in forelimbs; 7, tetraplegia; and 8, moribund.

3. Novel object recognition memory

We used the novel object recognition memory task in a L-maze (NOR) according to previously described procedures (Robin et al., 2018). The consolidation of this type of memory is deeply altered by acute immediate post-training administration of cannabinoids via hippocampal CB_1R (Puighermanal et al., 2009) as well as in GFAP-CB_1-KO mice (Robin et al., 2018). The task took place in a L-shaped maze made of dark gray polyvinyl chloride shaped by two identical perpendicular arms (35 cm and 30 cm long respectively for external and internal L walls, 4.5 cm wide and 15 cm high walls) placed on a white background. The task occurred in a room adjacent to the animal house with a light intensity fixed at 30 lux. The maze was overhung by a video camera allowing the detection and scoring offline of animal's behavior. The task consisted of 3 sequential daily trials of 9 min each. During the habituation session (day 1), mice were placed in the center of the maze and allowed to freely explore the arms in the absence of any objects. The

acquisition session (day 2) consisted in placing the mice again in the center of the maze in the presence of two identical objects positioned at the extremities of each arm and left to freely explore the maze and the objects. The memory test occurred 24 h later (day 3) by replacing one of the familiar objects by a novel object different in its shape, color and texture. Mice were left to explore both objects during the memory test. The position of the novel object and the associations of novel and familiar were randomized. All objects were previously tested to avoid biased preference. The apparatus as well as objects were cleaned with water before experimental use and between each animal testing. Memory performance was assessed by the discrimination index (DI). The DI was calculated as the difference between the time spent exploring the novel (TN) and the familiar object (TF) divided by the total exploration time (TN+TF): DI = [TN-TF]/[TN+TF]. Memory was also evaluated by directly comparing the exploration time of novel and familiar objects, respectively. Object exploration was defined as the orientation of the nose to the object at a distance of less than 2 cm. The exploration time was evaluated by an experienced investigator blind to the genotype of the animals.

4. Fiber photometry in freely behaving mice

We used fiber photometry based on GECIs to define the Ca^{2+} dynamics of cortical astrocytes during autoimmune demyelination *in vivo* and its regulation by astrocytic CB_1Rs. Specific astrocytic targeting was obtained using a short version (*Gfa*-ABC_1D) of the human GFAP promoter (Shigetomi et al., 2016).

4.1. Stereotaxic fiber implantation and AAV administration

For intracortical AAV delivery, mice (8-9 weeks of age) were anaesthetized by isoflurane and placed into a stereotaxic apparatus (David Kopf Instruments) with mouse adaptor and lateral ear bars. Virus v275-9 ssAAV-9/2-GFAP-hHBbI/E-GCaMP6f-bGHp(A) particles obtained from ETH Zürich were injected 0.4 µl per injection site at a rate of 0.12 µl per min with the help of a glass pipette attached to a *Nanoject III* (Drummond, Broomall, USA). Virus titres were 10^{12} genomic copies per ml. Injections were carried out in the somatosensory cortex according to the following coordinates: anterior-posterior -1.5; medial-lateral +2.5; dorsal-ventral -1.5. Following virus delivery, the syringe was left in place for 10 min before being slowly withdrawn from the brain. The optical fiber (400 µm diameter) was placed 250 µm above the injection site during the same surgical session. Mice were weighed daily and individuals that fail to return to their pre-surgery body weight will be excluded from subsequent experiments. Conditional mutant mice receive tamoxifen injections 1 week after the surgery. EAE was induced 3 weeks after the surgery in naïve mice and 3 weeks after tamoxifen injection in conditional mutant mice.

4.2. Fiber photometry imaging and data analysis.

Mice were habituated to being handled for 3 days. The day of recording each mouse was placed in a rectangular chamber and its behavior recorded using a camera placed above the chamber. In experiments aimed at evaluating the effect of Δ^9-THC in naïve mice, baseline recordings were made for 12-20 min. Animals were subsequently injected with vehicle solution (4% ethanol, 4% Cremophor-EL and 92% saline; i.p.) and recorded for further 30 min after injection (15 min *period 1* + 15 min *period 2*). Mice were returned to the home cage following vehicle recordings. At least 24 h after vehicle recordings mice were injected with Δ^9-THC solution (10 mg/Kg; i.p.) following a 12-20 min baseline recording period and imaged for the same time-windows. In experiments designed to address changes in astrocytic Ca^{2+} dynamics during

autoimmune demyelination, EAE was induced following the habituation period and recordings made every 2 days for 12 min starting 3 days before MOG administration. At the end of the experiment, mice were injected with vehicle and Δ^9-THC (10 mg/Kg; i.p.) administered in consecutive days (20-21 dpi) and recordings made as described above.

GCaMP6f was excited using 470 and 405 nm LEDs (Thorlabs) in order to measure cytosolic Ca^{2+} activity. The 470 nm LED was used to extract Ca^{2+}-dependent signals and the 405 nm LED to obtain Ca^{2+}-independent isosbestic signals as control for artifactual fluorescence. The GCaMP6f fluorescence from the astrocytes was collected with a sCMOS camera through an optic fiber divided in 2 sections: a short fiber implanted in the brain of the mouse and a long fiber (modified patchcord), both connected through a 1.25 mm ferrule-ferrule connection. Matlab software was used to control the LEDs and acquire fluorescence data at 1 KHz. LEDs will be alternately turned on and off at 40 Hz in a square pulse pattern. Custom-written MATLAB scripts (MathWorks Corporation) was used to compute fluorescent signals. To calculate fluorescence due specifically to fluctuations in Ca^{2+} and to remove bleaching and movement artefacts, the isosbestic 405 nm signal was subtracted from the 470 nm Ca^{2+} signal. Specifically, normalized fluorescence changes ($\Delta F/F_0$) were calculated by subtracting the mean fluorescence (2 min sliding window average) from the fluorescence recorded by the fiber at each time point and dividing this value by the mean fluorescence ($(F-F_{mean})/F_{mean}$), using a customized Matlab software. Subsequently, the Ca^{2+} independent signal (emitted after the 405 nm excitation) was subtracted to the raw signal (emitted after the 470 nm excitation) to eliminate unspecific fluorescence. The result will be the global Ca^{2+} signal ($\Delta F/F$ (%) = ΔF_{Ca} - ΔF_{isos}), that was used as an estimate of tonic activity of the astrocytes. Ca^{2+} transients were detected on the filtered trace (high filter) using a threshold to identify them (2 median absolute deviation -MAD- of the entire trace). Duration and frequency were calculated on the detected transients. Amplitude was determined as the MAD of each studied period. The effects of vehicle and Δ^9-THC injection were analyzed in 2 equal time periods after injection (*period 1* and *period 2*).

5. Histology and immunohistochemistry

For histological examination anesthetized mice were transcardially perfused with 0.1 M phosphate buffer (25 mM $NaH_2PO_4 \bullet H_2O$; 75 mM Na_2HPO_4; pH 7.4) followed by 4% paraformaldehyde (PFA) in the same buffer. After extraction, the spinal cords and brains were post-fixed in 4% PFA for 1-3 hours, respectively, and cryoprotected overnight in 20% sucrose at 4°C. Spinal cord tissue was re-equilibrated in 15% sucrose solution and embedded in 15% sucrose-7% porcine gelatin solution in PBS. Then, the tissue was frozen using 2-methylbutane and stored at -80°C until use. Postfixed brains were stored at 4°C in 0.1 M PB containing 0.02% sodium azide. Coronal sections (10 µm-thick) were obtained from lumbar spinal cords using a cryostat (Leica CM3050S) and stored at -20°C until use. Forebrains were sliced in the coronal plane (Paxinos and Franklin, 2012) on a vibratome (Leica VT1000S) and 40-µm-thick sections between 1.10 and 0.14 bregma containing the cortex were stored in 0.1 M PB containing 0.02% sodium azide until use.

5.1. Luxol fast blue myelin staining

Spinal cord tissue sections were treated overnight in a solution containing ethanol at 95%, 0.5% glacial acetic acid and 0.1% luxol fast blue (LFB) solvent 38 (Sigma-Aldrich) at 37-42°C, and then differentiated with a 0.01% lithium carbonate solution (Sigma-Aldrich). Tissues were

dehydrated by passing them through a series of increasing alcohol concentrations (50%-100%) and mounted in DPX (Sigma-Aldrich).

5.2. Immunofluorescence staining

Spinal cord and forebrain sections were incubated in Epitope Recovery Buffer (Aptum) (95°C, 5 min) for antigen retrieval rinsed in PBS (100 mM Tris Base, 150 mM NaCl; pH 7.4) and incubated in cold ethanol (10 min). Following extensive washing, spinal cord slices were blocked for 60 min in PBS supplemented with 5% normal goat serum (NGS, Vector Laboratories), 0.2% Triton X-100 and Fab fragment (3%; Jackson ImmunoResearch) followed by overnight incubation at 4°C with mouse anti-MBP (1:2000; Covance; Cat.no. SMI-99P), rabbit anti-MBP (1:250; Millipore; Cat.no. AB980); mouse anti-GFAP (1:40; Millipore; cat. no. MAB3402), rabbit anti-Iba1 (1:500; Wako; Cat.no. 019-19741), rat anti-CD3 (1:50; Bio-Rad; Cat.no. MCA1477), mouse anti-SMI32 (1:200; BioLegend; Cat.no. 801702) and rabbit anti-C3 (1:1500; Dako; Cat.no. A0063) in the same buffer. Free-floating forebrain sections were washed in PBS (3x10 min) and incubated for 60 min at RT in a blocking-permeabilization solution containing 3% NGS and 0.3% Triton X-100 in PBS and subsequently incubated overnight at 4°C with the corresponding primary antibodies diluted in PBS supplemented with 1% NGS and 0.1% Triton X-100. Tissue samples run in parallel without primary antibodies were always included as internal controls. Sections were washed in PBS (3x10 min) and primary antibodies were detected by incubation with appropriate Alexa Fluor 488 or 594 conjugated goat antibodies (1:400; Invitrogen) for 1-2 h at room temperature. Hoechst (1:300; Sigma-Aldrich) was used for chromatin staining. Sections were washed in PBS (3x10 min) and mounted in Glycergel (Dako).

For immunohistochemical staining related with fiber photometry experiments, free-floating forebrain sections were washed in PBS (3x5 min) and incubated with rabbit anti-GFP (1:500; Invitrogen; Cat.no. A11122) and chicken anti-GFAP (1:500; Abcam; Cat.no. ab4674) overnight at 4°C in a blocking-permeabilization solution containing 10% donkey serum and 0.3% Triton X-100 in PBS. Sections were washed in PBS (3x5 min) and primary antibodies were detected by incubation with donkey anti-rabbit Alexa Fluor 647 (1:500; Invitrogen; Cat.no. A31573) and donkey anti-chicken rhodamine (1:500; Jackson ImmunoResearch; Cat.no. 138258) for 2 h at room temperature. Sections were washed in PBS (3x5 min) and incubated with DAPI (1:20.000; Invitrogen; Cat.no. 11530306) for 5 min. Sections were washed in PBS (3x5min) and mounted in Fluoromount (Sigma-Aldrich).

5.3. Image acquisition and analysis

Optical images from tissue sections processed in parallel were acquired in the same session using a Zeiss Axioplan 2 microscope coupled to an Axiocam MRc5 digital camera using microscope fluorescence intensity settings at which the control sections without primary antibody gave no signal. LFB staining was quantified in 4 consecutive 10X objective pictures per spinal cord section. Immunolabeling was examined in 4 non-consecutive 20X objective pictures per spinal cord section. A total number of 3-5 coronal tissue sections per animal were examined for each experimental parameter. Colocalization analysis of GFAP and C3 dual-labelled tissue sections was performed using a laser scanning microscope (Leica). Series of optical sections (z-stacks) were taken through the tissue at a spacing of 0.7 µm using a 20X oil immersion objective. White matter $C3^+$ and $GFAP^+$ stained areas were quantified in 2 optical sections per tissue slice obtained from 4-5 slices per mouse.

Analysis of immunostained sections was carried out using Fiji Image J. Immunopositive cells were quantified by cell counting and data expressed as mean cell number per square millimeter (mm^2) of tissue area. Threshold analysis of GFAP immunostained area was carried out in 16-bit grey scale transformed pictures and the values were referred to the total white matter area in each optical section. Custom scripts were used for semiautomated image processing and analysis of co-localization in Fiji Image J (Schindelin et al., 2012).

6. Flow cytometry

For FACS analysis purposes naive and EAE mice were decapitated under isoflurane anesthesia (IsoVet®, B Braun) on days 7-8, 14-17 and 28-31, and cells purified from forebrain and spinal cord tissue according to previously described procedures (Manterola et al., 2018a). Mice were selected for FACS analysis so that each experimental group included animals immunized in 2-3 independent EAE experiments. Briefly, forebrain and spinal cord tissue were dissected and placed in enzymatic solution (116 mM NaCl, 5.4 mM KCl, 26 mM $NaHCO_3$, 1 mM NaH_2PO_4, 1.5 mM $CaCl_2$, 1 mM $MgSO_4$, 0.5 mM EDTA, 25 mM glucose, 1 mM L-cysteine) with papain (3 U/mL) and DNAse I (150 U/µL, Invitrogen) for digestion at 37**°**C for 25 min. Halfway through the incubation, the minced tissue was triturated 10 times using 5-ml serological pipettes. Following enzymatic digestion, cells were mechanically released by gentle passage through 23 G, 25 G and 27 G syringe needles. After homogenization, tissue clogs were removed by filtering the cell suspension through prewetted 40 µm cell strainers (Fisherbrand™) to a 50 mL Falcon tube quenched by 5 mL of 20% heat inactivated fetal bovine serum in Hank´s Balanced Salt Solution (HBSS, Thermo Fisher Scientific). The cell strainers were thoroughly rinsed with 15 ml HBSS in and cell suspensions were centrifuged 200 x *g* for 5 minutes. To purify astrocytes and microglia from myelin debris, cells were resuspended in 25% isotonic Percoll PLUS (GE Healthcare Europe GmbH) in HBSS and centrifuged at 200 x *g* without brake for 20 min at room temperature. The myelin top layer was aspirated and cells washed with HBSS to remove any traces of Percoll PLUS by centrifuging at 200 x *g* for 5 min. The total dissociated single cells were resuspended in 500 µL sorting buffer (25 mM HEPES, 5 mM EDTA, 1% BSA, in HBSS) containing Normal Rat Serum (1:100; Invitrogen, 10710C) and TruStain FcX™ (anti-mouse CD16/32) antibody (1:100; BioLegend, 101320). The cell suspension was then divided in 2 equivalent aliquots for the parallel purification of astrocytes and microglia. Isolated CNS cells were incubated with fluorochrome conjugated antibodies ACSA-2-PE (1:50; Miltenyi Biotec, REA969), A2B5-488 (1:100; R&D Systems, FAB1416G), CD11b-FITC (1:200; BioLegend, 101205), CD31-VioBright 515 (1:200; Miltenyi Biotec, REA784), CD45-FITC (1:200; Miltenyi Biotec, REA737) and O1-488 (1:100; R&D Systems, FAB1327G) for astrocyte isolation. Microglia was purified from a cell suspension aliquot incubated with antibodies to CD11b-FITC (1:100; BioLegend, 101205) and CD45-PE (1:100; BioLegend, 103105). In all cases, cell suspensions were incubated with LIVE/DEAD Fixable Green Dead Cell (1:1500; Thermo Fisher, L34969).

Astrocytes were sorted as ACSA-2^+ cells following exclusion of contaminating microglia, hematopoietic cells, oligodendrocytes, oligodendrocyte progenitors and endothelial cells grouped in a dump channel (Batiuk et al., 2017; Kantzer et al., 2017) (see **Results** section). Microglial cells were sorted as $CD11b^+$ cells with low CD45 expression (Szulzewsky et al., 2015). Samples were run on a BD FACS Jazz (2B/4YG) flow cytometer (BD Bioscience) controlled using BD FACS™ Software (version 1.1.0.84) and results were analyzed using FlowJo software. All gatings were set based on appropriate isotype controls. Debris and cell clumps were initially

gated out on the basis of FSC and SSC plots, allowing selection of only the population of interest. Further doublets were gated out using FSC/trigger pulse width plots. Typically, an average number of 50.000 astrocytes and 20.000 microglial cells were collected for each sample within 15-20 min. The purity of astrocytes was assessed by FACS analysis of sorted ACSA-2^+ cells following fixation and immunostaining with a C-terminal antibody against the astrocytic marker GLAST (Rothstein et al., 1994) (1:200; kindly donated by Rothstein). We further confirmed that we had isolated a relatively pure population of astrocytes and microglia by qPCR analysis for the expression of several cell-type specific markers (see **Results** section).

7. Nanofluidic RT-qPCR in purified astrocytes and microglia

FACS purified cells and cultured astrocytes were collected in lysis buffer (Qiagen) containing 1% β-mercaptoethanol for optimal template preservation and stored at -80°C until processing. Samples were transferred onto an RNeasyMin Elute spin column and RNA was purified with on-column DNAse treatment using RNeasy plus micro and mini kits (Qiagen, 74034 and 74104) following manufacturer's instructions. RNA was eluted with 14-35 µl of RNAse-free deionized water and stored at -80°C until transcriptomic analysis.

Synthesis of cDNA, pre-amplification and amplification steps were performed at the Genome Analysis Platform of the UPV/EHU following quality control of RNA samples with an Agilent 2100 Bioanalyzer (Agilent Technologies). Pre-amplified cDNA samples were measured with no reverse transcriptase and no template controls in the BioMark HD Real-Time PCR System using 96.96 and 48.48 Dynamic Arrays of integrated fluidic circuits (Fluidigm Corporation). This technology enables reliable and accurate gene expression analysis using very limited total RNA input (Jang 2011). We used commercial primers from IDT Integrated DNA Technologies or Fluidigm Corporation. Data pre-processing and analysis were completed using Fluidigm Melting Curve Analysis Software 1.1.0 and Real-time PCR Analysis Software 2.1.1 (Fluidigm Corporation) to determine valid PCR reactions. *Gapdh*, *Hprt*, *Ppia* and *B2m* were included as candidate reference genes for normalization purposes. Data were corrected for differences in input RNA using the geometric mean of reference genes selected according to results from the normalization algorithms geNorm (https://genorm.cmgg.be/) and Normfinder (https://moma.dk/normfinder-software). Relative expression values were calculated with the $2^{-\Delta\Delta Ct}$ method.

8. Astrocyte cultures

Astrocytes were isolated by magnetic activated cell sorting (MACS) from C57BL/6N mice (P5-6). Briefly, the forebrains were carefully dissected, meninges removed and tissue enzymatically dissociated using Neural Tissue Dissociation Kit (P) (Miltenyi Biotec, 130-092-628). Myelin was removed using a 35% Percoll PLUS (Merck) gradient and cells were sorted using Anti-ACSA-2^+ MicroBead Kit (Miltenyi Biotec, 130-097-679). Cells were seeded onto 14 mm diameter glass coverslips in 24-well plates at a density of 20.000 cells/well for immunocytochemistry and in 6-well plates at a density of 500.000/well for qPCR. Alternatively, astrocytes were seeded onto glass-bottom µ-dishes (Ibidi GmbH, Germany) at a density of 100.000 cells/plate for Ca^{2+} imaging. Cells were maintained in serum-free defined medium containing 50% neurobasal, 50% DMEM, 100 U/ml penicillin, 100 µg/ml streptomycin, 1 mM sodium pyruvate, 292 µg/ml l-glutamine, 1×SATO and 5 µg/ml of *N*-acetyl cysteine. This medium was supplemented with the astrocyte-required survival factor HBEGF (10 ng/ml; Preprotech) (Liddelow and Barres, 2017). The purity of the cultures was be routinely assessed by examining the characteristic cell

morphologies under phase-contrast microscopy and confirmed by immunostaining with mouse anti-GFAP (1:200; Merck, MAB3402) and mouse anti-S100β (1:400; Sigma Aldrich, S2532). After 6-7 days in culture $GFAP^+$ and $S100\beta^+$ cells represented 95±1% and 97±2% of total cells, respectively (*n* = 3 cultures, 1-2 coverslips per culture, 15 microscopic fields per coverslip).

Astrocyte polarization to a neurotoxic A1 phenotype was induced in astrocytes at 4-5 DIV by incubation with IL-1α (3 ng/ml; Sigma), TNFα (25 ng/ml; Cell Signaling Technology) and C1q (400 ng/ml; MyBioSource) for 18-24 h (Liddelow et al., 2017) and corroborated by qPCR analysis.

9. Cytosolic Ca^{2+} imaging

Astrocytes were loaded with Fluo-4 AM (1 mM; Molecular Probes) in culture media for for 20 min at 37°C followed by 10 min wash in HBSS (Sigma, H-4891) supplemented with 20 mM HEPES, 10 mM glucose, 2 mM $CaCl_2$, 1 mM $MgCl_2$ and 4 mM $NaHCO_3$ (pH 7.4) to allow de-esterification. Images were acquired through a 63X objective in a TCS SP8X STED CW confocal microscope (Leica) at an acquisition rate of 1 frame/15 s during 5 min. Following a baseline recording (1 min) cells were stimulated with glutamate (200 µM), ATP (200 µM) or WIN55,212-2 (100 nM), thapsigargin (1 µM) or FCCP (5 µM). Recordings aimed at testing mitochondrial and/or ER Ca^{2+} levels were carried out in the absence of extracellular Ca^{2+}. For data analysis, a homogeneous population of 15 cells was selected in the field of view and astrocyte somata selected as regions of interest (ROIs). Background values were always subtracted and data are expressed as F/F_0 in which F represents the fluorescence value for a given time point and F_0 represents the mean of the resting fluorescence level.

10. Data analysis and statistics

Data are presented as mean ± standard error of mean (S.E.M.) and *n* represents the number of animals or cultures tested. Statistical analyses were performed using GraphPad Prism 9 for Windows (GraphPad Software Inc). Time courses of EAE scores were analyzed using the unpaired Mann-Whitney *U*-test. Non-time course score and fiber photometry data, histological, biochemical and confocal imaging results were analyzed by unpaired Student's *t*-tests or with Mann-Whitney *U*-tests following application of normality tests or with two-way repeated-measures ANOVA followed by Šídák's multiple comparisons tests. Paired Student's *t*-tests or Wilcoxon matched-pairs signed rank tests were occasionally used for comparisons in cultured cells. In all instances, *p* values < 0.05 were considered statistically significant.

Table 2. Genes tested in RT-qPCR analysis.

	Gene symbol	Gene name
Target genes	*Abhd12*	Abhydrolase domain containing 12
	Abhd6	Abhydrolase domain containing 6
	Adora1	Adenosine A1 receptor
	Adora2a	Adenosine A2a receptor
	Adora2b	Adenosine A2b receptor
	Aldh1l1	Aldehyde dehydrogenase 1 family member L1
	Amigo2	Adhesion molecule with Ig like domain 2
	Aqp4	Aquaporin 4
	Aspg	Asparaginase
	Atp1b2	ATPase Na^+/K^+ transporting subunit beta 2
	Atp2a1	ATPase sarcoplasmic/endoplasmic reticulum Ca^{2+} transporting 1
	Axl	AXL receptor tyrosine kinase
	B3gnt5	UDP-GlcNAc:betaGal beta-1,3-N-acetylglucosaminyltransferase 5
	Bdnf	Brain derived neurotrophic factor
	C1ra	Complement component 1, r subcomponent A
	C3	Complement component 3
	Ccl2	Chemokine (C-C motif) ligand 2
	Ccl5	Chemokine (C-C motif) ligand 5
	Cd14	Monocyte Differentiation Antigen CD14
	Cd163	CD163 Molecule
	Cd44	CD44 Molecule
	Chil3	Chitinase 3 Like 1
	Cnr1	Cannabinoid receptor 1
	Cnr2	Cannabinoid receptor 2
	Cntf	Ciliary neurotrophic factor
	Csf2	Colony stimulating factor 2
	Cxcl10	Chemokine (C-X-C motif) ligand 10
	Cxcl2	Chemokine (C-X-C motif) ligand 2
	Dagla	Diacylglycerol lipase, alpha
	Daglb	Diacylglycerol lipase, beta
	Emp1	Epithelial membrane protein 1
	Faah	Fatty acid amide hydrolase
	Fabp7	Fatty acid binding protein 7
	Fkbp5	FKBP Prolyl Isomerase 5
	Gas6	Growth arrest specific 6
	Gbp2	Guanylate binding protein 2
	Gfap	Glial fibrillary acidic protein
	Ggta1	Glycoprotein galactosyltransferase alpha 1, 3
	Gnaq	Guanine nucleotide binding protein, alpha q polypeptide
	Gpc4	Glypican 4
	Gpc6	Glypican 6
	Gpr34	G protein-coupled receptor 34
	Grm1	Glutamate receptor, metabotropic 1
	Grm2	Glutamate receptor, metabotropic 2
	Grm3	Glutamate receptor, metabotropic 3
	Grm4	Glutamate receptor, metabotropic 4
	Grm5	Glutamate receptor, metabotropic 5
	Grm7	Glutamate receptor, metabotropic 7
	Grm8	Glutamate receptor, metabotropic 8
	H2-T23	Histocompatibility 2, T region locus 23
	Icam1	Intercellular adhesion molecule 1
	Igf1	Insulin-like growth factor 1
	Iigp1	Interferon-inducible GTPase 1
	Il12a	Interleukin 12a
	Il1b	Interleukin 1 beta
	Il6	Interleukin 6
	Irf9	Interferon regulatory factor 9
	Itgam	Integrin subunit alpha M
	Itpr1	Inositol 1,4,5-triphosphate receptor 1
	Itpr2	Inositol 1,4,5-triphosphate receptor 2
	Itpr3	Inositol 1,4,5-triphosphate receptor 3
	Mcu	Mitochondrial calcium uniporter
	Megf10	Multiple EGF-like-domains 10
	Mertk	MER proto-oncogene tyrosine kinase
	Mgll	monoglyceride lipase
	Mrc1	Mannose receptor C-type 1
	Mx1	MX dynamin-like GTPase 1
	Naaa	N-acylethanolamine acid amidase

Table 2. Genes tested in RT-qPCR analysis (continuation).

	Gene symbol	Gene name
Target genes	*Napepld*	N-acyl phosphatidylethanolamine phospholipase D
	Nfe2l2	Nuclear factor erythroid 2-related factor 2
	Nlgn1	Neuroligin 1
	Nos2	Nitric oxide synthase 2, inducible
	Nrg1	Neuregulin 1
	P2ry1	Purinergic receptor P2Y, G-protein coupled 1
	P2ry12	Purinergic receptor P2Y, G-protein coupled 12
	Pdgfa	Platelet derived growth factor, alpha
	Psmb8	Proteasome 20S subunit beta 8
	Ptgs2	Prostaglandin-endoperoxide synthase 2
	Rbfox3	RNA binding protein, fox-1 homolog
	Ryr1	Ryanodine receptor 1
	Ryr2	Ryanodine receptor 2
	Ryr3	Ryanodine receptor 3
	S100a10	S100 calcium binding protein A10 (calpactin)
	S100b	S100 calcium binding protein B
	S1pr3	Sphingosine-1-phosphate receptor 3
	Serpina3n	Serpin Family A Member 3
	Serping1	Serine (or cysteine) peptidase inhibitor, clade G, member 1
	Shank1	SH3 and multiple ankyrin repeat domains 1
	Shank3	SH3 and multiple ankyrin repeat domains 3
	Slc1a3	Solute carrier family 1 (glial high affinity glutamate transporter), member 3
	Slc8b1	Solute carrier family 8 (sodium/lithium/calcium exchanger), member B1
	Snap25	Synaptosomal-associated protein 25
	Sparcl1	SPARC-like 1 (Hevin)
	Stat1	Signal transducer and activator of transcription 1
	Stat2	Signal transducer and activator of transcription 2
	Stat3	Signal transducer and activator of transcription 3
	Stat6	Signal transducer and activator of transcription 6
	Syn1	Synapsin I
	Tgfb1	Transforming growth factor, beta 1
	Thbs1	Thrombospondin 1
	Thbs2	Thrombospondin 2
	Tmem119	Transmembrane protein 119
	Tnfa	Tumor necrosis factor alpha
	Vcam1	Vascular cell adhesion molecule 1
Housekeeping genes	*B2m*	Beta-2-Microglobulin
	Gapdh	Glyceraldehyde-3-phosphate dehydrogenase
	Hprt	Hypoxanthine phosphoribosyltransferase 1
	Ppia	Peptidylprolyl isomerase A

Table 3. List of primers used for RT-qPCR analysis.

	Gene symbol	Forward sequence	Reverse sequence
Target genes	*Abhd12*	GCAATTACTACCTCCAGCCA	AGCATCCTCATACCACATCTG
	Abhd6	TTTGTTGCGTCTTTCCTCCT	CTGATAGTCCTCATGGTGTGC
	Adora1	GTACCTCCGAGTCAAGATCCC	AAACATGGGTGTCAGGCCTA
	Adora2a	ACTCCGGTACAATGGCTTG	AATTCATGGGTACCACGTCC
	Adora2b	CCGCTCAGGTATAAAGGTTTGG	TTTACTGTTCCACCCCAGGA
	Aldh1l1	GACAATACCACAGACCCCAAC	CCATCCAGACCTTCCGATAC
	Amigo2	GGAGACGGTTGAGTTTGAGAG	GATAATGGCTGGTCCTACTGC
	Aqp4	CACTTGTGCCTACGATCCTC	AGTCCGATGGAGATTCTCTACT
	Aspg	AGCATGAAAGAGAGCACTGAG	GTGACATGACCATCACTGAGT
	Atp1b2	GTTGAGGAGTGGAAGGAGTT	ATGGTGAGGCTGAACATGG
	Atp2a1	GTTTGGCAGGAACGGAATG	GAGCCTTGATCCTTTGCACT
	Axl	GTACCGTGTCCGAAAGTCC	CCTTATGCCGATCTACCATGAC
	B3gnt5	TCCACTCAAAACCTTCAGCTC	ATAGTCCACCAAAGAATCAGTAGG
	Bdnf	TCCAAAGGCCAACTGAAGCA	CTGCAGCCTTCCTTGGTGTA
	C1ra	CCTTCAACTTACAGTGCCTGA	CCTTCCACCCCATAGAACAG
	C3	AGGGAGTGTTTGTGCTGAAC	GCCAATGTCTGCCTTCTCTAC
	Ccl2	AGCAGCAGGTGTCCCAAA	TTCTTGGGGTCAGCACAGAC
	Ccl5	CCTCTATCCTAGCTCATCTCCA	GCTCCAATCTTGCAGTCGT
	Cd14	AACTTTCAGAATCTACCGACCA	CAATCTGGCTTCGGATCTGAG
	Cd163	GCCATAACTGCAGGCACAAA	GTTGGTCAGCCTCAGAGACA
	Cd44	CACCATTTCCTGAGACTTGCT	TCTGATTCTTGCCGTCTGC
	Chil3	GCCCACCAGGAAAGTACACA	CCTCAGTGGCTCCTTCATTCA
	Cnr1	GTGCTGTTGCTGTTCATTGTG	CTTGCCATCTTCTGAGGTGTG
	Cnr2	ACGGTGGCTTGGAGTTCAAC	GCCGGGAGGACAGGATAAT
	Cntf	AGATAGAGCGGCTACAGAGG	GTGAAGACAGAAGCAAACCAG
	Csf2	CATGCCTGTCACGTTGAATG	GGGGCAGTATGTCTGGTAGT
	Cxcl10	TGATTTCAAGCTTCCCTATGGC	ATTTTCTGCCTCATCCTGCT
	Cxcl2	CACTCATGTTGCCTGTTCTTC	CGGTTGGTGCTTAGACTTGA
	Dagla	ATCTTGGCTTTCCTGTCTGG	GTAGCAGACTTCTTTGTAGCGT
	Daglb	TGATAGTCCTCCTTGTTCTCCT	GCAGCTTAGACATAGACTTCCG
	Emp1	GCCATTATGCTGTTTGTCTCC	ATCTTCATTGCCGTAGGACAG
	Faah	CTGGTACAGAAGTTACAGAGTGG	GATAGGAGGTCACACAGTTGG
	Fabp7	GAAGTGGGATGGCAAAGAAAC	CATAACAGCGAACAGCAACG
	Fkbp5	GACACCAAAGAAAAGCTGACG	ACTATCTTCCTGTACTGAATCACG
	Gas6	GACTACCACTCTACAAAGAAGCTC	CGCACACCTTGATTTCCATC
	Gbp2	GCAGAATTCACCTCATACATCTTG	GATGGCACCAACATAGGTCTG
	Gfap	AACCGCATCACCATTCCTG	GCATCTCCACAGTCTTTACCA
	Ggta1	TCCTGTTGATGCTGATTGTCTC	GTCCTTCTGCCATCTGTTCTC
	Gnaq	CCTTCCTATCTGCCTACACAAC	CCATTTTCTTCTCTCTGACCTTTG
	Gpc4	CCTTCAGTGCTCGATTCAGAC	GCTTGTTTCAGTTTCTCCTTGAC
	Gpc6	ACGTCAACTTCCAAGACACAA	GTGACAAACTCGAACTCCGT
	Gpr34	AGCTGACACAACCTGGTCTA	ACTTCAGAAGCTGCAGGAAC
	Grm1	ATGCACCTGGAAGGTATGAC	CTTCCCCTTTCCGTATGACC
	Grm2	GTGATTATCGGGTGCAGACC	TCTGTGGCTGGAAGAGGATA
	Grm3	TATTCTCAGTCCTCTGCAAGC	AGCACTTCGTCTAACAGCCT
	Grm4	GCAGTCACCATTCTTCCCAA	CCAGAACTCAGCAAACCAGAT
	Grm5	GACAGGTTGTGATTTGATCCC	AGTAACGAAGAGGGTGGCTA
	Grm7	TTCAATGGTAGTGCTGGAACC	TGCAGTTCATCTGTCCACTG
	Grm8	ACATCAGGAGGATATTGGAAGC	TCCTGCTGATAGACAGGTGC
	H2-T23	ACAGTCCCGACCCAGAGTAG	CCACGTAGCCGACAATGATGA
	Icam1	CTGTGCTTTGAGAACTGTGG	GGTCCTTGCCTACTTGCTG
	Igf1	CTCATGTGAAGAGCCTGTAGC	CTGACCCATGACTTCAAGCA
	Iigp1	CTCATGTGAAGAGCCTGTAGC	CTGACCCATGACTTCAAGCA
	Il12a	AAACCAGCACATTGAAGACC	GGAAGAAGTCTCTCTAGTAGCC
	Il1b	TGGCAACTGTTCCTGAACTCA	GGGTCCGTCAACTTCAAAGAAC
	Il6	CGATGATGCACTTGCAGAAA	ACTCCAGAAGACCAGAGGAA
	Irf9	CAACTGCAACTCTGAGCTAGA	ACCATAGATGAAGGTGAGCAG
	Itgam	TGTCCAGATTGAAGCCATGA	CCACAGTTCACACTTCTTTCAG
	Itpr1	TCATGGAAAGCAGACACGATAG	CATCCTCAAATTCCACTTCACC
	Itpr2	GTTCCCACTATGACCTTATCTTCC	GTCCTTTCTATGCCATCCTCAC
	Itpr3	CATGTTCCGTCTCTGCTACC	CAATCTGTGACTGCATCATCC
	Mcu	TACTCACCAGATGGCGTTC	AGGAGGTCTCTCTTTGGTGG
	Megf10	CTAACGTGTCAGTGCCTCAA	GTTCAGCCCATAAGTGCCAT
	Mertk	GCACATCATTCAATCACACAGT	CATCTTACAGAAGTACGACCCAT
	Mgll	GTCAATGCAGACGGACAGTA	CTCATCATAACGGCCACAGT
	Mrc1	CACAAAGCCATGCTGTAGTACC	GTAAAACCCATGCCGTTTCCA
	Mx1	ACCAAGTAAACATCCTGATACCT	GGTGTCGATGAGGTCAATACAG
	Naaa	CTGGCTGACGGTATCTTGG	CCAAAAGGATAGTCCAGGTTCC

Table 3. List of primers used for RT-qPCR analysis (continuation).

	Gene symbol	Forward sequence	Reverse sequence
Target genes	*Napepld*	CCATCGGAGCTTATGAACCAA	GCCACAGATCTCTTTGTTTGAAG
	Nfe2l2	TGATGGACTTGGAGTTGCC	TCAAACACTTCTCGACTTACTCC
	Nlgn1	GTTCTCGCTGGTCCATCTTAG	TCGTCATCACAGTCAACTATCG
	Nos2	GAGGAGCAGGTGGAAGACTA	GGAAAAGACTGCACCGAAGATA
	Nrg1	GCCATTCGCTATGTTCACCA	GCATCTGTATCGCCCTGTT
	P2ry1	TCAAGCAGAATGGAGACACG	TGGTCAATAGAGTGTTGCTTCT
	P2ry12	GATGCCAGTCTGCAAGTTCC	TTGACACCAGGCACATCCA
	Pdgfa	GTATCTCGTAAATGACCGTCCTG	ATTAACCATGTGCCCGAGAA
	Psmb8	GCTGCTTTCCAACATGATGC	CCGAGTCCCATTGTCATCTAC
	Ptgs2	CTTCTCCCTGAAGCCGTACA	TGTCACTGTAGAGGGCTTTCAA
	Rbfox3	AACAGCTAATCTGCCACCTTC	GTGACTTTATCCTTCGCCTGT
	Ryr1	CTGAGCTGAATGAATACAACGC	CCATGAGCCTTTCTAGCACTG
	Ryr2	GGTGGATGTGGAAAAGTGGA	CTGTAGGAATGGCGTAGCAA
	Ryr3	ACCAGTCAGGTTGTTTTGCC	CTTTTGTTGTCATCCCGCAC
	S100a10	CGACAAAGACCACTTGACAAAG	CATTATTTTGTCCACAGCCAGAG
	S100b	CAGGAGTTCATGGCCTTCGT	CCTCTTGTGACCCTCATGTCT
	S1pr3	AGATGCGCCTTGCAGAA	GTTACTTCAACAGTCCACGAGA
	Serpina3n	CGCGTAGAACTCAGACTTGAAC	GACATTGATGGTGCTGGTGA
	Serping1	CTACCAAGATGGCTAAGACCAA	GATGCTCTCCAAGTTGCTCT
	Shank1	ATCAGACGAAATGCCTACGC	GTCTTGTAGCGGAACTCCAG
	Shank3	GGAACTTGCTTCCATTCGGAG	CCCCTACAGATTTGGTCCGT
	Slc1a3	GAATTCACCTCCACGTAGCC	GTCTTGCACTTGTTCCCAGA
	Slc8b1	GACTATGGAGATGAATACCGGC	TGTGAGCAGCAACAAGAACT
	Snap25	CAGAATCGCCAGATCGACAG	CAAATTTAACCACTTCCCAGCA
	Sparcl1	CTGTGCTTCTCCTCCTGTG	TGTCACCAGTGTTGCAGTAG
	Stat1	GCAGGTGTTGTCAGATCGAAC	ATGCACGGCTGTCGTTCTA
	Stat2	AGCGAATCACTCAAAGCAGA	CCGAAGTCCCAAATTAAGCC
	Stat3	TGGGCATCAATCCTGTGGTA	CCAATTGGCGGCTTAGTGAA
	Stat6	TGACTTTCCACAACGCCTAC	CATCTGAACCGACCAGGAAC
	Syn1	TGTCTTAGTCAGTGCCACAAC	TCCTAATCACAAAGAGATGCTCAG
	Tgfb1	GCTGCGCTTGCAGAGATTAA	GTAACGCCAGGAATTGTTGCTA
	Thbs1	AGTTCCTGATGGTGAATGCTG	ACCACGTTGCTGAATTCCAT
	Thbs2	CTACTAATGCCACCTACCACTG	CATTGTCATCGTCCTCGTCAC
	Tmem119	GGAGTGACACAGAGTAGGC	GGTCCTTCACCCAGAGC
	Tnfa	GGGTGATCGGTCCCCAAA	TGAGGGTCTGGGCCATAGAA
	Vcam1	GCAAAGGACACTGGAAAAGAG	TGTGCAGTTGACAGTGACA
Housekeeping genes	*B2m*	ACTGACCGGCCTGTATGCTA	ATGTTCGGCTTCCCATTCTCC
	Gapdh	AGACGGCCGCATCTTCTT	TTCACACCGACCTTCACCAT
	Hprt	CAGTACAGCCCCAAAATGGTTA	AGTCTGGCCTGTATCCAACA
	Ppia	AGGGTTCCTCCTTTCACAGAA	TGCCGCCAGTGCCATTA

Results

1. Flow cytometry purification of astrocytes and microglia during EAE

1.1. FACS strategy for the purification of rodent astrocytes using ACSA-2

ACSA-2 has been recently postulated as a novel surface marker for astrocyte purification purposes (Kantzer et al., 2017). However, the results of Kantzer and collaborators (2017) also demonstrated that ACSA-2 is co-expressed to a certain extent in additional cellular populations in the adult rodent brain. Therefore, as first step in order to isolate a pure population of astrocytes from the mouse CNS we analyzed ACSA-2 expression in forebrain with spinal cord cell suspensions from adult animals. Anti-ACSA-2 labeled 64.7% of mouse CNS cells compared to isotype control staining (**Figure 1A**-**B**). Flow cytometry analysis of ACSA-2 expression allowed differentiating two populations of ACSA-2$^+$ cells displaying different fluorescent intensity (**Figure 1C**). We next analyzed the specificity of ACSA-2 expression in our cellular preparations using markers for microglia/macrophages (CD11b), hematopoietic cells (CD45), oligodendrocyte progenitors (A2B5), mature oligodendrocytes (O1) and endothelial cells (CD31) (**Figure 1D**-**I**). The microglia and the hematopoietic cell markers CD11b and CD45 were not co-expressed with ACSA-2 or only on a low percentage of the cells (**Figure 1D**-**E**). We detected overlapping of ACSA-2 and CD31 in ~4% of cells from the mouse CNS (**Figure 1F**). Nevertheless, around 60% of CD31$^+$ cells were also positive for the astrocyte marker (**Figure 1I**). By contrast, co-labelling analyses showed that ACSA-2 and the oligodendrocyte markers A2B5 and O1 overlapped in 25-26% of cells in the mouse CNS cells (**Figure 1G**-**H**). More specifically, ~80% A2B5 or O1 positive cells were ACSA-2$^+$, suggesting that immature glial-committed precursors and oligodendrocytes expressed low-intermediate levels of ACSA-2 (**Figure 1I**). These experiments also revealed a population of cells expressing high levels of ACSA-2 that were negative for oligodendrocyte markers. Overall, these results are in agreement with previous observations in cell suspensions of the adult rodent brain (Kantzer et al., 2017).

Based on the above-mentioned observations, we aimed at sorting a pure population or astrocytes by removing contaminating cells using a dump channel gating strategy that grouped antibodies against A2B5, O1, CD31, CD11b and CD45 together with a viability marker. When ACSA-2$^+$ events were plotted against the dump channel, we could identify a population of cells exclusively expressing the astrocyte marker (**Figure 2A**). The purity of astrocytes was assessed by FACS analysis of sorted cells following fixation and immunostaining with a C-terminal antibody against the astrocytic marker GLAST (Rothstein et al., 1994). Flow cytometry analysis showed that ~95% of purified ACSA-2$^+$ cells were GLAST$^+$ (**Figure 2C**), thus validating our gating strategy for the isolation of astrocytes from the adult mouse CNS.

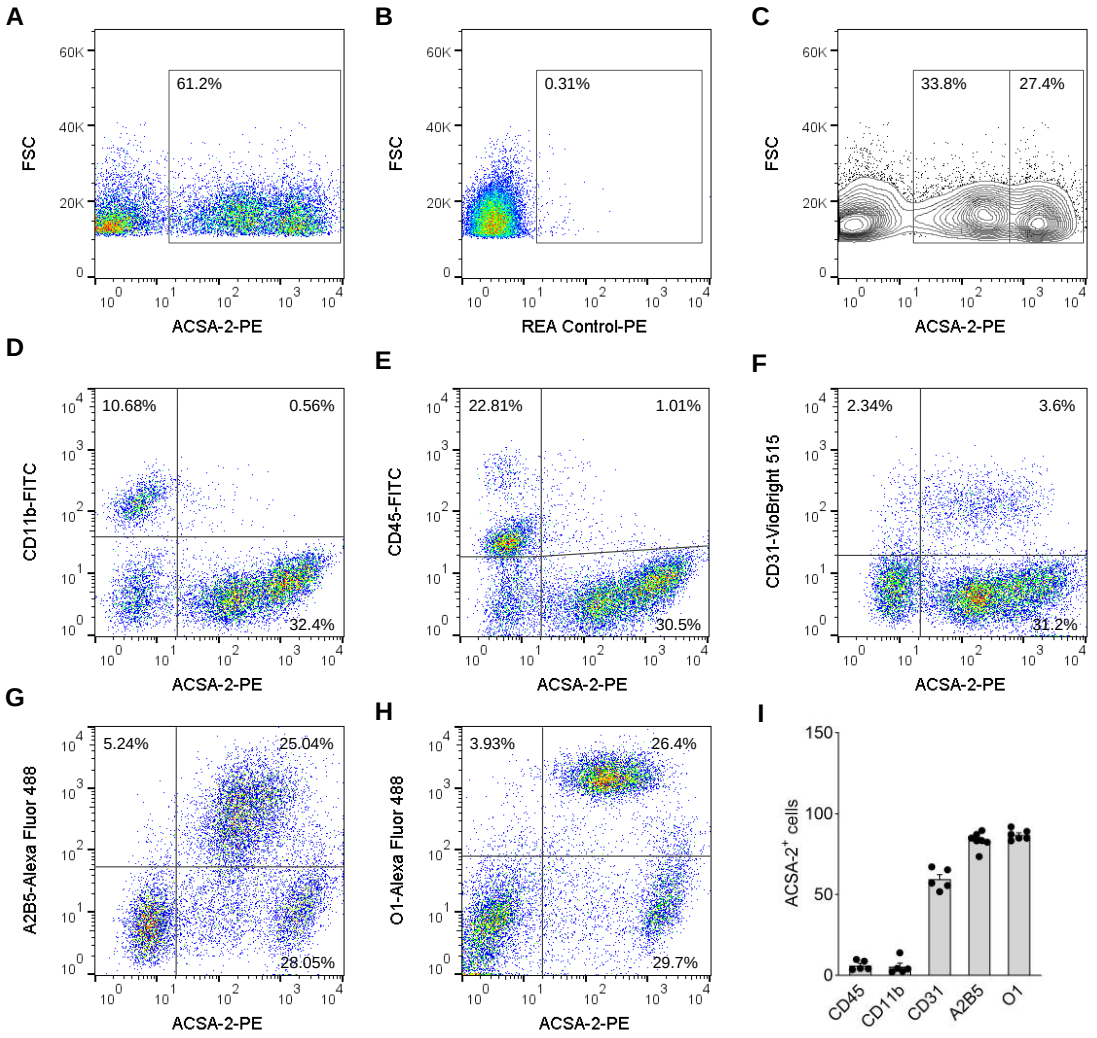

Figure 1. Flow cytometry analysis of ACSA-2 expression on mouse CNS. Single cell suspensions derived from adult mouse forebrain and spinal cord were labeled with the anti-ACSA-2 antibody. ACSA-2 was expressed by 64.7 ± 2.42% of cells in adult mouse brain (**A**) compared to isotype control staining (**B**) (*n* = 8 mice). (**C**) Representative contour plot of the experiment depicted in (**A**) shows two different cell clusters exhibiting low and high ACSA-2 intensity. (**D**-**H**) CNS cell suspensions were co-labeled with ACSA-2-PE and CD11b-FITC (**D**), CD45-FITC (**E**), CD31-VioBright (**F**), A2B5-488 (**G**) or O1-488 (**H**) as specific markers for microglia, hematopoietic cells, endothelial cells, oligodendrocyte precursors and mature oligodendrocytes, respectively. The specificity of each marker was previously tested versus isotype controls. (**I**) Bar graph depicting the proportion of ACSA-2$^+$ cells within each cell population in control mice (*n* = 5 - 7 mice). 100.000 events were analyzed for each sample.

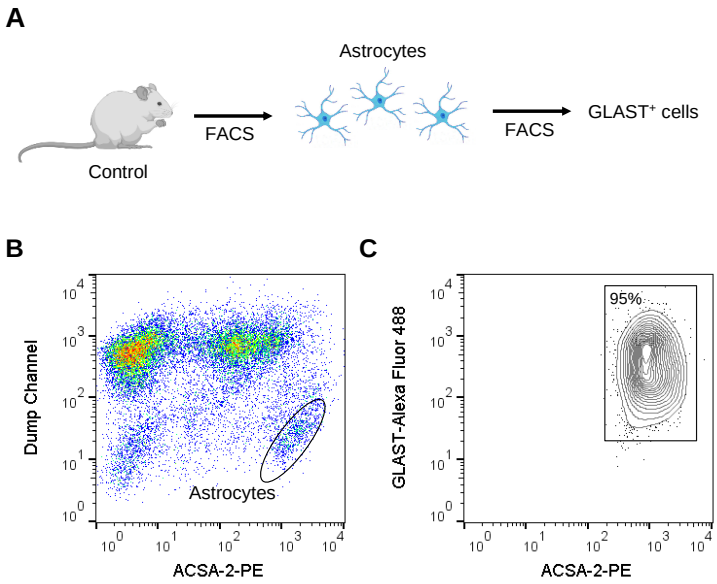

Figure 2. FACS sorting and purity of mouse CNS astrocytes. (**A**) Astroglial cells were isolated from the CNS of 8 week-old mice and GLAST expression analyzed by flow-cytometry. (**B**) Astrocytes were sorted as ACSA-2$^+$ cells following exclusion of contaminating oligodendrocyte progenitors (A2B5$^+$), oligodendrocytes (O1$^+$), endothelial cells (CD31$^+$), hematopoietic cells (CD45$^+$) and microglia/macrophages (CD11b$^+$/CD45$^+$), grouped in a dump channel. (**C**) FACS analysis of ACSA-2$^+$ astrocytes as defined in **B** following fixation and immunostaining with a C-terminal antibody against the astrocytic marker GLAST. Sorted cells were 95.9 ± 2.63% positive for GLAST (*n* = 6 mice).

1.2. Concomitant isolation of astrocytes and microglia during EAE

We next aimed at characterizing astrocytes and microglia purified at presymptomatic (7-8 dpi), acute (14-17 dpi) and recovery (28-31 dpi) stages of EAE. (**Figure 3B**). As readout of disease initiation and progression, we first evaluated the presence of different peripheral immune cell populations such as monocytes (CD11b$^+$CD45^{high}) and lymphocytes (CD11b$^-$CD45^{high}) during EAE time-course (**Figure 3C**)**.** Flow cytometry analysis demonstrated a significant increase in the number of monocytes (CD11b$^+$CD45^{high}) and lymphocytes (CD11b$^-$CD45^{high}) already in the presymptomatic phase of EAE in comparison to non-immunized mice. The presence of both cell populations reached the highest values at acute EAE and remained significantly increased during the recovery phase. Astrocytes and microglial cells were sequentially purified as ACSA-2$^+$ cells or CD11b$^+$ cells with low CD45 expression (Szulzewsky et al., 2015) respectively, from independent cell suspension aliquots obtained from the same animals at different time-points of EAE disease progression. RT-qPCR analysis confirmed that astrocyte and microglia sorted cell populations were enriched in astrocytic (*Aldh1l1*, *Aqp4*, *Atp1b2*, *Gfap*, *Slc1a3*) and microglial (*Gpr34*, *Itgam*, *P2ry12*, *Tmem119*) genes throughout EAE progression (**Figure 3D** shows results from cells purified at acute disease).

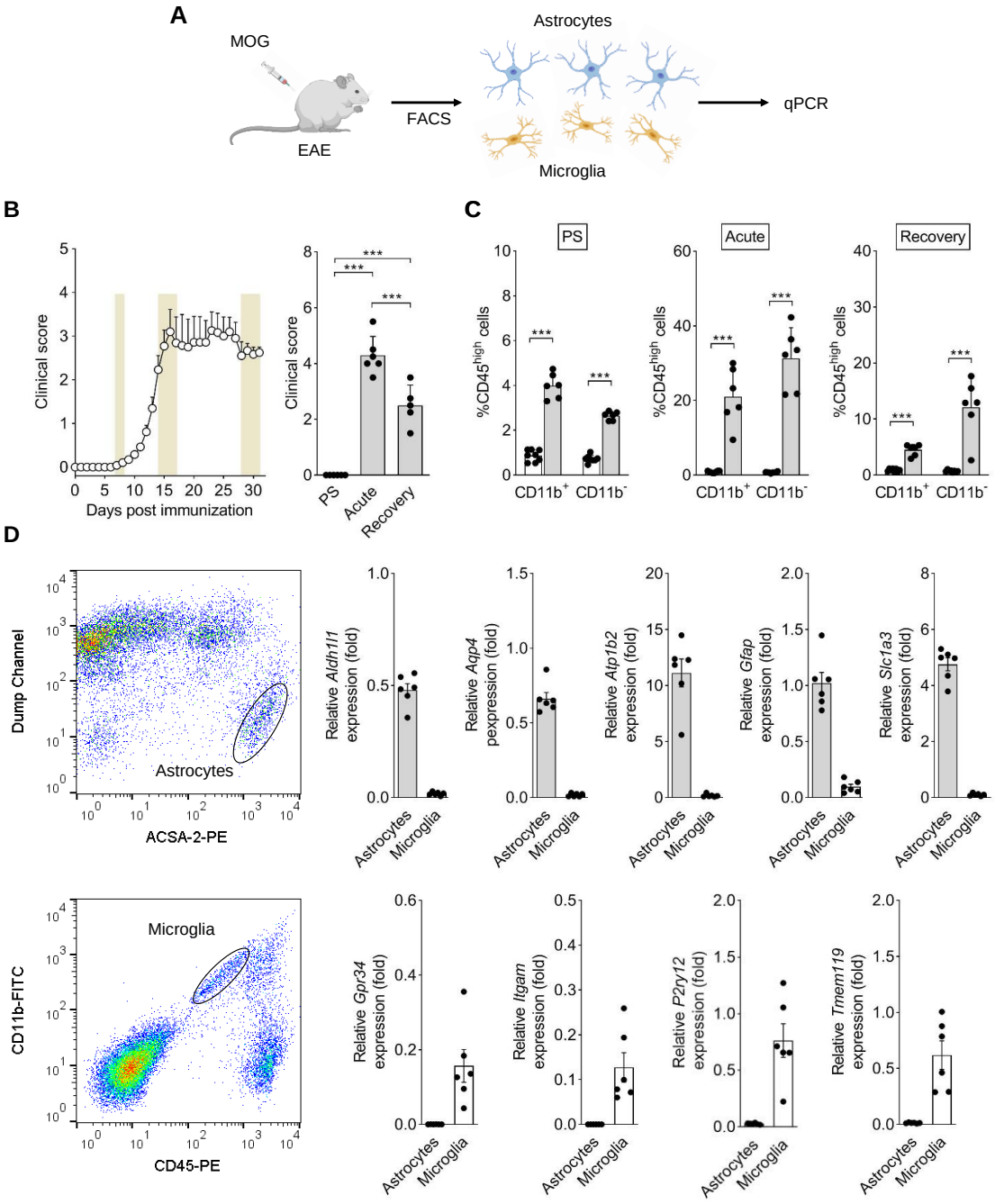

Figure 3. FACS sorting and purity of mouse CNS astrocytes and microglia purified during EAE. (**A**) Astrocytes and microglia were sequentially isolated from the forebrain and spinal cord of control and EAE mice. (**B**) Clinical score of the diseased animals used in the study (*n* = 18 mice; 2 independent EAE experiments). Cells were sorted from control and immunized mice at the presymptomatic (7-8 dpi), acute (14-17 dpi) and recovery (28-31 dpi) phases of the disease. *Right*: Neurological score of the EAE mice used for FACS analysis at each time-point (*n* = 6 mice per group). ***$p < 0.001$; 1-way ANOVA followed by Newman-Keuls tests. (**C**) Relative abundance of $CD11b^{+}CD45^{high}$ and $CD11b^{-}CD45^{high}$ peripheral immune cell populations in CNS single-cell suspensions from control (white bars) and EAE (grey bars) mice at presymptomatic, acute and recovery phases of the disease (*n* = 6-8 mice per condition). ***$p < 0.001$ referred to non-immunized mice; Student´s *t*-tests or Mann-Whitney *U*-tests. (**D**) Representative dot-plots and RT-qPCR analysis of astrocyte (*Aldh1l1*, *Aqp4*, *Atp1b2*, *Gfap*, *Slc1a3*) and microglia (*Gpr34*, *Itgam*, *P2ry12*, *Tmem119*) enriched genes in both cell types purified at acute EAE disease (*n* = 5-6 mice; normalized to astrocytic *Gfap*). PS, Presymptomatic.

2. Expression of neurotoxicity and inflammation related genes during EAE

2.1. EAE promotes neurotoxic astrocyte conversion

Recent tissue and cell-type specific transcriptomic studies suggest a relevant role for neurotoxic astrocytes in MS pathogenesis (Itoh 2018; Zhao 2020). However, the induction pattern of astrocytic A1 phenotype related genes in rodent models of the disease remains to be fully characterized. To address this question, we evaluated the expression of A1 phenotype associated genes in astrocytes purified by FACS at the different time-points of EAE progression. In parallel, we analyzed several genes associated to the protective A2 reactive phenotype, astrocyte pan-reactive genes as well as genes involved in astrocyte functions during autoimmune demyelination (Liddelow et al., 2017; Mayo et al., 2014; Rothhammer et al., 2016; Zamanian et al., 2012).

The results of our RT-qPCR screen show that astrocytes activated during EAE display increased levels of several pan-reactive genes (*Cxcl10*, *Gfap*, *Serpina3n*) (**Figure 4A**; **Table 4**) and reduced expression of several astrocytic markers (*Aldh1l1*, *Aqp4, Slc1a3*) (**Table 4**), thus matching previous observations (Itoh et al., 2018; Mayo et al., 2016). We also validated the up-regulation of genes involved in EAE, including *Ccl2*, *Ccl5* and *Nos2*, and genes of the interferon type I signaling pathway (*Stat1*, *Stat2*, *Irf9*, *Mx1*), at peak disease (**Table 4**) (Mayo et al., 2016; Rothhammer et al., 2016). In addition, astrocytes markedly upregulated the expression of several A1 reactive genes at acute EAE with many of these molecules remaining elevated during the recovery phase (**Figure 4A**; **Table 4**). Remarkably, a number of A1 genes were significantly up-regulated in astrocytes purified at asymptomatic disease, suggesting that transformation of these cells towards a neurotoxic phenotype is an early event during EAE and parallels the infiltration of peripheral immune cells into the CNS (**Figure 3C**; **Table 4**). Interestingly, we found a highly significant correlation between neurological disability and *C3* expression in astrocytes purified during acute EAE, but not in cells sorted at the recovery phase (**Figure 4B; Table 5**). However, the rest of A1 phenotype markers showed only non-significant trends or even inverse correlations with motor scores at acute or chronic disease stages (**Table 5**). On the other hand, the expression of astrocytic A2 signature genes was either unchanged or only modestly increased during the time-course of EAE (**Figure 4A**; **Table 4**). Normalization analysis of A1 and A2 genes indicated a greater induction of the neurotoxic-marker genes during the time-course of EAE progression (**Figure 4A**, *right panels*).

To corroborate the presence of A1 astrocytes in EAE we evaluated the expression of C3 in spinal cord astrocytes at the protein level. Double immunolabelling using antibodies for complement component C3 (Liddelow et al., 2017) and the astrocytic marker GFAP showed increased expression of C3 in white matter astrocytes from chronic EAE mice compared to naïve animals (**Figure 4E**). Our colocalization analyses also demonstrate a predominant C3 expression by astrocytes in white matter of EAE mice as ~75% of immunostaining lied on $GFAP^+$ processes (**Figure 4E**). Since astrocytic C3 has been associated with a neurotoxic phenotype of aberrant synapse stripping and myelin phagocytic activity (Lian et al., 2015; Liddelow et al., 2017), we analyzed the expression of several molecules regulating these functions in cells purified during EAE. The induction of astrocytic A1 reactive genes at acute disease was paralleled by a significant down-regulation of genes involved in neuroprotection (*Bdnf*), synapse formation (*Gpc4*, *Gpc6, Sparcl1*) and phagocytosis (*Megf10*, *Gas6*, *Axl*) (**Figure 4C**-**D**; **Table 4**). Cells purified at acute

disease also displayed increased levels of the astrocytic synaptogenic molecule *Thbs1* in good agreement with the changes reported following the *in vitro* and *in vivo* induction of A1 astrocytes (Liddelow et al., 2017; Tassoni et al., 2019). Most of these genes remained deregulated, albeit to a lesser extent, in astrocytes purified at the recovery phase of EAE thus mirroring deregulation of A1 phenotype markers (**Table 4**). Combined, these data suggest that astrocytes acquire neurotoxic phenotype associated to deficiencies in maintaining and/or promoting synapses and blunted myelin clearance capacity during the time-course of EAE.

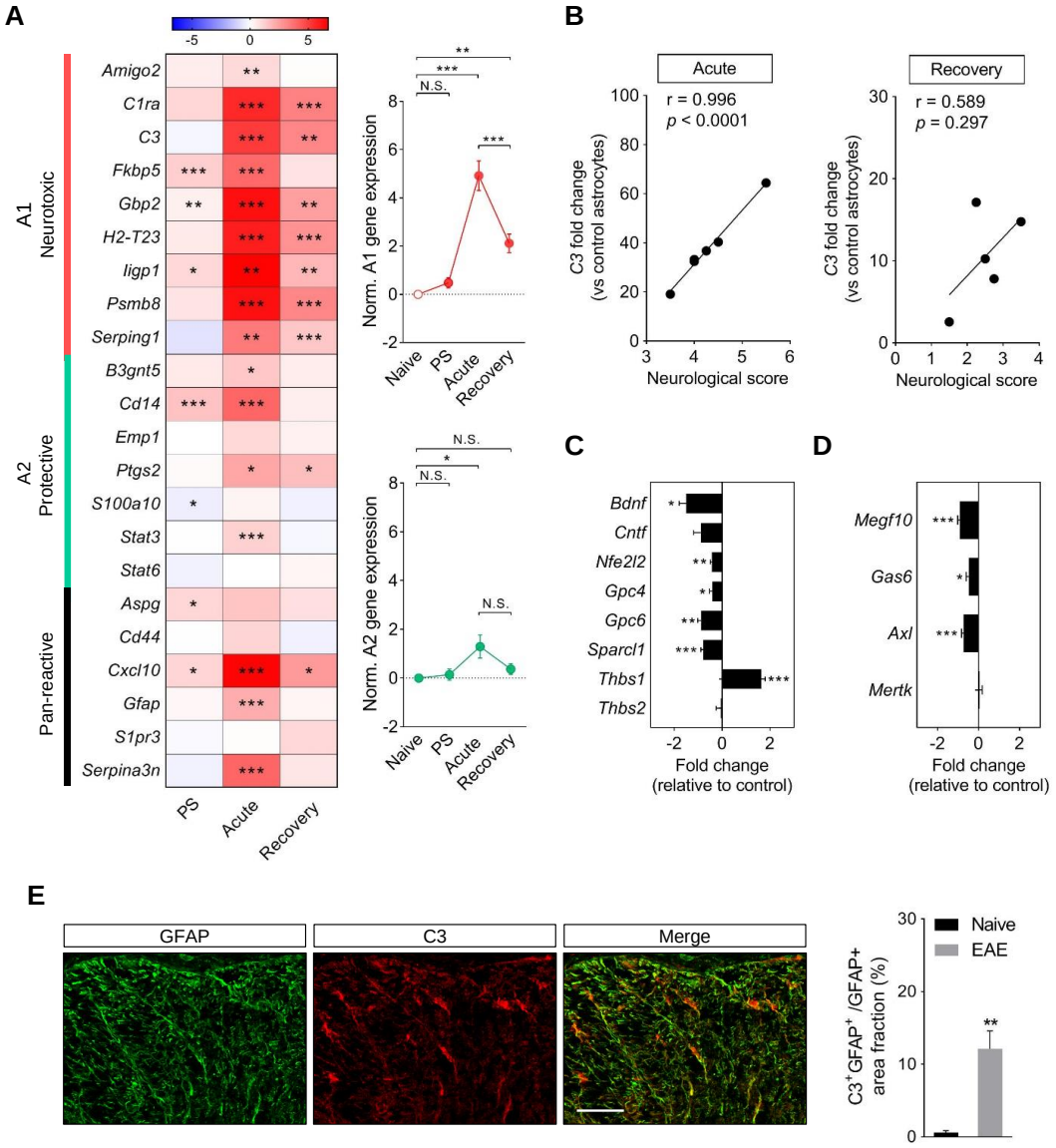

Figure 4. Modulation of astrocytic phenotype-associated genes during EAE. (**A**) Heat map depicting the mean expression of selected A1, A2 and pan-reactive genes in astrocytes purified from mice at the presymptomatic, acute and recovery stages of EAE as determined by RT-qPCR. *Right panel*: Histogram representation of normalized A1 and A2 gene expression during EAE progression. (**B**) Correlation between complement component *C3* gene expression in astrocytes ($2^{-\Delta\Delta Ct}$ values) and disease scores at acute and recovery EAE phases. (**C**-**D**) Fold change in mRNA expression of genes related to neuroprotection and synapse formation (**C**) and phagocytosis (**D**) in astrocytes sorted during acute EAE. Changes in relative expression were determined as $\log_2$. (**E**) Confocal images and quantification of C3 colocalization with the astrocytic marker GFAP in spinal cord white matter of chronic EAE mice (n = 3 mice; 35 dpi). Scale bar: 50 µm. PS, Presymptomatic. N.S., not statistically significant. *$p < 0.05$, **$p < 0.01$ and ***$p < 0.001$; referred to naïve astrocytes by Student´s *t*-tests or Mann-Whitney *U*-tests; 1-way ANOVA followed by Newman-Keuls tests (**A**, right panels).

2.2. Expression patterns of pro-inflammatory and protective genes in microglia

Activation of microglia in MS has been described as pro-inflammatory (also known as M1) and regenerating (regarded as M2) states (Chu et al., 2018; Hu et al., 2015) although more recent observations suggest a multidimensional model of activation (Ransohoff, 2016). Concerning findings during autoimmune demyelination, RNA-seq of microglia from EAE mice shows a changing phenotype over the course of the disease with an early-onset modulation of chemokines and molecules related to apoptotic cell uptake (Lewis et al., 2014). Consistent with these results, a number of genes associated to the induction and/or expression of pro-inflammatory responses by microglia such as *Ccl2*, *Ccl5*, *Cxcl2*, *Nos2* or *Stat1* displayed upregulated levels in cells purified from EAE mice, as determined by RT-qPCR (**Figure 5A**; **Table 6**). Although the induction of M1 phenotype genes was most remarkable at acute disease, some of these molecules were already upregulated in microglia isolated from animals at presymptomatic EAE, thus paralleling the early induction of A1 genes in astrocytes. These results sit well with the hypothesis that microglia activated during CNS disease facilitates the induction of a neurotoxic phenotype in astrocytes *in vivo* (Liddelow et al., 2017). It is also noteworthy, however, that some pro-inflammatory genes were either not modulated (*Il6*) or even down-regulated (*Il12a*, *Tnfa*) in microglia purified during EAE. On the other hand, most microglia M2 phenotype related genes displayed reduced expression (**Figure 5A**; **Table 6**). These observations regarding changes in the transcript levels of individual genes suggest that microglia in EAE predominantly display pro-inflammatory characteristics. However, normalization analysis showed no overall modulation of the M1 and M2 associated genes tested during the time-course of the disease (**Figure 5A**, *right panels*). These results contrast the marked induction of A1 genes in astrocytes (**Figure 4A**; **Table 4**) and match previous reports showing that a major subset of microglial cells exhibit an intermediate activation state during autoimmune demyelination (Vogel et al., 2013; Zabala et al., 2018).

2.3. EAE induces the expression of neurotoxic and pan-reactive astrocyte genes in microglia

According to recent reports, CNS disease conditions such as spinal cord injury and ALS induce an autologous expression of classical astrocyte-specific marker genes in microglia whose biological role is currently unknown (Chiu et al., 2013; Noristani et al., 2017). To understand if such processes are occurring in MS, we assessed the mRNA levels of pan-astrocytic genes and A1 phenotype markers in microglial cells purified during EAE. Consistent with previous observations (Noristani et al., 2017), microglia from EAE mice at acute disease over-expressed markers of reactive astrogliosis such as *Gfap*, *Serpina3n, S1pr3* and *Cd44* (**Figure 5B**; **Table 6**). Furthermore, gene expression responses of microglial cells during EAE mirrored the upregulated expression of A1 genes in astrocytes, with increased levels of complement components *C1ra* and *C3*, among other phenotype markers (**Figure 5B**; **Table 6**). However, none of the A1 genes tested exhibited significant correlation with disease scores at acute or chronic EAE (**Table 5**). These findings indicate that the induction of genes associated to the expression of a neurotoxic astrocyte phenotype is not exclusive to this cell population during EAE. However, deregulation of *C3* in microglia did not significantly correlate with the severity of disease scores at acute or chronic EAE disease (**Figure 5C**). In all, these results argue against the pathological relevance of A1 gene expression in microglial cells during EAE.

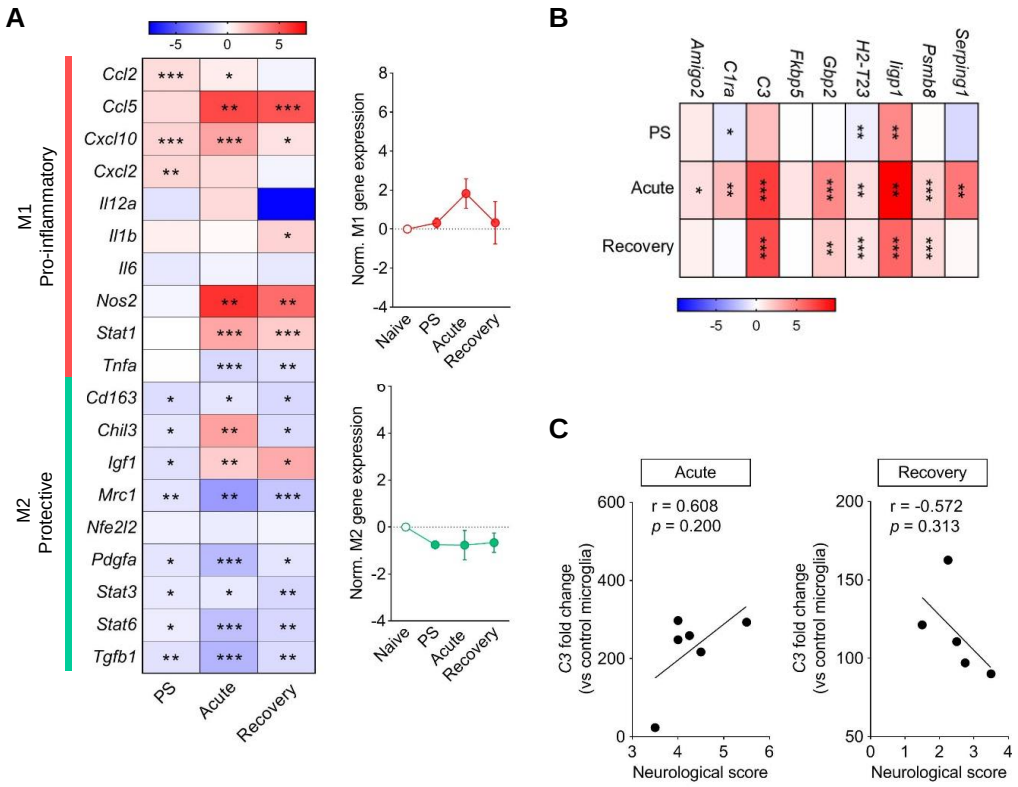

Figure 5. Pro-inflammatory and anti-inflammatory gene expressions in microglia isolated during EAE. Heat maps depict the mean expression of M1 and M2 phenotype-associated genes (**A**) and selected pan-reactive and A1 neurotoxic genes (**B**) in microglial cells purified from mice at presymptomatic, acute and recovery stages of EAE, as determined by RT-qPCR (n = 5-6 mice). Statistical analysis by 1-way ANOVA determined no overall deregulation of M1 or M2 gene transcripts during disease progression. *Right panel* in **A**: Histograms represent normalized M1 and M2 gene expression during EAE progression. (**C**) Correlation between complement *C3* gene expression in microglia ($2^{-\Delta\Delta Ct}$ values) and disease scores at acute and recovery EAE phases. PS, Presymptomatic. N.S., not statistically significant. *$p < 0.05$, **$p < 0.01$ and ***$p < 0.001$; referred to microglia purified from naïve mice by Student´s t-tests or Mann-Whitney U-tests.

3. Gene expression analysis of endocannabinoid system related genes during EAE

3.1. Early deregulation of endocannabinoid signaling genes in astrocytes

To investigate the role of endocannabinoids in regulating astrocyte dysfunction in MS we analyzed the expression of the principal endocannabinoid signaling molecules in cells purified during EAE progression using a microfluidic RT-qPCR screen. Interestingly, astrocytes isolated at asymptomatic disease showed significant modulation of several endocannabinoid system associated genes (**Figure 6A**-**C**; **Table 4**). In particular, we measured increased levels of *Napepld* together with a marked reduction in *Fabp7* thereby suggesting enhanced AEA dependent signaling, although these alterations were concomitant with augmented *Faah* levels. In addition, presymptomatic EAE astrocytes displayed down-regulated expression of the main 2-AG hydrolytic enzymes *Mgll* and *Abhd6* without changes in the α form of DAGL (*Dagla*), primary responsible of 2-AG synthesis in astroglial cells (Viader et al., 2016).

Astrocytes isolated from acute EAE mice exhibited reductions in all endocannabinoid metabolism-associated genes, with the exception of *Faah*, which persisted at chronic disease. Blunted expression of endocannabinoid hydrolysis genes was associated to reduced *Cnr1* levels both at acute and recovery phases suggesting deficient astrocytic CB_1R-mediated signaling associated to disease progression. Cannabinoid CB_2R transcripts were not detected in astrocytes from naïve or EAE mice at any stage of disease progression. This result is in general agreement with previous pharmacological studies in cultured cells that support only a marginal expression of CB_2R in astroglial cells (Stella, 2010). On the other hand, we also measured down-regulated expression of *Dagla* and/or *Daglb* without changes in *Napepld* levels, suggesting a selective impairment of astrocytic 2-AG biosynthesis that parallels deficits in hydrolysis-related genes at acute and chronic disease stages.

3.2. Modulation of endocannabinoid signaling genes in microglia

We next assessed the expression level of endocannabinoid signaling associated genes in microglia purified over the course of EAE. In contrast to our observations in astrocytes, expression of *Cnr1* was not detected by RT-qPCR in naïve or EAE microglia. Conversely, *Cnr2* transcripts were expressed in cells from non-immunized mice but not significantly modulated over the course of EAE (**Figure 6B**-**C**; **Table 6**). Interestingly, microglia isolated from the CNS of EAE mice displayed changes in the expression levels of genes involved in 2-AG metabolism reminiscent to the ones observed in astrocytes during disease progression, albeit to a higher extent. In particular, our results show down-regulation of 2-AG hydrolytic enzymes *Mgll*, *Abhd6* and *Abhd12* in microglia purified at asymptomatic disease as well as at the peak of the symptoms (**Figure 6B**-**C**; **Table 6**). In parallel, microglial cells exhibited an early onset reduction in the expression of *Dagla* and *Daglb* suggesting deficient 2-AG production at early EAE stages associated to impaired metabolism. Most of these transcriptional changes were present even though in lesser magnitude in microglial cells isolated from mice at the recovery phase of EAE. On the other hand, genes involved in AEA biosynthesis and metabolism were not significantly modulated in microglia at presymptomatic disease. Cells purified at acute and chronic disease stages, however, displayed a significant down-regulation of *Faah* paralleled by increased *Naaa* levels, without changes in the expression of *Napepld* or *Fabp7*. In sum, our results indicate that astrocytes and microglia differ in their transcriptional modulation of AEA signaling related genes during EAE.

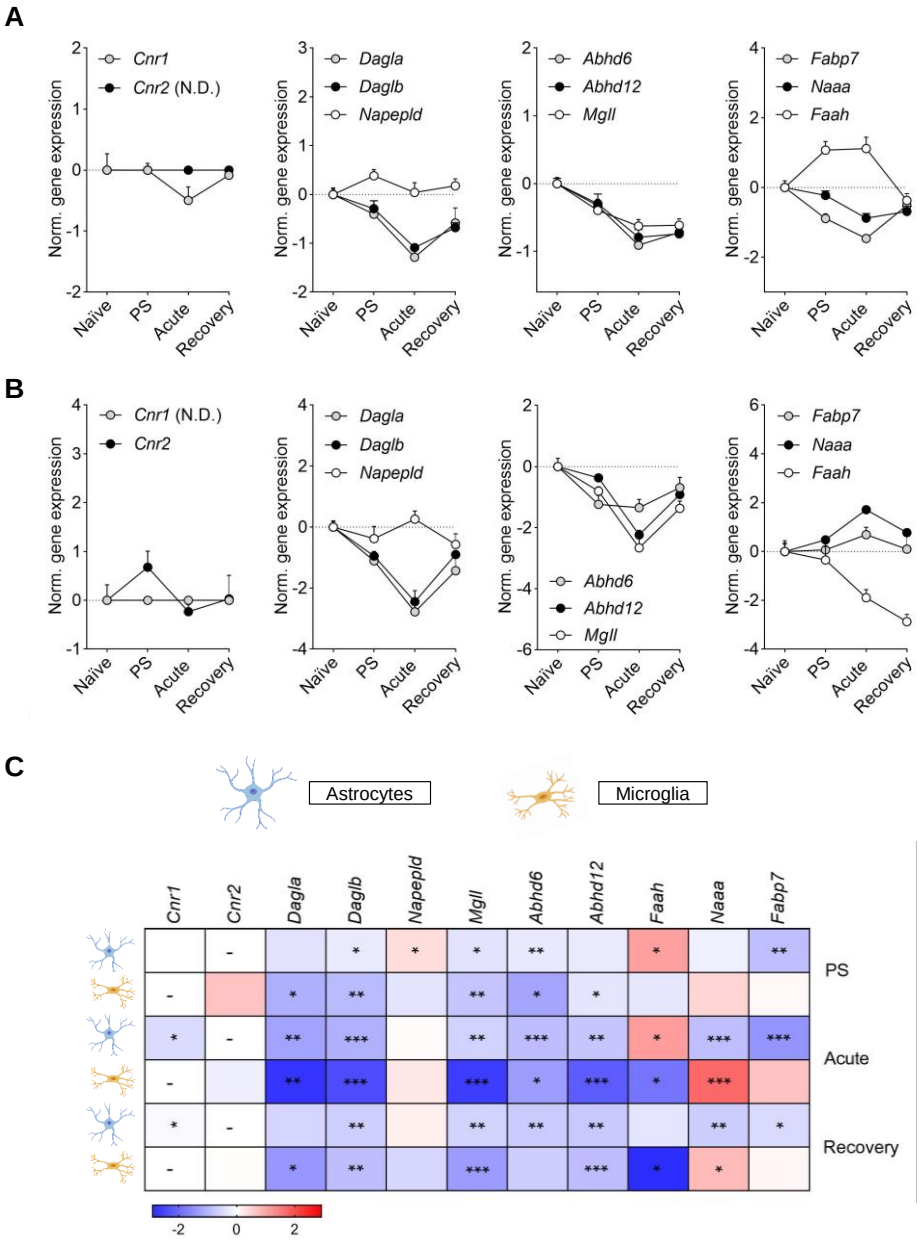

Figure 6. Deregulated expression of astrocytic and microglial endocannabinoid signaling genes during EAE. RT-qPCR analysis of endocannabinoid system-related genes in astrocytes (**A**) and microglia (**B**) purified at presymptomatic, acute and recovery phases of EAE. (**C**) Fold changes in relative expression compared to naïve cells were determined as $\log_2$ (n = 5-6 mice group). (-) not detected. PS, Presymptomatic. *p < 0.05, **p < 0.01, and ***p < 0.001; referred to naïve astrocytes or microglia by Student´s t-tests or Mann-Whitney U-tests.

4. Astrocyte Ca^{2+} dynamics during autoimmune demyelination

Fiber photometry based on GECIs has emerged as an ideal approach to dissect the functions of astrocytes in physiopathological conditions as it allows deep-tissue measurements in freely behaving animals, thus avoiding anesthesia and restrain-associated stress interferences in Ca^{2+} dynamics (Patel et al., 2020). In this study, we applied the fiber photometry approach to the analysis of astrocytic Ca^{2+} responses and their modulation by CB_1Rs in the mouse somatosensory cortex both in control and EAE mice.

4.1. Analysis of astrocyte Ca^{2+} activity in vivo

To study astrocytic Ca^{2+} responses in the cortex of freely behaving mice we used GCaMP6f because previous *in vivo* characterization studies have demonstrated its higher sensitivity compared to that of commonly used synthetic Ca^{2+} dyes (Chen et al., 2013). Mice were injected AAV-GFAP-GCaMP6f viral particles expressing the Ca^{2+} probe under the promoter of human GFAP. Histological analysis of *postmortem* tissue showed specific expression of the Ca^{2+} sensor in astrocytes in the area surrounding the viral injection (**Figure 7A**). We confirmed the specificity and selectivity of AAV-GFAP-GCaMP6f expression in astrocytes by double immunostaining for GFAP and GFP (**Figure 7C**).

4.1.1. Activation of CB_1 receptors enhances Ca^{2+} activity in cortical astrocytes

We next investigated the effect of cannabinoid treatment on astrocytic Ca^{2+} responses in the somatosensory cortex of CB_1-WT and CB_1-KO mice (Marsicano et al., 2002). Fiber photometry recordings were performed in mice carrying astroglial GCaMP6f treated with vehicle and Δ^9-THC (10 mg/Kg; i.p.) after a baseline recording period (**Figure 8**). The amplitude, duration and frequency of recorded Ca^{2+} events were analyzed in 2 equal time-periods of 15 min each after vehicle or Δ^9-THC injection (**Figure 7B**). Drug administration did not significantly modulate astrocyte Ca^{2+} signals during the first 15 min of recording. However, Δ^9-THC significantly increased the amplitude and duration of astroglial Ca^{2+} transients in the somatosensory cortex of CB_1-WT but not in CB_1-KO mice (**Figure 8A**-**D**). Treatment with Δ^9-THC did not modulate the frequency of Ca^{2+} transients in cortical astrocytes (**Figure 8E**). On the other hand, no significant differences were observed between CB_1-WT mice and CB_1-KO littermates concerning the dynamics of astroglial Ca^{2+} events recorded during the baseline period (**Figure 8F**). Thus, systemic Δ^9-THC increases astrocyte Ca^{2+} activity in the somatosensory cortex of freely behaving mice through the activation of CB_1Rs.

To decipher whether the increase of astroglial Ca^{2+} activity induced by Δ^9-THC is mediated by CB_1Rs present in astrocytes, we performed fiber photometry recordings in conditional mutant mice lacking CB_1Rs in GFAP-positive cells (GFAP-CB_1-KO mice) (Han et al., 2012) (**Figure 9A**-**D**). Animals received tamoxifen injections 1 week after the surgery and were used for *in vivo* imaging experiments after a 3 weeks washout period (see methods for further details). Systemic Δ^9-THC did not modulate the dynamics of astroglial Ca^{2+}events in the somatosensory cortex of GFAP-CB_1-KO mice while reliably increased the amplitude of Ca^{2+} signals in control littermates recorded in parallel (GFAP-CB_1-WT) (**Figure 9A**-**C**). By contrast, Δ^9-THC injection did not modulate the duration and frequency of astrocytic Ca^{2+} events in GFAP-CB_1-WT and GFAP-CB_1-KO mice (**Figure 9D**-**E**).

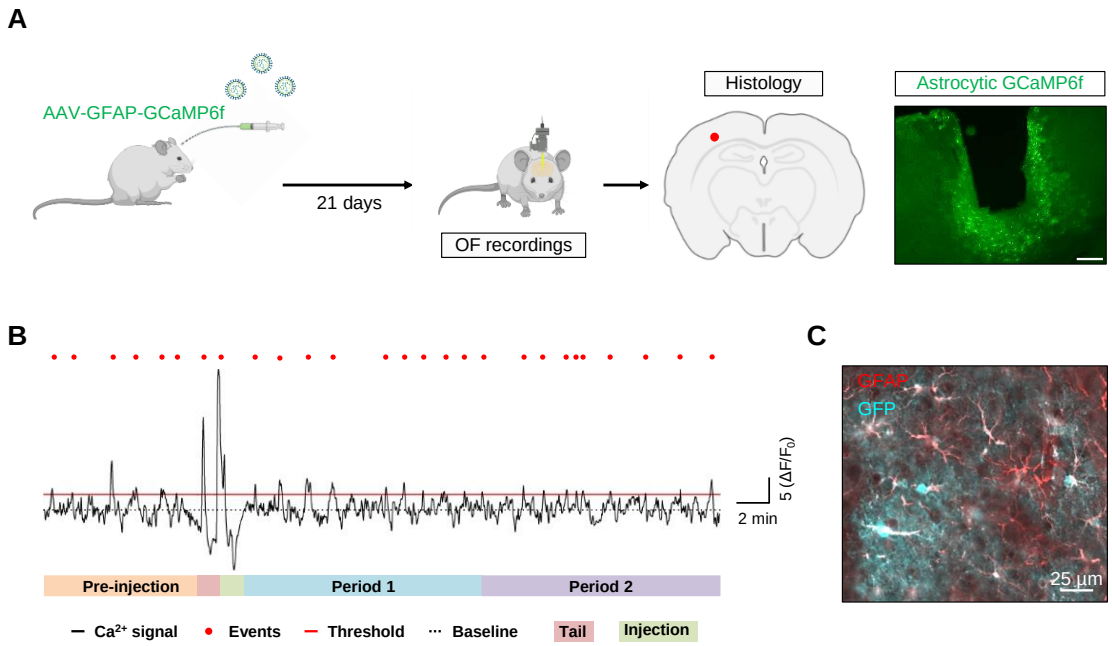

Figure 7. Monitoring astrocytic Ca^{2+} activity in freely behaving mice. (**A**) Experimental fiber photometry approach for *in vivo* recording of astrocytic Ca^{2+} dynamics in mouse cortex. Mice were injected stereotactically in the somatosensory cortex with AAV vectors encoding GCaMP6f under the control of the *Gfa*-ABC$_1$D promoter and the optical fiber (OF) placed above the injection site during the same surgical session. OF recordings were performed 3 weeks after the surgery and expression of AAV-GFAP-GCaMP6fs at the injection site corroborated by fluorescence microscopy. Scale bar: 150 µm. (**B**) Representative PF experiment showing 1) spontaneous astrocytic Ca^{2+} transients in the mouse cortex during the pre-injection period, 2) Ca^{2+} responses evoked by tail-holding and vehicle-injection and 3) Ca^{2+} dynamics during consecutive post-injection periods (Period 1 and Period 2). Red dots depict Ca^{2+} transients detected above threshold (median+2*MAD) and considered for the analysis of duration and frequency. (**C**) Representative image showing GFAP (red) and GFP (cyan) immunostaining in the cortex of mice injected with AAV-GFAP-GCaMP6f. GFP^+ cells surrounding the probe were 94.9 ± 4.88% positive for the astrocytic marker GFAP and 96.9 ± 3.25% of the $GFAP^+$ cells were immunopositive for GFP (*n* = 6 mice).

Noteworthy, GFAP-CB$_1$-KO mice displayed reduced duration and increased frequency of spontaneous Ca^{2+} events recorded during the baseline period as compared to GFAP-CB$_1$-WT littermates, whereas the amplitude of Ca^{2+} transients was unaffected (**Figure 9F**). These results indicate that astrocytic CB$_1$Rs mediate the increase in the amplitude of cytosolic Ca^{2+} transients induced by systemically administered Δ^9-THC and suggest the existence of an endocannabinoid tone positively modulating astroglial Ca^{2+} dynamics in the somatosensory cortex of living mice.

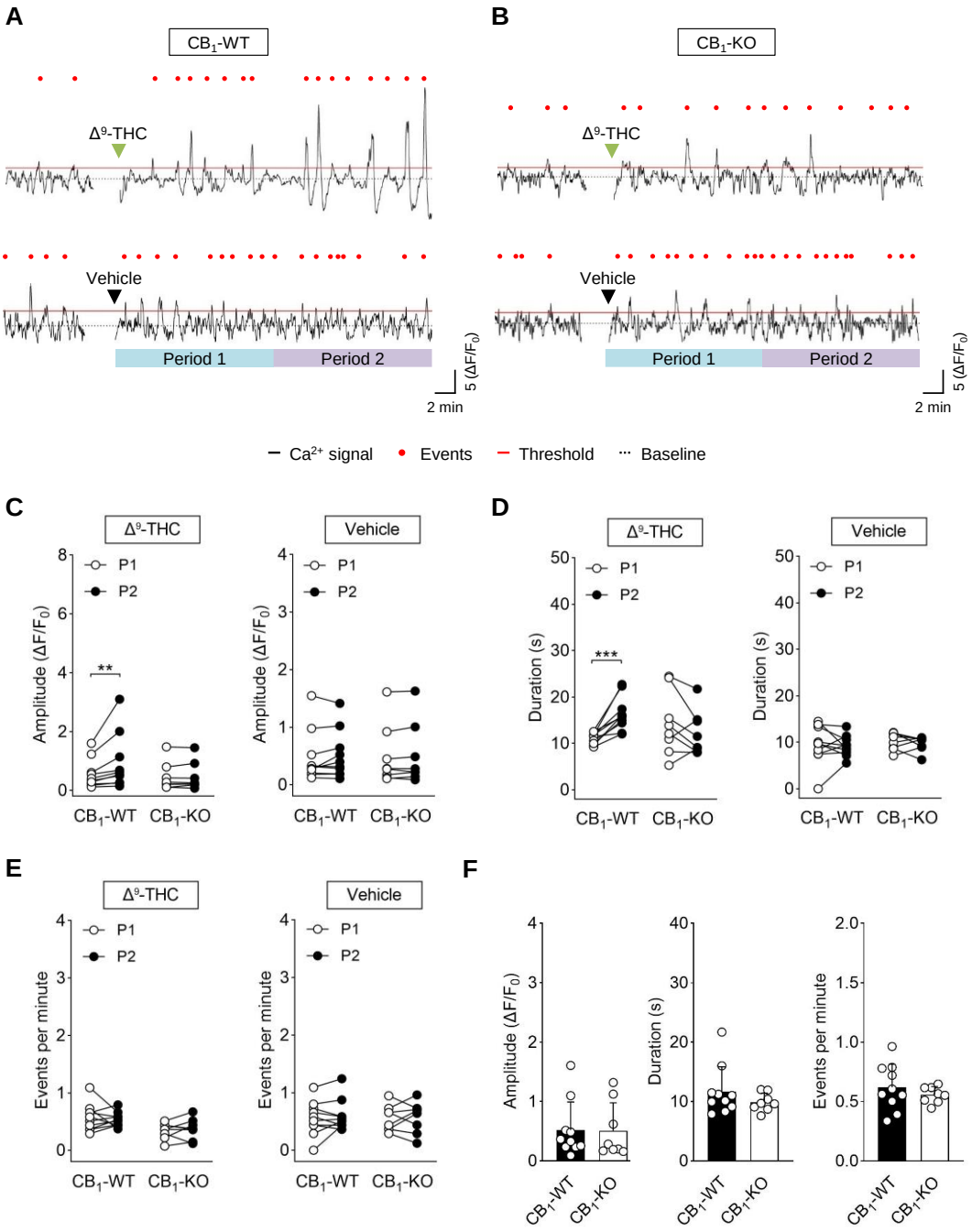

Figure 8. CB_1 receptor activation increases astrocytic Ca^{2+} in the cortex of freely behaving mice. Representative traces from the somatosensory cortex of CB_1-WT (**A**) and CB_1-KO (**B**) mice injected with AAV-GFAP-GCaMP6fs and treated with Δ^9-THC (10 mg/Kg; i.p.) (top panels) or vehicle (bottom panels). Colored rectangles depict post-injection periods (Period 1, blue; Period 2, purple) considered for analysis. Comparison of amplitude (**C**), duration (**D**) and frequency (**E**) of Ca^{2+} transients recorded from CB_1-WT and CB_1-KO mice following Δ^9-THC or vehicle injection (n = 8-10 mice per group). (**F**) Amplitude, duration and frequency of spontaneous Ca^{2+} transients recorded in CB_1-WT and CB_1-KO mice during the pre-injection period. P1, Period 1; P2, Period 2. $^{**}p < 0.01$ and $^{***}p < 0.001$; 2-way ANOVA followed by Šídák's multiple comparisons tests (**C**-**E**) and Student´s *t*-tests or Mann-Whitney *U*-tests (**F**).

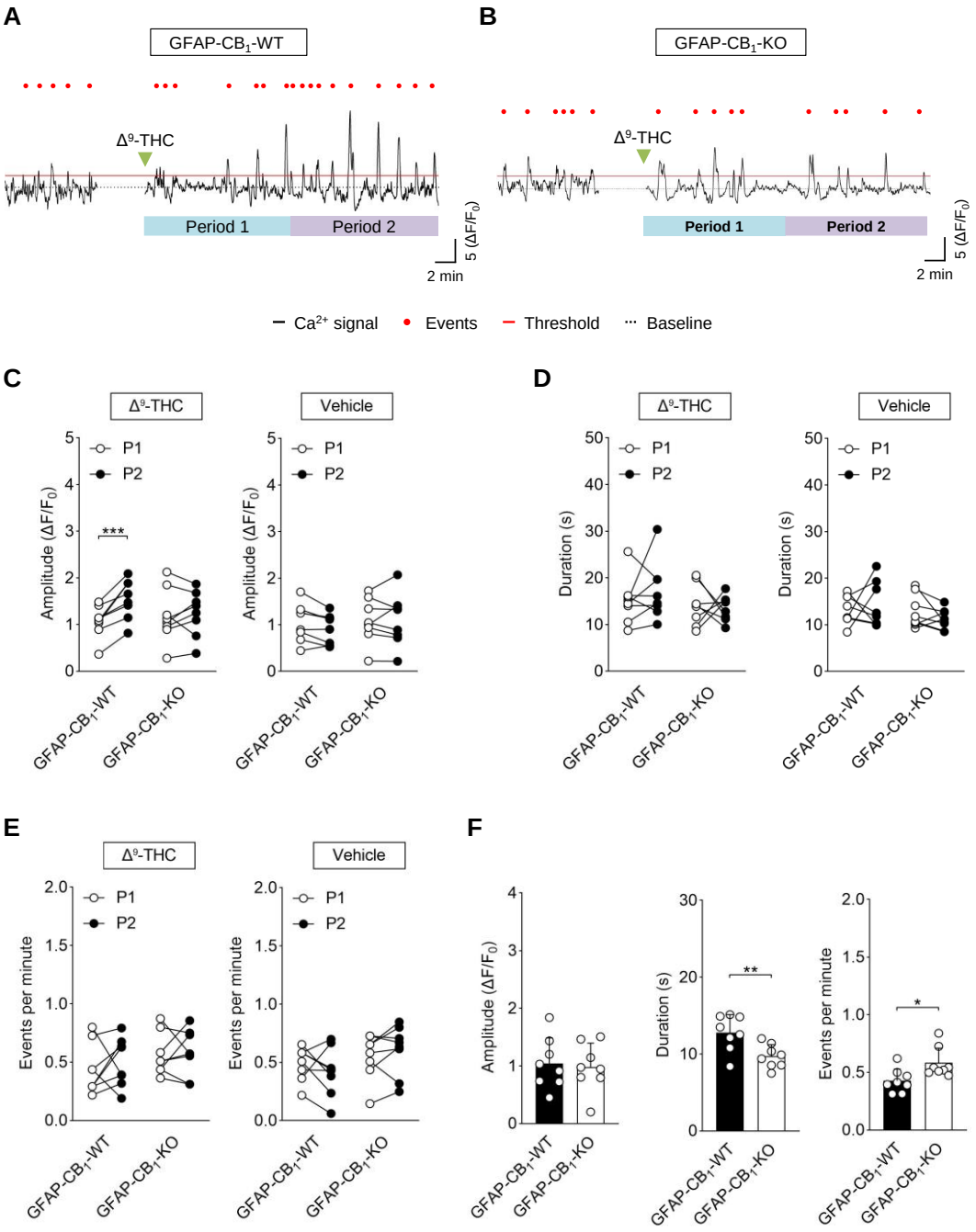

Figure 9. Astrocytic CB_1 receptors mediate Ca^{2+} responses in the mouse cortex by systemic Δ^9-THC. Representative recordings from the somatosensory cortex of GFAP-CB_1-WT (**A**) and GFAP-CB_1-KO (**B**) mice injected with AAV-GFAP-GCaMP6fs and treated with Δ^9-THC (10 mg/Kg; i.p.). Comparison of amplitude (**B**), duration (**C**) and frequency (**D**) of Ca^{2+} transients between GFAP-CB_1-KO and GFAP-CB_1-WT control littermates following vehicle and Δ^9-THC injection. (**E**) Amplitude, duration and frequency of Ca^{2+} transients recorded in GFAP-CB_1-WT and GFAP-CB_1-KO mice during baseline recordings. P1, Period 1; P2, Period 2. *$p < 0.05$, **$p < 0.01$ and ***$p < 0.001$; 2-way ANOVA followed by Šídák's multiple comparisons tests (**C**-**E**) and Student´s *t*-tests or Mann-Whitney *U*-tests (**F**).

4.1.2. Cortical astrocytes exhibit deregulated Ca^{2+} dynamics during EAE

A growing body of evidence suggest that aberrant astrocytic Ca^{2+} activity patterns may contribute to neuronal functional deficits in the diseased CNS (Mizuno et al., 2018; Verkhratsky and Nedergaard, 2018). Related to MS, recent reports suggest the existence of a dysregulated cortical network linked to elevated anxiety and neurodegeneration in the EAE mouse model (Ellwardt et al., 2018). However, whether EAE cortical pathology is associated to changes in astrocytic Ca^{2+} dynamics remains to be addressed. To answer this question we measured astroglial Ca^{2+} transients at different time points during EAE progression in animals carrying astroglial GCaMP6f. The first clinical manifestations occurred at 10 dpi with acute disease peaking at 18 dpi and attenuation of disease severity taking place at later time-points (**Figure 10A**).

Astrocyte Ca^{2+} signals in the mouse cortex can occur both spontaneously or in response to endogenous or exogenous stimuli such tail-holding or whisker stimulation (Qin et al., 2020; Wang et al., 2006). In our experimental settings, tail-holding evoked reliable Ca^{2+} responses in cortical astrocytes from control mice that remained stable in size during the chronic recording period (**Figure 10C**-**D**). Induction of EAE was associated to a significantly decreased amplitude of astrocytic Ca^{2+} responses evoked by tail-holding that paralleled symptom onset (**Figure 10B**-**C, E**). By contrast, the duration of evoked astrocyte Ca^{2+} signals remained unchanged during the time course of EAE. We next investigated the possible relationship between deregulated Ca^{2+} responses in cortical astrocytes and disease severity. We observed an inverse correlation between motor score values and astrocyte Ca^{2+} responses evoked by tail-holding during EAE progression that reached statistical significance at 17 and 19 dpi (**Figure 10F**).

We next analyzed the dynamics of spontaneous astrocytic Ca^{2+} signals during EAE progression. Reminiscent of our previous observations concerning evoked Ca^{2+} responses, the onset of EAE symptomatology was associated to a progressive decline in the amplitude of spontaneous Ca^{2+} transients in cortical astrocytes that reached a plateau at 14 dpi (**Figure 11A**-**C**). Further analysis showed that spontaneous Ca^{2+} activity in EAE astrocytes displays events of increased duration and reduced frequency as compared to control animals recorded in parallel (**Figure 11A**-**E**). The observed impairments in the amplitude of spontaneous Ca^{2+} transients correlated to EAE clinical severity during EAE progression (**Figure 12A**). However, changes in the duration and frequency of astroglial Ca^{2+} signals did not correlate to neurological disability at any of the time-points tested (**Figure 12B**-**C**). Overall, these results show that EAE induces a shift in astrocytic Ca^{2+} activity in the mouse cortex that could both reflect and contribute to disease symptomatology.

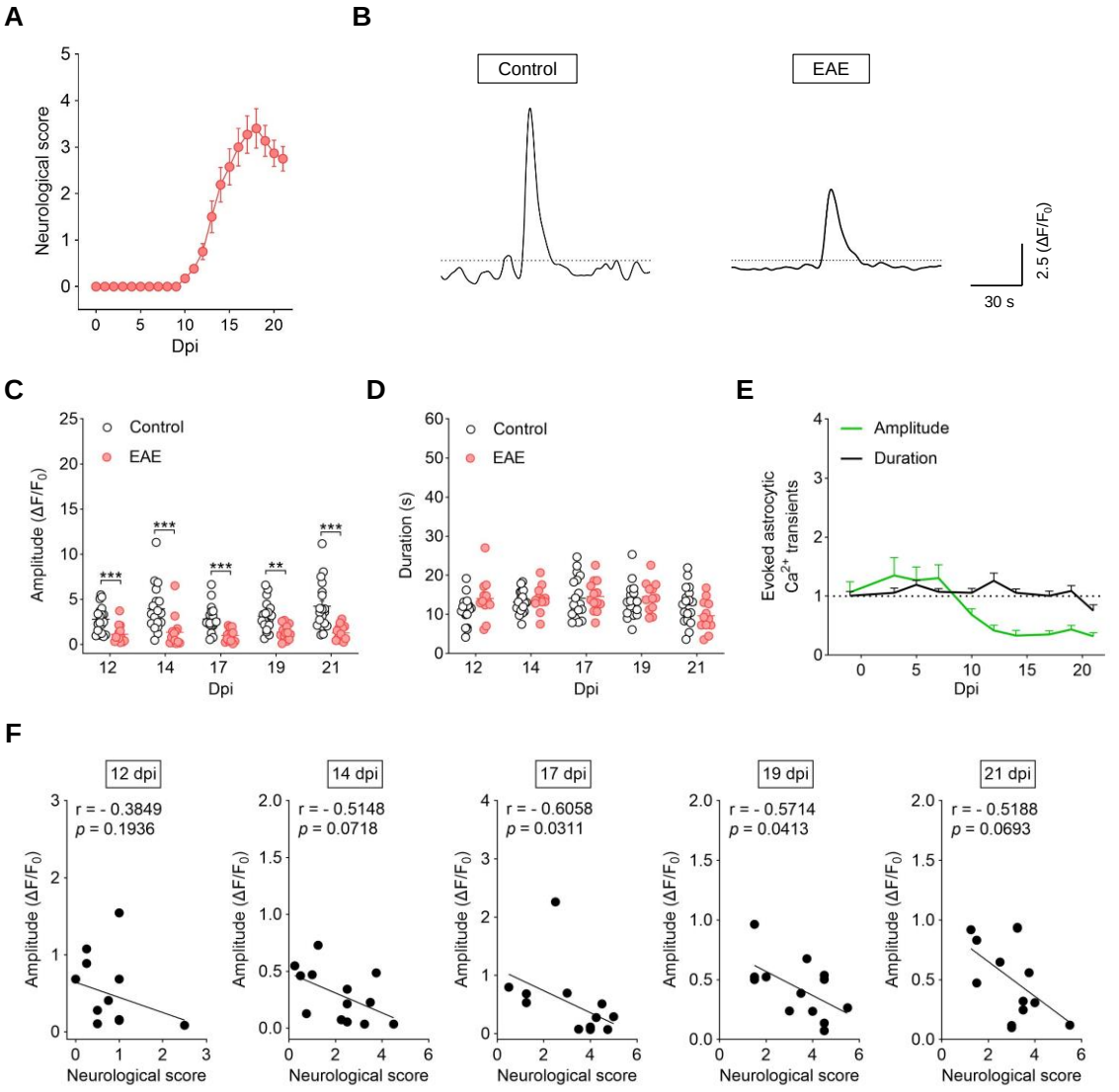

Figure 10. EAE impairs astrocytic Ca^{2+} responses evoked *in vivo*. (**A**) Neurological score of EAE mice included in the study (*n* = 13 mice; 3 independent EAE experiments). (**B**) Representative traces showing astrocytic Ca^{2+} responses evoked by tail-holding in the cortex of control (left panel) and EAE (right panel; 17 dpi) mice. Amplitude (**C**) and duration (**D**) of Ca^{2+} responses evoked in immunized mice at different time-points of disease progression as compared to control mice recorded in parallel (*n* = 19 mice). $^{**}p < 0.01$ and $^{***}p < 0.001$; Student´s *t*-tests or Mann-Whitney *U*-tests. (**E**) Time-course of normalized amplitude and duration of astrocytic Ca^{2+} transients during EAE progression. Raw data from immunized mice were expressed relative to values from control animals recorded in parallel at each time point. (**F**) Deregulation of evoked astrocytic Ca^{2+} responses and neurological disability during EAE progression. Raw data from EAE mice were normalized to pre-immunization values and plotted against disease scores. Pearson's or Spearman's correlation coefficients and *p* values are indicated in each dot plot.

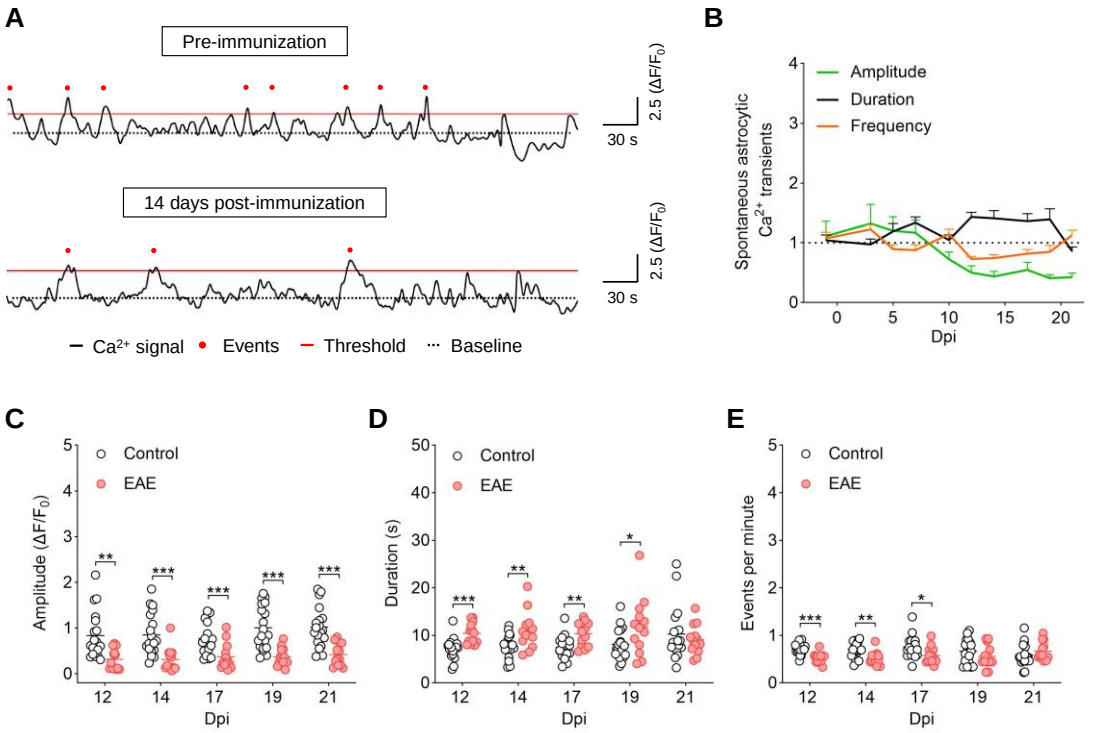

Figure 11. Aberrant spontaneous Ca^{2+} activity of cortical astrocytes during EAE. (**A**) Spontaneous Ca^{2+} transients in cortical astrocytes from a mouse injected with AAV-GFAP-GCaMP6fs and recorded during EAE (bottom panel; 14 dpi) as compared to the pre-immunization phase (top panel). (**B**) Time-course of normalized amplitude, duration and frequency of astrocytic Ca^{2+} transients recorded during EAE progression. Raw data recorded from EAE mice were expressed relative to values from control animals recorded in parallel (*n* = 13-19 mice). Amplitude (**C**), duration (**D**) and frequency (**E**) of spontaneous Ca^{2+} responses recorded from control and EAE mice at different time-points of disease progression. **p* < 0.05, ***p* < 0.01 and ****p* < 0.001; Student´s *t*-tests or Mann-Whitney *U*-tests.

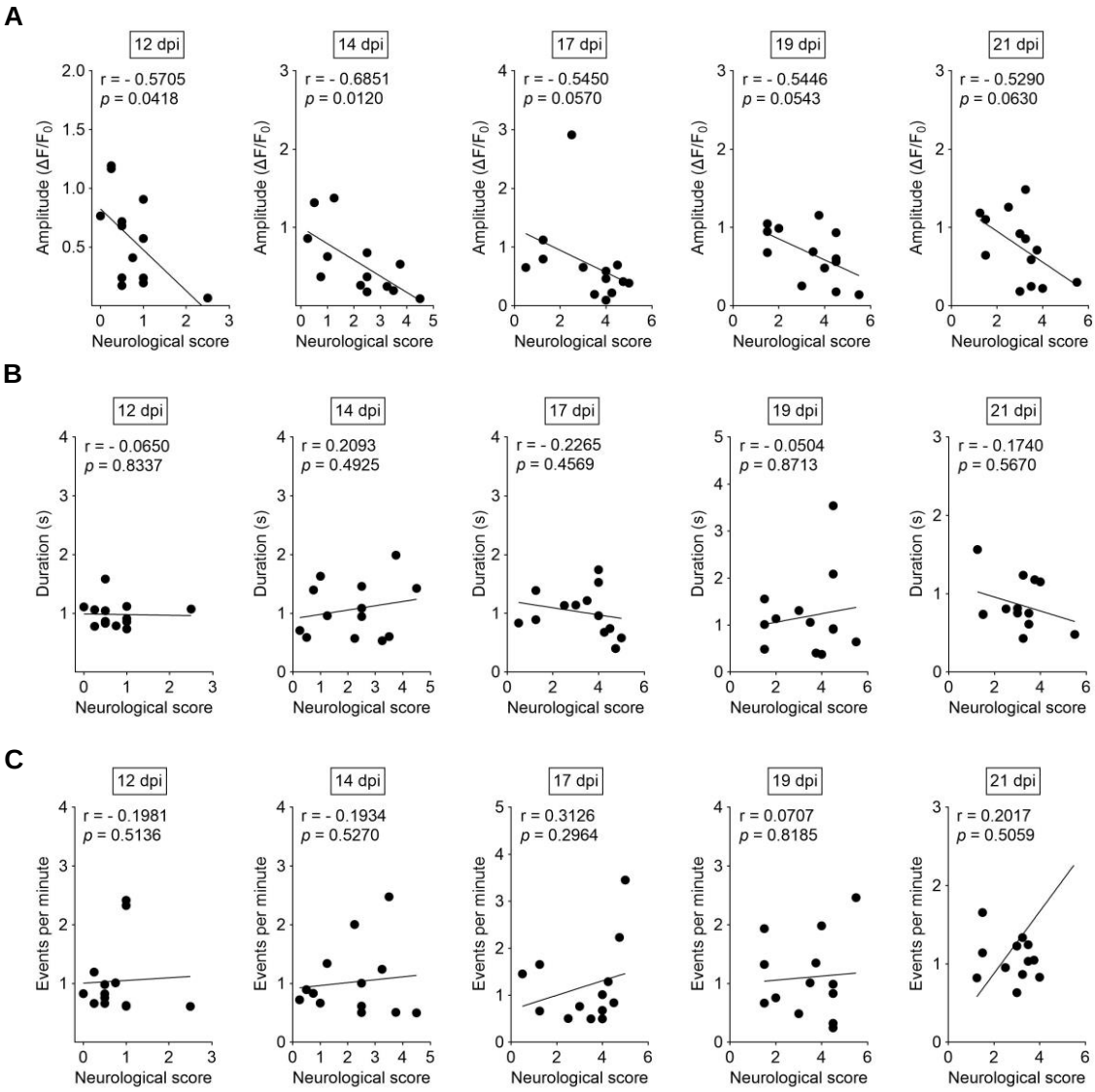

Figure 12. Deficient Ca^{2+} activity of cortical astrocytes during EAE: association to disease severity. (**A**) Amplitude, (**B**) Duration and (**C**) Frequency of astrocytic Ca^{2+} events. Raw data from EAE mice were normalized to pre-symptomatic phase (7 dpi) values and plotted against neurological scores. Pearson's or Spearman's correlation coefficients and *p* values are indicated in each dot plot.

4.1.3. EAE impairs CB_1 receptor-mediated Ca^{2+} responses in cortical astrocytes

Next, we explored whether the observed changes in the activity patterns of astrocytic Ca^{2+} during EAE involved deficient regulation of cytosolic Ca^{2+} levels by CB_1Rs. Mice subjected to EAE were sequentially challenged with vehicle and Δ^9-THC (10 mg/Kg; i.p.) at 20-21 dpi in 2 consecutive sessions separated 24 hours. Injection of Δ^9-THC did not significantly modulate the dynamics of astroglial Ca^{2+} events in the somatosensory cortex of EAE mice during the recording session (**Figure 13**). By contrast, and corroborating our previous observations (**Figures 8**-**9**), systemically administered Δ^9-THC effectively increased the amplitude and duration of astroglial Ca^{2+} transients during the second half of the recordings in control non-immunized mice chronically monitored over several weeks (**Figure 13B**-**C**). The cannabinoid agonist did not induce changes in the frequency of astrocyte Ca^{2+} events in control or EAE mice (**Figure 13C**-**D**). Thus, EAE is associated to deficient astrocytic Ca^{2+} responses mediated by CB_1Rs in the somatosensory cortex. These results suggest that impairments in spontaneous astrocytic Ca^{2+} activity during disease progression may reflect, at least in part, abnormal endocannabinoid mediated signaling through astrocyte CB_1Rs.

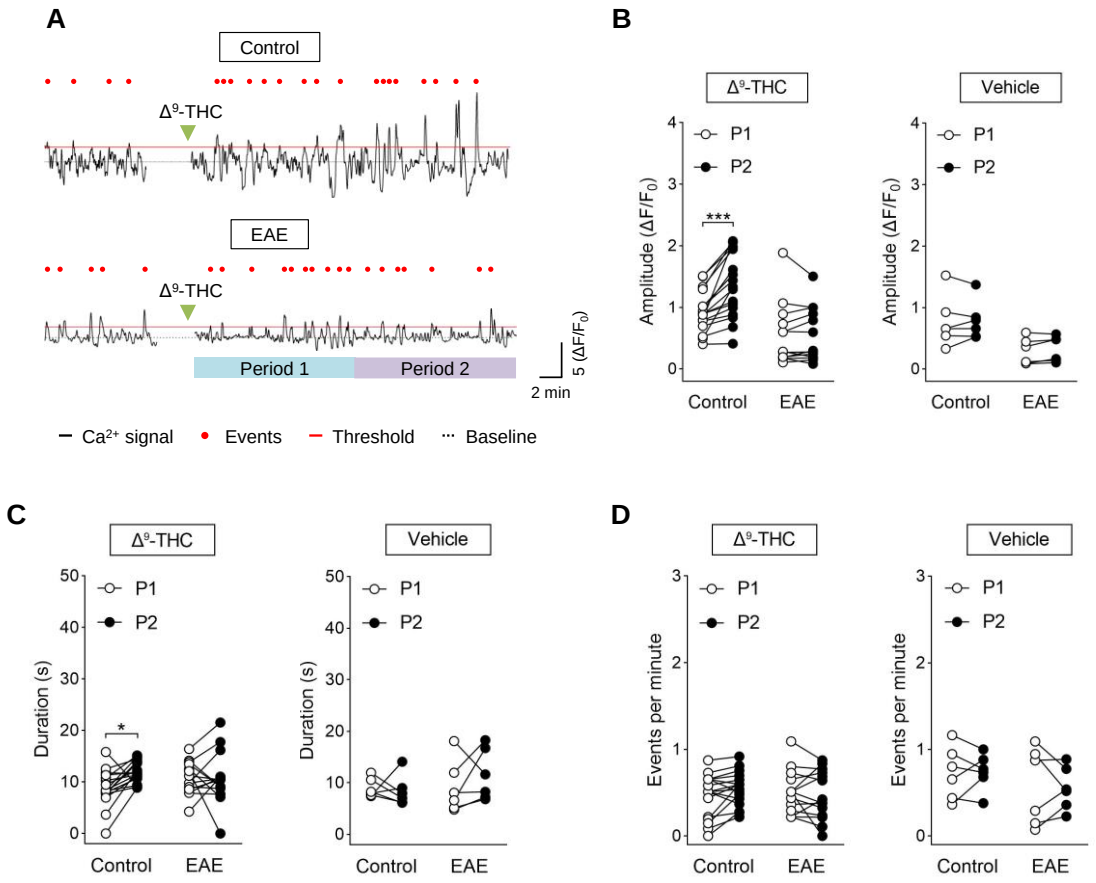

Figure 13. EAE impairs CB_1 receptor-mediated astrocytic Ca^{2+} responses in the mouse cortex. (**A**) Representative recordings from the mouse somatosensory cortex showing the effect of Δ^9-THC (10 mg/Kg; i.p.) on astrocytic Ca^{2+} activity in control (top panel) and EAE (21 dpi; bottom panel) mice. Amplitude (**B**), duration (**C**) and frequency (**D**) of astrocytic Ca^{2+} responses to Δ^9-THC or vehicle in control and EAE mice (n = 6-17 mice). P1, Period 1; P2, Period 2. ***p < 0.001; 2-way ANOVA followed by Šídák's multiple comparisons tests (**B**-**D**).

4.2. Expression of astrocyte Ca^{2+} handling genes during EAE

We next sought to investigate the factors driving aberrant Ca^{2+} activity in EAE mice. Our gene expression analysis in astrocytes purified from EAE mice suggests that impaired astroglial Ca^{2+} responses to systemic Δ^9-THC at acute disease may be related to reductions in the expression levels of astrocytic CB_1Rs (see Results 3.1). However, given the profound transformation of astrocytes during EAE disease, it is reasonable to speculate that reorganization of Ca^{2+} homeostasis and dynamic signaling *in vivo* may involve abnormal expression of additional membrane receptors coupled to intracellular Ca^{2+} regulation as well as changes affecting Ca^{2+} handling molecular cascades. To test this hypothesis we conducted mRNA analysis using RT-qPCR to determine the levels of selected Ca^{2+} signaling/homeostatic toolkits in astrocytes purified during acute EAE. Our results showed deregulated transcript levels of several Ca^{2+} handling receptors and molecules in astrocytes purified from the CNS of mice at acute EAE (**Figure 14C**; **Table 7**). Among the genes whose expression were altered, we found complex changes in several receptors mediating glutamate signaling to astrocytes, such as metabotropic

glutamate receptors 5 (*Grm5*) and 3 (*Grm3*) (Haustein et al., 2014; Sun et al., 2013) as well as decreased levels of several adenosine receptors (*Adora2a*, *Adora2b*). Our RT-qPCR analysis also shows reductions in the expression levels of molecules chiefly involved the regulation of astrocytic Ca^{2+} responses by the ER and the mitochondria, namely G_q protein subunits, IP_3R_2 and the MCU (*Gnaq, Itpr2, Mcu*). These results suggest that astrocytes at acute EAE disease display deficits in Ca^{2+} signaling pathways that are essential for their physiological functions in the CNS.

4.3. Ca^{2+} responsiveness in neurotoxic astrocytes in vitro

Pathological remodeling of astroglial Ca^{2+} handling toolkits leading to abnormal activity may be either cell autonomous or can develop in response to extrinsic stress. In the context of MS and EAE, it seems likely that abnormal astroglial Ca^{2+} activity reflects the transformation of these cells to reactive phenotypes associated to the accumulation of inflammatory mediators in the brain parenchyma (Yi et al., 2019). To address this possibility, we next examined the Ca^{2+} handling properties in astrocytes activated *in vitro* by incubation with pro-inflammatory factors that induce the phenotypic transformation of these cells to a neurotoxic phenotype (Liddelow et al., 2017). Astrocytes incubated with TNFα, IL-1α and C1q displayed upregulated expression of selected A1 neurotoxic genes, and, to a lesser extent, of A2 genes, together with deregulated expression levels of synaptogenesis-related genes (**Figure 12A**-**B**). These results in astrocytes activated *in vitro* are reminiscent of our observations in cells purified during acute EAE (**Figure 5**). Astrocytes activated with pro-inflammatory factors showed deregulated expression of a number of Ca^{2+} signaling molecules including glutamate (*Grm1*, *Grm3*, *Grm5*) and ATP/adenosine receptors (*P2ry1*, *Adora1*), molecules related to ER Ca^{2+} handling (*Gnaq*, *Itpr1*, *Ryr1*, *Ryr2*, *Ryr3*), and cytoplasmic Ca^{2+} binding proteins (*S100b*) (**Figure 14C**; **Table 7**). Some of these changes paralleled observations in astrocytes purified during acute EAE. Particularly, *Grm3*, *Gnaq* and *S100b* showed decreased gene expression in both experimental settings. However, genes such as *Grm1* and *Grm5* showed opposite changes in cells activated *in vitro* and *in vivo*.

Next, we wondered whether the observed deficits in the expression Ca^{2+} handling genes translated to deregulated cytosolic Ca^{2+} dynamics in astrocytes activated *in vitro*. Cultured astrocytes did not display spontaneous Ca^{2+} activity in our experimental settings but showed reliable cytosolic Ca^{2+} responses to glutamate and ATP (**Figure 14D**-**F**). Astrocytes activated by pro-inflammatory factors showed aberrant responses to both glutamate (**Figure 14E**-**F**) and ATP (**Figure 14F**). Incubation with the blocker of the sarco/endoplasmic reticulum Ca^{2+}-ATPase (SERCA) pump thapsigarging increased cytosolic Ca^{2+} to the same extent in control and activated astrocytes, ruling out significant alterations in the Ca^{2+} content of the ER (**Figure 14F**). However, astrocytes incubated with pro-inflammatory factors showed impaired cytosolic Ca^{2+} responses to the mitochondrial toxin FCCP (**Figure 14F**). Overall, these results suggest that astrocytes activated to a neurotoxic phenotype display Ca^{2+} signaling deficits that potentially contribute to the pathogenic profile of these cells during EAE.

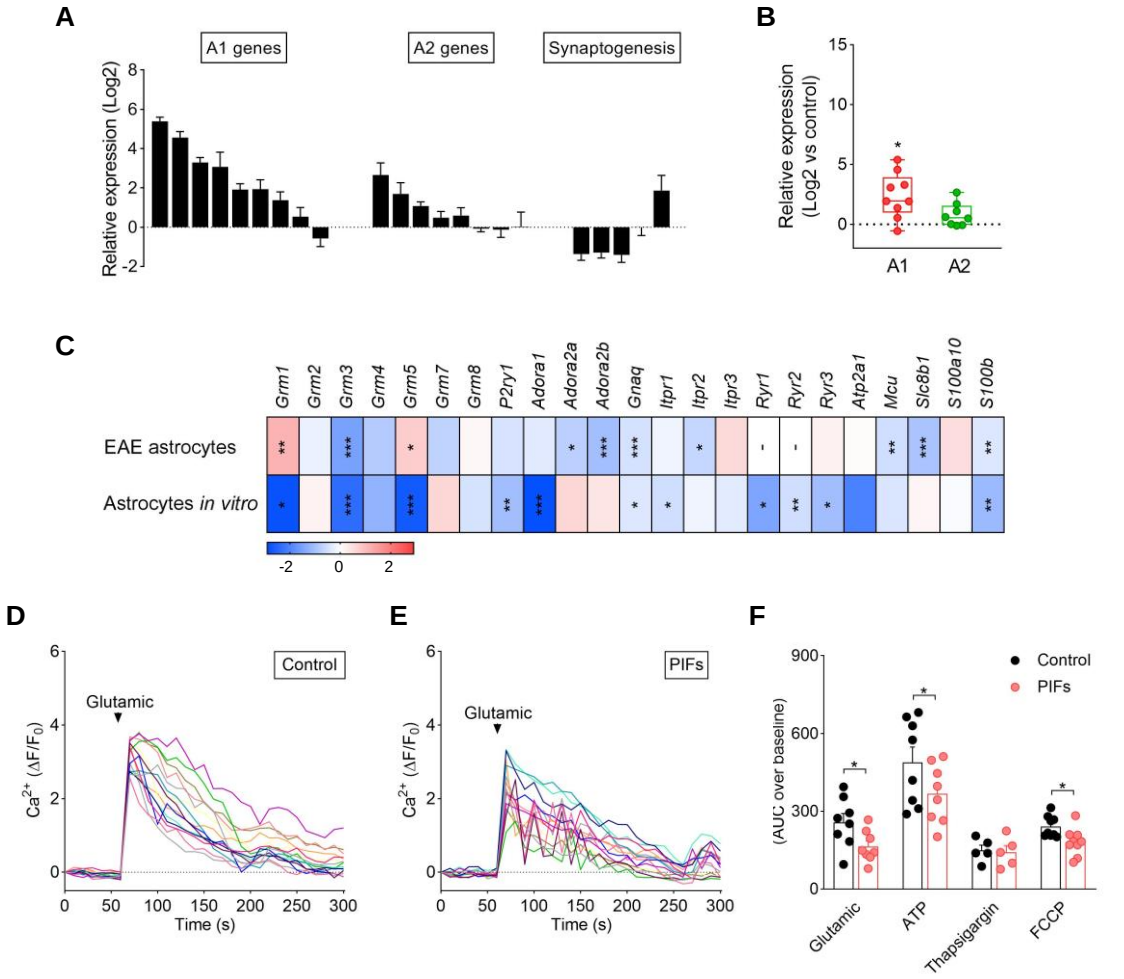

Figure 14. Expression of Ca^{2+} handling genes in astrocytes activated *in vivo* and *in vitro*. (**A**) Normalized expression of selected A1 (*C3*, *Gbp2*, *C1ra*, *Iigp1*, *Amigo2*, *Serping1, H2-T23*, *Ggta1*, *Fkbp5*), A2 (*Cd14*, *Clcf1*, *Stat3*, *Stat6*, *S1pr3, S100a10*, *B3gnt5*, *Emp1*) and synaptogenesis-related (*Gpc4*, *Gpc6*, *Sparcl1*, *Thbs1*, *Thbs2*) genes in astrocytes activated *in vitro* by incubation with the pro-inflammatory factors (PIFs) TNFα, IL-1α and C1q (n = 5-6 cultures). (**B**) Normalization analysis of A1 and A2 genes in astrocytes activated *in vitro*. *p < 0.05; Wilcoxon matched-pairs signed rank test vs control cultures. (**C**) Heat map depicting the mean expression of selected Ca^{2+} handling receptors and molecules in astrocytes purified from the CNS of mice at acute EAE (14-17 dpi; n = 6 mice) or activated *in vitro* by incubation with PIFs. Changes in relative expression were determined as log_2. Representative experiments showing cytosolic Ca^{2+} responses evoked by glutamate (200 µM) in individual control (**D**) and neurotoxic astrocytes (**E**). Cells were activated *in vitro* by incubation with PIFs and loaded with Fluo4 for Ca^{2+} imaging. (**F**) Quantitative analysis of cytosolic Ca^{2+} responses to glutamate (200 µM), ATP (200 µM), thapsigargin (1 µM) and FCCP (1 µM) in control and activated astrocytes (5-8 cultures). AUC, area under the curve; -, not detected. *p < 0.05, **p < 0.01 and ***p < 0.001; Student´s t-tests or Mann-Whitney U-tests relative to control animals or cultures.

5. Phenotype of mice lacking astrocyte CB_1 receptors in the EAE model

5.1. Astrocytic CB_1 receptor null mice exhibit attenuated EAE severity

To study the role of astroglial CB_1Rs in MS we analyzed the phenotype of conditional mutant mice lacking CB_1Rs in GFAP positive cells (Han et al., 2012) in the EAE model of autoimmune demyelination. Upon EAE induction, mice lacking CB_1Rs specifically in astrocytes (GFAP-CB_1-KO) displayed similar disease onset but significantly decreased clinical scores during the acute and chronic phases of the disease (***$p < 0.001$; Mann-Whitney *U*-tests for the comparison of score curves from the onset of EAE symptoms at 6 dpi to 35 dpi) (**Figure 15B**). We next carried out a histological evaluation of spinal cord sections from mice at the experimental end-point (35 dpi). Analysis of Hoechst and LFB patterns revealed that the number of inflammatory lesions, mostly associated to white matter areas close to the tissue edge, was reduced in GFAP-CB_1-KO mice as compared to GFAP-CB_1-WT controls (**Figure 15C**). Evaluation of white matter myelin integrity in tissue sections immunolabeled for the myelin protein MBP showed attenuated demyelination in spinal cord of GFAP-CB_1-KO mice (**Figure 15D**).

Grey matter damage plays a crucial role in MS pathogenesis and clinical course (Calabrese et al., 2015). In particular, functional and structural alterations affecting the cortex are present from the earliest stages of MS and have been associated a number of disease-related symptoms including slowly of voluntary movements, pain, cognitive impairment and depressive-like behaviors (Feinstein et al., 2014; Potter et al., 2016). Given our previous results showing deficient astrocytic Ca^{2+} dynamics in cortical astrocytes during EAE, we next sought for possible differences between genotypes in this brain area. Coronal brain sections were immunostained for the T cell marker CD3 to identify inflammatory lesions. GFAP-CB_1-KO mice displayed a significantly reduced lesion load in the brain cortex at chronic EAE stages (**Figure 15E**). Together, these histological findings are consistent with myelin-protective and anti-inflammatory mechanisms affecting both white and grey matter structures in mice lacking astrocyte CB_1Rs during EAE.

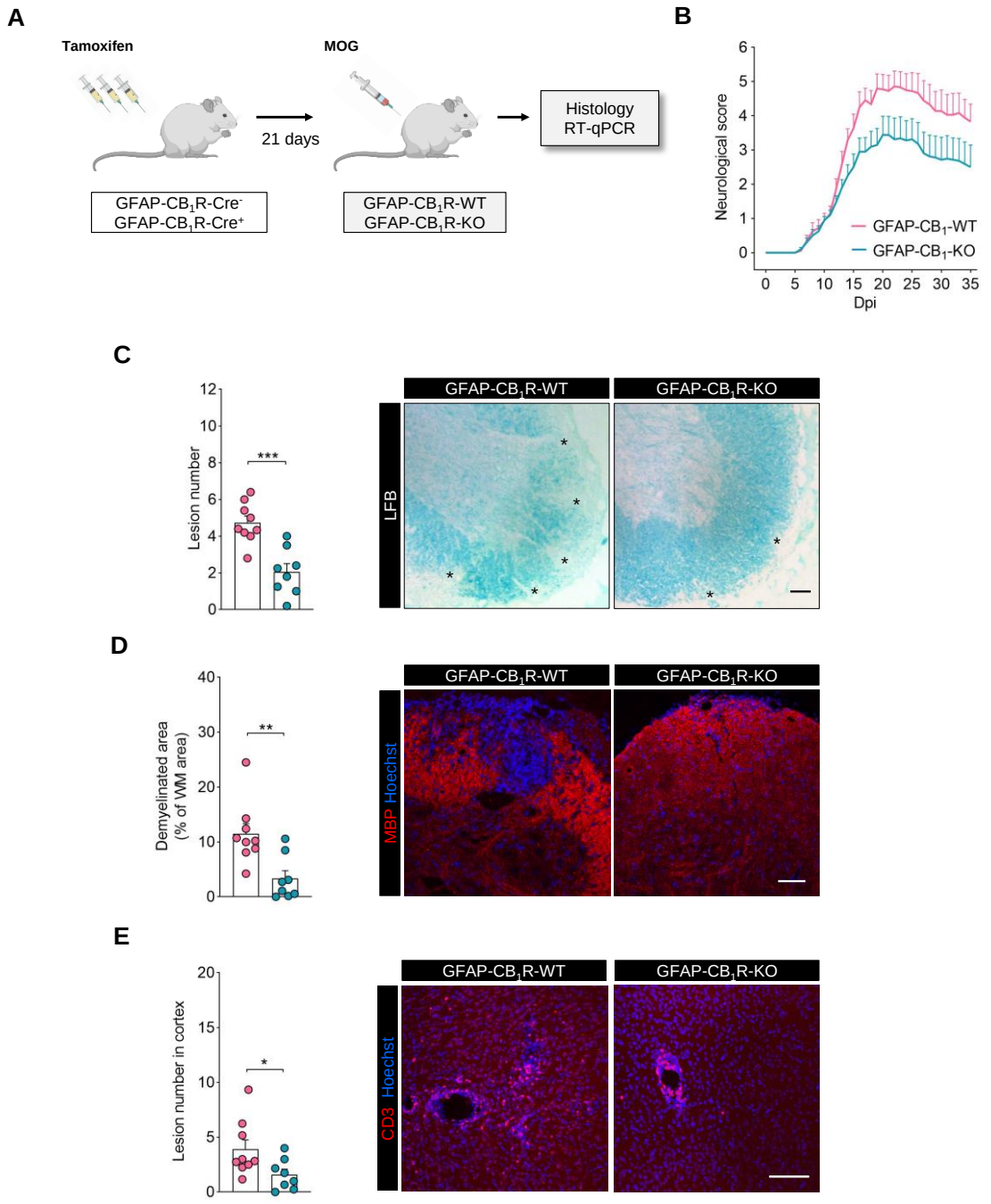

Figure 15. Astrocyte-specific CB_1 receptor null mice exhibit attenuated severity in the EAE model. (**A**) Experimental approach for EAE induction and tissue analysis in mice lacking astrocyte CB_1Rs. Mice were injected daily i.p. injections of tamoxifen for 7 days and EAE induced 3 weeks after tamoxifen treatment. Mice were perfused at 35 or 25 days post-immunization (dpi) for histology and RT-qPCR, respectively. (**B**) Neurological score of mutant mice lacking CB_1Rs from astroglial cells (GFAP-CB_1-KO) and littermate controls (GFAP-CB_1-WT) included in the histological study (*n* = 8-12 mice; 2 independent EAE experiments). (**C**) Quantification of demyelinating lesions by luxol fast blue (LFB) myelin staining (* depict demyelinating lesions) in spinal cord tissue. (**D**) Quantification of demyelinated area as determined by analysis of MBP immunostaining in spinal cord sections from GFAP-CB_1R-KO mice and GFAP-CB_1R-WT controls. (**E**) Quantification of the number of $CD3^+$ inflammatory lesions in the cortex of GFAP-CB_1R-KO mice at 35 dpi (*n* = 8-9 mice). WM, white matter. **p* <0.05, ***p* <0.01, ****p* <0.001; Student's *t*-test. Scale bars: 100 µm.

5.2. Genetic deletion of astrocyte CB_1 receptors alleviates neuroinflammation during EAE

Chronic inflammation exacerbates demyelination and neurodegeneration in MS and astrocytes are crucial mediators of inflammatory responses during EAE (Mayo et al., 2016; Rothhammer et al., 2016). Thus, we next sought to further investigate whether astrocyte-specific CB_1R null mice display altered inflammatory responses in the EAE model. Firstly, we analyzed the amount of infiltrating T lymphocytes, microglia/macrophages and reactive astrocytes in demyelinating lesions of the spinal cord white matter. Our histological analysis showed that GFAP-CB_1-KO mice exhibit a significant reduction in the number of $CD3^+$ T lymphocytes, lower numbers of $CD11b^+$ microglia/macrophages and reduced GFAP immunoreactivity in inflammatory lesions (**Figure 16A**-**B**). We next aimed at evaluating the expression of a variety of inflammatory mediators crucially involved in EAE pathology at an earlier time-point of disease progression. Corroborating our previous observations, mice lacking CB_1Rs specifically in astrocytes showed a significantly decreased EAE severity (**$p < 0.01$; Mann-Whitney *U*-tests for the comparison of score curves from 15 dpi to 25 dpi) (**Figure 16C**). RT-qPCR analysis of spinal cord tissue at 25 dpi evidenced down-regulated gene expression levels of the pro-inflammatory factors and cytokines/chemokines tested in GFAP-CB_1-KO mice as compared to GFAP-CB_1-WT animals (**Figure 16D**; **Table 8**). In particular, we measured significant reductions in the expression of the adhesion molecules *Vcam1* and *Icam1* (**Figure 16D**), implicated in the activation and migration of myelin-specific T cells across the BBB during EAE (Cerutti and Ridley, 2017; Haghayegh Jahromi et al., 2020). Altogether, these results indicate that astrocyte CB_1R ablation ameliorates inflammatory responses driven by infiltrating and resident immune cells during EAE.

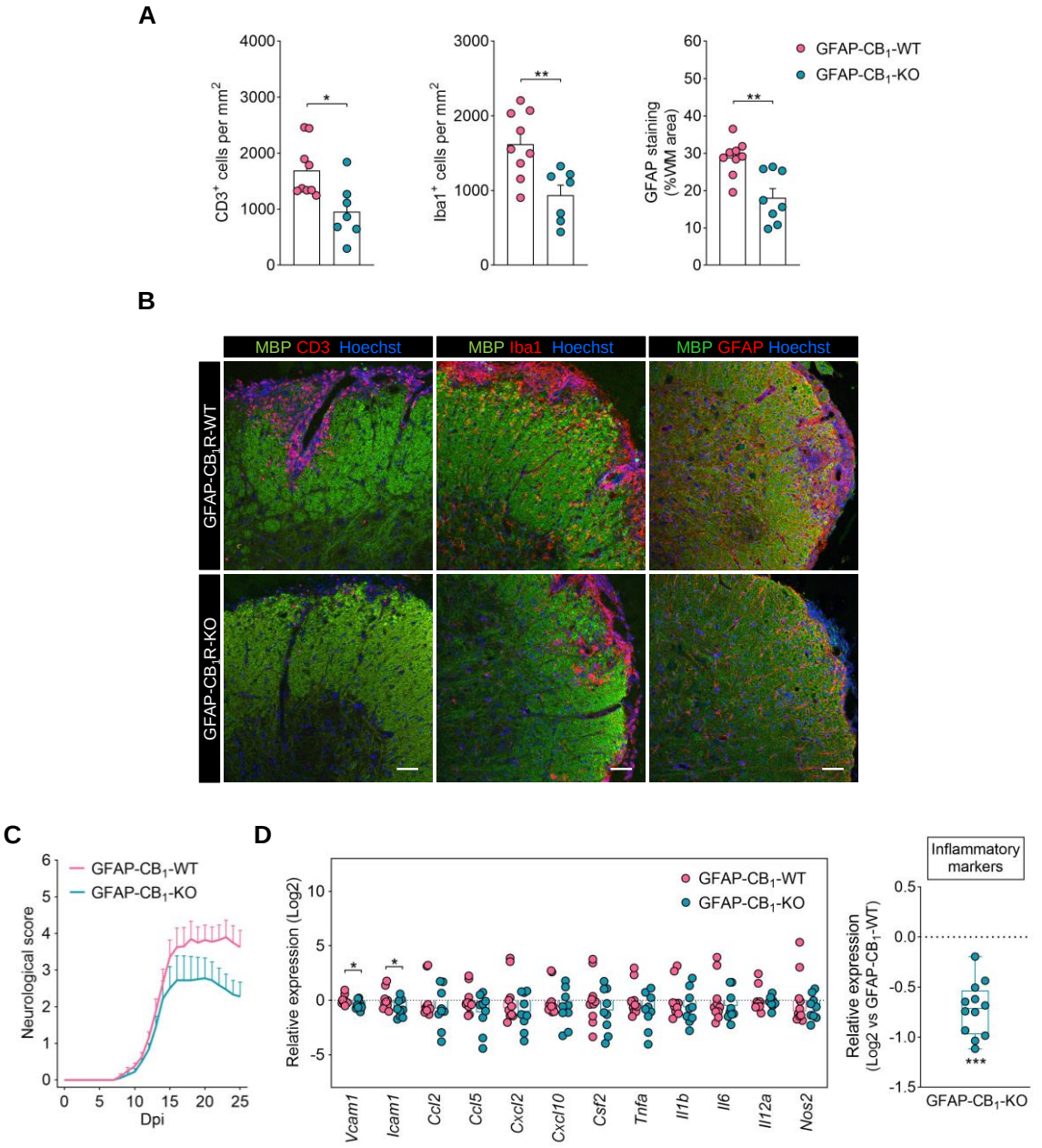

Figure 16. Astroglial CB_1 receptors promote inflammatory responses during EAE. (**A**) Histograms show quantification of $CD3^+$ T cells, $Iba1^+$ microglia/macrophages and GFAP immunostaining in demyelinated white matter (n = 8-12 mice; 2 independent EAE experiments). WM, white matter. *$p < 0.05$ and **$p < 0.01$; Student's t-test. (**B**) Representative immunofluorescence images depict T cells, microglia/macrophages and astrocytes in spinal cord sections from GFAP-CB_1R-KO mice and GFAP-CB_1R-WT littermates at 35 days post-immunization. Scale bars: 100 µm. (**C**) Neurological scores of GFAP-CB_1R-KO and GFAP-CB_1R-WT mice used for RT-qPCR assays (n = 9-10 mice). (**D**) Relative expression of individual inflammatory genes in spinal cord tissue from GFAP-CB_1R-KO mice and GFAP-CB_1R-WT mice at 25 days post-immunization. *$p < 0.05$; Student's t-tests or Mann Whitney U-tests relative to the control group. *Right*: Normalization analysis of the inflammatory genes tested. Comparison between genotypes evidenced significant downregulation in GFAP-CB_1R-KO mice. ***$p < 0.001$ for genotype effect; 2-way ANOVA.

5.3. Reduced presence of neurotoxic astrocytes and preserved neuroaxonal integrity in astrocyte CB_1 receptor null mice

Recent reports suggest that astrocyte conversion to a neurotoxic phenotype is pathogenic in the EAE model (Hou et al., 2020; Zhao et al., 2020), as supported by our own findings (see above). In addition, our results suggest that deregulation of CB_1R mediated signaling in astrocytes is an early event during EAE. Thus, we decided to further explore the relationship between astrocyte CB_1Rs and the acquisition of a neurotoxic phenotype by astroglial cells during EAE. With this aim, we performed immunohistochemistry to assess the presence of A1 reactive astrocytes immunopositive for C3 in GFAP-CB_1-KO mice. We found a reduced number of $C3^+$ profiles in spinal cord white matter of GFAP-CB_1-KO mice as compared to GFAP-CB_1-WT animals at 35 dpi. Double immunostaining with GFAP showed a reduced proportion of $C3^+$ astrocytic profiles in GFAP-CB_1-KO mice, thus suggesting an attenuated presence of neurotoxic astrocytes (**Figure 17A**-**B**). Next, we investigated the expression of several A1 reactive genes by RT-qPCR analysis in spinal cord tissue at 25 dpi. Our results showed a general down-regulation of A1 phenotype genes in GFAP-CB_1-KO mice compared to GFAP-CB_1-WT littermates that reached statistical significance for *C3*, *Fkbp5*, *Ggta1* and *Psmb8* (**Figure 17C**; **Table 8**). We also found a significant correlation between neurological disability scores and *C3* expression in spinal cord tissue of both genotypes (**Figure 17C**, *right panel*), which supports a pathogenic role for C3 during EAE pathology.

Astrocyte conversion to a neurotoxic phenotype has been associated to synapse loss and cognitive deficits in the EAE model (Hou et al., 2020). Thus, we next addressed the possibility that astrocyte CB_1R ablation prevents neurodegeneration as a mechanism of disease attenuation during EAE by immunofluorescence staining of non-phospho-neurofilament (SMI32) protein. Cross-sections of the spinal cord showed less SMI32 immunoreactivity in the white matter of GFAP-CB_1-KO mice, indicative of preserved neuroaxonal integrity (**Figure 18A**-**B**). These histological observations were paralleled by an increased gene expression of neuron/synaptic markers, such as *Rbfox3* and *Snap25*, in GFAP-CB_1-KO mice at 25 dpi (**Figure 18C**; **Table 8**). In sum, our results show that decreased EAE severity in astrocyte CB_1R null mice is associated to an attenuated presence of neurotoxic astrocytes and reduced axonal damage.

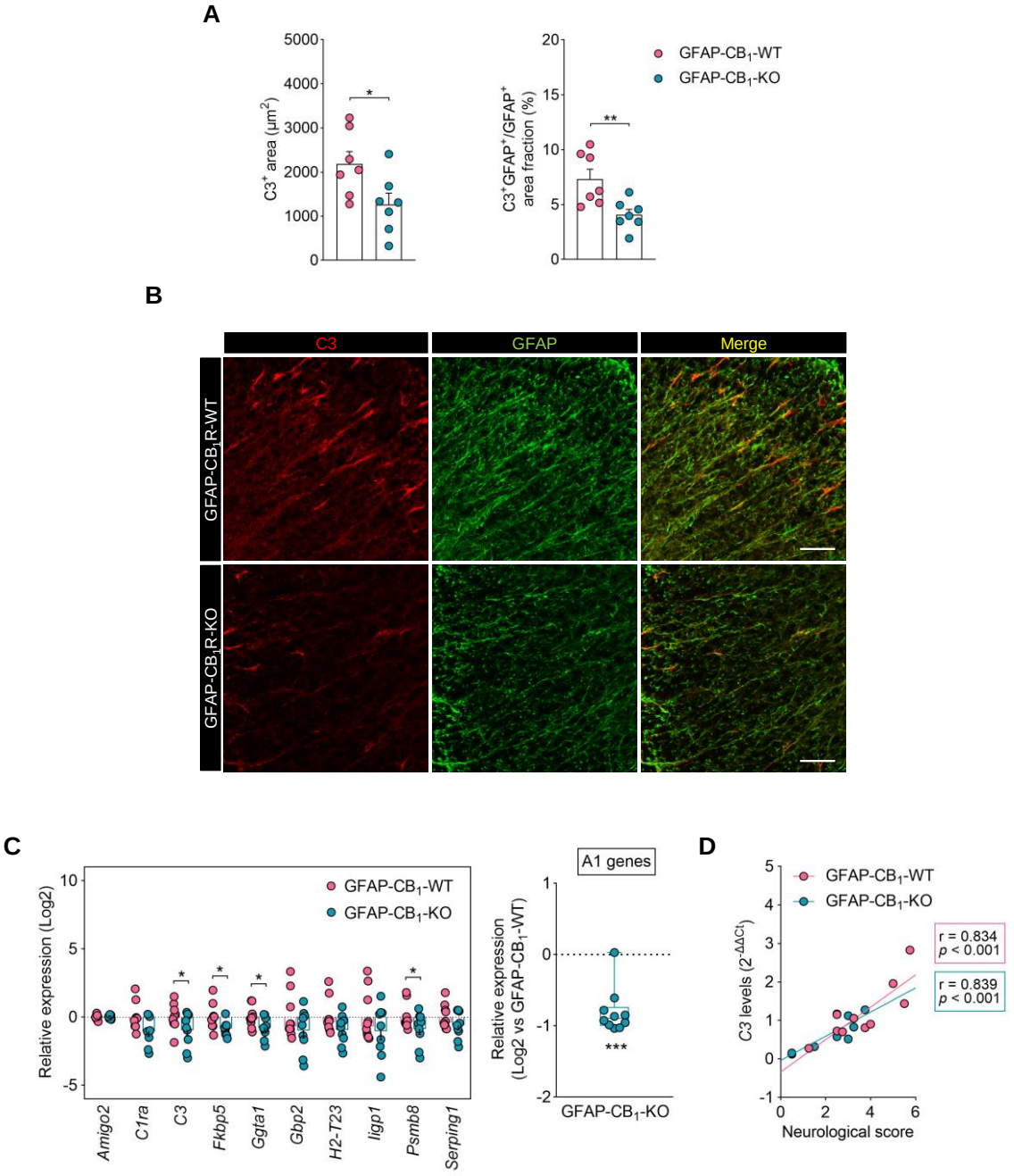

Figure 17. Astrocyte-specific CB_1 receptor ablation attenuates neurotoxic phenotype reactivity and gene expression at chronic EAE. (**A**) Histograms show quantification of $C3^+$ area and $C3^+/GFAP^+$ normalized to $GFAP^+$ area in spinal cord white matter (n = 7 mice). *p <0.05 and **p <0.01; Student's t-test. (**B**) Representative immunofluorescence images depict C3 and GFAP immunostaining in spinal cord sections from GFAP-CB_1R-KO mice and GFAP-CB_1R-WT controls at 35 days post-immunization. Scale bars: 50 µm (**C**) Relative expression of individual A1 phenotype related-genes in spinal cord tissue of GFAP-CB_1R-KO and GFAP-CB_1R-WT mice at 25 days post-immunization (n = 9-10 mice). *p < 0.05; Student's t- or Mann Whitney U-tests. *Right*: Normalized gene expression of the A1 phenotype genes tested. Comparison between genotypes evidenced downregulation in GFAP-CB_1R-KO mice. ***p < 0.001 for genotype effect; 2-way ANOVA. (**D**) Correlation between complement component C3 gene expression in spinal cord tissue ($2^{-\Delta\Delta ct}$ values) and disease scores in EAE. Pearson's correlation coefficients and p values are indicated in the dot plot.

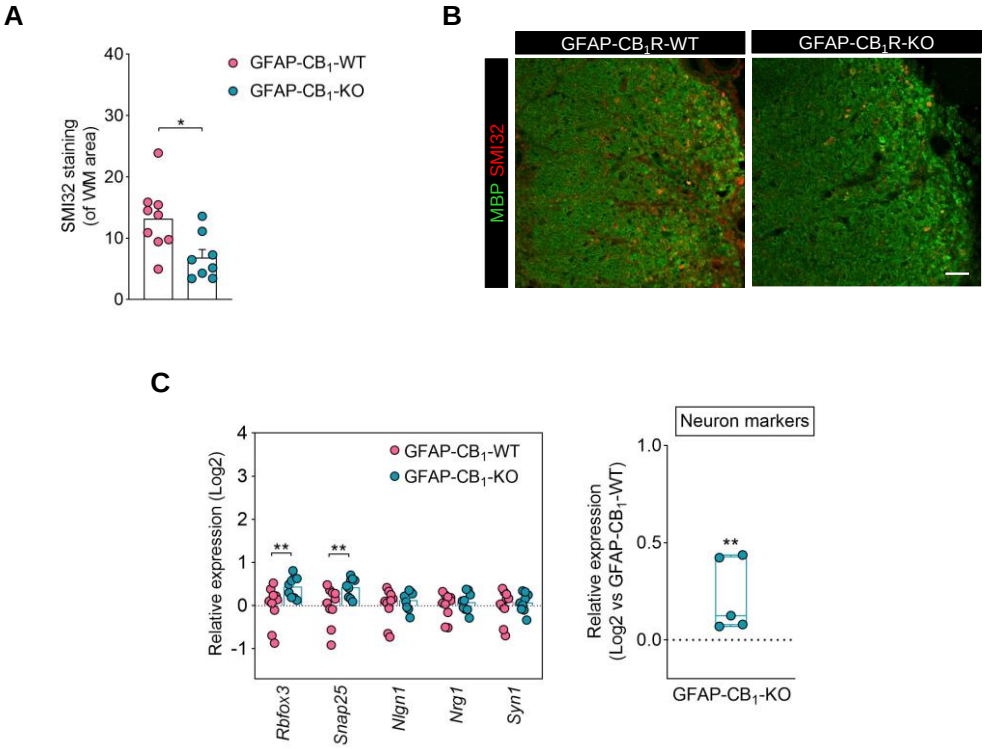

Figure 18. Astrocyte-specific CB_1 receptor null mice exhibit attenuated neuroaxonal damage during EAE. (**A**) Quantification of SMI32 immunostaining in spinal cord tissue from GFAP-CB_1R-KO mice at 35 days post-immunization (n = 8-9 mice). Representative images are shown in **B.** Scale bars: 100 µm. (**C**) Gene expression of individual neuron/synaptic markers in spinal cord tissue from GFAP-CB_1R-KO and GFAP-CB_1R-WT mice at 25 days post-immunization. *p < 0.05 and **p <0.01; Student's t-tests or Mann Whitney U-tests. *Right*: Gene expression of the neuronal markers in astrocyte CB_1R null mice normalized to the control group. Comparison between genotypes evidenced downregulation in GFAP-CB_1R-KO mice. ***p < 0.001 for genotype effect; 2-way ANOVA.

5.4. Genetic deletion of astrocyte CB_1 receptors prevents deregulation of astroglial Ca^{2+} activity during EAE

Our fiber photometry results demonstrate that EAE is associated to an impairment of astrocytic Ca^{2+} responses in the mouse cortex that correlates with disease severity (see above). At the light of these observations, we next wondered whether attenuation of EAE motor deficits in GFAP-CB_1-KO mice was associated to improvement at the astrocyte Ca^{2+} handling level. Thus, we next aimed at analyzing astrocyte Ca^{2+} responses in GFAP-CB_1-KO mice during EAE disease progression.

It is well established that CB_1R removal from astrocytes leads to deficits in a long-term novel object recognition memory task in an L-maze (NOR) (Robin et al., 2018). As internal control of fiber photometry experiments in astrocyte CB_1R mutants, we aimed at corroborating the memory phenotype of GFAP-CB_1-KO mice used for Ca^{2+} analysis *in vivo* before EAE induction. Conditional mutant mice receive tamoxifen injections 1 week after stereotaxic fiber implantation and AAV administration, and were used for behavioral assessments and EAE induction analysis 3 weeks later. GFAP-CB_1-KO mice displayed a significant memory deficit as

compared to their control littermates as well as a non-significant attenuation of disease scores during EAE as compared to the control group (**Figure 19A**-**B**). Reminiscent of our previous observations in wild-type animals, acute EAE disease was paralleled by a significant decrease in the amplitude of Ca^{2+} responses evoked by tail-holding in cortical astrocytes of GFAP-CB_1-WT mice that was not detected in GFAP-CB_1-KO mutants (**Figure 19C**-**D**). On the other hand, the duration of astrocyte Ca^{2+} signals in response to tail-handling was not altered in either genotype during the time-course of EAE (**Figure 19C**-**F***)*. Regarding the dynamics of spontaneous astrocytic Ca^{2+} signals, GFAP-CB_1-WT mice displayed slight reductions in the amplitude and increased duration of the responses that reached statistical significance at 17-19 dpi and were absent in GFAP-CB_1-KO mice (**Figure 20A**-**D**). These results suggest that attenuation of EAE neurological disability astrocyte CB_1R null mice is accompanied by a normalization of astrocytic Ca^{2+} handling properties. Finally, we evaluated potential alterations in the regulation of cytosolic Ca^{2+} levels by Δ^9-THC in conditional mutant mice. Corroborating our previous observations, systemically administered Δ^9-THC effectively increased the amplitude of astroglial Ca^{2+} transients during the second half of the recordings in control, non-immunized GFAP-CB_1R-WT mice without significantly modulating the duration and frequency of the events (**Figure 21**). As expected, administration of the cannabinoid agonist had no significant effect on astrocyte Ca^{2+} responses in GFAP-CB_1R-WT at acute EAE stages (21 dpi), nor in control or immunized GFAP-CB_1-KO animals (**Figure 21**). Altogether, these results further demonstrate that EAE disrupts astrocytic Ca^{2+} responses mediated by CB_1Rs in the mouse somatosensory cortex.

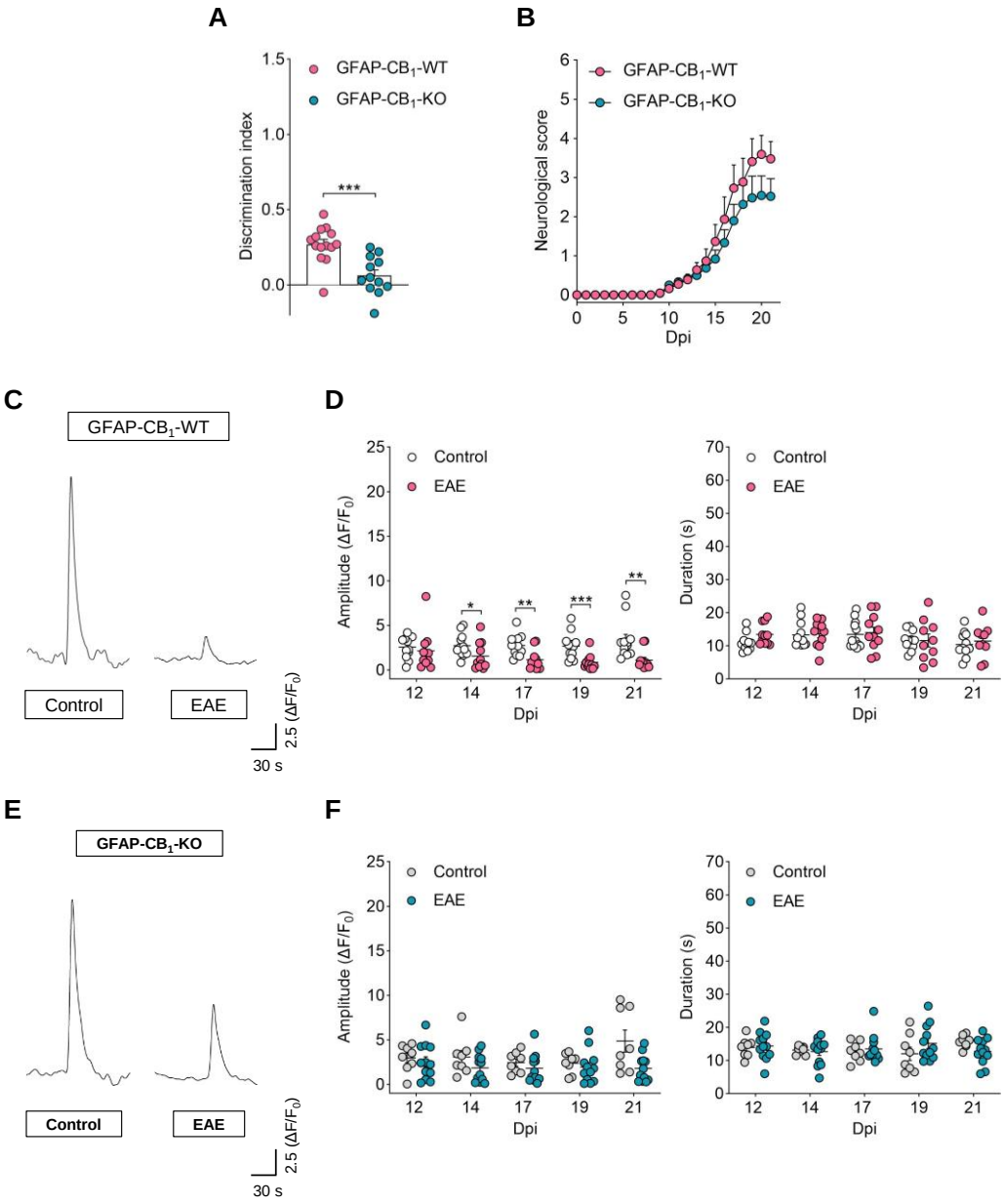

Figure 19. Deregulation of evoked astrocytic Ca^{2+} responses in astrocyte-specific CB_1 receptor null mice during EAE. (**A**) Memory performance of GFAP-CB_1R-KO and GFAP-CB_1R-WT mice in the NOR task. (**B**) Neurological score of mutant mice included in Ca^{2+} imaging experiments (*n* = 11-12 mice; 2 independent EAE experiments). (**C**, **E**) Representative traces show astrocytic Ca^{2+} responses evoked by tail-holding in the cortex of GFAP-CB_1-WT (**C**) and GFAP-CB_1-KO (**E**) control and EAE mice (17 dpi). (**D**, **F**) Amplitude and duration of Ca^{2+} responses evoked in GFAP-CB_1R-WT (**D**) and GFAP-CB_1R-KO (**F**) mice at different time-points of disease progression as compared to control mice recorded in parallel (*n* = 8-12 mice). **p* < 0.05, ***p* < 0.01 and ****p* < 0.001; Student´s *t*-tests or Mann-Whitney *U*-tests.

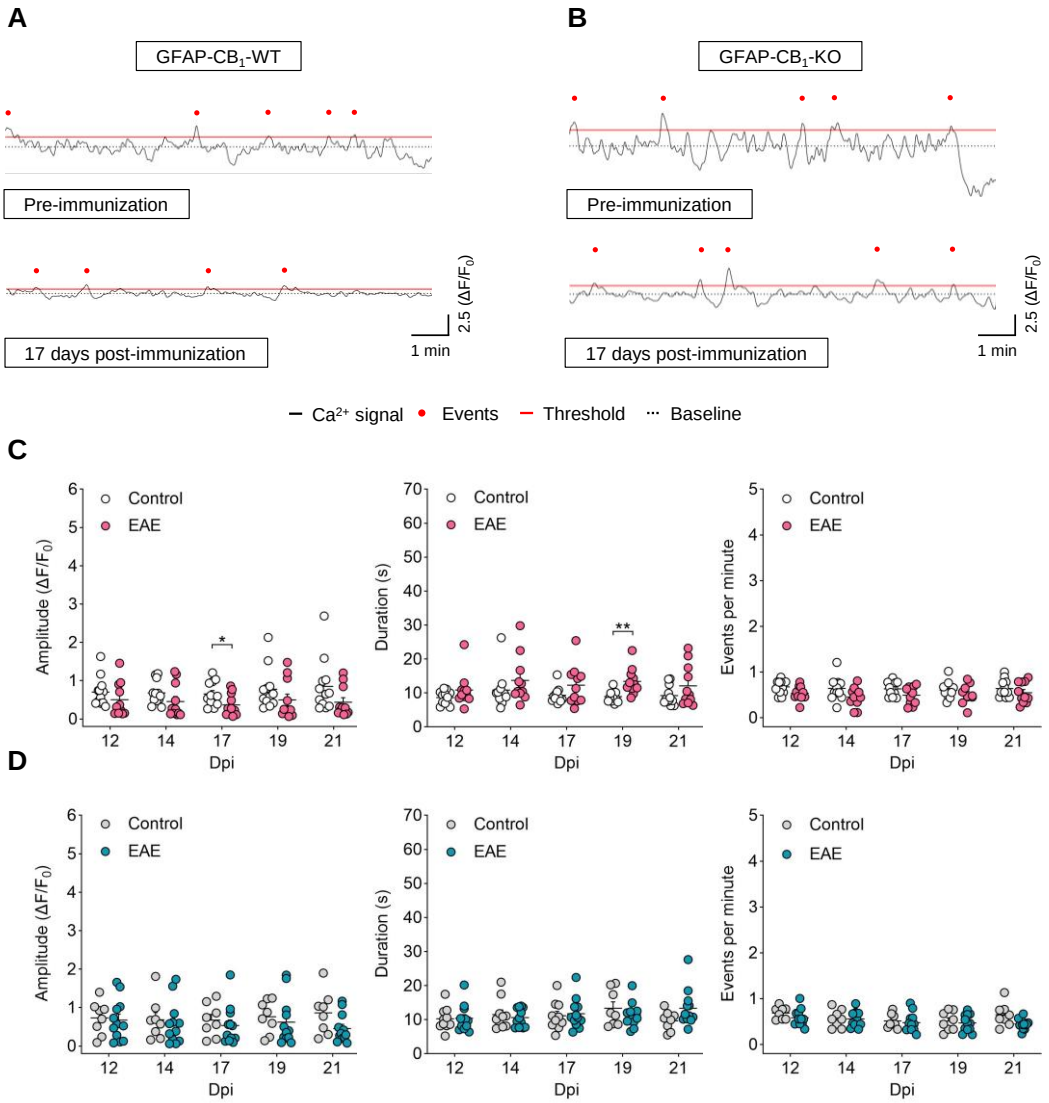

Figure 20. Spontaneous Ca^{2+} activity of cortical astrocytes in astrocytic CB_1 receptor null mice during EAE. Representative recordings show spontaneous Ca^{2+} activity in cortical astrocytes from GFAP-CB_1R -WT (**A**) and GFAP-CB_1R-KO (**B**) mice injected with AAV-GFAP-GCaMP6fs and recorded during EAE (bottom panel) as compared to the pre-immunization phase (top panel). Amplitude, duration and frequency of spontaneous Ca^{2+} responses recorded from GFAP-CB_1R-WT (**C**) and GFAP-CB_1R -KO (**D**) control and EAE mice at different time-points of disease progression. *$p < 0.05$ and **$p < 0.01$; Student´s *t*-tests or Mann-Whitney *U*-tests.

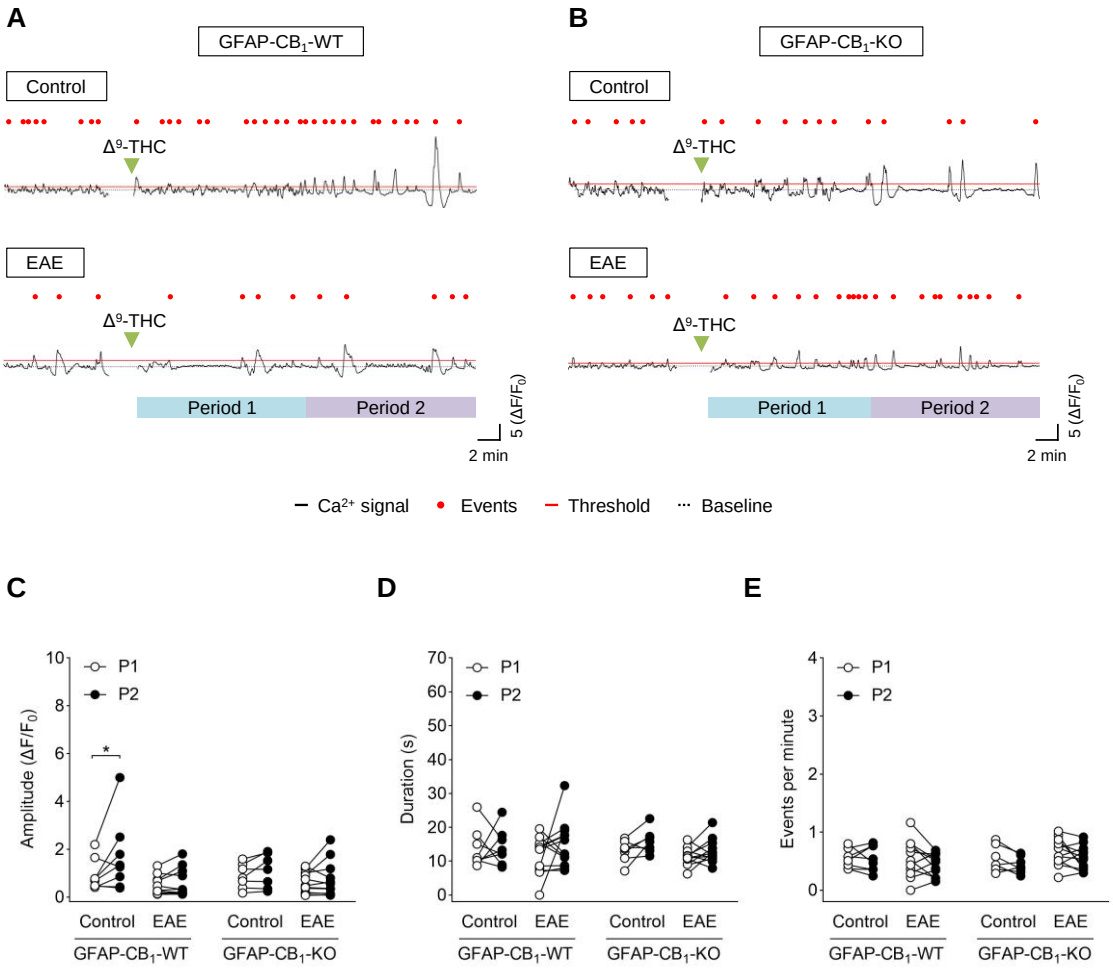

Figure 21. Astrocytic Ca^{2+} responses to Δ^9-THC in conditional mutant mice during EAE. Representative recordings from the mouse somatosensory cortex showing the effect of Δ^9-THC (10 mg/Kg; i.p.) on astrocytic Ca^{2+} activity in GFAP-CB_1R-WT (**A**) and GFAP-CB_1R-KO (**B**) control (top panel) and EAE (21 dpi; bottom panel) mice. Amplitude (**C**), duration (**D**) and frequency (**E**) of astrocytic Ca^{2+} responses to Δ^9-THC in control and EAE mice (*n* = 7-12 mice). P1, Period 1; P2, Period 2. **p* < 0.05; 2-way ANOVA followed by Šídák's multiple comparison tests (**C**-**E**).

Table 4. Gene expression analysis of astrocytes purified during EAE time-course.

Gene symbol	Presymptomatic		Acute		Chronic	
	Log_2FC	*p* value	Log_2FC	*p* value	Log_2FC	*p* value
Abhd12	-0.2958	1.32E-01	-0.7912	2.16E-03	-0.7403	4.33E-03
Abhd6	-0.3260	3.95E-02	-0.9070	1.81E-04	-0.7198	2.59E-03
Aldh1l1	-0.2086	9.31E-02	-0.4887	1.51E-03	-0.5920	1.13E-03
Amigo2	0.4574	1.97E-01	0.9601	9.81E-03	0.0677	9.57E-01
Aqp4	-0.3681	1.52E-02	-1.0820	2.16E-03	-0.7385	1.00E-03
Aspg	1.0457	7.58E-02	1.5157	9.34E-02	0.8380	1.11E-01
Atp1b2	-0.0256	9.36E-01	-0.6689	4.00E-02	-0.3878	2.45E-03
Axl	-0.1703	3.81E-01	-0.7354	4.38E-05	-0.3534	1.13E-02
B3gnt5	0.5680	1.37E-01	1.4538	1.30E-02	0.4544	2.15E-01
Bdnf	-0.5618	5.48E-01	-1.7650	1.59E-02	-0.7419	5.48E-01
C1ra	1.0253	8.07E-02	5.6156	6.01E-05	3.2730	4.46E-04
C3	-0.2392	5.89E-01	5.1450	1.33E-04	3.1307	3.14E-03
Ccl2	-0.0922	9.63E-01	6.2203	2.16E-03	2.6472	5.95E-04
Ccl5	0.8433	2.30E-03	5.7783	1.59E-05	2.4616	2.72E-02
Cd14	1.5763	6.70E-04	3.9730	2.73E-03	0.4278	2.50E-01
Cd44	0.0215	6.49E-01	1.1253	7.55E-02	-0.3682	1.54E-01
Cnr1	-0.2541	1.39E-01	-0.7481	1.44E-02	-0.3372	4.89E-02
Cntf	-0.2403	5.32E-01	-0.8945	5.22E-02	-0.3806	6.91E-01
Cxcl10	1.0978	1.61E-02	6.5725	1.72E-06	2.6462	2.69E-02
Dagla	-0.4039	9.31E-02	-1.2845	2.16E-03	-0.5846	3.29E-01
Daglb	-0.2901	2.60E-02	-1.0867	2.49E-07	-0.6780	1.36E-04
Emp1	-0.0149	8.92E-01	1.0155	1.14E-01	0.3568	3.37E-01
Faah	1.0725	2.16E-02	1.1180	2.98E-02	-0.3671	2.40E-01
Fabp7	-0.8868	1.31E-03	-1.4619	5.93E-05	-0.5146	3.69E-02
Fkbp5	1.2543	4.53E-04	3.9361	4.04E-04	0.7152	5.94E-02
Gas6	-0.2751	1.69E-01	-0.4668	1.32E-02	-0.4357	1.08E-02
Gbp2	0.3728	3.67E-01	6.2841	5.98E-03	2.4958	2.93E-04
Gfap	0.2068	2.97E-01	2.1071	6.98E-06	0.2481	1.80E-01
Gpc4	-0.0273	9.39E-01	-0.4136	3.37E-02	-0.4002	7.84E-02
Gpc6	-0.4054	2.28E-02	-0.8763	1.01E-03	-0.4390	4.71E-02
Gpr34	4.7079	6.58E-05	1.7543	2.24E-02	2.5456	3.75E-07
H2-T23	0.5347	4.80E-01	5.9328	8.28E-04	2.8608	6.85E-04
Iigp1	0.9752	1.37E-02	6.6471	4.33E-03	1.8828	4.55E-03
Irf9	-0.4988	1.56E-01	2.1240	3.90E-09	0.4724	4.07E-02
Itgam	7.4676	2.77E-04	8.9446	8.81E-03	0.5823	6.41E-02
Megf10	-0.2899	2.20E-01	-0.9127	9.92E-07	-0.7813	1.52E-04
Mertk	0.1891	8.18E-01	0.0585	5.39E-01	-0.1858	9.40E-02
Mgll	-0.3937	1.92E-02	-0.6254	1.09E-03	-0.6124	2.25E-03
Mx1	-0.5919	2.86E-03	4.2962	2.62E-03	4.3201	8.79E-07
Naaa	-0.2253	1.60E-01	-0.8791	9.65E-05	-0.6861	1.55E-03
Napepld	0.3823	4.70E-02	0.0409	7.00E-01	0.1787	2.94E-01
Nfe2l2	-0.0994	5.56E-01	-0.4310	8.88E-03	-0.6098	6.99E-03
Nos2	0.5536	8.44E-03	5.1443	5.22E-03	-7.8606	6.40E-08
P2ry12	0.2283	4.19E-01	0.6321	3.00E-02	0.1262	5.87E-01
Psmb8	0.6830	6.11E-02	6.2725	3.62E-04	3.1408	1.68E-04
Ptgs2	0.1140	6.16E-01	2.3021	1.08E-02	1.6962	3.03E-02
S100a10	-0.4520	3.43E-02	0.2866	4.03E-01	-0.3923	6.81E-02
S1pr3	-0.2910	3.94E-01	0.0671	6.14E-01	0.3833	3.57E-01
S1pr3	-0.1582	6.94E-01	0.1836	6.64E-01	0.9933	7.01E-02
Serpina3n	-0.3440	1.16E-01	3.9841	1.04E-04	0.6363	1.16E-01
Serping1	-0.7536	4.11E-02	3.4705	2.16E-03	1.4702	2.57E-04
Slc1a3	-0.1687	3.10E-01	-0.7289	2.16E-03	-0.4696	9.91E-03
Sparcl1	-0.3934	7.49E-02	-0.7929	4.24E-04	-0.5069	1.66E-02
Stat1	0.0620	7.73E-01	3.7181	2.16E-03	1.1288	8.67E-05
Stat2	-0.2720	2.52E-01	2.1939	6.05E-06	0.2231	4.29E-01
Stat3	-0.0277	8.40E-01	1.1582	3.88E-04	-0.2226	1.70E-01
Stat6	-0.3474	4.84E-01	-0.0079	7.57E-01	0.2566	5.22E-01
Thbs1	-0.2094	9.59E-01	1.6377	7.76E-04	0.7992	3.75E-02
Thbs2	-0.7781	1.42E-01	-0.0510	8.21E-01	0.1025	7.96E-01
Tmem119	1.1464	7.56E-03	1.3720	3.97E-03	1.5985	3.15E-03

Table 5. Correlation between neurological disability and A1 phenotype gene expression in astrocytes and microglia purified during EAE.

Gene symbol	Astrocytes			
	Acute EAE		Chronic EAE	
	r value	*p* value	r value	*p* value
Amigo2	-0.5911	0.2166	0.5835	0.3017
C1ra	0.2209	0.6740	0.4372	0.4616
C3	0.9955	< 0.001	0.5890	0.2970
Fkbp5	-0.4541	0.3657	-0.1111	0.8589
Gbp2	-0.8021	0.0549	-0.3315	0.5858
H2-T23	-0.8490	0.0325	-0.8037	0.1013
Iigp1	-0.7904	0.0613	-0.6500	0.2351
Psmb8	-0.9082	0.0123	-0.3019	0.6215
Serping1	-0.1739	0.7500	-0.1572	0.8007
Gene symbol	**Microglia**			
	Acute EAE		**Chronic EAE**	
	r value	***p* value**	**r value**	***p* value**
Amigo2	-0.1299	0.8063	0.6000	0.3500
C1ra	0.0811	0.8786	0.3336	0.5832
C3	0.6080	0.2004	-0.5721	0.3135
Fkbp5	0.7440	0.0899	0.3431	0.5718
Gbp2	0.2677	0.6080	-0.4208	0.4805
H2-T23	0.1160	0.8389	0.3217	0.5976
Iigp1	-0.1768	0.7375	-0.5220	0.3670
Psmb8	0.2899	0.6000	0.4918	0.4001
Serping1	0.1160	0.8389	0.4089	0.4943

Table 6. Gene expression analysis in microglial cells purified during EAE time-course.

Gene symbol	Presymptomatic		Acute		Chronic	
	Log_2FC	*p* value	Log_2FC	*p* value	Log_2FC	*p* value
Abhd12	-0.3685	3.53E-02	-2.2369	8.02E-07	-0.9160	2.53E-04
Abhd6	-1.2380	1.78E-02	-1.3443	1.07E-02	-0.6903	1.34E-01
Aldh1l1	-1.8121	2.95E-02	-1.0359	1.32E-01	-2.3467	1.15E-02
Amigo2	0.7924	6.49E-02	1.1548	1.52E-02	0.5408	8.23E-02
Aqp4	-1.2754	7.52E-01	-1.2896	1.69E-01	-1.1119	4.34E-01
Atp1b2	-0.1750	6.63E-01	0.9971	1.26E-01	0.6212	1.54E-01
C1ra	-0.5156	2.08E-02	2.9594	1.65E-03	0.1950	3.36E-01
C3	2.4360	6.21E-04	7.4494	9.65E-04	6.8301	1.83E-05
Ccl2	1.0033	3.88E-04	0.5604	3.91E-02	-0.3471	4.29E-01
Ccl5	1.0954	1.21E-01	5.4235	6.70E-03	5.0439	1.54E-04
Cd163	-1.0196	1.09E-02	-0.7727	3.33E-02	-1.1434	2.82E-02
Cd44	0.5860	1.60E-01	2.7387	2.53E-03	2.0072	1.63E-04
Chil3	-0.7727	3.67E-02	2.7977	4.19E-03	-1.0488	2.12E-02
Cnr2	0.6786	1.84E-01	-0.2327	9.14E-01	0.0285	7.25E-01
Cxcl2	1.1945	1.15E-03	1.0228	1.15E-01	-0.3391	2.48E-01
Cxcl10	1.2742	8.17E-05	2.7016	2.39E-05	0.8101	2.80E-02
Dagla	-1.1077	3.03E-02	-2.7762	4.33E-03	-1.4266	1.07E-02
Daglb	-0.9503	8.66E-03	-2.4466	7.69E-05	-0.8968	5.85E-03
Faah	-0.3459	1.11E-01	-1.8949	1.90E-02	-2.8732	1.59E-02
Fabp7	0.0705	9.52E-01	0.6877	2.93E-01	0.0979	7.29E-01
Fkbp5	-0.0562	7.24E-01	1.0307	1.20E-01	-0.0510	8.90E-01
Gbp2	-0.0906	5.65E-01	4.4800	1.49E-04	1.9637	2.51E-03
Gfap	1.8609	6.19E-01	3.5182	1.51E-02	1.9257	7.19E-01
Gpr34	-0.8013	8.66E-03	-4.8053	2.42E-06	-1.8605	1.42E-04
H2-T23	-0.6233	8.94E-03	1.1600	4.33E-03	1.0186	2.19E-05
Igf1	0.5896	4.62E-02	3.6732	7.14E-02	4.5030	3.10E-06
Iigp1	4.5378	4.33E-03	9.7732	4.33E-03	5.8057	7.94E-03
Il1b	0.4626	4.51E-01	0.1753	8.77E-01	1.2967	2.03E-02
Il6	-0.6975	1.74E-01	-0.3659	3.56E-01	-0.7097	1.91E-01
Il12a	-0.8565	2.77E-01	1.0768	5.33E-01	-7.5319	1.10E-01
Itgam	-0.4558	6.43E-02	-2.2144	1.45E-04	-0.6837	3.45E-02
Mgll	-0.8032	8.66E-03	-2.6620	1.55E-05	-1.3662	1.02E-04
Mrc1	-0.7967	3.56E-03	-3.0272	4.33E-03	-1.6962	1.75E-04
Naaa	0.4747	2.01E-01	1.7152	1.23E-04	0.7763	2.36E-02
Napepld	-0.3803	7.31E-01	0.2620	4.13E-01	-0.5686	2.10E-01
Nfe2l2	-0.4292	1.39E-01	-0.5719	8.72E-02	-0.3284	2.26E-01
Nos2	-0.3254	6.99E-01	6.1096	2.16E-03	4.3729	4.33E-03
P2ry12	-1.3593	1.27E-06	-4.4317	9.00E-09	-2.0111	7.72E-07
Pdgfa	-0.7770	4.58E-02	-2.0694	2.37E-05	-0.7946	3.55E-02
Psmb8	0.0903	7.09E-01	1.7021	1.01E-05	1.3510	2.13E-04
S1pr3	4.7146	4.33E-03	6.0021	4.33E-03	5.4616	7.94E-03
Serpina3n	4.6570	4.33E-03	7.5980	4.33E-03	5.4031	7.94E-03
Serping1	-1.4736	1.32E-01	5.1970	1.50E-03	0.2370	3.93E-01
Slc1a3	-1.0226	1.55E-01	-0.2796	1.85E-01	-0.4825	4.33E-01
Stat1	-0.0252	8.19E-01	2.6262	2.01E-08	1.5463	5.77E-04
Stat3	-0.6832	4.46E-02	-0.6641	2.81E-02	-1.1886	7.44E-03
Stat6	-0.5660	1.87E-02	-1.8860	6.90E-05	-1.2146	1.20E-03
Tgfb1	-0.8759	4.14E-03	-2.2616	9.82E-05	-1.0800	3.80E-03
Tmem119	-0.9231	4.10E-03	-2.8893	4.63E-05	-1.4083	1.33E-03
Tnf	0.0245	8.52E-01	-1.1451	1.96E-04	-0.9015	3.81E-03

FC, fold change

Table 7. Expression of Ca^{2+} signaling genes in astrocytes purified at acute EAE disease and in cells activated *in vitro.*

Gene symbol	Astrocytes in acute EAE		Astrocytes *in vitro*	
	Log_2FC	*p* value	Log_2FC	*p* value
Adora1	-0.3429	2.30E-01	-2.9300	1.52E-04
Adora2a	-0.7776	3.34E-02	0.6377	4.66E-01
Adora2b	-1.0510	8.99E-04	0.4480	1.43E-01
Atp2a1	0.0484	9.62E-01	-1.1720	1.25E-01
Gnaq	-0.4946	7.42E-04	-0.3997	4.25E-02
Grm1	1.1480	2.16E-03	-2.3580	1.37E-02
Grm2	-0.2322	4.85E-01	0.2718	5.82E-01
Grm3	-1.5310	9.91E-06	-2.2800	8.22E-05
Grm4	-0.8506	1.36E-01	-1.1070	6.25E-02
Grm5	0.7527	1.13E-02	-2.5870	2.78E-04
Grm7	-0.7304	2.40E-01	0.3815	2.93E-01
Grm8	0.1196	8.02E-01	-0.5238	8.13E-01
Itpr1	-0.1915	6.63E-01	-0.3860	1.08E-02
Itpr2	-0.6645	1.39E-02	-0.0662	8.20E-01
Itpr3	0.5561	4.25E-01	-0.3716	2.27E-01
Mcu	-0.5402	8.34E-03	-0.2314	3.84E-01
P2ry1	-0.4607	3.88E-01	-0.9850	2.94E-03
Ryr1	ND	-	-1.8480	4.48E-02
Ryr2	ND	-	-0.7168	1.46E-03
Ryr3	0.2036	5.96E-01	-0.8797	3.59E-02
S100a10	0.5130	1.59E-01	-0.1565	5.43E-01
S100b	-0.3959	2.60E-02	-1.0370	6.58E-03
Slc8b1	-0.9622	2.11E-04	0.1485	6.63E-01

FC, fold change

Table 8. Gene expression analysis of spinal cord tissue from astrocyte CB_1 receptor null mice at acute EAE.

Gene symbol	Spinal cord tissue in EAE	
	Log_2FC	*p* value
Amigo2	-0.9164	7.06E-01
C1ra	-1.0360	7.82E-02
C3	-0.9544	3.62E-02
Ccl2	-0.7424	1.78E-01
Ccl5	-1.1170	1.78E-01
Csf2	-0.9323	2.75E-01
Cxcl10	-0.6828	2.24E-01
Cxcl2	-1.0360	6.04E-01
Fkbp5	-0.8480	1.35E-02
Gbp2	-0.9882	9.88E-02
Ggta1	-0.7814	4.74E-02
H2-T23	-0.9253	9.12E-02
Icam1	-0.7494	4.74E-02
Iigp1	-1.0270	2.39E-01
Il12a	-0.1947	2.75E-01
Il1b	-0.6197	1.78E-01
Il6	-0.5053	2.48E-01
Nlgn1	0.1248	2.03E-01
Nos2	-0.6465	4.52E-01
Nrg1	0.0795	2.62E-01
Psmb8	-0.8672	4.82E-02
Rbfox3	0.4369	9.50E-03
Serping1	-0.6091	2.11E-01
Snap25	0.4234	9.20E-03
Syn1	0.0698	3.12E-01
Tnfa	-0.9846	1.78E-01
Vcam1	-0.4365	1.75E-02

FC, fold change

Discussion

In this work, we addressed several unanswered questions concerning the role of endocannabinoids in modulating astroglial cell function in MS. First, we investigated gene expression changes in astrocyte endocannabinoid signaling molecules during EAE disease progression. Our results show that deregulation of cannabinoid receptors and endocannabinoid metabolic enzymes at the gene expression level takes place early during astrocyte activation in the EAE model and parallels the induction of neurotoxic phenotype-associated genes. Secondly, we defined cytosolic Ca^{2+} responses mediated by CB_1Rs in astrocytes of the mouse cortex *in vivo* and deciphered changes in the Ca^{2+} handling properties of astroglial cells activated in a demyelinating pro-inflammatory context. Using a combination of experimental approaches, we unveil dysfunctional Ca^{2+} signaling in astrocytes from EAE mice that include impaired CB_1R coupling to cytosolic signals *in vivo*. Finally, we show that mice lacking CB_1Rs in astroglial cells display a protective phenotype in the EAE model, as evidenced by lower neurological disability scores, reduced lesion load and tissue inflammation and improved neuroaxonal integrity. Deletion of astrocyte CB_1Rs was also associated to an attenuated presence of neurotoxic astrocytes and preserved astrocyte Ca^{2+} signaling during EAE. Altogether, these results point to the endocannabinoid system as an important modulator of astrocyte dyshomeostasis in MS as well as to dysfunctional Ca^{2+} dynamics in astroglial cells as possible mechanisms underlying disease symptomatology.

1. Gene expression analysis of astrocytes and microglia during EAE: neurotoxic activation and endocannabinoid signaling

1.1. Activation characteristics of astrocytes and microglia during EAE

In this study, we analyzed the expression of selected target genes related to neurotoxic astrocyte activation in cells purified at different stages of EAE progression. We report that CNS astrocytes dynamically and highly up-regulate A1-like genes as compared to A2 phenotype markers. We also establish that astroglial cells over-express a number of A1 reactive genes at early, asymptomatic stages, with most of these molecules exhibiting significantly increased transcript levels both at acute and recovery phases. Early gene expression changes in astrocytes are consistent with the presence of infiltrating cells - lymphocytes and monocytes - already in the presymptomatic phase of EAE, as well as with the concept that astroglial cells activated at initial stages contribute actively to disease development (Linnerbauer et al., 2020). Using immunohistochemistry, we corroborated that a population of reactive astrocytes in spinal cord white matter up-regulates complement component C3, a putative marker of neurotoxic astrocytes, at the protein level. Consistent with the acquisition of pathogenic functions, our RT-qPCR analysis also demonstrates that induction of astrocytic A1 phenotype marker genes during autoimmune demyelination is associated with the deregulation of specific genes involved in neuroprotection, synaptogenesis, and phagocytosis, thus matching previous observations (Liddelow et al., 2017; Tassoni et al., 2019). These results add to the growing body of evidence showing the presence of a population of neurotoxic astrocytes in brain aging and chronic neurodegenerative diseases that compromise synaptic function in part through the release of C3 (Chao et al., 2019; Clarke et al., 2018; Guttenplan et al., 2020; Lian et al., 2015; Yun et al., 2018). Furthermore, in this study, the increase in astrocytic *C3* transcripts strongly correlated with motor disability scores at acute disease. Although neurological deficits in a complex disease model such as EAE cannot be ascribed to variations in a single gene, this result is reminiscent of

the negative correlation between astroglial C3 expression and retinal ganglion cell density in optic neuritis (Tassoni et al., 2019), and lead us to postulate a relevant connection between astrocytic complement expression in white matter tracts and neurodegeneration in MS. On the other hand, the transcriptional induction of additional astrocytic A1 markers displayed, however, a complex profile in terms of association with disease severity, with many of them showing non-significant correlations or even inversely correlating with neurological scores. When interpreting these results, it should be kept in mind that although the general up-regulation of A1 genes reported here supports the expression of a pathogenic neurotoxic astrocytic phenotype (Clarke et al., 2018; Liddelow et al., 2017; Zamanian et al., 2012), each one of these individual genes might play opposite roles in regulating astrocyte function in terms of disease outcome. Indeed, the inverse correlation astrocytic IFN inducible genes such as *Iigp1* and *Psmb8* and disease severity is not surprising in the context of protective responses driven by this signaling pathway in experimental MS (Hindinger et al., 2012; Smith et al., 2020). In addition, most of the A1-like genes assayed in this study are not expected to be exclusively expressed in the population of so-called neurotoxic astrocytes during EAE. Instead, a complex pattern of expression in several astrocyte populations displaying different phenotypic states may be suggested for the different genes tested based on the existing literature. Importantly, single-cell microfluidic qPCR of astrocytes purified from experimental models for astrocyte polarization have validated *C3* among other A1 genes as the most appropriate marker to visualize the population of neurotoxic astrocytes in disease conditions, based on its selective expression in this subset of reactive astroglia (Liddelow et al., 2017). In this scenario, our results corroborate the pathological relevance of A1 astrocytes expressing C3 during autoimmune demyelination and highlight the complexity of studying astrocyte phenotypic responses in MS.

Microfluidic RT-qPCR analysis of isolated microglia revealed a preferential activation toward a pro-inflammatory phenotype with increased expressions of chemokines such as *Ccl2*, *Ccl5*, *Cxcl2* and *Cxcl10* that can promote hematopoietic cell recruitment, hence matching previous transcriptomic analyses (Lewis et al., 2014). However, it is also noteworthy that the induction of these injury-promoting molecules was paralleled by the overexpression of genes involved in the expression of microglia protective functions such as *Igf1* and *Chil3*. In this regard, our observations support the hypothesis that microglial cells acquire complex phenotypes during autoimmune demyelination that may promote both tissue damage and repair (Vogel et al., 2013; Zhang et al., 2016). On the other hand, we also demonstrate the induction of genes associated with reactive astrogliosis and neurotoxic A1 functions in microglia during EAE. The expression of microglial *Gfap* and *Serpina3n* transcripts shown in this study has been previously reported in mouse models of injury and disease, and it is speculated that it might suppress pro-inflammatory pathways (Chiu et al., 2013; Noristani et al., 2017). Our results in the EAE model encourage additional studies using cell-type-specific transcriptomic analysis of microglia and complementary *in vitro* analyses to uncover the precise role of astrocyte population marker genes within these cells in MS pathophysiology. With regard to astrocytic A1-like genes, overexpression of *C1ra* and *C3* is in line with previous results from transcriptomic and *in situ* hybridization studies demonstrating the up-regulation of the complement pathway in microglia and monocyte-derived macrophages from EAE mice (Bourel et al., 2021; Lewis et al., 2014). A causal role of complement in the context of demyelination has been established based on previous reports showing that genetic loss of C3 protects EAE mice from synapse loss, reduces

microglial activation and decreases the severity of the clinical score (Hammond et al., 2020; Szalai et al., 2007). However, in this study only astrocytes displayed a significant correlation between *C3* induction and disease severity, which points to the possibility that microglial C3 expression is not crucially involved in disease pathogenesis. This hypothesis is consistent with recent reports that microglial $C3^+$ clusters are present in chronic but not in acute human MS lesions, suggesting that they do not drive formation of new lesions and could instead represent a physiological mechanism to remove damaged axons or myelin at advanced disease stages (Michailidou et al., 2017). Further supporting the hypothesis that astrocytes, and not microglial cells, are the main mediators of pathogenic C3 signaling in EAE, in our study C3 expression was predominantly associated to astrocytic profiles in spinal cord white matter from EAE mice. Altogether, these observations thus confer cell-type specificity to the protective phenotype C3 knockout mice in this MS mouse model with regard to white matter innate immune cells.

1.2. Deregulation of endocannabinoid signaling genes in astrocytes and microglia during EAE

The study of factors and mechanisms regulating astrocyte and microglia activation in MS has important therapeutic implications and is a matter of intense research. Findings of the current study indicate that these cell populations undergo gene expression changes affecting multiple endocannabinoid signaling molecules concomitant to their phenotypic activation in the EAE model and that these changes occur early during disease progression.

A role for endocannabinoids as modulators of MS pathology is supported by a number of studies reporting altered levels of these lipids in patients and rodent models of the disease. Increased concentrations of AEA have been determined in brain tissue, cerebrospinal fluid, and plasma from MS patients (Centonze et al., 2007; Eljaschewitsch et al., 2006; Di Filippo et al., 2008; Jean-Gilles et al., 2009). These observations have been replicated in EAE and correlated to increased NAPE-PLD and reduced FAAH expression and activities (Baker et al., 2001; Centonze et al., 2007). Concerning 2-AG, the majority of the studies report unaltered concentrations both in animal models and MS patients (Centonze et al., 2007; Manterola et al., 2018a; Maresz et al., 2007), although higher 2-AG levels have also been proposed in EAE mice (Baker et al., 2001). Although it is generally assumed that changes in endocannabinoid levels may be, at least in part, associated to the inflammatory reaction driven by innate immune cells in MS tissue, whether the transcriptional reprogramming of astrocytes and microglia during disease progression involves changes in the endocannabinoid biosynthetic and metabolic machinery has never been assessed. In this study, we show that both cell populations display significant reductions in 2-AG hydrolysis genes *Mgll*, *Abhd6*, and *Abhd12* at the early stages of EAE, paralleled or followed by reductions in *Dagla* and *Daglb* transcripts. Altogether, these results suggest that time-dependent transcriptional changes in astrocytes and microglial cells may contribute to the dysregulation of 2-AG levels in MS, and help explain some inconsistencies between previous studies. On the other hand, astrocytes and microglia purified over the course of EAE differ in the timing, extent, and sign of transcriptional changes affecting AEA production and metabolism machinery. Astroglia transiently and selectively over-expressed *Napepld* transcripts at presymptomatic disease while displaying early and persistent down-regulation of *Naaa* and *Fabp7* expression levels. However, astrocytes at asymptomatic and acute EAE also displayed increased transcript levels for *Faah*, consistent with the predominant localization of FAAH proteins in hypertrophic astroglia associated to active plaques in human MS (Benito et al., 2007). Conversely, isolated microglial cells showed selective down-regulation of *Faah* transcripts

paralleled by increased *Naaa* expression levels at acute and chronic stages. In sum, these findings illustrate the cell-type specificity of transcriptomic alterations regarding AEA biosynthesis and hydrolysis genes in a demyelinating context and suggest that both astroglia and microglial cells participate in the misbalance of AEA levels in MS.

A hurdle when interpreting the biological impact of changes in the gene expression pattern of endocannabinoid synthetic and metabolic machinery in purified cells is the absence of results showing parallel modifications in 2-AG and AEA levels. In this study, the low number of astrocytes and microglial cells purified for analysis precluded us from providing experimental evidence of changes in endocannabinoid contents. In this regard, the development of high-sensitivity liquid chromatography-mass spectrometry techniques allows nowadays the detection of very low amounts of endocannabinoids, but this experimental approach requires a $>10^6$ cells for accurate and reliable detection of changes in AEA and 2-AG levels (Chicca et al., 2017; Hermes et al., 2018; Marrs et al., 2010; Muccioli et al., 2007). When evaluating the utility of endocannabinoid measurements as readout of unbalanced production/metabolism, it should also be kept in mind that these alterations may be activity-dependent *in vivo* and, therefore, not faithfully mirrored upon determination of basal levels in purified cells. Experimental limitations concerning cell availability in this study also applied to the detection of proteins for the main components of the endocannabinoid system, which is further hindered by the low expression levels of several of these molecules in astrocytes and microglia as well as by antibody specificity issues (Ashton, 2012; Grimsey et al., 2008; Metna-Laurent and Marsicano, 2015). Although the outcome of expression changes in the production and metabolic genes on endocannabinoid levels in the vicinity of the cells remains, thus, to be established, gene expression results in astrocytes purified at asymptomatic EAE lead us to postulate an imbalance in 2-AG mediated activity at early disease stages. Indeed, down-regulated *Mgll* and *Abhd6* transcript levels in astrocytes without concomitant reductions in *Dagla* expression may be associated with enhanced 2-AG levels in the context of previous work. This possibility is supported by lipase profiling experiments demonstrating that MAGL and ABHD6 are responsible for approximately 85% and 8% of brain 2-AG hydrolysis (Blankman et al., 2007), as well as by results from global pharmacological or genetic inactivation studies showing that both enzymes control the accumulation and biological activity of this lipid mediator (Long et al., 2009; Marrs et al., 2010). Further, the analysis of astrocyte-specific MAGL knockout mice has consistently demonstrated that astrocytic MAGL plays a substantive role in 2-AG metabolism and its inactivation leads to deficient endocannabinoid clearance. In particular, conditional deletion of MAGL in astrocytes leads to a 40% reduction in brain 2-AG hydrolysis and 3-fold increases in 2-AG levels while enabling the spatial diffusion of endocannabinoid signaling at neuronal CB_1Rs (Chen et al., 2016; Liu et al., 2016; Viader et al., 2015). On the other hand, there is also consensus that MAGL inactivation triggers CB_1Rs down-regulation upon sustained exposure to increased endocannabinoid levels (Bernal-Chico et al., 2015; Schlosburg et al., 2010). Consistently, astrocytes purified during acute, but not asymptomatic, EAE disease showed reduced *Cnr1* transcript levels that persisted at the recovery phase. Although changes in endocannabinoid levels cannot be inferred based only on transcriptional deregulation and caution is thus needed when interpreting these data, altogether our results point to an early shift toward enhanced 2-AG mediated activity onto astrocytic CB_1Rs that may be followed by deficits at more progressive stages of the autoimmune demyelination process.

Our data concerning deregulation of *Mgll*, *Abhd6*, *Dagla*, *Faah*, and *Fabp7* transcript levels in astrocytes purified during acute EAE confirm results from a recent transcriptomic study in EAE mice at 45 days post-immunization (Itoh et al., 2018). These authors used RiboTag technology applied to Gfap-Cre mice to determine astrocyte-specific gene expression networks in multiple regions of the CNS but did not validate RNA-seq results using RT-qPCR and did not report changes in additional endocannabinoid system genes. It is noteworthy, however, that two studies using fundamentally different experimental approaches show similar alterations regarding endocannabinoid activity associated genes at acute/chronic EAE stages. Altogether, these observations indicate that deregulated astrocytic expression of endocannabinoid biosynthesis and metabolism genes is a consistent finding in the EAE mouse model of MS.

A role for endocannabinoids in preventing or attenuating reactive astrogliosis and microglial reaction in MS mouse models is supported by a number of studies using genetic and pharmacological tools (Bernal-Chico et al., 2015; Maresz et al., 2007; Ortega-Gutiérrez et al., 2005; Palazuelos et al., 2008). However, how these observations translate to disease progression in terms of pathogenic versus protective astrocyte and microglia functions and the detailed mechanisms underlying such effects remain to be fully elucidated. The early deregulation of endocannabinoid system genes in astrocytic and microglia during EAE reported here supports the possibility that these lipid mediators tune the phenotypic transformation of these cells in demyelinating conditions. Indeed, endocannabinoids have been pointed out to promote the acquisition of an alternative, regenerating phenotype in microglia *in vitro* (Mecha et al., 2015), although similar analyses have not yet been performed in astrocytes. Together with previously published results, our observations warrant further investigation on the role of endocannabinoids in the phenotypic activation of innate immune cells using cell-specific gain or loss-of-function strategies and *in vivo* disease models. In the same context, the extent to which alterations in the expression pattern of endocannabinoid system genes in innate immune cells determines the general neuroprotective and regenerative role of these endogenous lipids in MS requires further analysis. In this regard, a role for astroglial and microglial endocannabinoid systems in neurodegenerative conditions is supported by accumulating evidence demonstrating the relevance of endocannabinoid-mediated crosstalk mechanisms between innate immune cells and neurons in regulating brain functions (Araque et al., 2017; Scheller and Kirchhoff, 2016). Concerning endocannabinoid signaling in MS, neuronal CB_1Rs and CB_2Rs in T cells have been established as crucial determinants of cannabinoid-mediated EAE suppression based, in part, on studies using cell-type-specific knockdown strategies (Maresz et al., 2007). However, with the exception of our present results using astrocyte-specific CB_1R null mice in the EAE model, similar experimental approaches have not yet been applied to the analysis of the neuroglial endocannabinoid system in MS. In the light of these results, further studies using transgenic mice or virus-mediated strategies to specifically modulate endocannabinoid system elements in astrocytes and microglia are needed to decipher the relevance of these cell types as targets and mediators of endocannabinoid signaling in MS.

2. Calcium dynamics in astrocytes during EAE

2.1. CB_1 receptor activation increases cytosolic calcium in astrocytes in vivo

A number of previous studies in rodent and human settings have convincingly demonstrated that activation of astrocyte CB_1Rs increases cytosolic Ca^{2+} activity in these cells leading to the modulation of synaptic transmission and behavior through the release of gliotransmitters (Araque et al., 2017; Covelo et al., 2021). Most of the data available at the present time, however, derive from studies performed in tissue slices (Carlsen et al., 2021; Martin-Fernandez et al., 2017; Robin et al., 2018). Results from *ex vivo* experimental conditions often differ from findings in living animals and, with regard to astrocytic function, it is also well established that Ca^{2+} transients in these cells are affected by anesthesia and restraint-induced stress (Qin et al., 2020). Imaging studies in freely moving mice are therefore necessary to elucidate both the mechanisms and implications of CB_1Rs in modulating astrocyte Ca^{2+} dynamics in health and disease. Using fiber photometry, we show that systemically administered Δ^9-THC increases the amplitude and duration of astrocyte Ca^{2+} transients in the mouse cortex thus supporting the *in vivo* relevance of astroglial cells as targets and mediators of cannabinoid effects. Assessments in CB_1-KO mice corroborate that modulation of cytosolic Ca^{2+} activity in cortical astrocytes by Δ^9-THC depends on the activation of CB_1Rs. Interestingly, systemic Δ^9-THC enhanced the amplitude (but not the duration) of astrocyte Ca^{2+} transients in GFAP-CB_1-WT mice, and this effect was absent in GFAP-CB_1-KO mice. This latest result demonstrates that cytosolic Ca^{2+} increases by systemically administered Δ^9-THC are mediated by the astrocytic pool of CB_1Rs and highlights the relevance of this receptor population in the effects of cannabinoids in living mice. Our observations in this regard are in good agreement with recent pharmacological studies showing that Ca^{2+} responses by acute cannabinoids in the somas and main processes of astrocytes are absent in GFAP-CB_1-KO mice (Martin-Fernandez et al., 2017; Robin et al., 2018). These results also points to cytosolic Ca^{2+} increases as a parameter that faithfully reflects astrocyte CB_1R function *in vivo*. On the other hand, discrepancies in the ability of the cannabinoid agonist to modulate the duration of astrocyte Ca^{2+} signals between mouse strains may originate from to differences in methodological approaches or reflect divergent baseline astrocyte or network activities. In this regard, it is worth mentioning that the duration of astrocyte Ca^{2+} signals was selectively reduced in GFAP-CB_1-KO mice - and not in CB_1-KO mice - as compared to their respective littermate controls recorded in parallel. This observation may suggest a tonic control of astrocyte Ca^{2+} dynamics in terms of duration by astrocyte CB_1Rs in GFAP-CB_1-WT mice that masks the effects of the exogenous cannabinoid agonist. To the best of our knowledge, changes in the duration of astrocyte Ca^{2+} signals mediated by CB_1Rs have not been previously reported in studies *ex vivo* and may be restricted to *in vivo* activity in freely moving mice. Unfortunately, the mechanisms that determine dynamic changes in the amplitude and duration of astrocyte Ca^{2+} activity *in vivo* remain to be fully characterized and our observations regarding the effect Δ^9-THC on these parameters are difficult to interpret at the present time.

Our fiber photometry results add to the growing body of evidence pointing to a crucial role of astrocyte CB_1Rs in the regulation of brain physiology as well as mediators of the pharmacological effects of exogenous cannabinoids. Although *in vivo* studies assessing the impact of astrocyte CB_1Rs on synaptic activity are scarce, available evidence indicates that activation of this receptor population translates into variety of short- and long-term synaptic effects underlying complex brain functions such as memory and sensory remodeling (Covelo et

al., 2021). In this regard, it is worth mentioning that astrocyte CB_1Rs mediate hippocampal long-term depression (LTD) induced *in vivo* by systemically administered Δ^9-THC through a mechanism that involves the release of glutamate as gliotransmitter and the activation of extrasynaptic NMDA receptors (Han et al., 2012). These observations sit well with the fact that GFAP-CB_1-KO mice display memory deficits in the NOR task likely resulting from alterations of astrocyte Ca^{2+} dynamics and subsequent gliotransmitter release (Covelo and Araque, 2018; Martin-Fernandez et al., 2017; Robin et al., 2018). Concerning cortical activity, astrocyte CB_1Rs have been critically involved in spike timing-dependent depression at neocortical synapses *ex vivo* through a signaling cascade that implies Ca^{2+} increases and subsequent glutamate release (Min and Nevian, 2012). In the context of these results, our present findings support the hypothesis that astrocyte CB_1Rs may promote glutamate release as gliotransmitter in the mouse cortex *in vivo*. It should be highlighted, however, that the mechanisms underlying the modulation of synaptic transmission and plasticity by astroglial CB_1Rs in the neocortex remain incompletely explored and most likely involve additional gliotransmitters such as ATP or D-serine, as described in other brain regions (Araque et al., 2014; Martin-Fernandez et al., 2017; Robin et al., 2018).

Astrocytes express CB_1Rs both at the plasmatic and mitochondrial membranes (mtCB_1Rs) whose specific roles in the regulation of astrocyte biology are nowadays beginning to be elucidated. The mechanisms underlying crosstalk between plasma and mtCB_1Rs in the control of astrocyte Ca^{2+} dynamics are poorly understood but a recent study proposes that the mtCB_1R population actively promotes mitochondrial Ca^{2+} intake through ER/IP_3R/AKT pathways in these cells (Serrat et al., 2021). Using fiber photometry with a mitochondria-specific Ca^{2+} sensor for astrocytes, Serrat and collaborators (2021) showed that systemic Δ^9-THC increases Ca^{2+} levels in these organelles in the somatosensory cortex and hippocampus and of freely behaving mice. Furthermore, the mtCB_1R pool seems to be specifically involved in the lateral synaptic potentiation of hippocampal synapses. Interestingly, assessments in astrocytes *in vitro* suggest that mitochondrial Ca^{2+} uptake upon activation of mtCB_1R takes place independently of Ca^{2+} levels in the cytosol, and therefore, the extent to which systemic Δ^9-THC increases cytosolic Ca^{2+} activity in astrocytes remained an open question (Serrat et al., 2021). Indeed, another remarkable difference between both studies is that Δ^9-THC increased the duration of the Ca^{2+} transients in the cytosol but not in the mitochondria of cortical astrocytes, thus highlighting specificities in cannabinoid modulation of astrocyte Ca^{2+} responses between both intracellular compartments. Altogether, these results support a scenario in which Δ^9-THC promotes both cytosolic and mitochondrial Ca^{2+} increases in rodent astrocytes *in vivo* by activating distinct subcellular pools of CB_1Rs in astroglial cells.

2.2. Astrocytes activated during EAE display dysfunctional calcium signaling properties

Reactive astrocytes exhibit a wide variety of physiopathological responses closely associated with the onset and/or development of CNS diseases. In addition to extensive changes in gene expression profiles, functional changes involving aberrant Ca^{2+} signaling in astrocytes have been pinpointed in several neurodegenerative conditions (Shigetomi et al., 2019). In particular, cortical astrocytes in the APP/PS1 mouse model display higher frequency of spontaneous Ca^{2+} events but diminished responses to sensory stimulation as determined by *in vivo* imaging in anesthetized mice (Lines et al., 2022). In this study, spontaneous Ca^{2+} hyperactivity was related to Aβ density and associated to dysregulated electrical cortical activity. In the same line, cortical

astrocytes nearby Aβ plaques display Ca^{2+} hyperactivity associated to local blood flow changes in anesthetized APP/PS1 mice evaluated using multiphoton microscopy (Delekate et al., 2014). Pharmacological assessments suggested that astroglial network dysfunction in the APP/PS1 mouse is mediated by purinergic signaling through P_2Y_1 receptors coupled to $G_{\alpha q}$ in reactive astrocytes. In the R6/2 mouse model of HD, by contrast, striatal astrocytes show significant reductions in the amplitude, duration, and frequency of spontaneous Ca^{2+} signals *ex vivo* (Jiang et al., 2016). Interestingly, this study proposes that the loss of spontaneous Ca^{2+} in R6/2 mice occurs in the absence of overt reactive astrogliosis and may reflect lower ER store capacity in HD astrocytes. Remarkably, dysfunctional astrocyte Ca^{2+} signaling was associated to altered medium spiny neuron (MSN) activity and repetitive self-grooming behaviors in HD mice (Yu et al., 2018). A follow-up study of the same laboratory unveiled that $G_{\alpha i}$ signaling pathways are consistently inhibited in HD astrocytes and that activation of astrocytic $G_{\alpha i}$-GPCRs using pharmacogenetic tools rescues spontaneous Ca^{2+} handling deficits and behavioral phenotypes behaviors in HD mice (Yu et al., 2020). These studies show that astrocyte Ca^{2+} signaling is dysregulated during CNS pathology in a disease-specific manner and is relevant to neuromodulatory deficits underlying behavioral abnormalities in neurodegenerative conditions.

To the best of our knowledge, this is the first study to explore the *in vivo* dynamics of astrocyte Ca^{2+} activity during autoimmune demyelination. Our results in freely-behaving mice show dysfunctional spontaneous and stimulus-evoked astrocytic Ca^{2+} signals associated to EAE progression. In particular, cortical astrocytes in EAE mice showed spontaneous Ca^{2+} transients of reduced amplitude and frequency but increased duration, whereas sensory-evoked Ca^{2+} events were impaired only in terms of amplitude. The onset of astrocytic Ca^{2+} deregulation paralleled the appearance of neurological disability at 12 dpi raising the possibility that these changes may reflect motor deficits. Indeed, locomotion is directly associated to increases in astrocytic Ca^{2+} activity *in vivo* (Bojarskaite et al., 2020; Qin et al., 2020) and we cannot discard that loss of motor coordination and muscle tone associated to EAE progression may underlie, at least in part, aberrant astrocyte Ca^{2+} dynamics in the somatosensory cortex. Supporting this hypothesis, deficits in the amplitude of astrocyte Ca^{2+} transients correlated to disease severity at different time-points of EAE progression. By contrast, neither the frequency deficits nor the observed increase in the duration of astrocyte Ca^{2+} signals during EAE correlated with motor symptoms, which suggests that different disease-associated regulatory mechanisms underlie changes in each parameter. Unfortunately, the activity patterns and characteristics of astrocytic Ca^{2+} signals are complex and highly heterogeneous *in vivo* and have not been characterized in detail. The mechanistic implications of the observed changes in astrocyte Ca^{2+} dynamics during EAE require, therefore, further *ex vivo* and *in vivo* analysis. In this context, it is important to highlight that our targeted gene expression analysis suggests that astrocyte Ca^{2+} deficits during EAE do not merely reflect deficient motor activity. Indeed, astrocytes purified from EAE mice or activated *in vitro* to a neurotoxic phenotype displayed changes in the expression of several GPCRs (*Cnr1*, *Grm1*, *Grm3*, *Grm5*, *P2ry1*, *Adora1*, *Adora2a*, *Adora2b*) and G-protein effectors (*Gnaq*, *Itpr1*, *Itpr2*, *Ryr1, Ryr2*, *Ryr3*) implicated in Ca^{2+} signaling as well as aberrant responses to glutamate and ATP. These observations are in good agreement with previously published results showing that inflammatory stimuli significantly deregulates, mostly down, astrocyte Ca^{2+} signaling stimulated by multiple GPCR both at the gene expression and functional level, in parallel to the upregulation of immune signaling and cell injury molecular networks (Hamby et al., 2012). Comparison of the study of Hamby and coworkers (2012) and our present findings in

cultured cells highlights commonly down-regulated genes, such as *P2ry1* and *Adora1*, but also certain discrepancies most likely related to the different pro-inflammatory stimuli used. For instance, microarray analysis of whole-genome expression in astrocytes activated with TGF-ß1, LPS and IFNγ did not highlight changes in *Gnaq* and *Itpr2* (Hamby et al., 2012), in contrast to our observations in cells stimulated with TNFα, IL-1α and C1q. Altogether, these results suggest that reactive astrogliosis is associated to stimulus-specific deficits in Ca^{2+} handling mechanisms and point to the (co)existence of heterogeneous populations of dysfunctional astrocytes in terms of Ca^{2+} signaling contributing to CNS pathologies. Remarkably, down-regulated expression of *Gnaq* and *Itpr2* in neurotoxic astrocytes induced *in vitro* was corroborated in cells purified during acute EAE. Given the central role of both molecules in astrocyte Ca^{2+} responses (Sherwood et al., 2021; Srinivasan et al., 2015), at the light of our results it seems plausible to speculate that reductions in intracellular Ca^{2+} mobilization via the PLC-IP_3 pathway may underlie, at least in part, attenuated cytosolic Ca^{2+} responses in cortical astrocytes during autoimmune demyelination. When interpreting these results it should be kept in mind that reduction of astrocyte Ca^{2+} signaling may be accompanied with changes in gene expression, which makes it difficult to dissociate primary from secondary effects. This problem was recently addressed by generating a new transgenic mouse line to achieve inducible astrocyte Ca^{2+} signaling attenuation *in vivo* by expressing a plasma membrane Ca^{2+} pump that constitutively excludes cytosolic Ca^{2+} (CalEx) (Yu et al., 2018). This approach reduced the amplitude and duration of spontaneous and GPCR-mediated astrocyte Ca^{2+} signals by ~70% in striatal slices, altered MSN activity and induced self-grooming behaviors. In this study, *in vivo* attenuation of astrocyte Ca^{2+} signaling did not promote the expression of pan-reactive of neurotoxic A1 genes but induced cell autonomous and non-autonomous effects on astrocyte gene expression selectively affecting molecules involved in membrane protein trafficking and stabilization. In a recent study of the same laboratory, specific attenuation of G_q GPCR signaling in striatal astrocytes *in vivo* did not affect gene expression or spontaneous Ca^{2+} signaling (Nagai et al., 2021). None of these studies highlighted gene expression changes affecting Ca^{2+} handling pathways following attenuation of astrocyte Ca^{2+} signaling *in vivo*. Together with our *in vitro* and *in vivo* results, these observations support the hypothesis that reduction in astrocyte Ca^{2+} signaling in EAE mice occurs because of cell activation and relies on gene expression changes associated to the phenotypic transformation of these cells in an inflammatory environment.

In this study, deficits in spontaneous and stimulus-evoked astrocyte Ca^{2+} activities were accompanied by impaired Ca^{2+} responses to Δ^9-THC in mice at acute EAE disease. These observations point to deficient Ca^{2+} signaling by astrocytic CB_1Rs and might reflect reductions in the size of the astrocytic receptor pool during EAE, as suggested by the down-regulated expression levels of *Cnr1* in cells purified at acute and chronic disease stages. Alternatively, changes in the expression of additional molecules mediating cytosolic Ca^{2+} responses by G_q GPCRs might also contribute to the observed deficits in CB_1R-mediated astrocyte Ca^{2+} increases in EAE mice. Regardless of the underlying mechanisms, according to the existing literature in the field (Covelo et al., 2021), it seems plausible that deficient Ca^{2+} signaling by astrocyte CB_1Rs translates to deficits in gliotransmitter release and astrocyte-to-neuron communication and contributes to cortical pathology in MS. The extent to which dysfunctional astrocyte Ca^{2+} signaling stimulated by CB_1Rs contributes to deficits in spontaneous and stimulus-evoked activity of cortical astrocytes during EAE remains uncertain. Arguing against this possibility,

conditional mutant mice lacking astrocyte CB_1Rs did not display changes in the amplitude of astrocyte Ca^{2+} transients and showed instead signals of reduced duration and increased frequency. In the same line, ablation of astrocyte G_q GPCR signaling *in vivo* did not affect spontaneous Ca^{2+} signaling in striatal cells (Nagai et al., 2021). Indeed, astrocyte Ca^{2+} signals are nowadays recognized to be diverse and mediated by both GPCR dependent and independent mechanisms (Semyanov et al., 2020; Shigetomi et al., 2016; Volterra et al., 2014). On the other hand, our gene expression data and Ca^{2+} imaging results in cultured cells suggest that changes in GPCRs mediating glutamate and ATP signaling may also contribute to impairments in astrocyte Ca^{2+} activity during EAE. In particular, astrocytes activated *in vitro* and purified at acute disease displayed significant reductions in the gene expression of mGluR3, which predominates in adult astrocytes compared to mGluR5 (Haustein et al., 2014; Jiang et al., 2016; Sun et al., 2013) and represents the only mGluR whose expression is down-regulated in both experimental settings. This result is consistent with previous observations in astrocytes purified from RiboTag mice at chronic EAE disease (Itoh et al., 2018). Noteworthy, glutamate mGluR3 receptors promote cytosolic Ca^{2+} elevations in adult astroglial cells despite being $G_{\alpha i/o}$ coupled (Haustein et al., 2014; Jiang et al., 2016) and deficits in the expression of this receptor proteins might thus contribute to dysregulated astrocyte Ca^{2+} responses during autoimmune demyelination *in vivo*. Concerning ATP responses, our gene expression results show downregulated levels of *Adora2a* and *Adora2b* in EAE astrocytes that were not mirrored in cells activated *in vitro* with PIFs. In parallel, we measured reduced expression of *P2ry1* and *Adora1* that reached statistical significance in the *in vitro* setting. Discrepancies in gene expression results between astrocytes from EAE mice and cultured cells stimulated with PIFs may originate from differences associated to the *in vivo* versus *in vitro* inflammatory environments and/or reflect a more complex and dynamic deregulation of Ca^{2+} signaling tools in astroglia activated in the context of neuroinflammation *in vivo*. Mechanistic considerations notwithstanding, these observations suggest that impaired responses to ATP and adenosine could contribute to dysfunctional spontaneous and stimulus-evoked astrocyte Ca^{2+} signals during EAE. Indeed, it is well stablished that astrocytes in the adult mouse brain express a variety of ATP and adenosine GPCRs that are $G_{\alpha i}$ coupled (*Adora1*), as well as adenosine receptors coupled to $G_{\alpha s}$ (*Adora2a*, *Adora2b*), whose activation leads to cytosolic Ca^{2+} responses (Blanca et al., 2019; Durkee and Araque, 2019; Nagai et al., 2021; Verkhratsky and Nedergaard, 2018). Furthermore, Ca^{2+} signals induced by ATP in astrocytes *ex vivo* seem to be mediated by a combination of $G_{\alpha i}$ coupled P_2Y receptors and adenosine receptors, but not markedly by $G_{\alpha q}$ protein coupled receptors (Nagai et al., 2021). Altogether, these observations point to deficits in astrocyte Ca^{2+} signaling evoked by glutamate, ATP and adenosine as underlying mechanisms of dysfunctional astrocyte Ca^{2+} responses in cortical astrocytes during EAE. From a mechanistic perspective, imaging experiments in cells activated *in vitro* suggest that astrocyte Ca^{2+} impairments do not reflect changes in ER store capacity but may instead involve deregulation of mitochondria Ca^{2+} handling mechanisms. This hypothesis is consistent with deficits in the expression of *Mcu* and *Slc8b1* in astrocytes purified at acute EAE. A role of mitochondria in the development of MS is nowadays supported by multiple lines of evidence including both functional and anatomical studies. Diffuse mitochondrial respiratory chain defects are seen in axons, oligodendrocytes and astrocytes in *postmortem* MS tissue (Mahad et al., 2008) and focal intra-axonal mitochondrial pathology is the earliest ultrastructural sign of damage preceding demyelination in the EAE model of MS (Nikić et al., 2011). Reports on astrocyte mitochondrial dysfunction in MS are still scarce, but

available data show upregulated mitochondrial oxidative phosphorylation (OXPHOS) and decreased production of lactate available for the metabolic support of neurons during EAE (Chao et al., 2019). OXPHOS depends critically on Ca^{2+} entry into the mitochondria, which guides ATP synthesis by modulating dehydrogenase activity and mitochondrial membrane potential (Wescott et al., 2019) and it is envisaged that altered mitochondrial calcium dynamics may have profound pathogenic implications in MS that have only recently begun to be addressed. In this context, our results suggest that deregulated astrocyte mitochondrial Ca^{2+} handling may be associated to dysfunctional bioenergetics contributing to MS pathogenesis.

Concerning the pathogenic implications of dysfunctional astrocyte Ca^{2+} signaling during autoimmune demyelination, accumulating studies show that changes in the Ca^{2+} dynamics of astroglial cells affect synaptic transmission leading to behavioral abnormalities in neurodegenerative diseases (Nagai et al., 2021; Shigetomi et al., 2019; Yu et al., 2020). It is also well established that MS is associated to grey matter damage affecting brain cortical structures. In particular, functional and structural alterations affecting the cortex are present from the earliest stages of MS and have been associated a number of disease-related symptoms including slowly of voluntary movements, pain, cognitive impairment and depressive-like behaviors (Calabrese et al., 2015; Feinstein et al., 2014; Potter et al., 2016). Recent studies have shown a widespread and pronounced loss of dendritic spines in MS cortex that occurs independently of cortical demyelination and axon loss, suggesting that synaptic dysfunctions might be a primary event in MS (Jürgens et al., 2016). In this regard, electrophysiological evidence suggests that an early excitatory-inhibitory imbalance leading to excitotoxicity contributes to the synaptic loss and neurodegeneration observed in MS (Ellwardt et al., 2018; Potter et al., 2016). The pathogenic mechanisms underlying cortical pathology in MS have not been investigated in detail but experiment evidence in the EAE model suggest that microglial cells are activated at early disease stages (Potter et al., 2016). However, the contribution of astroglial cells to cortical dysfunction in MS remains largely unexplored in MS. In this context, our results support the hypothesis that deficits in astrocyte Ca^{2+} handling properties may contribute to cortical synaptic deregulation and cognitive impairments in MS and lays the foundation for future mechanistic analyses.

3. Astrocyte CB_1 receptors exacerbate EAE severity

In this study, we assessed for the first time the role of astrocyte CB_1Rs during neuroinflammation *in vivo* using conditional mice as experimental strategy to reduce receptor function. Our results show that astrocyte CB_1R ablation ameliorates neurological disability in the EAE model thus suggesting that the pool of CB_1Rs located on astroglial cells play a deleterious role during autoimmune demyelination. The protective phenotype of astrocyte CB_1R null involved attenuated myelin loss, inflammatory reactions and axonal damage in spinal cord tissue. Reducing astrocyte CB_1R signaling also ameliorated cortical pathology and astrocyte Ca^{2+} activity deregulation during EAE. In all, these observations suggest that astrocyte CB_1R signaling promotes pathogenic functions in MS and, potentially, other neurological disorders.

The relevance of CB_1Rs as regulators of astrocyte function in neuropathological conditions remains largely unexplored. Given the complexity of CB_1R signaling in astrocytes, which involves both plasma and mitochondrial receptor pools regulating Ca^{2+} signaling, gliotransmitter release and metabolism (Covelo et al., 2021; Jimenez-Blasco et al., 2020; Serrat et al., 2021), it seems

likely that the protective phenotype of astrocyte CB_1R null mice in the EAE model involves several faces of astrocyte biology. In this study, we do not provide a definitive mechanistic explanation for the protective effects resulting from knocking down astrocyte CB_1Rs during autoimmune demyelination, although our histological and gene expression analysis may provide some insights. In particular, astrocyte CB_1R deletion was associated to a reduced presence of demyelinating lesions at chronic EAE which points to several non-exclusive possibilities. Firstly, CB_1Rs might negatively modulate the production of pro-myelinating factors by astroglial cells and thus attenuate the efficacy of the remyelination process during chronic EAE disease (Lundgaard et al., 2014), which should be further evaluated using more specific *in vivo* models of myelin repair. Alternatively, astrocyte CB_1Rs may positively coupled to the modulation of pro-inflammatory signaling pathways that promote autoimmune demyelination. Indeed, amelioration of EAE disease severity in astrocyte CB_1Rs deficient mice was associated to a reduction in the numbers of infiltrating T lymphocytes and microglia/macrophages in lesion sites. In addition, gene expression data show a global down-regulation in the expression of pro-inflammatory molecules in spinal cord tissue of mice lacking astrocyte CB_1R during EAE. Among these, we found a significant reduction in the expression of *Vcam1* and *Icam1* adhesion molecules, which are overexpressed by reactive astrocytes in neurodegenerative contexts, including MS and EAE, and crucially involved in the recruitment of pathogenic T cells into the CNS (Gimenez et al., 2004; Lee et al., 2000). These observations suggest pro-inflammatory functions of astrocyte CB_1Rs in autoimmune demyelinating contexts.

Several lines of evidence demonstrate that neurotoxic astrocytes are present in MS and participate to disease pathogenesis (Liddelow et al., 2017; Hou et al., 2020) as supported by our results in cells purified from EAE mice. In this study, astrocyte CB_1R null mice displayed an attenuated presence of C3 immunopositive reactive astroglial profiles in the spinal cord white matter at chronic EAE, which was consistent with reduced expression levels of several A1 phenotype associated genes (*C3*, *Fkbp5*, *Ggta1*, *Psmb8*) at earlier disease stages. These findings were paralleled by significant reductions in axonal damage, measured by SMI-32 immunostaining, and increased expression levels of neuron/synaptic markers (*Rbfox3* and *Snap25*) in mice lacking astrocyte CB_1Rs. Overall, these results are consistent with previous reports showing that astrocyte conversion to a neurotoxic phenotype is pathogenic in the EAE model (Hou et al., 2020; Zhao et al., 2020), further supported by the positive correlation between C3 expression and neurological disability scores in spinal cord tissue observed in this study. Taken together, these observations also support the possibility that astrocyte CB_1R signaling facilitates cell conversion to a neurotoxic phenotype during EAE through cell autonomous or non cell-autonomous mechanisms and thus exacerbates neuroaxonal damage and neurological disability during disease progression. The extent to which astrocyte CB_1Rs are coupled to the activation of pro-inflammatory pathways promoting pathogenic upregulation of C3 remains in these cells a matter of future research.

This study also provides evidence that genetic loss of astrocyte CB_1Rs ameliorates Ca^{2+} signaling deficits associated to EAE in freely behaving mice. In particular, our results in conditional mutants show that astrocyte CB_1R deletion prevents dysregulation of spontaneous and stimulus-evoked Ca^{2+} activity in cortical astrocytes during EAE in parallel to the amelioration of motor symptomatology. This particular observation strengthens the hypothesis that cytosolic Ca^{2+} deregulation in cortical astrocytes is associated to neurological disability during EAE and

would suggest shared underlying mechanisms. Remarkably, astrocyte CB_1R deletion reduced the number of T cell containing inflammatory lesions in the cortex of EAE mice. Based on these results, we postulate that inflammatory responses driven by astrocyte CB_1Rs in the brain cortex may underlie dysfunctional Ca^{2+} activity during EAE. Our combined observations in the brain cortex extends the protective phenotype astrocyte CB_1R null mice from white matter cells to astrocytes in the grey matter thus highlighting the pathogenic relevance of the CB_1R receptor pool expressed by astroglial cells in demyelinating contexts.

The attenuated disease phenotype of astrocyte CB_1R null mice that we describe here contrasts to the general neuroprotective and anti-inflammatory effects ascribed to (endo)cannabinoids in rodent models of MS and other neurodegenerative conditions (Chiurchiù et al., 2018; Cristino et al., 2020). Up to the date, however, only a limited number of studies have addressed the specific role of CB_1Rs in regulating the function of innate immune cells in neuroinflammatory contexts. Remarkably, the recent generation and characterization of a conditional mouse model of CB_1R deletion specifically in microglia has revealed pro-inflammatory functions of this receptor pool in response to an immune challenge despite being expressed at very low levels (De Meij et al., 2021). In this study, genetic deletion of CB_1Rs in CX3CR1-positive cells attenuated brain cytokine production by LPS. These results are in line with previous reports showing protection from inflammation by pharmacological CB_1R blockade and/or global CB_1R deletion (Huang et al., 2010; Mehrpouya-Bahrami et al., 2017; Suárez et al., 2019). Concerning astroglial cells, a role for CB_1Rs as mediators of astrocyte inflammatory responses can be inferred from studies using genetic and pharmacological strategies to modulate FAAH activities and thus enhance endocannabinoid signaling by AEA. Mice bearing deletion of FAAH exhibit increased astrocyte hemichannel activity and ATP release leading to exacerbated *in vivo* microglial responses to injury through mechanisms that involve the activation of CB_1Rs (Vázquez et al., 2015a). In the same line, FAAH inactivation potentiated neuroinflammation in the 5xFAD mouse model of AD as evidenced by the increased expression levels of TNF-α, IL-1β and IL-6 in 5xAD/FAAH null mice (Vázquez et al., 2015b). Remarkably, pharmacological CB_1R blockade normalized the levels of pro-inflammatory cytokines in 5xAD mice lacking FAAH thus suggesting that CB_1R signaling is pro-inflammatory in an AD context. It should be noted, however, that pharmacological CB_1R blockade exacerbated neuroinflammation in this mouse models of AD (Vázquez et al., 2015b). Further support for a pathogenic role of astrocyte CB_1Rs is provided by the study of Coiret and collaborators (2012) in a model in which astrocyte Ca^{2+} elevations sustains seizure-like activity in the hippocampus. In this study, CB_1R blockade reduced epileptiform discharges while abolishing cytosolic Ca^{2+} signals in astrocytes thus suggesting that endocannabinoid signaling to CB_1Rs in astroglia contributes to the pathogenesis of seizures (Coiret et al., 2012). Altogether, these studies highlight a dual and complex role of CB_1R in the context of neuroinflammation and suggest that the astrocyte receptor pool may promote pro-inflammatory and neurodegenerative effects of (endo)cannabinoids in disease models.

Conclusions

In this Thesis, we sought to characterize the role of endocannabinoids and CB_1Rs in regulating the functional activity of astroglial cells in MS. Our results unveil astrocyte activation in a demyelinating context is associated to deregulated expression of endocannabinoid signaling genes and that pathogenic responses to autoimmune demyelination are astrocyte CB_1R dependent. Furthermore, we identify CB_1Rs as crucial regulators of astrocyte Ca^{2+} dynamics in the mouse cortex *in vivo* and uncover aberrant Ca^{2+} signaling in MS pointing out to a novel role of the endocannabinoid system in the pathophysiology of myelin.

The main **Conclusions** of our study are as follows:

I. Astrocytes upregulate the expression of neurotoxic phenotype associated genes early during EAE progression thus supporting a pathogenic role of this subset of reactive astrocytes in MS. On the other hand, microglia exhibit an intermediate polarization state regarding the expression of inflammatory genes during EAE.

II. Astrocytes and microglia activated during autoimmune demyelination display cell-type-specific transcriptional alterations affecting endocannabinoid system associated molecules that suggest deregulated endocannabinoid signaling onto and by innate immune cells in MS.

III. Cortical astrocytes display spontaneous and stimulus-evoked Ca^{2+} signaling deficits during EAE that correlate in part to neurological disability thus highlighting the involvement of common underlying mechanisms.

IV. Astrocytes activated *in vitro* and *in vivo* show deregulated gene expression of Ca^{2+} handling molecules as well as impaired cytosolic Ca^{2+} responses to glutamate and ATP that may contribute to Ca^{2+} signaling deficits during demyelination *in vivo*.

V. Activation of astrocyte CB_1Rs elicits robust cytosolic Ca^{2+} responses in cortical astrocytes in freely behaving mice that are impaired during EAE. In the context of previous studies, these observations suggest deficits in endocannabinoid mediated astrocyte-to-neuron communication leading to synaptic dysfunction in MS.

VI. Genetic deletion of astrocyte CB_1Rs attenuates EAE severity and prevents Ca^{2+} handling deficits associated to disease progression through mechanisms that may involve the modulation of T cell and microglia/macrophage recruitment and neurotoxic astrocyte conversion. As a whole, these results point to an unexpected pro-inflammatory role of astrocyte CB_1Rs in demyelinating contexts.

Altogether, these findings broaden current understanding on the mechanisms mediating the benefits/side effects of currently available MS treatment approaches targeting CB_1Rs and lay the foundation for future research aimed at developing novel, more efficacious endocannabinoid system-modulating drugs to treat MS.

References

Abbott, N.J., Rönnbäck, L., and Hansson, E. (2006). Astrocyte-endothelial interactions at the blood-brain barrier. Nat. Rev. Neurosci. *7*, 41–53.

Aebischer, J., Cassina, P., Otsmane, B., Moumen, A., Seilhean, D., Meininger, V., Barbeito, L., Pettmann, B., and Raoul, C. (2011). IFNγ triggers a LIGHT-dependent selective death of motoneurons contributing to the non-cell-autonomous effects of mutant SOD1. Cell Death Differ. *18*, 754–768.

Agarwal, A., Wu, P.-H., Hughes, E.G., Fukaya, M., Tischfield, M.A., Langseth, A.J., Wirtz, D., and Bergles, D.E. (2017). Transient opening of the mitochondrial permeability transition Pore induces microdomain calcium transients in astrocyte processes. Neuron *93*, 587–605.

Aguado, T., Huerga-Gómez, A., Sánchez-de la Torre, A., Resel, E., Chara, J.C., Matute, C., Mato, S., Galve-Roperh, I., Guzman, M., and Palazuelos, J. (2021). Δ9-Tetrahydrocannabinol promotes functional remyelination in the mouse brain. Br. J. Pharmacol. *178*, 4176–4192.

Aguzzi, A., Barres, B.A., and Bennett, M.L. (2013). Microglia: scapegoat, saboteur, or something else? Science *339*, 156–161.

Aharoni, R., Eilam, R., and Arnon, R. (2021). Astrocytes in multiple sclerosis—essential constituents with diverse multifaceted functions. Int. J. Mol. Sci. *22*, 5904.

Ahn, K., McKinney, M.K., and Cravatt, B.F. (2008). Enzymatic pathways that regulate endocannabinoid signaling in the nervous system. Chem Rev *108*, 1687–1707.

Alle, H., Roth, A., and Geiger, J.R.P. (2009). Energy-Efficient action potentials in hippocampal mossy fibers. Science (80-.). *325*, 1405–1408.

Allen, N.J., Bennett, M.L., Foo, L.C., Wang, G.X., Chakraborty, C., Smith, S.J., and Barres, B.A. (2012). Astrocyte glypicans 4 and 6 promote formation of excitatory synapses via GluA1 AMPA receptors. Nature *486*, 410–414.

Alvarez, J.I., Dodelet-Devillers, A., Kebir, H., Ifergan, I., Fabre, P.J., Terouz, S., Sabbagh, M., Wosik, K., Bourbonnière, L., Bernard, M., et al. (2011). The hedgehog pathway promotes blood-brain barrier integrity and CNS immune quiescence. Science (80-.). *334*, 1727–1731.

André, A., and Gonthier, M.P. (2010). The endocannabinoid system: its roles in energy balance and potential as a target for obesity treatment. Int J Biochem Cell Biol *42*, 1788–1801.

Anlauf, E., and Derouiche, A. (2013). Glutamine synthetase as an astrocytic marker: its cell type and vesicle localization. Front. Endocrinol. (Lausanne). *4*, 144.

Araque, A., Parpura, V., Sanzgiri, R.P., and Haydon, P.G. (1999). Tripartite synapses: glia, the unacknowledged partner. Trends Neurosci. *22*, 208–215.

Araque, A., Carmignoto, G., Haydon, P.G., Oliet, S.H., Robitaille, R., and Volterra, A. (2014). Gliotransmitters travel in time and space. Neuron *81*, 728–739.

Araque, A., Castillo, P.E., Manzoni, O.J., and Tonini, R. (2017). Synaptic functions of endocannabinoid signaling in health and disease. Neuropharmacology *124*, 13–24.

Arévalo-Martín, A., Vela, J.M., Molina-Holgado, E., Borrell, J., and Guaza, C. (2003). Therapeutic action of cannabinoids in a murine model of multiple sclerosis. J Neurosci *23*, 2511–2516.

Arranz, A.M., Hussein, A., Alix, J.J., Pérez-Cerdá, F., Allcock, N., Matute, C., and Fern, R. (2008). Functional glutamate transport in rodent optic nerve axons and glia. Glia *56*, 1353–1367.

Arregui, L., Benítez, J.A., Razgado, L.F., Vergara, P., and Segovia, J. (2011). Adenoviral astrocyte-specific expression of BDNF in the striata of mice transgenic for Huntington's disease delays the

onset of the motor phenotype. Cell. Mol. Neurobiol. *31*, 1229–1243.

Ashton, J.C. (2012). The use of knockout mice to test the specificity of antibodies for cannabinoid receptors. Hippocampus *22*, 643–644.

Attwell, D. (1994). Glia and neurons in dialogue. Nature *369*, 707–708.

Atwood, B.K., and Mackie, K. (2010). CB_2: a cannabinoid receptor with an identity crisis. Br J Pharmacol *160*, 467–479.

Bak, L.K., Walls, A.B., Schousboe, A., and Waagepetersen, H.S. (2018). Astrocytic glycogen metabolism in the healthy and diseased brain. J. Biol. Chem. *293*, 7108–7116.

Baker, D., Pryce, G., Croxford, J.L., Brown, P., Pertwee, R.G., Makriyannis, A., Khanolkar, A., Layward, L., Fezza, F., Bisogno, T., et al. (2001). Endocannabinoids control spasticity in a multiple sclerosis model. FASEB J *15*, 300–302.

Baker, D., Pryce, G., Jackson, S.J., Bolton, C., and Giovannoni, G. (2012). The biology that underpins the therapeutic potential of cannabis-based medicines for the control of spasticity in multiple sclerosis. Mult. Scler. Relat. Disord. *1*, 11.

Bannerman, P., Hahn, A., Soulika, A., Gallo, V., and Pleasure, D. (2007). Astrogliosis in EAE spinal cord: derivation from radial glia, and relationships to oligodendroglia. Glia *55*, 57–64.

Barnett, M.H., and Prineas, J.W. (2004). Relapsing and remitting multiple sclerosis: pathology of the newly forming lesion. Ann Neurol *55*, 458–468.

Barros, L.F., and Deitmer, J.W. (2010). Glucose and lactate supply to the synapse. Brain Res. Rev. *63*, 149–159.

Batiuk, M.Y., De Vin, F., Duqué, S.I., Li, C., Saito, T., Saido, T., Fiers, M., Belgard, T.G., and Holt, M.G. (2017). An immunoaffinity-based method for isolating ultrapure adult astrocytes based on ATP1B2 targeting by the ACSA-2 antibody. J. Biol. Chem. *292*, 8874–8891.

Bazargani, N., and Attwell, D. (2016). Astrocyte calcium signaling: the third wave. Nat Neurosci *19*, 182–189.

Behrens, P.F., Franz, P., Woodman, B., Lindenberg, K.S., and Landwehrmeyer, G.B. (2002). Impaired glutamate transport and glutamate-glutamine cycling: downstream effects of the Huntington mutation. Brain *125*, 1908–1922.

Bélanger, M., Allaman, I., and Magistretti, P.J. (2011). Brain energy metabolism: focus on astrocyte-neuron metabolic cooperation. Cell Metab. *14*, 724–738.

Bellot-Saez, A., Kékesi, O., Morley, J.W., and Buskila, Y. (2017). Astrocytic modulation of neuronal excitability through K+ spatial buffering. Neurosci. Biobehav. Rev. *77*, 87–97.

Bénard, G., Massa, F., Puente, N., Lourenço, J., Bellocchio, L., Soria-Gómez, E., Matias, I., Delamarre, A., Metna-Laurent, M., Cannich, A., et al. (2012). Mitochondrial CB_1 receptors regulate neuronal energy metabolism. Nat. Neurosci. *15*, 558–564.

Benito, C., Romero, J.P., Tolón, R.M., Clemente, D., Docagne, F., Hillard, C.J., Guaza, C., and Romero, J. (2007). Cannabinoid CB_1 and CB_2 receptors and fatty acid amide hydrolase are specific markers of plaque cell subtypes in human multiple sclerosis. J Neurosci *27*, 2396–2402.

Berdyshev, E. V (2000). Cannabinoid receptors and the regulation of immune response. Chem Phys Lipids *108*, 169–190.

Bergersen, L.H., Morland, C., Ormel, L., Rinholm, J.E., Larsson, M., Wold, J.F.H., Røe, A.T.,

Stranna, A., Santello, M., Bouvier, D., et al. (2012). Immunogold detection of L-glutamate and D-serine in small synaptic-like microvesicles in adult hippocampal astrocytes. Cereb. Cortex *22*, 1690–1697.

Bernal-Chico, A., Canedo, M., Manterola, A., Victoria Sánchez-Gómez, M., Pérez-Samartín, A., Rodríguez-Puertas, R., Matute, C., and Mato, S. (2015). Blockade of monoacylglycerol lipase inhibits oligodendrocyte excitotoxicity and prevents demyelination in vivo. Glia *63*, 163–176.

Bernardi, P., and Petronilli, V. (1996). The permeability transition pore as a mitochondrial calcium release channel: a critical appraisal. J. Bioenerg. Biomembr. *28*, 131–138.

Berrendero, F., Sánchez, A., Cabranes, A., Puerta, C., Ramos, J.A., García-Merino, A., and Fernández-Ruiz, J. (2001). Changes in cannabinoid CB_1 receptors in striatal and cortical regions of rats with experimental allergic encephalomyelitis, an animal model of multiple sclerosis. Synapse *41*, 195–202.

Berridge, M.J. (2005). Unlocking the secrets of cell signaling. Annu. Rev. Physiol. *67*, 1–21.

Berridge, M.J., Bootman, M.D., and Roderick, H.L. (2003). Calcium signalling: Dynamics, homeostasis and remodelling. Nat. Rev. Mol. Cell Biol. *4*, 517–529.

Bezzi, P., Gundersen, V., Galbete, J.L., Seifert, G., Steinhäuser, C., Pilati, E., and Volterra, A. (2004). Astrocytes contain a vesicular compartment that is competent for regulated exocytosis of glutamate. Nat. Neurosci. *7*, 613–620.

Bi, F., Huang, C., Tong, J., Qiu, G., Huang, B., Wu, Q., Li, F., Xu, Z., Bowser, R., Xia, X.-G., et al. (2013). Reactive astrocytes secrete lcn2 to promote neuron death. Proc. Natl. Acad. Sci. U. S. A. *110*, 4069–4074.

Bianchini, D., De Martini, I., Cadoni, A., Zicca, A., Tabaton, M., Schenone, A., Anfosso, S., Akkad Wattar, A.S., Zaccheo, D., and Mancardi, G.L. (1992). GFAP expression of human Schwann cells in tissue culture. Brain Res. *570*, 209–217.

Bittner, C.X., Valdebenito, R., Ruminot, I., Loaiza, A., Larenas, V., Sotelo-Hitschfeld, T., Moldenhauer, H., San Martín, A., Gutiérrez, R., Zambrano, M., et al. (2011). Fast and reversible Stimulation of astrocytic glycolysis by K^+ and a delayed and persistent effect of glutamate. J. Neurosci. *31*, 4709 LP – 4713.

Blanca, D.-C., R., G.M., Xinzhu, Y., Giovanni, C., and S., K.B. (2019). Astrocyte molecular signatures in Huntington's disease. Sci. Transl. Med. *11*, eaaw8546.

Blankman, J.L., Simon, G.M., and Cravatt, B.F. (2007). A comprehensive profile of brain enzymes that hydrolyze the endocannabinoid 2-arachidonoylglycerol. Chem Biol *14*, 1347–1356.

Blaustein, M.P. (1993). Physiological effects of endogenous ouabain: control of intracellular Ca^{2+} stores and cell responsiveness. Am. J. Physiol. *264*, C1367–C1387.

De Bock, M., Wang, N., Decrock, E., Bol, M., Gadicherla, A.K., Culot, M., Cecchelli, R., Bultynck, G., and Leybaert, L. (2013). Endothelial calcium dynamics, connexin channels and blood-brain barrier function. Prog. Neurobiol. *108*, 1–20.

Boddum, K., Jensen, T.P., Magloire, V., Kristiansen, U., Rusakov, D.A., Pavlov, I., and Walker, M.C. (2016). Astrocytic GABA transporter activity modulates excitatory neurotransmission. Nat. Commun. *7*, 1–10.

Bojarskaite, L., Bjørnstad, D.M., Pettersen, K.H., Cunen, C., Hermansen, G.H., Åbjørsbråten, K.S., Chambers, A.R., Sprengel, R., Vervaeke, K., Tang, W., et al. (2020). Astrocytic Ca2+ signaling is reduced during sleep and is involved in the regulation of slow wave sleep. Nat. Commun. *11*,

3240.

Bolton, C., and Paul, C. (1997). MK-801 limits neurovascular dysfunction during experimental allergic encephalomyelitis. J Pharmacol Exp Ther *282*, 397–402.

Boscia, F., Elkjaer, M.L., Illes, Z., and Kukley, M. (2021). Altered expression of ion channels in white matter lesions of progressive multiple sclerosis: what do we know about their function? Front. Cell. Neurosci. *15*, 1–40.

Bosier, B., Bellocchio, L., Metna-Laurent, M., Soria-Gomez, E., Matias, I., Hebert-Chatelain, E., Cannich, A., Maitre, M., Leste-Lasserre, T., Cardinal, P., et al. (2013). Astroglial CB_1 cannabinoid receptors regulate leptin signaling in mouse brain astrocytes. Mol Metab *2*, 393–404.

Bouaboula, M., Poinot-Chazel, C., Bourrié, B., Canat, X., Calandra, B., Rinaldi-Carmona, M., Le Fur, G., and Casellas, P. (1995). Activation of mitogen-activated protein kinases by stimulation of the central cannabinoid receptor CB_1. Biochem J *312 (Pt 2)*, 637–641.

Boumezbeur, F., Petersen, K.F., Cline, G.W., Mason, G.F., Behar, K.L., Shulman, G.I., and Rothman, D.L. (2010). The contribution of blood lactate to brain energy metabolism in humans measured by dynamic 13C nuclear magnetic resonance spectroscopy. J. Neurosci. *30*, 13983–13991.

Bourel, J., Planche, V., Dubourdieu, N., Oliveira, A., Séré, A., Ducourneau, E.-G., Tible, M., Maitre, M., Lesté-Lasserre, T., Nadjar, A., et al. (2021). Complement C3 mediates early hippocampal neurodegeneration and memory impairment in experimental multiple sclerosis. Neurobiol. Dis. *160*, 105533.

Bradley, S.J., and Challiss, R.A.J. (2012). G protein-coupled receptor signalling in astrocytes in health and disease: a focus on metabotropic glutamate receptors. Biochem. Pharmacol. *84*, 249–259.

Brambilla, R. (2019). The contribution of astrocytes to the neuroinflammatory response in multiple sclerosis and experimental autoimmune encephalomyelitis. Acta Neuropathol. *137*, 757–783.

Brambilla, R., Bracchi-Ricard, V., Hu, W.-H., Frydel, B., Bramwell, A., Karmally, S., Green, E.J., and Bethea, J.R. (2005). Inhibition of astroglial nuclear factor kappaB reduces inflammation and improves functional recovery after spinal cord injury. J. Exp. Med. *202*, 145–156.

Briggs, C.A., Chakroborty, S., and Stutzmann, G.E. (2017). Emerging pathways driving early synaptic pathology in Alzheimer's disease. Biochem. Biophys. Res. Commun. *483*, 988–997.

Brosnan, C.F., and Raine, C.S. (2013). The astrocyte in multiple sclerosis revisited. Glia *61*, 453–465.

Brownlee, W.J., Hardy, T.A., Fazekas, F., and Miller, D.H. (2017). Diagnosis of multiple sclerosis: progress and challenges. Lancet (London, England) *389*, 1336–1346.

Brozzi, F., Arcuri, C., Giambanco, I., and Donato, R. (2009). S100B Protein regulates astrocyte shape and migration via interaction with Src kinase: implications for astrocyte development, activation, and tumor growth. J. Biol. Chem. *284*, 8797–8811.

Burda, J.E., and Sofroniew, M. V. (2014). Reactive gliosis and the multicellular response to CNS damage and disease. Neuron *81*, 229–248.

Burrows, D.J., McGown, A., Jain, S.A., De Felice, M., Ramesh, T.M., Sharrack, B., and Majid, A. (2019). Animal models of multiple sclerosis: From rodents to zebrafish. Mult. Scler. *25*, 306–324.

Bush, T.G., Puvanachandra, N., Horner, C.H., Polito, A., Ostenfeld, T., Svendsen, C.N., Mucke, L., Johnson, M.H., and Sofroniew, M. V (1999). Leukocyte infiltration, neuronal degeneration, and neurite outgrowth after ablation of scar-forming, reactive astrocytes in adult transgenic mice. Neuron *23*, 297–308.

Bushong, E.A., Martone, M.E., Jones, Y.Z., and Ellisman, M.H. (2002). Protoplasmic astrocytes in CA1 stratum radiatum occupy separate anatomical domains. J. Neurosci. *22*, 183 LP – 192.

Busquets-Garcia, A., Puighermanal, E., Pastor, A., de la Torre, R., Maldonado, R., and Ozaita, A. (2011). Differential role of anandamide and 2-arachidonoylglycerol in memory and anxiety-like responses. Biol Psychiatry *70*, 479–486.

Busquets-Garcia, A., Desprez, T., Metna-Laurent, M., Bellocchio, L., Marsicano, G., and Soria-Gomez, E. (2015). Dissecting the cannabinergic control of behavior: The where matters. BioEssays *37*, 1215–1225.

Butt, A.M., Fern, R.F., and Matute, C. (2014). Neurotransmitter signaling in white matter. Glia *62*, 1762–1779.

Cabranes, A., Venderova, K., de Lago, E., Fezza, F., Sánchez, A., Mestre, L., Valenti, M., García-Merino, A., Ramos, J.A., Di Marzo, V., et al. (2005). Decreased endocannabinoid levels in the brain and beneficial effects of agents activating cannabinoid and/or vanilloid receptors in a rat model of multiple sclerosis. Neurobiol Dis *20*, 207–217.

Cabranes, A., Pryce, G., Baker, D., and Fernández-Ruiz, J. (2006). Changes in CB_1 receptors in motor-related brain structures of chronic relapsing experimental allergic encephalomyelitis mice. Brain Res *1107*, 199–205.

Cahoy, J.D., Emery, B., Kaushal, A., Foo, L.C., Zamanian, J.L., Christopherson, K.S., Xing, Y., Lubischer, J.L., Krieg, P.A., Krupenko, S.A., et al. (2008). A transcriptome database for astrocytes, neurons, and oligodendrocytes: A new resource for understanding brain development and function. J. Neurosci. *28*, 264–278.

Calabrese, M., Magliozzi, R., Ciccarelli, O., Geurts, J.J., Reynolds, R., and Martin, R. (2015). Exploring the origins of grey matter damage in multiple sclerosis. Nat Rev Neurosci *16*, 147–158.

Carlsen, E.M.M., Falk, S., Skupio, U., Robin, L., Pagano Zottola, A.C., Marsicano, G., and Perrier, J.-F. (2021). Spinal astroglial cannabinoid receptors control pathological tremor. Nat. Neurosci. *24*, 658–666.

Castillo, P.E., Younts, T.J., Chávez, A.E., and Hashimotodani, Y. (2012). Endocannabinoid signaling and synaptic function. Neuron *76*, 70–81.

Castro Dias, M., Coisne, C., Baden, P., Enzmann, G., Garrett, L., Becker, L., Hölter, S.M., Hrabě de Angelis, M., Deutsch, U., and Engelhardt, B. (2019). Claudin-12 is not required for blood-brain barrier tight junction function. Fluids Barriers CNS *16*, 30.

Celarain, N., and Tomas-Roig, J. (2020). Aberrant DNA methylation profile exacerbates inflammation and neurodegeneration in multiple sclerosis patients. J. Neuroinflammation *17*, 21.

Centonze, D., Bari, M., Rossi, S., Prosperetti, C., Furlan, R., Fezza, F., De Chiara, V., Battistini, L., Bernardi, G., Bernardini, S., et al. (2007). The endocannabinoid system is dysregulated in multiple sclerosis and in experimental autoimmune encephalomyelitis. Brain *130*, 2543–2553.

Centonze, D., Muzio, L., Rossi, S., Cavasinni, F., De Chiara, V., Bergami, A., Musella, A., D'Amelio, M., Cavallucci, V., Martorana, A., et al. (2009). Inflammation triggers synaptic alteration and

degeneration in experimental autoimmune encephalomyelitis. J. Neurosci. *29*, 3442–3452.

Cerutti, C., and Ridley, A.J. (2017). Endothelial cell-cell adhesion and signaling. Exp. Cell Res. *358*, 31–38.

Chai, H., Diaz-Castro, B., Shigetomi, E., Monte, E., Octeau, J.C., Yu, X., Cohn, W., Rajendran, P.S., Vondriska, T.M., Whitelegge, J.P., et al. (2017). Neural circuit-specialized astrocytes: transcriptomic, proteomic, morphological, and functional evidence. Neuron *95*, 531–549.

Chang, A., Staugaitis, S.M., Dutta, R., Batt, C.E., Easley, K.E., Chomyk, A.M., Yong, V.W., Fox, R.J., Kidd, G.J., and Trapp, B.D. (2012). Cortical remyelination: a new target for repair therapies in multiple sclerosis. Ann Neurol *72*, 918–926.

Chao, C.-C., Gutiérrez-Vázquez, C., Rothhammer, V., Mayo, L., Wheeler, M.A., Tjon, E.C., Zandee, S.E.J., Blain, M., de Lima, K.A., Takenaka, M.C., et al. (2019). Metabolic control of astrocyte pathogenic activity via cPLA2-MAVS. Cell *179*, 1483–1498.

Chen, T.-W., Wardill, T.J., Sun, Y., Pulver, S.R., Renninger, S.L., Baohan, A., Schreiter, E.R., Kerr, R.A., Orger, M.B., Jayaraman, V., et al. (2013). Ultrasensitive fluorescent proteins for imaging neuronal activity. Nature *499*, 295–300.

Chen, Y., Liu, X., Vickstrom, C.R., Liu, M.J., Zhao, L., Viader, A., Cravatt, B.F., and Liu, Q.S. (2016). Neuronal and Astrocytic Monoacylglycerol Lipase Limit the Spread of Endocannabinoid Signaling in the Cerebellum. ENeuro *3*.

Cheng, A., Jia, W., Kawahata, I., and Fukunaga, K. (2021). A novel fatty acid-binding protein 5 and 7 inhibitor ameliorates oligodendrocyte injury in multiple sclerosis mouse models. EBioMedicine *72*, 103582.

Cheng, Y.-Y., Zhao, H.-K., Chen, L.-W., Yao, X.-Y., Wang, Y.-L., Huang, Z.-W., Li, G.-P., Wang, Z., and Chen, B.-Y. (2020). Reactive astrocytes increase expression of proNGF in the mouse model of contused spinal cord injury. Neurosci. Res. *157*, 34–43.

Chevaleyre, V., Takahashi, K.A., and Castillo, P.E. (2006). Endocannabinoid-mediated synaptic plasticity in the CNS. Annu Rev Neurosci *29*, 37–76.

Chiarlone, A., Bellocchio, L., Blázquez, C., Resel, E., Soria-Gómez, E., Cannich, A., Ferrero, J.J., Sagredo, O., Benito, C., Romero, J., et al. (2014). A restricted population of CB_1 cannabinoid receptors with neuroprotective activity. Proc Natl Acad Sci U S A *111*, 8257–8262.

Chicca, A., Nicolussi, S., Bartholomäus, R., Blunder, M., Aparisi Rey, A., Petrucci, V., Reynoso-Moreno, I. del C., Viveros-Paredes, J.M., Dalghi Gens, M., Lutz, B., et al. (2017). Chemical probes to potently and selectively inhibit endocannabinoid cellular reuptake. Proc. Natl. Acad. Sci. *114*, E5006 LP-E5015.

Chiu, I.M., Morimoto, E.T.A., Goodarzi, H., Liao, J.T., O'Keeffe, S., Phatnani, H.P., Muratet, M., Carroll, M.C., Levy, S., Tavazoie, S., et al. (2013). A neurodegeneration-specific gene-expression signature of acutely isolated microglia from an amyotrophic lateral sclerosis mouse model. Cell Rep. *4*, 385–401.

Chiurchiù, V., van der Stelt, M., Centonze, D., and Maccarrone, M. (2018). The endocannabinoid system and its therapeutic exploitation in multiple sclerosis: Clues for other neuroinflammatory diseases. Prog Neurobiol *160*, 82–100.

Chou, S.-Y., Weng, J.-Y., Lai, H.-L., Liao, F., Sun, S.H., Tu, P.-H., Dickson, D.W., and Chern, Y. (2008). Expanded-Polyglutamine huntingtin protein suppresses the secretion and production of a chemokine (CCL5/RANTES) by astrocytes. J. Neurosci. *28*, 3277–3290.

Christopherson, K.S., Ullian, E.M., Stokes, C.C.A., Mullowney, C.E., Hell, J.W., Agah, A., Lawler, J., Mosher, D.F., Bornstein, P., and Barres, B.A. (2005). Thrombospondins are astrocyte-secreted proteins that promote CNS synaptogenesis. Cell *120*, 421–433.

Chu, F., Shi, M., Zheng, C., Shen, D., Zhu, J., Zheng, X., and Cui, L. (2018). The roles of macrophages and microglia in multiple sclerosis and experimental autoimmune encephalomyelitis. J Neuroimmunol *318*, 1–7.

Chung, W.-S., Verghese, P.B., Chakraborty, C., Joung, J., Hyman, B.T., Ulrich, J.D., Holtzman, D.M., and Barres, B.A. (2016). Novel allele-dependent role for APOE in controlling the rate of synapse pruning by astrocytes. Proc. Natl. Acad. Sci. U. S. A. *113*, 10186–10191.

Clapham, D.E. (2007). Calcium signaling. Cell *131*, 1047–1058.

Clarke, L.E., Liddelow, S.A., Chakraborty, C., Münch, A.E., Heiman, M., and Barres, B.A. (2018). Normal aging induces A1-like astrocyte reactivity. Proc. Natl. Acad. Sci. U. S. A. *115*, E1896–E1905.

Coiret, G., Ster, J., Grewe, B., Wendling, F., Helmchen, F., Gerber, U., and Benquet, P. (2012). Neuron to astrocyte communication via cannabinoid receptors is necessary for sustained epileptiform activity in rat hippocampus. PLoS One *7*, e37320.

Compston, A., and Coles, A. (2008). Multiple sclerosis. Lancet *372*, 1502–1517.

Consroe, P. (1998). Brain cannabinoid systems as targets for the therapy of neurological disorders. Neurobiol Dis *5*, 534–551.

Cornell-Bell, A.H., Finkbeiner, S.M., Cooper, M.S., and Smith, S.J. (1990). Glutamate induces calcium waves in cultured astrocytes: long-range glial signaling. Science *247*, 470–473.

Correale, J., Gaitán, M.I., Ysrraelit, M.C., and Fiol, M.P. (2017). Progressive multiple sclerosis: from pathogenic mechanisms to treatment. Brain *140*, 527–546.

Cotsapas, C., and Mitrovic, M. (2018). Genome-wide association studies of multiple sclerosis. Clin. Transl. Immunol. *7*, e1018.

Covelo, A., and Araque, A. (2018). Neuronal activity determines distinct gliotransmitter release from a single astrocyte. Elife *7*, e32237.

Covelo, A., Eraso-Pichot, A., Fernández-Moncada, I., Serrat, R., and Marsicano, G. (2021). CB_1R-dependent regulation of astrocyte physiology and astrocyte-neuron interactions. Neuropharmacology *195*, 108678.

Cravatt, B.F., Demarest, K., Patricelli, M.P., Bracey, M.H., Giang, D.K., Martin, B.R., and Lichtman, A.H. (2001). Supersensitivity to anandamide and enhanced endogenous cannabinoid signaling in mice lacking fatty acid amide hydrolase. Proc Natl Acad Sci U S A *98*, 9371–9376.

Cristino, L., Bisogno, T., and Di Marzo, V. (2020). Cannabinoids and the expanded endocannabinoid system in neurological disorders. Nat. Rev. Neurol. *16*, 9–29.

D'Ascenzo, M., Fellin, T., Terunuma, M., Revilla-Sanchez, R., Meaney, D.F., Auberson, Y.P., Moss, S.J., and Haydon, P.G. (2007). mGluR5 stimulates gliotransmission in the nucleus accumbens. Proc. Natl. Acad. Sci. U. S. A. *104*, 1995–2000.

Danbolt, N.C. (2001). Glutamate uptake. Prog. Neurobiol. *65*, 1–105.

Dani, J.W., Chernjavsky, A., and Smith, S.J. (1992). Neuronal activity triggers calcium waves in hippocampal astrocyte networks. Neuron *8*, 429–440.

Das, A.M. (2003). Regulation of the mitochondrial ATP-synthase in health and disease. Mol. Genet. Metab. *79*, 71–82.

Delekate, A., Füchtemeier, M., Schumacher, T., Ulbrich, C., Foddis, M., and Petzold, G.C. (2014). Metabotropic P2Y1 receptor signalling mediates astrocytic hyperactivity in vivo in an Alzheimer's disease mouse model. Nat. Commun. *5*, 5422.

Dendrou, C.A., Fugger, L., and Friese, M.A. (2015). Immunopathology of multiple sclerosis. Nat. Rev. Immunol. *15*, 545–558.

Devane, W.A., Hanus, L., Breuer, A., Pertwee, R.G., Stevenson, L.A., Griffin, G., Gibson, D., Mandelbaum, A., Etinger, A., and Mechoulam, R. (1992). Isolation and structure of a brain constituent that binds to the cannabinoid receptor. Science (80-.). *258*, 1946–1949.

Duan, S., Anderson, C.M., Keung, E.C., Chen, Y., Chen, Y., and Swanson, R.A. (2003). P2X7 receptor-mediated release of excitatory amino acids from astrocytes. J. Neurosci. *23*, 1320–1328.

Durkee, C.A., and Araque, A. (2019). Diversity and specificity of astrocyte-neuron communication. Neuroscience *396*, 73–78.

Eljaschewitsch, E., Witting, A., Mawrin, C., Lee, T., Schmidt, P.M., Wolf, S., Hoertnagl, H., Raine, C.S., Schneider-Stock, R., Nitsch, R., et al. (2006). The endocannabinoid anandamide protects neurons during CNS inflammation by induction of MKP-1 in microglial cells. Neuron *49*, 67–79.

Ellwardt, E., Pramanik, G., Luchtman, D., Novkovic, T., Jubal, E.R., Vogt, J., Arnoux, I., Vogelaar, C.F., Mandal, S., Schmalz, M., et al. (2018). Maladaptive cortical hyperactivity upon recovery from experimental autoimmune encephalomyelitis. Nat Neurosci *21*, 1392–1403.

Emsley, J.G., and Macklis, J.D. (2006). Astroglial heterogeneity closely reflects the neuronal-defined anatomy of the adult murine CNS. Neuron Glia Biol. *2*, 175–186.

Enders, M., Heider, T., Ludwig, A., and Kuerten, S. (2020). Strategies for neuroprotection in multiple sclerosis and the role of calcium. Int. J. Mol. Sci. *21*, 1663.

Eng, L.F., Ghirnikar, R.S., and Lee, Y.L. (2000). Glial fibrillary acidic protein: GFAP-thirty-one years (1969-2000). Neurochem. Res. *25*, 1439–1451.

Eng LF, Gerstl B, Vanderhaeghen, J. (1970). A study of proteins in old multiple sclerosis plaques. Trans Am Soc Neurochem *1*, 42.

Eroglu, C. (2009). The role of astrocyte-secreted matricellular proteins in central nervous system development and function. J. Cell Commun. Signal. *3*, 167–176.

Escartin, C., Galea, E., Lakatos, A., O'Callaghan, J.P., Petzold, G.C., Serrano-Pozo, A., Steinhäuser, C., Volterra, A., Carmignoto, G., Agarwal, A., et al. (2021). Reactive astrocyte nomenclature, definitions, and future directions. Nat. Neurosci. *24*, 312–325.

Ezan, P., André, P., Cisternino, S., Saubaméa, B., Boulay, A.-C., Doutremer, S., Thomas, M.-A., Quenech'du, N., Giaume, C., and Cohen-Salmon, M. (2012). Deletion of astroglial connexins weakens the blood–brain barrier. J. Cereb. Blood Flow Metab. *32*, 1457–1467.

Fan, Y.Y., and Huo, J. (2021). A1/A2 astrocytes in central nervous system injuries and diseases: Angels or devils? Neurochem. Int. *148*, 105080.

Feinstein, A., Magalhaes, S., Richard, J.F., Audet, B., and Moore, C. (2014). The link between multiple sclerosis and depression. Nat Rev Neurol *10*, 507–517.

Feliú, A., Bonilla Del Río, I., Carrillo-Salinas, F.J., Hernández-Torres, G., Mestre, L., Puente, N.,

Ortega-Gutiérrez, S., López-Rodríguez, M.L., Grandes, P., Mecha, M., et al. (2017). 2-Arachidonoylglycerol reduces proteoglycans and enhances remyelination in a progressive model of demyelination. J Neurosci *37*, 8385–8398.

Fellin, T., Pascual, O., Gobbo, S., Pozzan, T., Haydon, P.G., and Carmignoto, G. (2004). Neuronal synchrony mediated by astrocytic glutamate through activation of extrasynaptic NMDA receptors. Neuron *43*, 729–743.

Fernández-Ruiz, J. (2009). The endocannabinoid system as a target for the treatment of motor dysfunction. Br J Pharmacol *156*, 1029–1040.

Fernández-Ruiz, J., Pazos, M.R., García-Arencibia, M., Sagredo, O., and Ramos, J.A. (2008). Role of CB_2 receptors in neuroprotective effects of cannabinoids. Mol Cell Endocrinol *286*, S91-6.

Fernández-Ruiz, J., García, C., Sagredo, O., Gómez-Ruiz, M., and de Lago, E. (2010). The endocannabinoid system as a target for the treatment of neuronal damage. Expert Opin Ther Targets *14*, 387–404.

Ferraiuolo, L., Higginbottom, A., Heath, P.R., Barber, S., Greenald, D., Kirby, J., and Shaw, P.J. (2011). Dysregulation of astrocyte-motoneuron cross-talk in mutant superoxide dismutase 1-related amyotrophic lateral sclerosis. Brain *134*, 2627–2641.

Filippi, M., Bar-Or, A., Piehl, F., Preziosa, P., Solari, A., Vukusic, S., and Rocca, M.A. (2018). Multiple sclerosis. Nat Rev Dis Prim. *4*, 43.

Di Filippo, M., Pini, L.A., Pelliccioli, G.P., Calabresi, P., and Sarchielli, P. (2008). Abnormalities in the cerebrospinal fluid levels of endocannabinoids in multiple sclerosis. J Neurol Neurosurg Psychiatry *79*, 1224–1229.

Foo, L.C., Allen, N.J., Bushong, E.A., Ventura, P.B., Chung, W.S., Zhou, L., Cahoy, J.D., Daneman, R., Zong, H., Ellisman, M.H., et al. (2011). Development of a method for the purification and culture of rodent astrocytes. Neuron *71*, 799–811.

Franklin, R.J.M., and Ffrench-Constant, C. (2017). Regenerating CNS myelin - from mechanisms to experimental medicines. Nat Rev Neurosci *18*, 753–769.

Fulmer, C.G., VonDran, M.W., Stillman, A.A., Huang, Y., Hempstead, B.L., and Dreyfus, C.F. (2014). Astrocyte-derived BDNF supports myelin protein synthesis after cuprizone-induced demyelination. J. Neurosci. *34*, 8186–8196.

Galve-Roperh, I., Rueda, D., del Pulgar, T., Velasco, G., and Guzmán, M. (2002). Mechanism of extracellular signal-regulated kinase activation by the CB_1 cannabinoid receptor. Mol Pharmacol *62*, 1385–1392.

Gao, Y.-J., and Ji, R.-R. (2010). Targeting astrocyte signaling for chronic pain. Neurother. J. Am. Soc. Exp. Neurother. *7*, 482–493.

Gaoni, Y., and Mechoulam, R. (1964). Isolation, structure, and partial synthesis of an active constituent of hashish. J. Am. Chem. Soc. *86*, 1646–1647.

Garcia, A.D.R., Doan, N.B., Imura, T., Bush, T.G., and Sofroniew, M. V (2004). GFAP-expressing progenitors are the principal source of constitutive neurogenesis in adult mouse forebrain. Nat. Neurosci. *7*, 1233–1241.

Gimenez, M.A.T., Sim, J.E., and Russell, J.H. (2004). TNFR1-dependent VCAM-1 expression by astrocytes exposes the CNS to destructive inflammation. J. Neuroimmunol. *151*, 116–125.

Go, L.O., Moschella, M.C., Watras, J., Handa, K.K., Fyfe, B.S., and Marks, A.R. (1995). Differential

regulation of two types of intracellular calcium release channels during end-stage heart failure. J. Clin. Invest. *95*, 888–894.

Gómez-Gonzalo, M., Navarrete, M., Perea, G., Covelo, A., Martín-Fernández, M., Shigemoto, R., Luján, R., and Araque, A. (2015). Endocannabinoids induce lateral long-term potentiation of transmitter release by stimulation of gliotransmission. Cereb Cortex *25*, 3699–3712.

Gomez, O., Arevalo-Martin, A., Garcia-Ovejero, D., Ortega-Gutierrez, S., Cisneros, J.A., Almazan, G., Sánchez-Rodriguez, M.A., Molina-Holgado, F., and Molina-Holgado, E. (2010). The constitutive production of the endocannabinoid 2-arachidonoylglycerol participates in oligodendrocyte differentiation. Glia *58*, 1913–1927.

Gomez, O., Sanchez-Rodriguez, A., Le, M.Q.U., Sanchez-Caro, C., Molina-Holgado, F., and Molina-Holgado, E. (2011). Cannabinoid receptor agonists modulate oligodendrocyte differentiation by activating PI3K/Akt and the mammalian target of rapamycin (mTOR) pathways. Br. J. Pharmacol. *163*, 1520–1532.

Gómez del Pulgar, T., Velasco, G., and Guzmán, M. (2000). The CB_1 cannabinoid receptor is coupled to the activation of protein kinase B/Akt. Biochem. J. *347*, 369–373.

Gorzkiewicz, A., and Szemraj, J. (2018). Brain endocannabinoid signaling exhibits remarkable complexity. Brain Res Bull *142*, 33–46.

Griebel, G., Stemmelin, J., Lopez-Grancha, M., Fauchey, V., Slowinski, F., Pichat, P., Dargazanli, G., Abouabdellah, A., Cohen, C., and Bergis, O.E. (2018). The selective reversible FAAH inhibitor, SSR411298, restores the development of maladaptive behaviors to acute and chronic stress in rodents. Sci. Rep. *8*, 2416.

Grigoriadis, N., van Pesch, V., and Group, P. (2015). A basic overview of multiple sclerosis immunopathology. Eur J Neurol *22 Suppl 2*, 3–13.

Grimsey, N.L., Goodfellow, C.E., Scotter, E.L., Dowie, M.J., Glass, M., and Graham, E.S. (2008). Specific detection of CB_1 receptors; cannabinoid CB_1 receptor antibodies are not all created equal! J. Neurosci. Methods *171*, 78–86.

Guerra-Gomes, S., Sousa, N., Pinto, L., and Oliveira, J.F. (2018). Functional roles of astrocyte calcium elevations: From synapses to behavior. Front. Cell. Neurosci. *11*, 1–7.

Gutiérrez-Rodríguez, A., Puente, N., Elezgarai, I., Ruehle, S., Lutz, B., Reguero, L., Gerrikagoitia, I., Marsicano, G., and Grandes, P. (2017). Anatomical characterization of the cannabinoid CB_1 receptor in cell-type-specific mutant mouse rescue models. J Comp Neurol *525*, 302–318.

Gutiérrez-Rodríguez, A., Bonilla-Del Río, I., Puente, N., Gómez-Urquijo, S.M., Fontaine, C.J., Egaña-Huguet, J., Elezgarai, I., Ruehle, S., Lutz, B., Robin, L.M., et al. (2018). Localization of the cannabinoid type-1 receptor in subcellular astrocyte compartments of mutant mouse hippocampus. Glia *66*, 1417–1431.

Guttenplan, K.A., Weigel, M.K., Adler, D.I., Couthouis, J., Liddelow, S.A., Gitler, A.D., and Barres, B.A. (2020). Knockout of reactive astrocyte activating factors slows disease progression in an ALS mouse model. Nat. Commun. *11*, 3753.

Guttenplan, K.A., Weigel, M.K., Prakash, P., Wijewardhane, P.R., Hasel, P., Rufen-Blanchette, U., Münch, A.E., Blum, J.A., Fine, J., Neal, M.C., et al. (2021). Neurotoxic reactive astrocytes induce cell death via saturated lipids. Nature *599*, 102–107.

Göbel, J., Engelhardt, E., Pelzer, P., Sakthivelu, V., Jahn, H.M., Jevtic, M., Folz-Donahue, K., Kukat, C., Schauss, A., Frese, C.K., et al. (2020). Mitochondria-Endoplasmic reticulum contacts in

reactive astrocytes promote vascular remodeling. Cell Metab *31*, 791–808.

Hablitz, L.M., Gunesch, A.N., Cravetchi, O., Moldavan, M., and Allen, C.N. (2020). Cannabinoid signaling recruits astrocytes to modulate presynaptic function in the suprachiasmatic nucleus. ENeuro *7*, 0081–19.

Hachem, S., Aguirre, A., Vives, V., Marks, A., Gallo, V., and Legraverend, C. (2005). Spatial and temporal expression of S100B in cells of oligodendrocyte lineage. Glia *51*, 81–97.

Hafler, D.A., Compston, A., Sawcer, S., Lander, E.S., Daly, M.J., De Jager, P.L., de Bakker, P.I.W., Gabriel, S.B., Mirel, D.B., Ivinson, A.J., et al. (2007). Risk alleles for multiple sclerosis identified by a genomewide study. N. Engl. J. Med. *357*, 851–862.

Haghayegh Jahromi, N., Marchetti, L., Moalli, F., Duc, D., Basso, C., Tardent, H., Kaba, E., Deutsch, U., Pot, C., Sallusto, F., et al. (2020). Intercellular adhesion molecule-1 (ICAM-1) and ICAM-2 differentially contribute to peripheral activation and CNS entry of autoaggressive Th1 and Th17 cells in experimental autoimmune encephalomyelitis. Front. Immunol. *10*, 3056.

Ben Haim, L., and Rowitch, D.H. (2016). Functional diversity of astrocytes in neural circuit regulation. Nat. Rev. Neurosci. *18*, 31–41.

Hainfellner, J.A., Voigtländer, T., Ströbel, T., Mazal, P.R., Maddalena, A.S., Aguzzi, A., and Budka, H. (2001). Fibroblasts can express glial fibrillary acidic protein (GFAP) in vivo. J. Neuropathol. Exp. Neurol. *60*, 449–461.

Haj-Dahmane, S., Shen, R.Y., Elmes, M.W., Studholme, K., Kanjiya, M.P., Bogdan, D., Thanos, P.K., Miyauchi, J.T., Tsirka, S.E., Deutsch, D.G., et al. (2018). Fatty-acid-binding protein 5 controls retrograde endocannabinoid signaling at central glutamate synapses. Proc. Natl. Acad. Sci. U. S. A. *115*, 3482–3487.

Halassa, M.M., and Haydon, P.G. (2010). Integrated brain circuits: astrocytic networks modulate neuronal activity and behavior. Annu. Rev. Physiol. *72*, 335–355.

Hamby, M.E., Coppola, G., Ao, Y., Geschwind, D.H., Khakh, B.S., and Sofroniew, M. V (2012). Inflammatory mediators alter the astrocyte transcriptome and calcium signaling elicited by multiple G-protein-coupled receptors. J. Neurosci. *32*, 14489–14510.

Hamilton, N.B., and Attwell, D. (2010). Do astrocytes really exocytose neurotransmitters? Nat. Rev. Neurosci. *11*, 227–238.

Hamilton, N., Vayro, S., Wigley, R., and Butt, A.M. (2010). Axons and astrocytes release ATP and glutamate to evoke calcium signals in NG2-glia. Glia *58*, 66–79.

Hammond, J.W., Bellizzi, M.J., Ware, C., Qiu, W.Q., Saminathan, P., Li, H., Luo, S., Ma, S.A., Li, Y., and Gelbard, H.A. (2020). Complement-dependent synapse loss and microgliosis in a mouse model of multiple sclerosis. Brain. Behav. Immun. *87*, 739–750.

Han, J., Kesner, P., Metna-Laurent, M., Duan, T., Xu, L., Georges, F., Koehl, M., Abrous, D.N., Mendizabal-Zubiaga, J., Grandes, P., et al. (2012). Acute cannabinoids impair working memory through astroglial CB 1 receptor modulation of hippocampal LTD. Cell *148*, 1039–1050.

Hara, M., Kobayakawa, K., Ohkawa, Y., Kumamaru, H., Yokota, K., Saito, T., Kijima, K., Yoshizaki, S., Harimaya, K., Nakashima, Y., et al. (2017). Interaction of reactive astrocytes with type I collagen induces astrocytic scar formation through the integrin-N-cadherin pathway after spinal cord injury. Nat. Med. *23*, 818–828.

Haustein, M.D., Kracun, S., Lu, X.-H., Shih, T., Jackson-Weaver, O., Tong, X., Xu, J., Yang, X.W., O'Dell, T.J., Marvin, J.S., et al. (2014). Conditions and constraints for astrocyte calcium signaling

in the hippocampal mossy fiber pathway. Neuron *82*, 413–429.

Hayakawa, K., Pham, L.-D.D., Arai, K., and Lo, E.H. (2014). Reactive astrocytes promote adhesive interactions between brain endothelium and endothelial progenitor cells via HMGB1 and beta-2 integrin signaling. Stem Cell Res. *12*, 531–538.

Hayakawa, K., Esposito, E., Wang, X., Terasaki, Y., Liu, Y., Xing, C., Ji, X., and Lo, E.H. (2016). Transfer of mitochondria from astrocytes to neurons after stroke. Nature *535*, 551–555.

Hebert-Chatelain, E., Desprez, T., Serrat, R., Bellocchio, L., Soria-Gomez, E., Busquets-Garcia, A., Pagano Zottola, A.C., Delamarre, A., Cannich, A., Vincent, P., et al. (2016). A cannabinoid link between mitochondria and memory. Nature *539*, 555–559.

Hegyi, Z., Oláh, T., Koszeghy, Á., Pisticelli, F., Holló, K., Pál, B., Csernoch, L., Di Marzo, V., and Antal, M. (2018). CB_1 receptor activation induces intracellular Ca^{2+} mobilization and 2-arachidonoylglycerol release in rodent spinal cord astrocytes. Sci. Rep. *8*, 1–16.

Heppner, F.L., Ransohoff, R.M., and Becher, B. (2015). Immune attack: the role of inflammation in Alzheimer disease. Nat. Rev. Neurosci. *16*, 358–372.

Herculano-Houzel, S. (2014). The glia/neuron ratio: how it varies uniformly across brain structures and species and what that means for brain physiology and evolution. Glia *62*, 1377–1391.

Herkenham, M., Lynn, A.B., Little, M.D., Johnson, M.R., Melvin, L.S., de Costa, B.R., and Rice, K.C. (1990). Cannabinoid receptor localization in brain. Proc Natl Acad Sci U S A *87*, 1932–1936.

Hermes, D.J., Xu, C., Poklis, J.L., Niphakis, M.J., Cravatt, B.F., Mackie, K., Lichtman, A.H., Ignatowska-Jankowska, B.M., and Fitting, S. (2018). Neuroprotective effects of fatty acid amide hydrolase catabolic enzyme inhibition in a HIV-1 Tat model of neuroAIDS. Neuropharmacology *141*, 55–65.

Hernández-Torres, G., Cipriano, M., Hedén, E., Björklund, E., Canales, Á., Zian, D., Feliú, A., Mecha, M., Guaza, C., Fowler, C.J., et al. (2014). A reversible and selective inhibitor of monoacylglycerol lipase ameliorates multiple sclerosis. Angew Chem Int Ed Engl *53*, 13765–13770.

Herrmann, J.E., Imura, T., Song, B., Qi, J., Ao, Y., Nguyen, T.K., Korsak, R.A., Takeda, K., Akira, S., and Sofroniew, M. V (2008). STAT3 is a critical regulator of astrogliosis and scar formation after spinal cord injury. J. Neurosci. *28*, 7231–7243.

Herz, J., Zipp, F., and Siffrin, V. (2010). Neurodegeneration in autoimmune CNS inflammation. Exp Neurol *225*, 9–17.

Higashi, K., Fujita, A., Inanobe, A., Tanemoto, M., Doi, K., Kubo, T., and Kurachi, Y. (2001). An inwardly rectifying K(+) channel, Kir4.1, expressed in astrocytes surrounds synapses and blood vessels in brain. Am. J. Physiol. Cell Physiol. *281*, 922–931.

Hindinger, C., Bergmann, C.C., Hinton, D.R., Phares, T.W., Parra, G.I., Hussain, S., Savarin, C., Atkinson, R.D., and Stohlman, S.A. (2012). IFN-γ signaling to astrocytes protects from autoimmune mediated neurological disability. PLoS One *7*, e42088.

Hou, B., Zhang, Y., Liang, P., He, Y., Peng, B., Liu, W., Han, S., Yin, J., and He, X. (2020). Inhibition of the NLRP3-inflammasome prevents cognitive deficits in experimental autoimmune encephalomyelitis mice via the alteration of astrocyte phenotype. Cell Death Dis. *11*, 377.

Howland, D.S., Liu, J., She, Y., Goad, B., Maragakis, N.J., Kim, B., Erickson, J., Kulik, J., DeVito, L., Psaltis, G., et al. (2002). Focal loss of the glutamate transporter EAAT2 in a transgenic rat model

of SOD1 mutant-mediated amyotrophic lateral sclerosis (ALS). Proc. Natl. Acad. Sci. U. S. A. *99*, 1604–1609.

Howlett, A.C. (2002). The cannabinoid receptors. Prostaglandins Other Lipid Mediat *68–69*, 619–631.

Hu, X., Leak, R.K., Shi, Y., Suenaga, J., Gao, Y., Zheng, P., and Chen, J. (2015). Microglial and macrophage polarization—new prospects for brain repair. Nat Rev Neurol *11*, 56–64.

Huang, N., Juang, J., Wang, Y., Hsueh, C., Liang, Y., Lin, J., Tsai, C., and Lai, L. (2010). Rimonabant inhibits TNF-α-induced endothelial IL-6 secretion via CB1 receptor and cAMP-dependent protein kinase pathway. Acta Pharmacol. Sin. *31*, 1447–1453.

Hundehege, P., Epping, L., and Meuth, S. (2017). Calcium homeostasis in multiple sclerosis. Neurol. Int. Open *01*, E127–E135.

Iannotti, F.A., Di Marzo, V., and Petrosino, S. (2016). Endocannabinoids and endocannabinoid-related mediators: Targets, metabolism and role in neurological disorders. Prog Lipid Res *62*, 107–128.

Ishibashi, M., Egawa, K., and Fukuda, A. (2019). Diverse actions of astrocytes in GABAergic signaling. Int. J. Mol. Sci. *20*, 2964.

Itoh, N., Itoh, Y., Tassoni, A., Ren, E., Kaito, M., Ohno, A., Ao, Y., Farkhondeh, V., Johnsonbaugh, H., Burda, J., et al. (2018). Cell-specific and region-specific transcriptomics in the multiple sclerosis model: Focus on astrocytes. Proc Natl Acad Sci U S A *115*, E302–E309.

Jackson, J.G., and Robinson, M.B. (2018). Regulation of mitochondrial dynamics in astrocytes: Mechanisms, consequences, and unknowns. Glia *66*, 1213–1234.

Jean-Gilles, L., Feng, S., Tench, C.R., Chapman, V., Kendall, D.A., Barrett, D.A., and Constantinescu, C.S. (2009). Plasma endocannabinoid levels in multiple sclerosis. J Neurol Sci *287*, 212–215.

Ji, R.-R., Donnelly, C.R., and Nedergaard, M. (2019). Astrocytes in chronic pain and itch. Nat. Rev. Neurosci. *20*, 667–685.

Jiang, R., Diaz-Castro, B., Looger, L.L., and Khakh, B.S. (2016). Dysfunctional calcium and glutamate signaling in striatal astrocytes from Huntington's disease model mice. J. Neurosci. *36*, 3453–3470.

Jimenez-Blasco, D., Busquets-Garcia, A., Hebert-Chatelain, E., Serrat, R., Vicente-Gutierrez, C., Ioannidou, C., Gómez-Sotres, P., Lopez-Fabuel, I., Resch-Beusher, M., Resel, E., et al. (2020). Glucose metabolism links astroglial mitochondria to cannabinoid effects. Nature *583*, 603–608.

John Lin, C.-C., Yu, K., Hatcher, A., Huang, T.-W., Lee, H.K., Carlson, J., Weston, M.C., Chen, F., Zhang, Y., Zhu, W., et al. (2017). Identification of diverse astrocyte populations and their malignant analogs. Nat. Neurosci. *20*, 396–405.

Jourdain, P., Bergersen, L.H., Bhaukaurally, K., Bezzi, P., Santello, M., Domercq, M., Matute, C., Tonello, F., Gundersen, V., and Volterra, A. (2007). Glutamate exocytosis from astrocytes controls synaptic strength. Nat Neurosci *10*, 331–339.

Jukkola, P., Guerrero, T., Gray, V., and Gu, C. (2013). Astrocytes differentially respond to inflammatory autoimmune insults and imbalances of neural activity. Acta Neuropathol. Commun. *1*, 70.

Jungblut, M., Tiveron, M.C., Barral, S., Abrahamsen, B., Knöbel, S., Pennartz, S., Schmitz, J.,

Perraut, M., Pfrieger, F.W., Stoffel, W., et al. (2012). Isolation and characterization of living primary astroglial cells using the new GLAST-specific monoclonal antibody ACSA-1. Glia *60*, 894–907.

Jürgens, T., Jafari, M., Kreutzfeldt, M., Bahn, E., Brück, W., Kerschensteiner, M., and Merkler, D. (2016). Reconstruction of single cortical projection neurons reveals primary spine loss in multiple sclerosis. Brain *139*, 39–46.

Kaczocha, M., Glaser, S.T., and Deutsch, D.G. (2009). Identification of intracellular carriers for the endocannabinoid anandamide. Proc Natl Acad Sci U S A *106*, 6375–6380.

Kaczocha, M., Glaser, S.T., Maher, T., Clavin, B., Hamilton, J., O'Rourke, J., Rebecchi, M., Puopolo, M., Owada, Y., and Thanos, P.K. (2015). Fatty acid binding protein deletion suppresses inflammatory pain through endocannabinoid/N-acylethanolamine-dependent mechanisms. Mol Pain *11*, 52.

Kanemaru, K., Sekiya, H., Xu, M., Satoh, K., Kitajima, N., Yoshida, K., Okubo, Y., Sasaki, T., Moritoh, S., Hasuwa, H., et al. (2014). In vivo visualization of subtle, transient, and local activity of astrocytes using an ultrasensitive Ca2+ indicator. Cell Rep. *8*, 311–318.

Kang, J., Kang, N., Lovatt, D., Torres, A., Zhao, Z., Lin, J., and Nedergaard, M. (2008). Connexin 43 hemichannels are permeable to ATP. J. Neurosci. *28*, 4702–4711.

Kantzer, C.G., Boutin, C., Herzig, I.D., Wittwer, C., Reiß, S., Tiveron, M.C., Drewes, J., Rockel, T.D., Ohlig, S., Ninkovic, J., et al. (2017). Anti-ACSA-2 defines a novel monoclonal antibody for prospective isolation of living neonatal and adult astrocytes. Glia *65*, 990–1004.

Kato, H., Yamamoto, T., Yamamoto, H., Ohi, R., So, N., and Iwasaki, Y. (1990). Immunocytochemical characterization of supporting cells in the enteric nervous system in Hirschsprung's disease. J. Pediatr. Surg. *25*, 514–519.

Katona, I., and Freund, T.F. (2008). Endocannabinoid signaling as a synaptic circuit breaker in neurological disease. Nat Med *14*, 923–930.

Katona, I., and Freund, T.F. (2012). Multiple functions of endocannabinoid signaling in the brain. Annu Rev Neurosci *35*, 529–558.

Kawamura, Y., Fukaya, M., Maejima, T., Yoshida, T., Miura, E., Watanabe, M., Ohno-Shosaku, T., and Kano, M. (2006). The CB_1 cannabinoid receptor is the major cannabinoid receptor at excitatory presynaptic sites in the hippocampus and cerebellum. J Neurosci *26*, 2991–3001.

Kendall, D.A., and Yudowski, G.A. (2017). Cannabinoid receptors in the central nervous system: their signaling and roles in disease. Front. Cell. Neurosci. *10*, 294.

Khakh, B.S., and Deneen, B. (2019). The emerging nature of astrocyte diversity. Annu. Rev. Neurosci. *42*, 187–207.

Khakh, B.S., and McCarthy, K.D. (2015). Astrocyte calcium signaling: From observations to functions and the challenges therein. Cold Spring Harb. Perspect. Biol. *7*, 1–17.

Khakh, B.S., and Sofroniew, M. V (2015). Diversity of astrocyte functions and phenotypes in neural circuits. Nat. Neurosci. *18*, 942–952.

Kim, C.K., Yang, S.J., Pichamoorthy, N., Young, N.P., Kauvar, I., Jennings, J.H., Lerner, T.N., Berndt, A., Lee, S.Y., Ramakrishnan, C., et al. (2016). Simultaneous fast measurement of circuit dynamics at multiple sites across the mammalian brain. Nat. Methods *13*, 325–328.

Kirichok, Y., Krapivinsky, G., and Clapham, D.E. (2004). The mitochondrial calcium uniporter is a

highly selective ion channel. Nature *427*, 360–364.

Kjetil, B., Marianna, C., C., H.B., Jens, K., J., M.M., Yumei, L., J., E.S., W., N.D., I., S.A., L., M.K., et al. (2022). Longitudinal analysis reveals high prevalence of Epstein-Barr virus associated with multiple sclerosis. Science (80-.). *375*, 296–301.

Kmietowicz, Z. (2010). Cannabis based drug is licensed for spasticity in patients with MS. BMJ *340*, c3363.

Kremer, D., Akkermann, R., Küry, P., and Dutta, R. (2018). Current advancements in promoting remyelination in multiple sclerosis. Mult Scler *25*, 7–14.

Kucukdereli, H., Allen, N.J., Lee, A.T., Feng, A., Ozlu, M.I., Conatser, L.M., Chakraborty, C., Workman, G., Weaver, M., Sage, E.H., et al. (2011). Control of excitatory CNS synaptogenesis by astrocyte-secreted proteins Hevin and SPARC. Proc. Natl. Acad. Sci. *108*, 12983–12984.

Kurnellas, M.P., Donahue, K.C., and Elkabes, S. (2007). Mechanisms of neuronal damage in multiple sclerosis and its animal models: role of calcium pumps and exchangers. Biochem. Soc. Trans. *35*, 923–926.

Lalo, U., Verkhratsky, A., and Pankratov, Y. (2011). Ionotropic ATP receptors in neuronal-glial communication. Semin. Cell Dev. Biol. *22*, 220–228.

Lassmann, H. (2014). Mechanisms of white matter damage in multiple sclerosis. Glia *62*, 1816–1830.

Lassmann, H. (2018). Pathogenic mechanisms associated with different clinical courses of multiple sclerosis. Front. Immunol. *9*, 3116.

Lau, B.K., Cota, D., Cristino, L., and Borgland, S.L. (2017). Endocannabinoid modulation of homeostatic and non-homeostatic feeding circuits. Neuropharmacology *124*, 38–51.

Lee, S.J., Drabik, K., Van Wagoner, N.J., Lee, S., Choi, C., Dong, Y., and Benveniste, E.N. (2000). ICAM-1-Induced expression of proinflammatory cytokines in astrocytes: involvement of extracellular signal-regulated kinase and p38 mitogen-activated protein kinase pathways. J. Immunol. *165*, 4658–4666.

Lenhossék, M. (1893). Der feinere Bau des Nervensystems im Lichte neuester Forschungen.

Leterrier, C., Bonnard, D., Carrel, D., Rossier, J., and Lenkei, Z. (2004). Constitutive endocytic cycle of the CB_1 cannabinoid receptor. J Biol Chem *279*, 36013–36021.

Lewis, N.D., Hill, J.D., Juchem, K.W., Stefanopoulos, D.E., and Modis, L.K. (2014). RNA sequencing of microglia and monocyte-derived macrophages from mice with experimental autoimmune encephalomyelitis illustrates a changing phenotype with disease course. J. Neuroimmunol. *277*, 26–38.

Li, D., Ropert, N., Koulakoff, A., Giaume, C., and Oheim, M. (2008). Lysosomes are the major vesicular compartment undergoing Ca^{2+}-regulated exocytosis from aortical astrocytes. J. Neurosci. *28*, 7648–7658.

Li, D., Chen, M., Meng, T., and Fei, J. (2020). Hippocampal microglial activation triggers a neurotoxic-specific astrocyte response and mediates etomidate-induced long-term synaptic inhibition. J. Neuroinflammation *17*, 1–15.

Li, K., Li, J., Zheng, J., and Qin, S. (2019). Reactive astrocytes in neurodegenerative diseases. Aging Dis. *10*, 664–675.

Lian, H., Yang, L., Cole, A., Sun, L., Chiang, A.C.-A., Fowler, S.W., Shim, D.J., Rodriguez-Rivera, J.,

Taglialatela, G., Jankowsky, J.L., et al. (2015). NFκB-activated astroglial release of complement C3 compromises neuronal morphology and function associated with Alzheimer's disease. Neuron *85*, 101–115.

Lian, H., Litvinchuk, A., Chiang, A.C.A., Aithmitti, N., Jankowsky, J.L., and Zheng, H. (2016). Astrocyte-microglia cross talk through complement activation modulates amyloid pathology in mouse models of Alzheimer's disease. J. Neurosci. *36*, 577–589.

Liddelow, S.A., and Barres, B.A. (2017). Reactive astrocytes: production, function, and therapeutic potential. Immunity *46*, 957–967.

Liddelow, S.A., and Sofroniew, M. V (2019). Astrocytes usurp neurons as a disease focus. Nat. Neurosci. *22*, 512–513.

Liddelow, S.A., Guttenplan, K.A., Clarke, L.E., Bennett, F.C., Bohlen, C.J., Schirmer, L., Bennett, M.L., Münch, A.E., Chung, W.S., Peterson, T.C., et al. (2017). Neurotoxic reactive astrocytes are induced by activated microglia. Nature *541*, 481–487.

Ligresti, A., Cascio, M.G., Pryce, G., Kulasegram, S., Beletskaya, I., De Petrocellis, L., Saha, B., Mahadevan, A., Visintin, C., Wiley, J.L., et al. (2006). New potent and selective inhibitors of anandamide reuptake with antispastic activity in a mouse model of multiple sclerosis. Br J Pharmacol *147*, 83–91.

Lim, D., Semyanov, A., and Genazzani, A. (2021). Calcium signaling in neuroglia (Elsevier Inc.).

Lines, J., Baraibar, A.M., Fang, C., Martin, E.D., Aguilar, J., Lee, M.K., Araque, A., and Kofuji, P. (2022). Astrocyte-neuronal network interplay is disrupted in Alzheimer's disease mice. Glia *70*, 368–378.

Linnerbauer, M., and Rothhammer, V. (2020). Protective functions of reactive astrocytes following central nervous system insult. Front. Immunol. *11*, 1–18.

Linnerbauer, M., Wheeler, M.A., and Quintana, F.J. (2020). Astrocyte crosstalk in CNS inflammation. Neuron *108*, 608–622.

Liu, X., Chen, Y., Vickstrom, C.R., Li, Y., Viader, A., Cravatt, B.F., and Liu, Q. (2016). Coordinated regulation of endocannabinoid-mediated retrograde synaptic suppression in the cerebellum by neuronal and astrocytic monoacylglycerol lipase. Sci. Rep. *6*, 35829.

Long, J.Z., Li, W., Booker, L., Burston, J.J., Kinsey, S.G., Schlosburg, J.E., Pavón, F.J., Serrano, A.M., Selley, D.E., Parsons, L.H., et al. (2009). Selective blockade of 2-arachidonoylglycerol hydrolysis produces cannabinoid behavioral effects. Nat Chem Biol *5*, 37–44.

Loría, F., Petrosino, S., Mestre, L., Spagnolo, A., Correa, F., Hernangómez, M., Guaza, C., Di Marzo, V., and Docagne, F. (2008). Study of the regulation of the endocannabinoid system in a virus model of multiple sclerosis reveals a therapeutic effect of palmitoylethanolamide. Eur J Neurosci *28*, 633–641.

Lucchinetti, C., Brück, W., Parisi, J., Scheithauer, B., Rodriguez, M., and Lassmann, H. (2000). Heterogeneity of multiple sclerosis lesions: implications for the pathogenesis of demyelination. Ann Neurol *47*, 707–717.

Lundgaard, I., Osório, M.J., Kress, B.T., Sanggaard, S., and Nedergaard, M. (2014). White matter astrocytes in health and disease. Neuroscience *276*, 161–173.

Luongo, T.S., Lambert, J.P., Gross, P., Nwokedi, M., Lombardi, A.A., Shanmughapriya, S., Carpenter, A.C., Kolmetzky, D., Gao, E., van Berlo, J.H., et al. (2017). The mitochondrial Na(+)/Ca(2+) exchanger is essential for Ca(2+) homeostasis and viability. Nature *545*, 93–97.

Lutz, B., Marsicano, G., Maldonado, R., and Hillard, C.J. (2015). The endocannabinoid system in guarding against fear, anxiety and stress. Nat Rev Neurosci *16*, 705–718.

Ma, B., Buckalew, R., Du, Y., Kiyoshi, C.M., Alford, C.C., Wang, W., McTigue, D.M., Enyeart, J.J., Terman, D., and Zhou, M. (2016). Gap junction coupling confers isopotentiality on astrocyte syncytium. Glia *64*, 214–226.

Magistretti, P.J., and Allaman, I. (2015). A cellular perspective on brain energy metabolism and functional imaging. Neuron *86*, 883–901.

Mahad, D., Ziabreva, I., Lassmann, H., and Turnbull, D. (2008). Mitochondrial defects in acute multiple sclerosis lesions. Brain *131*, 1722–1735.

Manterola, A., Bernal-Chico, A., Cipriani, R., Canedo-Antelo, M., Moreno-García, Á., Martín-Fontecha, M., Pérez-Cerdá, F., Sánchez-Gómez, M. V, Ortega-Gutiérrez, S., Brown, J.M., et al. (2018a). Deregulation of the endocannabinoid system and therapeutic potential of ABHD6 blockade in the cuprizone model of demyelination. Biochem Pharmacol *157*, 189–201.

Manterola, A., Bernal-Chico, A., Cipriani, R., Ruiz, A., Pérez-Samartín, A., Moreno-Rodríguez, M., Hsu, K.L., Cravatt, B.F., Brown, J.M., Rodríguez-Puertas, R., et al. (2018b). Re-examining the potential of targeting ABHD6 in multiple sclerosis: Efficacy of systemic and peripherally restricted inhibitors in experimental autoimmune encephalomyelitis. Neuropharmacology *141*, 181–191.

Marchi, S., Patergnani, S., Missiroli, S., Morciano, G., Rimessi, A., Wieckowski, M.R., Giorgi, C., and Pinton, P. (2018). Mitochondrial and endoplasmic reticulum calcium homeostasis and cell death. Cell Calcium *69*, 62–72.

Maresz, K., Pryce, G., Ponomarev, E.D., Marsicano, G., Croxford, J.L., Shriver, L.P., Ledent, C., Cheng, X., Carrier, E.J., Mann, M.K., et al. (2007). Direct suppression of CNS autoimmune inflammation via the cannabinoid receptor CB_1 on neurons and CB_2 on autoreactive T cells. Nat. Med. *13*, 492–497.

Marinelli, S., Pacioni, S., Bisogno, T., Di Marzo, V., Prince, D.A., Huguenard, J.R., and Bacci, A. (2008). The endocannabinoid 2-arachidonoylglycerol is responsible for the slow self-inhibition in neocortical interneurons. J Neurosci *28*, 13532–13541.

Maroso, M., Szabo, G.G., Kim, H.K., Alexander, A., Bui, A.D., Lee, S.H., Lutz, B., and Soltesz, I. (2016). Cannabinoid control of learning and memory through HCN channels. Neuron *89*, 1059–1073.

Marrs, W.R., Blankman, J.L., Horne, E.A., Thomazeau, A., Lin, Y.H., Coy, J., Bodor, A.L., Muccioli, G.G., Hu, S.S., Woodruff, G., et al. (2010). The serine hydrolase ABHD6 controls the accumulation and efficacy of 2-AG at cannabinoid receptors. Nat Neurosci *13*, 951–957.

Marsicano, G., and Lafenêtre, P. (2009). Roles of the endocannabinoid system in learning and memory. Curr Top Behav Neurosci *1*, 201–230.

Marsicano, G., and Lutz, B. (1999). Expression of the cannabinoid receptor CB_1 in distinct neuronal subpopulations in the adult mouse forebrain. Eur J Neurosci *11*, 4213–4225.

Marsicano, G., Wotjak, C.T., Azad, S.C., Bisogno, T., Rammes, G., Cascio, M.G., Hermann, H., Tang, J., Hofmann, C., Zieglgänsberger, W., et al. (2002). The endogenous cannabinoid system controls extinction of aversive memories. Nature *418*, 530–534.

Marsicano, G., Goodenough, S., Monory, K., Hermann, H., Eder, M., Cannich, A., Azad, S.C., Cascio, M.G., Gutiérrez, S.O., van der Stelt, M., et al. (2003). CB_1 cannabinoid receptors and on-

demand defense against excitotoxicity. Science (80-.). *302*, 84–88.

Martin-Fernandez, M., Jamison, S., Robin, L.M., Zhao, Z., Martin, E.D., Aguilar, J., Benneyworth, M.A., Marsicano, G., and Araque, A. (2017). Synapse-specific astrocyte gating of amygdala-related behavior. Nat Neurosci *20*, 1540–1548.

Martín, R., Bajo-Grañeras, R., Moratalla, R., Perea, G., and Araque, A. (2015). Circuit-specific signaling in astrocyte-neuron networks in basal ganglia pathways. Science (80-.). *349*, 730–734.

Matsuda, L.A., Lolait, S.J., Brownstein, M.J., Young, A.C., and Bonner, T.I. (1990). Structure of a cannabinoid receptor and functional expression of the cloned cDNA. Nature *346*, 561–564.

Matute, C., Domercq, M., Fogarty, D.J., de Zulueta, M., and Sánchez-Gómez, M. V (1999). On how altered glutamate homeostasis may contribute to demyelinating diseases of the CNS. Adv Exp Med Biol *468*, 97–107.

Matyash, M., Matyash, V., Nolte, C., Sorrentino, V., and Kettenmann, H. (2002). Requirement of functional ryanodine receptor type 3 for astrocyte migration. FASEB J. Off. Publ. Fed. Am. Soc. Exp. Biol. *16*, 84–86.

Mayo, L., Quintana, F.J., and Weiner, H.L. (2012). The innate immune system in demyelinating disease. Immunol Rev *248*, 170–187.

Mayo, L., Trauger, S.A., Blain, M., Nadeau, M., Patel, B., Jorge, I., Mascanfroni, I.D., Yeste, A., Kivisäkk, P., Kallas, K., et al. (2014). B4GALT6 regulates astrocyte activation during CNS inflammation. Nat. Med. *20*, 1147–1156.

Mayo, L., Cunha, A.P., Madi, A., Beynon, V., Yang, Z., Alvarez, J.I., Prat, A., Sobel, R.A., Kobzik, L., Lassmann, H., et al. (2016). IL-10-dependent Tr1 cells attenuate astrocyte activation and ameliorate chronic central nervous system inflammation. Brain *139*, 1939–1957.

McCarthy, K.D., and de Vellis, J. (1980). Preparation of separate astroglial and oligodendroglial cell cultures from rat cerebral tissue. J Cell Biol *85*, 890–902.

Mecha, M., Feliú, A., Carrillo-Salinas, F.J., Rueda-Zubiaurre, A., Ortega-Gutiérrez, S., de Sola, R.G., and Guaza, C. (2015). Endocannabinoids drive the acquisition of an alternative phenotype in microglia. Brain Behav Immun *49*, 233–245.

Mecha, M., Carrillo-Salinas, F.J., Feliú, A., Mestre, L., and Guaza, C. (2016). Microglia activation states and cannabinoid system: Therapeutic implications. Pharmacol Ther *166*, 40–55.

Mechoulam, R. (1986). The pharmacohistory of cannabis, in cannabis as therapeutic agents (1st ed.). CRC Press Boca Rat.

Mehrpouya-Bahrami, P., Chitrala, K.N., Ganewatta, M.S., Tang, C., Murphy, E.A., Enos, R.T., Velazquez, K.T., McCellan, J., Nagarkatti, M., and Nagarkatti, P. (2017). Blockade of CB1 cannabinoid receptor alters gut microbiota and attenuates inflammation and diet-induced obesity. Sci. Rep. *7*, 15645.

De Meij, J., Alfanek, Z., Morel, L., Decoeur, F., Leyrolle, Q., Picard, K., Carrier, M., Aubert, A., Séré, A., Lucas, C., et al. (2021). Microglial Cannabinoid Type 1 Receptor Regulates Brain Inflammation in a Sex-Specific Manner. Cannabis Cannabinoid Res. *6*, 488–507.

Mergenthaler, P., Lindauer, U., Dienel, G.A., and Meisel, A. (2013). Sugar for the brain: the role of glucose in physiological and pathological brain function. Trends Neurosci. *36*, 587–597.

Metna-Laurent, M., and Marsicano, G. (2015). Rising stars: modulation of brain functions by astroglial type-1 cannabinoid receptors. Glia *63*, 353–364.

Michailidou, I., Naessens, D.M.P., Hametner, S., Guldenaar, W., Kooi, E.-J., Geurts, J.J.G., Baas, F., Lassmann, H., and Ramaglia, V. (2017). Complement C3 on microglial clusters in multiple sclerosis occur in chronic but not acute disease: Implication for disease pathogenesis. Glia *65*, 264–277.

Micu, I., Jiang, Q., Coderre, E., Ridsdale, A., Zhang, L., Woulfe, J., Yin, X., Trapp, B.D., McRory, J.E., Rehak, R., et al. (2006). NMDA receptors mediate calcium accumulation in myelin during chemical ischaemia. Nature *439*, 988–992.

Middeldorp, J., and Hol, E.M. (2011). GFAP in health and disease. Prog. Neurobiol. *93*, 421–443.

Miller, S.J. (2018). Astrocyte heterogeneity in the adult central nervous system. Front. Cell. Neurosci. *12*, 1–6.

Miller, R.H., and Raff, M.C. (1984). Fibrous and protoplasmic astrocytes are biochemically and developmentally distinct. J. Neurosci. *4*, 585–592.

Min, R., and Nevian, T. (2012). Astrocyte signaling controls spike timing-dependent depression at neocortical synapses. Nat Neurosci *15*, 746–753.

Minagar, A., and Alexander, J.S. (2003). Blood-brain barrier disruption in multiple sclerosis. Mult. Scler. *9*, 540–549.

Mizuno, G.O., Wang, Y., Shi, G., Sun, J., Papadopoulos, S., Broussard, G.J., Unger, E.K., Deng, W., Weick, J., Bhattacharyya, A., et al. (2018). Aberrant calcium signaling in astrocytes inhibits neuronal excitability in a human Down Syndrome stem cell model. Cell Rep *24*, 355–365.

Moldrich, G., and Wenger, T. (2000). Localization of the CB_1 cannabinoid receptor in the rat brain. An immunohistochemical study. Peptides *21*, 1735–1742.

Molina-Gonzalez, I., and Miron, V.E. (2019). Astrocytes in myelination and remyelination. Neurosci. Lett. *713*, 134532.

Monory, K., Massa, F., Egertová, M., Eder, M., Blaudzun, H., Westenbroek, R., Kelsch, W., Jacob, W., Marsch, R., Ekker, M., et al. (2006). The endocannabinoid system controls key epileptogenic circuits in the hippocampus. Neuron *51*, 455–466.

Montana, V., Malarkey, E.B., Verderio, C., Matteoli, M., and Parpura, V. (2006). Vesicular transmitter release from astrocytes. Glia *54*, 700–715.

Morales, P., and Reggio, P.H. (2017). An update on non-CB_1, non-CB_2 cannabinoid related G-protein-coupled receptors. Cannabis Cannabinoid Res *2*, 265–273.

Morel, L., Chiang, M.S.R., Higashimori, H., Shoneye, T., Iyer, L.K., Yelick, J., Tai, A., and Yang, Y. (2017). Molecular and functional properties of regional astrocytes in the adult brain. J. Neurosci. *37*, 8706–8717.

Morgan, T.E., Xie, Z., Goldsmith, S., Yoshida, T., Lanzrein, A.S., Stone, D., Rozovsky, I., Perry, G., Smith, M.A., and Finch, C.E. (1999). The mosaic of brain glial hyperactivity during normal ageing and its attenuation by food restriction. Neuroscience *89*, 687–699.

Muccioli, G.G., Xu, C., Odah, E., Cudaback, E., Cisneros, J.A., Lambert, D.M., López Rodríguez, M.L., Bajjalieh, S., and Stella, N. (2007). Identification of a novel endocannabinoid-hydrolyzing enzyme expressed by microglial cells. J. Neurosci. *27*, 2883–2889.

Munro, S., Thomas, K.L., and Abu-Shaar, M. (1993). Molecular characterization of a peripheral receptor for cannabinoids. Nature *365*, 61–65.

Murphy-Royal, C., Dupuis, J., Groc, L., and Oliet, S.H.R. (2017). Astroglial glutamate transporters

in the brain: Regulating neurotransmitter homeostasis and synaptic transmission. J. Neurosci. Res. *95*, 2140–2151.

Nagai, J., Bellafard, A., Qu, Z., Yu, X., Ollivier, M., Gangwani, M.R., Diaz-Castro, B., Coppola, G., Schumacher, S.M., Golshani, P., et al. (2021). Specific and behaviorally consequential astrocyte Gq GPCR signaling attenuation in vivo with iβARK. Neuron *109*, 2256–2274.

Nagelhus, E.A., and Ottersen, O.P. (2013). Physiological roles of aquaporin-4 in brain. Physiol. Rev. *93*, 1543–1562.

Navarrete, M., and Araque, A. (2008). Endocannabinoids mediate neuron-astrocyte communication. Neuron *57*, 883–893.

Navarrete, M., and Araque, A. (2010). Endocannabinoids potentiate synaptic transmission through stimulation of astrocytes. Neuron *68*, 113–126.

Navarrete, M., Perea, G., Maglio, L., Pastor, J., de Sola, R., and Araque, A. (2013). Astrocyte calcium signal and gliotransmission in human brain tissue. Cereb Cortex *23*, 1240–1246.

Navarro, G., Morales, P., Rodríguez-Cueto, C., Fernández-Ruiz, J., Jagerovic, N., and Franco, R. (2016). Targeting cannabinoid CB_2 receptors in the central nervous system. Medicinal chemistry approaches with focus on neurodegenerative disorders. Front Neurosci *10*, 406.

Neal, M., Luo, J., Harischandra, D.S., Gordon, R., Sarkar, S., Jin, H., Anantharam, V., Désaubry, L., Kanthasamy, A., and Kanthasamy, A. (2018). Prokineticin-2 promotes chemotaxis and alternative A2 reactivity of astrocytes. Glia *66*, 2137–2157.

Nedergaard, M. (1994). Direct signaling from astrocytes to neurons in cultures of mammalian brain cells. Science *263*, 1768–1771.

Newman, E.A., and Zahs, K.R. (1997). Calcium waves in retinal glial cells. Science *275*, 844–847.

Nichols, N.R., Day, J.R., Laping, N.J., Johnson, S.A., and Finch, C.E. (1993). GFAP mRNA increases with age in rat and human brain. Neurobiol. Aging *14*, 421–429.

Nikić, I., Merkler, D., Sorbara, C., Brinkoetter, M., Kreutzfeldt, M., Bareyre, F.M., Brück, W., Bishop, D., Misgeld, T., and Kerschensteiner, M. (2011). A reversible form of axon damage in experimental autoimmune encephalomyelitis and multiple sclerosis. Nat. Med. *17*, 495–499.

Nizar, K., Uhlirova, H., Tian, P., Saisan, P.A., Cheng, Q., Reznichenko, L., Weldy, K.L., Steed, T.C., Sridhar, V.B., MacDonald, C.L., et al. (2013). In vivo stimulus-induced vasodilation occurs without IP3 receptor activation and may precede astrocytic calcium increase. J. Neurosci. *33*, 8411–8422.

Nolte, C., Matyash, M., Pivneva, T., Schipke, C.G., Ohlemeyer, C., Hanisch, U.K., Kirchhoff, F., and Kettenmann, H. (2001). GFAP promoter-controlled EGFP-expressing transgenic mice: a tool to visualize astrocytes and astrogliosis in living brain tissue. Glia *33*, 72–86.

Noristani, H.N., Gerber, Y.N., Sabourin, J.C., Le Corre, M., Lonjon, N., Mestre-Frances, N., Hirbec, H.E., and Perrin, F.E. (2017). RNA-Seq Analysis of microglia reveals time-dependent activation of specific genetic programs following spinal cord injury. Front Mol Neurosci *10*, 90.

Oberheim, N.A., Takano, T., Han, X., He, W., Lin, J.H.C., Wang, F., Xu, Q., Wyatt, J.D., Pilcher, W., Ojemann, J.G., et al. (2009). Uniquely hominid features of adult human astrocytes. J. Neurosci. *29*, 3276–3287.

Oberheim, N.A., Goldman, S.A., and Nedergaard, M. (2012). Heterogeneity of astrocytic form and function. Methods Mol. Biol. *814*, 23–45.

Okada, S., Nakamura, M., Katoh, H., Miyao, T., Shimazaki, T., Ishii, K., Yamane, J., Yoshimura, A., Iwamoto, Y., Toyama, Y., et al. (2006). Conditional ablation of Stat3 or Socs3 discloses a dual role for reactive astrocytes after spinal cord injury. Nat. Med. *12*, 829–834.

Okubo, Y., Kanemaru, K., Suzuki, J., Kobayashi, K., Hirose, K., and Iino, M. (2019). Inositol 1,4,5-trisphosphate receptor type 2-independent Ca^{2+} release from the endoplasmic reticulum in astrocytes. Glia *67*, 113–124.

Olsson, T., Barcellos, L.F., and Alfredsson, L. (2017). Interactions between genetic, lifestyle and environmental risk factors for multiple sclerosis. Nat. Rev. Neurol. *13*, 25–36.

Orellana, J.A., Froger, N., Ezan, P., Jiang, J.X., Bennett, M.V.L., Naus, C.C., Giaume, C., and Sáez, J.C. (2011a). ATP and glutamate released via astroglial connexin 43 hemichannels mediate neuronal death through activation of pannexin 1 hemichannels. J. Neurochem. *118*, 826–840.

Orellana, J.A., Shoji, K.F., Abudara, V., Ezan, P., Amigou, E., Sáez, P.J., Jiang, J.X., Naus, C.C., Sáez, J.C., and Giaume, C. (2011b). Amyloid β-induced death in neurons involves glial and neuronal hemichannels. J. Neurosci. *31*, 4962–4977.

Ortega-Gutiérrez, S., Molina-Holgado, E., Arévalo-Martín, A., Correa, F., Viso, A., López-Rodríguez, M.L., Di Marzo, V., and Guaza, C. (2005). Activation of the endocannabinoid system as therapeutic approach in a murine model of multiple sclerosis. FASEB J *19*, 1338–1340.

Palazuelos, J., Davoust, N., Julien, B., Hatterer, E., Aguado, T., Mechoulam, R., Benito, C., Romero, J., Silva, A., Guzmán, M., et al. (2008). The CB_2 cannabinoid receptor controls myeloid progenitor trafficking: involvement in the pathogenesis of an animal model of multiple sclerosis. J Biol Chem *283*, 13320–13329.

Patel, A.A., McAlinden, N., Mathieson, K., and Sakata, S. (2020). Simultaneous electrophysiology and fiber photometry in freely behaving mice. Front. Neurosci. *14*, 148.

Pekny, M., Pekna, M., Messing, A., Steinhäuser, C., Lee, J.-M., Parpura, V., Hol, E.M., Sofroniew, M. V, and Verkhratsky, A. (2016). Astrocytes: a central element in neurological diseases. Acta Neuropathol. *131*, 323–345.

Pellerin, L., and Magistretti, P.J. (1994). Glutamate uptake into astrocytes stimulates aerobic glycolysis: a mechanism coupling neuronal activity to glucose utilization. Proc. Natl. Acad. Sci. U. S. A. *91*, 10625–10629.

Perea, G., Navarrete, M., and Araque, A. (2009). Tripartite synapses: astrocytes process and control synaptic information. Trends Neurosci. *32*, 421–431.

Pertwee, R.G., Howlett, A.C., Abood, M.E., Alexander, S.P., Di Marzo, V., Elphick, M.R., Greasley, P.J., Hansen, H.S., Kunos, G., Mackie, K., et al. (2010). International Union of Basic and Clinical Pharmacology. LXXIX. Cannabinoid receptors and their ligands: beyond CB_1 and CB_2. Pharmacol Rev *62*, 588–631.

Petravicz, J., Fiacco, T.A., and McCarthy, K.D. (2008). Loss of IP3 receptor-dependent Ca^{2+} increases in hippocampal astrocytes does not affect baseline CA1 pyramidal neuron synaptic activity. J. Neurosci. *28*, 4967–4973.

Phatnani, H.P., Guarnieri, P., Friedman, B.A., Carrasco, M.A., Muratet, M., O'Keeffe, S., Nwakeze, C., Pauli-Behn, F., Newberry, K.M., Meadows, S.K., et al. (2013). Intricate interplay between astrocytes and motor neurons in ALS. Proc. Natl. Acad. Sci. U. S. A. *110*, 756–765.

Pitt, D., Werner, P., and Raine, C.S. (2000). Glutamate excitotoxicity in a model of multiple sclerosis. Nat Med *6*, 67–70.

Ponath, G., Park, C., and Pitt, D. (2018). The role of astrocytes in multiple sclerosis. Front. Immunol. *9*, 1–12.

Potter, L.E., Paylor, J.W., Suh, J.S., Tenorio, G., Caliaperumal, J., Colbourne, F., Baker, G., Winship, I., and Kerr, B.J. (2016). Altered excitatory-inhibitory balance within somatosensory cortex is associated with enhanced plasticity and pain sensitivity in a mouse model of multiple sclerosis. J Neuroinflammation *13*, 142.

Pryce, G., Ahmed, Z., Hankey, D.J., Jackson, S.J., Croxford, J.L., Pocock, J.M., Ledent, C., Petzold, A., Thompson, A.J., Giovannoni, G., et al. (2003). Cannabinoids inhibit neurodegeneration in models of multiple sclerosis. Brain *126*, 2191–2202.

Pryce, G., Cabranes, A., Fernández-Ruiz, J., Bisogno, T., Di Marzo, V., Long, J.Z., Cravatt, B.F., Giovannoni, G., and Baker, D. (2013). Control of experimental spasticity by targeting the degradation of endocannabinoids using selective fatty acid amide hydrolase inhibitors. Mult Scler *19*, 1896–1904.

Puighermanal, E., Marsicano, G., Busquets-Garcia, A., Lutz, B., Maldonado, R., and Ozaita, A. (2009). Cannabinoid modulation of hippocampal long-term memory is mediated by mTOR signaling. Nat Neurosci *12*, 1152–1158.

Qin, H., He, W., Yang, C., Li, J., Jian, T., Liang, S., Chen, T., Feng, H., Chen, X., Liao, X., et al. (2020). Monitoring astrocytic Ca^{2+} activity in freely behaving mice. Front. Cell. Neurosci. *14*, 603095.

Rahman, M.H., and Suk, K. (2020). Mitochondrial dynamics and bioenergetic alteration during inflammatory activation of astrocytes. Front. Aging Neurosci. *12*, 614410.

Rangaraju, V., Calloway, N., and Ryan, T.A. (2014). Activity-driven local ATP synthesis is required for synaptic function. Cell *156*, 825–835.

Ransohoff, R.M. (2016). A polarizing question: do M1 and M2 microglia exist? Nat. Neurosci. *19*, 987–991.

Rao, E., Singh, P., Li, Y., Zhang, Y., Chi, Y.-I., Suttles, J., and Li, B. (2015). Targeting epidermal fatty acid binding protein for treatment of experimental autoimmune encephalomyelitis. BMC Immunol. *16*, 28.

Rapizzi, E., Pinton, P., Szabadkai, G., Wieckowski, M.R., Vandecasteele, G., Baird, G., Tuft, R.A., Fogarty, K.E., and Rizzuto, R. (2002). Recombinant expression of the voltage-dependent anion channel enhances the transfer of Ca^{2+} microdomains to mitochondria. J. Cell Biol. *159*, 613–624.

Raymond, L.A. (2017). Striatal synaptic dysfunction and altered calcium regulation in Huntington disease. Biochem. Biophys. Res. Commun. *483*, 1051–1062.

Regan, M.R., Huang, Y.H., Kim, Y.S., Dykes-Hoberg, M.I., Jin, L., Watkins, A.M., Bergles, D.E., and Rothstein, J.D. (2007). Variations in promoter activity reveal a differential expression and physiology of glutamate transporters by glia in the developing and mature CNS. J. Neurosci. *27*, 6607–6619.

Reich, D.S., Lucchinetti, C.F., and Calabresi, P.A. (2018). Multiple Sclerosis. N. Engl. J. Med. *378*, 169–180.

Reyes, R.C., and Parpura, V. (2008). Mitochondria modulate Ca^{2+}-dependent glutamate release from rat cortical astrocytes. J. Neurosci. *28*, 9682–9691.

Rizor, A., Pajarillo, E., Johnson, J., Aschner, M., and Lee, E. (2019). Astrocytic oxidative/nitrosative stress contributes to Parkinson's disease pathogenesis: the dual role of reactive astrocytes. Antioxidants (Basel, Switzerland) *8*, 265.

Robin, L.M., Oliveira da Cruz, J.F., Langlais, V.C., Martin-Fernandez, M., Metna-Laurent, M., Busquets-Garcia, A., Bellocchio, L., Soria-Gomez, E., Papouin, T., Varilh, M., et al. (2018). Astroglial CB_1 receptors determine synaptic D-Serine availability to enable recognition memory. Neuron *98*, 935–944.

Rocha, S.M., Cristovão, A.C., Campos, F.L., Fonseca, C.P., and Baltazar, G. (2012). Astrocyte-derived GDNF is a potent inhibitor of microglial activation. Neurobiol. Dis. *47*, 407–415.

Rodriguez, J.J., Mackie, K., and Pickel, V.M. (2001). Ultrastructural localization of the CB_1 cannabinoid receptor in mu-opioid receptor patches of the rat caudate putamen nucleus. J Neurosci *21*, 823–833.

Rolls, A., Shechter, R., and Schwartz, M. (2009). The bright side of the glial scar in CNS repair. Nat. Rev. Neurosci. *10*, 235–241.

Rosario, R., Marisa, B., Marta, M., and Tullio, P. (1993). Microdomains with high Ca^{2+} close to IP3-sensitive channels that are sensed by neighboring mitochondria. Science (80-.). *262*, 744–747.

Rothhammer, V., Mascanfroni, I.D., Bunse, L., Takenaka, M.C., Kenison, J.E., Mayo, L., Chao, C.C., Patel, B., Yan, R., Blain, M., et al. (2016). Type I interferons and microbial metabolites of tryptophan modulate astrocyte activity and central nervous system inflammation via the aryl hydrocarbon receptor. Nat Med *22*, 586–597.

Rothhammer, V., Borucki, D.M., Tjon, E.C., Takenaka, M.C., Chao, C.C., Ardura-Fabregat, A., de Lima, K.A., Gutiérrez-Vázquez, C., Hewson, P., Staszewski, O., et al. (2018). Microglial control of astrocytes in response to microbial metabolites. Nature *557*, 724–728.

Rothstein, J.D., Martin, L., Levey, A.I., Dykes-Hoberg, M., Jin, L., Wu, D., Nash, N., and Kuncl, R.W. (1994). Localization of neuronal and glial glutamate transporters. Neuron *13*, 713–725.

Rothstein, J.D., Dykes-Hoberg, M., Pardo, C.A., Bristol, L.A., Jin, L., Kuncl, R.W., Kanai, Y., Hediger, M.A., Wang, Y., Schielke, J.P., et al. (1996). Knockout of glutamate transporters reveals a major role for astroglial transport in excitotoxicity and clearance of glutamate. Neuron *16*, 675–686.

Rowitch, D.H., and Kriegstein, A.R. (2010). Developmental genetics of vertebrate glial-cell specification. Nature *468*, 214–222.

Rueda, D., Galve-Roperh, I., Haro, A., and Guzmán, M. (2000). The CB_1 cannabinoid receptor is coupled to the activation of c-Jun N-terminal kinase. Mol Pharmacol *58*, 814–820.

Sánchez-Gómez, M. V, Alberdi, E., Ibarretxe, G., Torre, I., and Matute, C. (2003). Caspase-dependent and caspase-independent oligodendrocyte death mediated by AMPA and kainate receptors. J Neurosci *23*, 9519–9528.

Sarchielli, P., Greco, L., Floridi, A., and Gallai, V. (2003). Excitatory amino acids and multiple sclerosis: evidence from cerebrospinal fluid. Arch Neurol *60*, 1082–1088.

Savinainen, J.R., Saario, S.M., and Laitinen, J.T. (2012). The serine hydrolases MAGL, ABHD6 and ABHD12 as guardians of 2-arachidonoylglycerol signalling through cannabinoid receptors. Acta Physiol *204*, 267–276.

Savtchouk, I., and Volterra, A. (2018). Gliotransmission: beyond black-and-white. J. Neurosci. *38*, 14–25.

Scheller, A., and Kirchhoff, F. (2016). Endocannabinoids and heterogeneity of glial cells in brain function. Front. Integr. Neurosci. *10*, 24.

Schindelin, J., Arganda-Carreras, I., Frise, E., Kaynig, V., Longair, M., Pietzsch, T., Preibisch, S., Rueden, C., Saalfeld, S., Schmid, B., et al. (2012). Fiji: an open-source platform for biological-image analysis. Nat. Methods *9*, 676–682.

Schlosburg, J.E., Blankman, J.L., Long, J.Z., Nomura, D.K., Pan, B., Kinsey, S.G., Nguyen, P.T., Ramesh, D., Booker, L., Burston, J.J., et al. (2010). Chronic monoacylglycerol lipase blockade causes functional antagonism of the endocannabinoid system. Nat Neurosci *13*, 1113–1119.

Schmitt, A., Asan, E., Püschel, B., and Kugler, P. (1997). Cellular and regional distribution of the glutamate transporter GLAST in the CNS of rats: nonradioactive in situ hybridization and comparative immunocytochemistry. J. Neurosci. *17*, 1–10.

Schmitt, A., Asan, E., Lesch, K.-P., and Kugler, P. (2002). A splice variant of glutamate transporter GLT1/EAAT2 expressed in neurons: cloning and localization in rat nervous system. Neuroscience *109*, 45–61.

Schmitt, C., Strazielle, N., and Ghersi-Egea, J.-F. (2012). Brain leukocyte infiltration initiated by peripheral inflammation or experimental autoimmune encephalomyelitis occurs through pathways connected to the CSF-filled compartments of the forebrain and midbrain. J. Neuroinflammation *9*, 187.

Schroeter, C.B., Herrmann, A.M., Bock, S., Vogelsang, A., Eichler, S., Albrecht, P., Meuth, S.G., and Ruck, T. (2021). One Brain—All cells: a comprehensive protocol to isolate all principal CNS-resident cell types from brain and spinal cord of adult healthy and EAE mice. Cells *10*, 651.

Schüle, L.-L., Glasmacher, S., Gertsch, J., Roggan, M.D., Transfeld, J.-L., Bindila, L., Lutz, B., Kolbe, C.-C., Bilkei-Gorzo, A., Zimmer, A., et al. (2021). Diacylglycerol lipase alpha in astrocytes is involved in maternal care and affective behaviors. Glia *69*, 377–391.

Seehusen, F., and Baumgärtner, W. (2010). Axonal pathology and loss precede demyelination and accompany chronic lesions in a spontaneously occurring animal model of multiple sclerosis. Brain Pathol *20*, 551–559.

Semyanov, A., Henneberger, C., and Agarwal, A. (2020). Making sense of astrocytic calcium signals — from acquisition to interpretation. Nat. Rev. Neurosci. *21*, 551–564.

Serrat, R., Covelo, A., Kouskoff, V., Delcasso, S., Ruiz-Calvo, A., Chenouard, N., Stella, C., Blancard, C., Salin, B., Julio-Kalajzić, F., et al. (2021). Astroglial ER-mitochondria calcium transfer mediates endocannabinoid-dependent synaptic integration. Cell Rep. *37*, 110133.

Sharif, A., and Prevot, V. (2010). ErbB receptor signaling in astrocytes: a mediator of neuron-glia communication in the mature central nervous system. Neurochem. Int. *57*, 344–358.

Shelton, M.K., and McCarthy, K.D. (1999). Mature hippocampal astrocytes exhibit functional metabotropic and ionotropic glutamate receptors in situ. Glia *26*, 1–11.

Sherwood, M.W., Arizono, M., Panatier, A., Mikoshiba, K., and Oliet, S.H.R. (2021). Astrocytic IP3Rs: Beyond IP3R2. Front. Cell. Neurosci. *15*, 1–12.

Shibata, T., Yamada, K., Watanabe, M., Ikenaka, K., Wada, K., Tanaka, K., and Inoue, Y. (1997). Glutamate transporter GLAST is expressed in the radial glia–astrocyte lineage of developing mouse spinal cord. J. Neurosci. *17*, 9212–9219.

Shigetomi, E., Kracun, S., and Khakh, B.S. (2010). Monitoring astrocyte calcium microdomains with improved membrane targeted GCaMP reporters. Neuron Glia Biol. *6*, 183–191.

Shigetomi, E., Patel, S., and Khakh, B.S. (2016). Probing the complexities of astrocyte calcium signaling. Trends Cell Biol *26*, 300–312.

Shigetomi, E., Saito, K., Sano, F., and Koizumi, S.C. (2019). Aberrant calcium signals in reactive astrocytes: A key process in neurological disorders. Int. J. Mol. Sci. *20*.

Siffrin, V., Birkenstock, J., Luchtman, D.W., Gollan, R., Baumgart, J., Niesner, R.A., Griesbeck, O., and Zipp, F. (2015). FRET based ratiometric Ca^{2+} imaging to investigate immune-mediated neuronal and axonal damage processes in experimental autoimmune encephalomyelitis. J. Neurosci. Methods *249*, 8–15.

Simard, M., and Nedergaard, M. (2004). The neurobiology of glia in the context of water and ion homeostasis. Neuroscience *129*, 877–896.

Smith, B.C., Sinyuk, M., Jenkins, J.E., Psenicka, M.W., and Williams, J.L. (2020). The impact of regional astrocyte interferon-γ signaling during chronic autoimmunity: a novel role for the immunoproteasome. J. Neuroinflammation *17*, 184.

Sofroniew, M. V. (2015). Astrocyte barriers to neurotoxic inflammation. Nat. Rev. Neurosci. *16*, 249–263.

Sofroniew, M. V. (2020). Astrocyte reactivity: subtypes, states, and functions in CNS innate immunity. Trends Immunol. *41*, 758–770.

Sofroniew, M. V., and Vinters, H. V. (2010). Astrocytes: Biology and pathology. Acta Neuropathol. *119*, 7–35.

Srinivasan, R., Sailasuta, N., Hurd, R., Nelson, S., and Pelletier, D. (2005). Evidence of elevated glutamate in multiple sclerosis using magnetic resonance spectroscopy at 3 T. Brain *128*, 1016–1025.

Srinivasan, R., Huang, B.S., Venugopal, S., Johnston, A.D., Chai, H., Zeng, H., Golshani, P., and Khakh, B.S. (2015). Ca(2+) signaling in astrocytes from Ip3r2(-/-) mice in brain slices and during startle responses in vivo. Nat. Neurosci. *18*, 708–717.

Srinivasan, R., Lu, T.Y., Chai, H., Xu, J., Huang, B.S., Golshani, P., Coppola, G., and Khakh, B.S. (2016). New transgenic mouse lines for selectively targeting astrocytes and studying calcium signals in astrocyte processes in situ and in vivo. Neuron *92*, 1181–1195.

Steiner, J., Bernstein, H.-G., Bielau, H., Berndt, A., Brisch, R., Mawrin, C., Keilhoff, G., and Bogerts, B. (2007). Evidence for a wide extra-astrocytic distribution of S100B in human brain. BMC Neurosci. *8*, 2.

Steinhäuser, C., Seifert, G., and Bedner, P. (2012). Astrocyte dysfunction in temporal lobe epilepsy: K^+ channels and gap junction coupling. Glia *60*, 1192–1202.

Stella, N. (2010). Cannabinoid and cannabinoid-like receptors in microglia, astrocytes, and astrocytomas. Glia *58*, 1017–1030.

Stoffels, J.M.J., de Jonge, J.C., Stancic, M., Nomden, A., van Strien, M.E., Ma, D., Sisková, Z., Maier, O., Ffrench-Constant, C., Franklin, R.J.M., et al. (2013). Fibronectin aggregation in multiple sclerosis lesions impairs remyelination. Brain *136*, 116–131.

Suárez, J., Rivera, P., Aparisi Rey, A., Pérez-Martín, M., Arrabal, S., Rodríguez de Fonseca, F., Ruiz de Azua, I., and Lutz, B. (2019). Adipocyte cannabinoid CB1 receptor deficiency alleviates high fat diet-induced memory deficit, depressive-like behavior, neuroinflammation and impairment in adult neurogenesis. Psychoneuroendocrinology *110*, 104418.

Sugiura, T., Kondo, S., Sukagawa, A., Nakane, S., Shinoda, A., Itoh, K., Yamashita, A., and Waku, K. (1995). 2-Arachidonoylglycerol: a possible endogenous cannabinoid receptor ligand in brain. Biochem Biophys Res Commun *215*, 89–97.

Sugiura, T., Kobayashi, Y., Oka, S., and Waku, K. (2002). Biosynthesis and degradation of anandamide and 2-arachidonoylglycerol and their possible physiological significance. Prostaglandins Leukot Essent Fat. Acids *66*, 173–192.

Sun, W., McConnell, E., Pare, J.-F., Xu, Q., Chen, M., Peng, W., Lovatt, D., Han, X., Smith, Y., and Nedergaard, M. (2013). Glutamate-dependent neuroglial calcium signaling differs between young and adult brain. Science *339*, 197–200.

Surmeier, D.J., Schumacker, P.T., Guzman, J.D., Ilijic, E., Yang, B., and Zampese, E. (2017). Calcium and Parkinson's disease. Biochem. Biophys. Res. Commun. *483*, 1013–1019.

Sweeney, M.D., Sagare, A.P., and Zlokovic, B. V (2018). Blood–brain barrier breakdown in Alzheimer disease and other neurodegenerative disorders. Nat. Rev. Neurol. *14*, 133–150.

Szalai, A.J., Hu, X., Adams, J.E., and Barnum, S.R. (2007). Complement in experimental autoimmune encephalomyelitis revisited: C3 is required for development of maximal disease. Mol. Immunol. *44*, 3132–3136.

Szatkowski, M., Barbour, B., and Attwell, D. (1990). Non-vesicular release of glutamate from glial cells by reversed electrogenic glutamate uptake. Nature *348*, 443–446.

Szulzewsky, F., Pelz, A., Feng, X., Synowitz, M., Markovic, D., Langmann, T., Holtman, I.R., Wang, X., Eggen, B.J., Boddeke, H.W., et al. (2015). Glioma-associated microglia/macrophages display an expression profile different from M1 and M2 polarization and highly express Gpnmb and Spp1. PLoS One *10*, e0116644.

Takata, N., and Hirase, H. (2008). Cortical layer 1 and layer 2/3 astrocytes exhibit distinct calcium dynamics in vivo. PLoS One *3*, e2525.

Tanaka, K., Watase, K., Manabe, T., Yamada, K., Watanabe, M., Takahashi, K., Iwama, H., Nishikawa, T., Ichihara, N., Kikuchi, T., et al. (1997). Epilepsy and exacerbation of brain injury in mice lacking the glutamate transporter GLT-1. Science *276*, 1699–1702.

Tassoni, A., Farkhondeh, V., Itoh, Y., Itoh, N., Sofroniew, M. V, and Voskuhl, R.R. (2019). The astrocyte transcriptome in EAE optic neuritis shows complement activation and reveals a sex difference in astrocytic C3 expression. Sci. Rep. *9*, 10010.

Thompson, A.J., Baranzini, S.E., Geurts, J., Hemmer, B., and Ciccarelli, O. (2018). Multiple sclerosis. Lancet *391*, 1622–1636.

Valdor, R., and Macian, F. (2010). Mechanisms of self-inactivation in anergic T cells. Inmunología *29*, 20–33.

Vázquez, C., Tolón, R.M., Pazos, M.R., Moreno, M., Koester, E.C., Cravatt, B.F., Hillard, C.J., and Romero, J. (2015a). Endocannabinoids regulate the activity of astrocytic hemichannels and the microglial response against an injury: In vivo studies. Neurobiol. Dis. *79*, 41–50.

Vázquez, C., Tolón, R.M., Grande, M.T., Caraza, M., Moreno, M., Koester, E.C., Villaescusa, B., Ruiz-Valdepeñas, L., Fernández-Sánchez, F.J., Cravatt, B.F., et al. (2015b). Endocannabinoid regulation of amyloid-induced neuroinflammation. Neurobiol. Aging *36*, 3008–3019.

Vercellino, M., Masera, S., Lorenzatti, M., Condello, C., Merola, A., Mattioda, A., Tribolo, A., Capello, E., Mancardi, G.L., Mutani, R., et al. (2009). Demyelination, inflammation, and neurodegeneration in multiple sclerosis deep gray matter. J Neuropathol Exp Neurol *68*, 489–502.

Verkhratsky, A., and Nedergaard, M. (2018). Physiology of astroglia. Physiol. Rev. *98*, 239–389.

Viader, A., Blankman, J.L., Zhong, P., Liu, X., Schlosburg, J.E., Joslyn, C.M., Liu, Q.S., Tomarchio, A.J., Lichtman, A.H., Selley, D.E., et al. (2015). Metabolic interplay between astrocytes and neurons regulates endocannabinoid action. Cell Rep *12*, 798–808.

Viader, A., Ogasawara, D., Joslyn, C.M., Sanchez-Alavez, M., Mori, S., Nguyen, W., Conti, B., and Cravatt, B.F. (2016). A chemical proteomic atlas of brain serine hydrolases identifies cell type-specific pathways regulating neuroinflammation. Elife *5*, e12345.

Vives, V., Alonso, G., Solal, A.C., Joubert, D., and Legraverend, C. (2003). Visualization of S100B-positive neurons and glia in the central nervous system of EGFP transgenic mice. J. Comp. Neurol. *457*, 404–419.

Vogel, D.Y.S., Vereyken, E.J.F., Glim, J.E., Heijnen, P.D.A.M., Moeton, M., van der Valk, P., Amor, S., Teunissen, C.E., van Horssen, J., and Dijkstra, C.D. (2013). Macrophages in inflammatory multiple sclerosis lesions have an intermediate activation status. J. Neuroinflammation *10*, 35.

Volterra, A., Magistretti, P.J., and Haydon, P.G. (2002). The tripartite synapse: glia in synaptic transmission (Oxford University Press).

Volterra, A., Liaudet, N., and Savtchouk, I. (2014). Astrocyte Ca^{2+} signalling: an unexpected complexity. Nat. Rev. Neurosci. *15*, 327–335.

Wallin, M.T., Culpepper, W.J., Nichols, E., Bhutta, Z.A., Gebrehiwot, T.T., Hay, S.I., Khalil, I.A., Krohn, K.J., Liang, X., Naghavi, M., et al. (2019). Global, regional, and national burden of multiple sclerosis 1990–2016: a systematic analysis for the Global Burden of Disease Study 2016. Lancet Neurol. *18*, 269–285.

Wang, X., Lou, N., Xu, Q., Tian, G.-F., Peng, W.G., Han, X., Kang, J., Takano, T., and Nedergaard, M. (2006). Astrocytic Ca^{2+} signaling evoked by sensory stimulation in vivo. Nat. Neurosci. *9*, 816–823.

Weber, B., and Barros, L.F. (2015). The astrocyte: Powerhouse and recycling center. Cold Spring Harb. Perspect. Biol. *7*, 1–15.

Weiner, H.L. (2004). Multiple sclerosis is an inflammatory T-cell-mediated autoimmune disease. Arch Neurol *61*, 1613–1615.

Weissert, R. (2013). The immune pathogenesis of multiple sclerosis. J Neuroimmune Pharmacol *8*, 857–866.

Werner, P., Pitt, D., and Raine, C.S. (2001). Multiple sclerosis: altered glutamate homeostasis in lesions correlates with oligodendrocyte and axonal damage. Ann Neurol *50*, 169–180.

Werth, J.L., and Thayer, S.A. (1994). Mitochondria buffer physiological calcium loads in cultured rat dorsal root ganglion neurons. J. Neurosci. *14*, 348–356.

Wescott, A.P., Kao, J.P.Y., Lederer, W.J., and Boyman, L. (2019). Voltage-energized Calcium-sensitive ATP Production by Mitochondria. Nat Metab *1*, 975–984.

Wiley, M.B., Perez, P.A., Argueta, D.A., Avalos, B., Wood, C.P., and DiPatrizio, N. V. (2021). UPLC-MS/MS method for analysis of endocannabinoid and related lipid metabolism in mouse mucosal tissue. Front. Physiol. *12*, 1–12.

Wilson, E.L., and Metzakopian, E. (2021). ER-mitochondria contact sites in neurodegeneration: genetic screening approaches to investigate novel disease mechanisms. Cell Death Differ. *28*, 1804–1821.

Witting, A., Chen, L., Cudaback, E., Straiker, A., Walter, L., Rickman, B., Möller, T., Brosnan, C.,

and Stella, N. (2006). Experimental autoimmune encephalomyelitis disrupts endocannabinoid-mediated neuroprotection. Proc Natl Acad Sci U S A *103*, 6362–6367.

Wójtowicz, A.M., Dvorzhak, A., Semtner, M., and Grantyn, R. (2013). Reduced tonic inhibition in striatal output neurons from Huntington mice due to loss of astrocytic GABA release through GAT-3. Front. Neural Circuits *7*, 188.

Woodhams, S.G., Chapman, V., Finn, D.P., Hohmann, A.G., and Neugebauer, V. (2017). The cannabinoid system and pain. Neuropharmacology *124*, 105–120.

Yang, Y., Vidensky, S., Jin, L., Jie, C., Lorenzini, I., Frankl, M., and Rothstein, J.D. (2011). Molecular comparison of GLT1+ and ALDH1L1+ astrocytes in vivo in astroglial reporter mice. Glia *59*, 200–207.

Ye, Z.-C., Wyeth, M.S., Baltan-Tekkok, S., and Ransom, B.R. (2003). Functional hemichannels in astrocytes: a novel mechanism of glutamate release. J. Neurosci. *23*, 3588–3596.

Yi, W., Schlüter, D., and Wang, X. (2019). Astrocytes in multiple sclerosis and experimental autoimmune encephalomyelitis: Star-shaped cells illuminating the darkness of CNS autoimmunity. Brain. Behav. Immun. *80*, 10–24.

Yu, X., Taylor, A.M.W., Nagai, J., Golshani, P., Evans, C.J., Coppola, G., and Khakh, B.S. (2018). Reducing astrocyte calcium signaling in vivo alters striatal microcircuits and causes repetitive behavior. Neuron *99*, 1170–1187.

Yu, X., Nagai, J., Marti-Solano, M., Soto, J.S., Coppola, G., Babu, M.M., and Khakh, B.S. (2020). Context-specific striatal astrocyte molecular responses are phenotypically exploitable. Neuron *108*, 1146–1162.

Yun, S.P., Kam, T.-I., Panicker, N., Kim, S., Oh, Y., Park, J.-S., Kwon, S.-H., Park, Y.J., Karuppagounder, S.S., Park, H., et al. (2018). Block of A1 astrocyte conversion by microglia is neuroprotective in models of Parkinson's disease. Nat. Med. *24*, 931–938.

Zabala, A., Vazquez-Villoldo, N., Rissiek, B., Gejo, J., Martin, A., Palomino, A., Perez-Samartín, A., Pulagam, K.R., Lukowiak, M., Capetillo-Zarate, E., et al. (2018). P2X4 receptor controls microglia activation and favors remyelination in autoimmune encephalitis. EMBO Mol Med *10*, e8743.

Zador, Z., Stiver, S., Wang, V., and Manley, G.T. (2009). Role of aquaporin-4 in cerebral edema and stroke. Handb. Exp. Pharmacol. 159–170.

Zamanian, J.L., Xu, L., Foo, L.C., Nouri, N., Zhou, L., Giffard, R.G., and Barres, B.A. (2012). Genomic analysis of reactive astrogliosis. J Neurosci *32*, 6391–6410.

Zhang, Y., Sloan, S.A., Clarke, L.E., Caneda, C., Plaza, C.A., Blumenthal, P.D., Vogel, H., Steinberg, G.K., Edwards, M.S., Li, G., et al. (2016). Purification and characterization of progenitor and mature human astrocytes reveals transcriptional and functional differences with mouse. Neuron *89*, 37–53.

Zhang, Z., Chen, G., Zhou, W., Song, A., Xu, T., Luo, Q., Wang, W., Gu, X., and Duan, S. (2007). Regulated ATP release from astrocytes through lysosome exocytosis. Nat. Cell Biol. *9*, 945–953.

Zhang, Z., Ma, Z., Zou, W., Guo, H., Liu, M., Ma, Y., and Zhang, L. (2019). The appropriate marker for astrocytes: comparing the distribution and expression of three astrocytic markers in different mouse cerebral regions. Biomed Res. Int. *2019*, 9605265.

Zhao, Y., Yamasaki, R., Yamaguchi, H., Nagata, S., Une, H., Cui, Y., Masaki, K., Nakamuta, Y., Iinuma, K., Watanabe, M., et al. (2020). Oligodendroglial connexin 47 regulates neuroinflammation upon autoimmune demyelination in a novel mouse model of multiple

sclerosis. Proc Natl Acad Sci U S A *117*, 2160–2169.

Zheng, J., Zeng, X., and Wang, S. (2015). Calcium ion as cellular messenger. Sci. China. Life Sci. *58*, 1–5.

Zhou, Y., and Danbolt, N. (2013). GABA and glutamate transporters in brain. Front. Endocrinol. (Lausanne). *4*, 165.

Zhuo, L., Sun, B., Zhang, C.L., Fine, A., Chiu, S.Y., and Messing, A. (1997). Live astrocytes visualized by green fluorescent protein in transgenic mice. Dev. Biol. *187*, 36–42.

Zou, S., and Kumar, U. (2018). Cannabinoid receptors and the endocannabinoid system: signaling and function in the central nervous system. Int J Mol Sci *19*, 833.